The Dissertation Committee for Rebecca Suzanne Zimmerman Certifies that this is the approved version of the following dissertation:

Studies of Anion Binding in Pyrrole-containing Supramolecular Motifs

Committee:

Jonathan L. Sessler, Supervisor

Alan H. Cowley

Brent L. Iverson

Sean M. Kerwin

Michael J. Krische

Studies of Anion Binding in Pyrrole-containing Supramolecular Motifs

by

Rebecca Suzanne Zimmerman, B.A., B.S.

Dissertation

Presented to the Faculty of the Graduate School of

The University of Texas at Austin

in Partial Fulfillment

of the Requirements

for the Degree of

Doctor of Philosophy

The University of Texas at Austin

May, 2002

Dedication

For my mother and father

Suzanne and Dennis

Who have freely given their love, support, and encouragement to me.

Thank you for teaching me to reach for the sky.

Acknowledgements

I would like to first and foremost acknowledge my supervisor, Jonathan Sessler, and thank him for taking a chance on me so long ago and for giving me this opportunity to make my way in the world. I am forever indebted to him. For those who helped get me started, Andreas Gebauer and John Genge, I thank you. You took me under your wing when I was uncertain and frightened, and gave me the courage to take my first steps; I will never forget what you did for me. Vladimír Král, thank you for pointing me in the right direction and teaching me how to complete a project. Others of you were not only mentors but good friends: Bruno Andrioletti, Christophe Bucher, and Greg Kirkovits. Without the patience and caring of the three of you, the content of this dissertation and the quality of my experience these past years would have been vastly compromised.

I made many friends along the way who made my stay enjoyable, and met many Sesslerites who taught me the meaning of belonging to something bigger than myself: Sharon, Daniel, Leah, Julian, Jim, Pavel and Karolina, Wyeth, Janan. I need to separately mention my two good friends who are fine people and amazing chemists, and who helped me survive my last year and a half: Dan Pantos and Mike Huggins. Dan, especially, thank you for your patience and for

helping me see the world and myself with new eyes. You have made a tremendous difference in my life. Thanks also to Greg and Mike for proofreading this beast, to Daniel for making this time in my life more bearable, and of course to my family and friends for being so supportive and understanding these past six years.

Finally, there are three people who are of utmost importance to me, and without whom I would have quit many times over on this long journey.

Muhunthan, you always stood by me, even when you didn't understand me. You helped me, you mentored me, you taught me, you let me cry on your shoulder, you yelled at me, you drove me crazy, you expected the best of me, and I could never ask for a better friend or a more entertaining labmate.

Maya, you lived with me and were my closest friend for almost six years. You have been there beside me every step of the way, through everything no matter good or bad. You lifted me up when I was down, you gave it to me straight even if I didn't want to hear it, and you kept me true to myself. You are that rarest of finds, a true friend.

And, finally, Nicolai. Nobody meant more to me than you. You were the light in my darkness, the strong hand on my back for such a long time. Thank you for sharing your life with me, for showing me what real love is, for teaching me about happiness, and for ultimately helping me to see that the answers I'd been looking for all this time are exactly where you said they'd be: right in my own heart. Never doubt that the most important lessons I learned in graduate school had nothing to do with chemistry.

Studies of Anion Binding in Pyrrole-containing Supramolecular Motifs

Publication No._____

Rebecca Suzanne Zimmerman, Ph.D.

The University of Texas at Austin, 2002

Supervisor: Jonathan L. Sessler

Anions are important in a wide range of biological as well as chemical processes. In addition to their importance in the areas of medicine and catalysis, many environmental pollutants are anionic, such as phosphates, nitrates, and pertechnetate. Anions are more difficult to sense *via* electrostatic interactions than cations because of their lower charge to radius ratio; the majority of neutral anion receptors thus utilize hydrogen bonding as the predominant binding mode. Anions also have a wide range of geometries and require a high degree of complementarity in receptor design in order to achieve selectivity. Additionally, an anion receptor must successfully compete with the solvent environment. Anions are very strongly solvated, and the free energy gained upon binding must exceed the free energy lost as the result of dehydrating the anion. This can make binding in protic or hydroxylic solvents particularly challenging.

Because of the inherent difficulties associated with anion recognition, the development of anion binding agents has lagged behind corresponding work on cation receptors. Currently, there are two general classes of synthetic anion receptors, those that are positively charged and those that are neutral. The major advantage of neutral hosts is that the absence of a positive charge generally provides for more selective binding, for the simple reason that positive charges are nondirectional and lead to electrostatic attractions that cannot by definition be selective for a particular anion. Another advantage to neutral hosts is that there is no inherent competition with a receptor associated with a counterion, which can often result in a weaker affinity for the intended guest.

This dissertation focuses on the anion binding behavior of neutral, pyrrole containing supramolecular systems. The first chapter will discuss the ability of ferrocene-pyrrole conjugates to sense anions electrochemically. Chapter 2 investigates the anion binding ability of an expanded calixphyrin and a strapped calixpyrrole. Chapter 3 focuses on crown ether appended dipyrrolylquinoxalines and their effectiveness as ditopic receptors. Chapter 4 provides experimental methods and characterization data.

Table of Contents

List of Tables

List of Figures

List of Illustrations

Chapter 1: The Design, Synthesis and Study of Ferrocene-Pyrrole Conjugates for the Electrochemical Sensing of Anions

1.1 INTRODUCTION

The development of receptors for the purpose of anion recognition has been the focus of increasing attention over the past thirty years. One class of receptors are organic based, examples of which consist of polyammonium receptors,[1-3] guanadinium-based receptors,[4-6] and expanded porphyrins,[7] all of which require protonation in order to bind anions. More recently amide and thiourea functionalities have been used to construct anion receptors that allow for anion binding without a pH restriction.[8-11] The rapidly growing field of organic receptor-based anion recognition chemistry has been widely reviewed,[12] however, and lies outside the scope of this discussion. More germane to the present work are anion receptors containing metal centers. These so-called inorganic anion receptors have been the focus of considerable effort and offer a number of advantages over their organic counterparts.[12] For example, the fact that metal centers are generally either positively charged or formally electron deficient, leads to an enhanced electrostatic interaction with the anion and one that is often independent of pH. Additionally, metal ions often display redox activity, UV-vis spectroscopic properties, fluorescent and energy-transfer properties, and radioactivity, all of which can allow for a measurement of the anion-binding event. Examples of inorganic receptors include those containing Lewis acid metals such as tin,[13-15] boron,[16-18] silicon,[19,20] germanium,[21,22] or mercury,[23,24] as

well as multiple positively charged metal ion based receptors.[25] All of these utilize orbital overlap interactions in addition to pure electrostatics to achieve anion binding.

Redox-based receptors containing ruthenium, cobalt, and iron have been in development over the past twelve years.[26] As a result of the redox-active metal center and the guest communicating with one another, a change in the potential of the metal center can occur in the presence of a guest. This communication can take place *via* a variety of interactions, including ones mediated through-space, through-bond, or as the result of direct coordination between the metal center and the guest. Induced conformational changes of the redox center upon binding of the guest, and interruption in the interaction between two redox centers are other ways whereby anion binding can be made to induce a measurable change at a metal center.[27] In the case of the redox-based receptors this change is often manifest in terms of the electrochemical properties of the system. An ideal electrochemical sensor will retain the reversibility of the redox couple in the presence of an anion, causing the potential of the metal center to shift cathodically. This is because the close proximity of an anion rich in electron density lowers the oxidation potential of the metal center. It is possible to correlate the magnitude of the cathodic shift to the strength of anion binding in the two redox states of the receptor. With the caveat that the affinity to one redox state is known, it becomes possible to calculate the enhancement in the binding affinity due to the oxidation of the metal center (referred to as reaction coupling efficiency, or RCE).[28]

1.1.1 Cobaltocenium Based Electrochemical Anion Sensors

One of the poineers in the area of redox-active inorganic-based anion sensing is Professor Paul Beer of Oxford University. His initial foray involved the positively charged, pH independent dicobaltocenium ester receptor **1.1** which he and his coworkers published in 1989.[29] This system was found to bind bromide anion through electrostatic interactions and to induce a cathodic shift in the electrochemical spectrum. However, its poor solubility, challenging synthesis, inability to bind a wider variety of anions, and the fact that it was prone to hydrolysis, led to a different approach involving amide linkages.

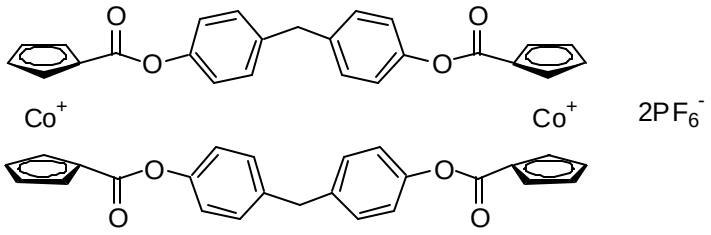

1.1

A wide range of amide-linked sensors were developed beginning with **1.2**, **1.3** and **1.4**.[30] The use of amide linkages introduced an additional hydrogen bonding anion recognition motif that complemented those arising from the positively charged colbaltocenium center. Proton NMR spectroscopic titrations of **1.2** and **1.3** in CD_3CN and $(CD_3)_2SO$ showed a downfield shift of the amide protons in the presence of anions, whereas the tertiary amide **1.4** displayed no evidence of anion binding, leading to the conclusion that the amide functionalities participate in the anion binding process.

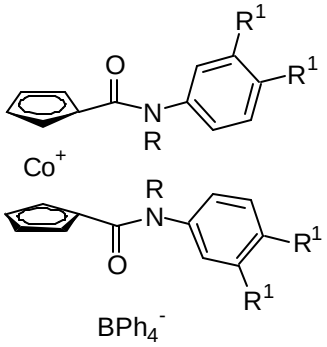

1.2 R = R^1 = H
1.3 R = H; R^1 = OMe
1.4 R = Me; R^1 = H

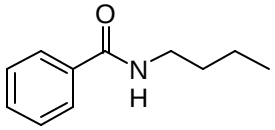

1.5

Control experiments with **1.5** provided support for the importance of the presumed electrostatic component to the anion binding process; in particular, ^{1}H NMR spectroscopic titrations of **1.5** showed much weaker binding interactions than **1.2** or **1.3**. The electrochemical results showed a cathodic shift in the reversible signal; the bound anion makes the cobaltocenium cation more difficult to reduce. The tertiary amide **1.4** did not show any signal perturbation, ruling out ion-pairing effects and supporting the hypothesis that signal perturbation was occurring as a result of hydrogen bonding interactions. Other receptors prepared by the Beer group included the tripodal systems **1.6** and **1.7**, which resulted in substantial downfield shifts of the amide protons upon addition of one equivalent of Cl^- as well as cathodic shifts in the elctrochemical spectrum.[31] These initial systems provided the first true indication that metallocene systems could function as effective anion-binding sensors.

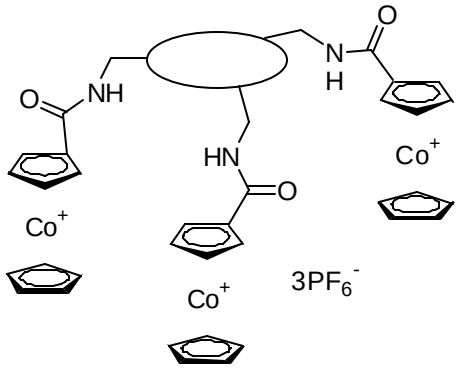

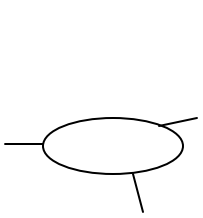

=

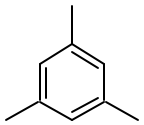

1.6

1.7

Studies on the effect of the accessibility of the hydrogen bond donor sites to the anion were conducted with **1.8**, **1.9**, and **1.10**,[31,32] which have the orientation of the amino donor group on the aryl substituent positioned *ortho*, *meta*, and *para*, respectively. The *ortho* and *meta* receptors were found to bind chloride anion (studied as its tetrabutylammonium salt) with a strength of 770 M^{-1} and 630 M^{-1} in CD_3CN, respectively, compared to only 24 M^{-1} for the *para* substituted receptor. Although the amide is the dominant hydrogen bond donor, the amines participate in hydrogen bonding as well. The low anion binding affinity of **1.10** is rationalized in terms of an inability of the *para* amino group to hydrogen bond to the chloride center as a result of the large distance of the amine from the amide NH. On a more fundamental level the fact that differences were seen was considered as underscoring the importance of a cooperative orientation of the hydrogen bond donor groups as a predicate for optimal binding.

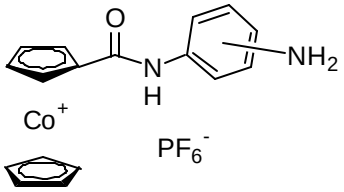

1.8 = ortho
1.9 = meta
1.10 = para

An investigation was undertaken to explore variables that influence anion binding strength and selectivity. A series of biscobaltocenium subunits linked by various alkyl and aryl spacers were prepared and studied.[33] Studies of the stability constants of the alkyl linked systems **1.11**, **1.12**, and **1.13** supported the expected 1:1 binding stoichiometry for chloride and bromide. The shorter alkyl chain receptor was found to exhibit a preference for binding chloride over bromide. However, as the chain length increased, this selectivity for chloride decreased and was replaced by a selectivity for bromide. In addition, the overall magnitude of the stability constants was found to decrease as the chain length increased. For instance, receptor **1.11** displayed an association constant of 2,500 M^{-1} for chloride anion and one of only 330 M^{-1} for bromide anion in CD_3CN. By contrast, receptor **1.13** displayed an association constant of 280 M^{-1} for chloride and 260 M^{-1} for bromide. When larger spacers were used as in **1.14**, the receptors formed 2:1 complexes with the halides. This result was taken as evidence that careful consideration must be given to receptor design in regards to size exclusion. It was also used to highlight the important role conformational ridigity of the receptor plays in maintaining high binding affinities.

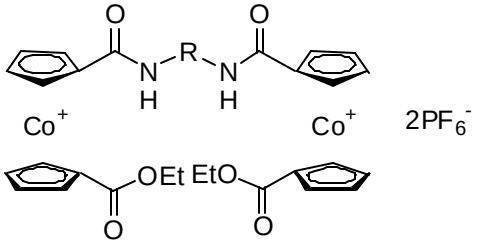

1.11 R = $-(CH_2)_2-$
1.12 R = $-(CH_2)_3-$
1.13 R = $-(CH_2)_4-$

1.14 R = 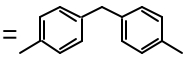

The majority of cobaltocenium electrochemical anion sensors display selectivity for dihydrogen phosphate anion in preference to chloride anion. In an

attempt to create unique topologies at the anion binding site that might deviate from this inherent selectivity, a series of three cobaltocenium-substituted calixarenes were prepared, **1.15**-**1.17**.[34,35] By altering the lower rim functionalities it proved possible to switch the selectivity difference between $H_2PO_4^-$ and Cl^-. For instance, receptor **1.15**, bearing lower-rim methoxy substituents on 1,3 alternate phenyl groups adjacent to the phenyl groups on which the cobaltocenium subunits are appended, displayed higher affinity for Cl^- than for $H_2PO_4^-$ (5,035 M^{-1} vs. 2,800 M^{-1} in $(CD_3)_2SO$). By changing these lower rim substituents from methoxy groups to tosyl functionalities, as in **1.16**, it proved possible to reverse the selectivity. For instance, this latter system displayed association constants of 400 M^{-1} and 2500 M^{-1} for Cl^- and $H_2PO_4^-$, respectively. This reversal in selectivity is rationalized in terms of the bulky tosyl substituents forcing the cobaltoceniums together, favoring $H_2PO_4^-$ binding. The smaller methoxy substituents of **1.15**, on the other hand, allow the cobaltocenium groups to move further apart, favoring the larger anion, Cl^-.

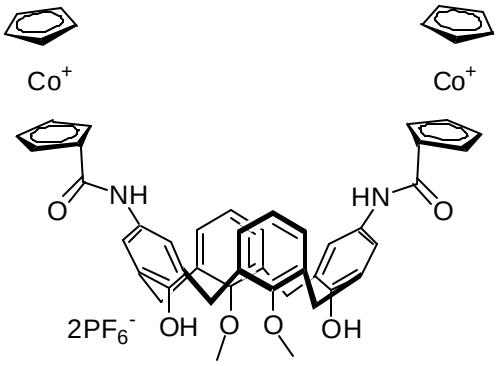

1.15

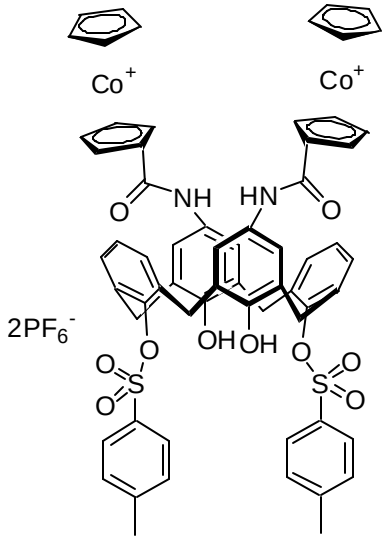

1.16

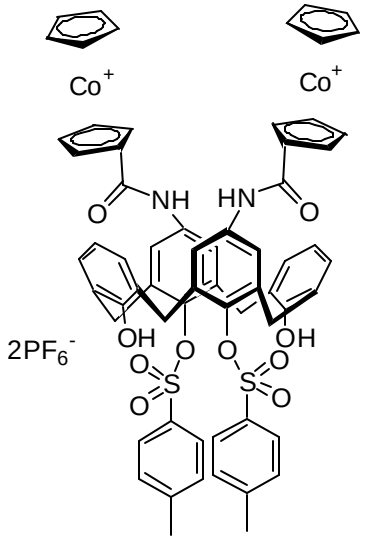

1.17

An even more dramatic example of selectivity switching was attained when the lower rim tosyl substituents were placed on the same phenyl groups as the cobaltocenium units, as in receptor **1.17**. This modification caused the selectivity difference between $H_2PO_4^-$ and Cl^- to become more enhanced, with the association constant for Cl^- now dropping to only 10 M^{-1} compared to 3,100 M^{-1}

for $H_2PO_4^-$. These systems demonstrate that remarkable versatility and sensitivity can be achieved through the careful design of electrochemical anion sensors.

In addition to topology, the importance of ridigity was illustrated through a comparison of systems **1.18** and **1.19**. The acyclic cobaltocenium receptor **1.18** displays a binding constant of 20 M^{-1} for Cl^- in $(CD_3)_2SO$, while the cyclic analog **1.19** binds the same anion with an affinity of 250 M^{-1}. This "macrocyclic effect" is presumably due to the greater preorganization induced by the cyclic system, an effect that is manifest in a lowered entropy cost for anion binding.

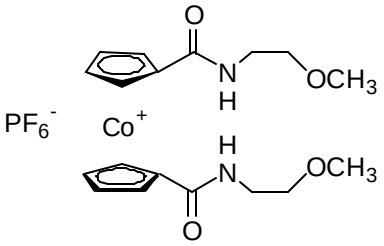

1.18

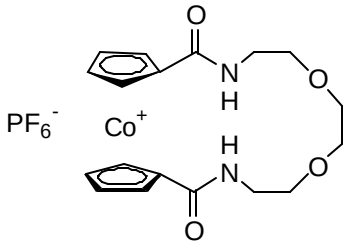

1.19

During the course of the development of these systems, cobaltocenium centers were also successfully tethered to porphyrins[36] and calixarenes.[33,34,37] Numerous other ruthenium-bipyridyl systems were also investigated for their anion binding properties.[12] These examples provide the solid foundation upon which the utility and versatility of redox anion binding systems was initially set and is currently sustained.[12]

1.1.2 Ferrocene Based Electrochemical Anion Sensors

Shortly after the development of cobaltocenium anion sensors, attention turned to analogous ferrocene based systems.[12,28,38,39] In contrast to cobaltocenium systems, in the case of these newer, neutral receptors, anion

binding is thought to occur as the result of hydrogen bonding interactions only. Although this results in a lower intrinsic binding affinity compared to systems wherein coulombic attractions are inherent, these ferrocene based systems are attractive because their electrostatic interaction with the anion can be switched on by oxidation of the Fe(II) ferrocene to the corresponding Fe(III) ferrocenium form; consequently, these kinds of molecular receptors exhibit considerable potential for use as amperometric sensors.

The first indication that ferrocene-based systems could be used to sense anions electrochemically came from studying the electrochemical properties of the multimetallocene receptor **1.20**.[40] Proton NMR spectroscopic titrations with $H_2PO_4^-$, HSO_4^-, and Cl^- in acetonitrile provided evidence for the formation of 1:1 complexes. Electrochemical studies in the presence of $H_2PO_4^-$ showed a cathodic perturbation not only of the cobaltocenium center (230 mV), but also of the ferrocene centers (90 mV). Inspired by the results of these studies, the first solely ferrocene-containing amide derivatives were prepared, examples of which include **1.21**-**1.23**.[40,41] Each of these latter receptor systems exhibited downfield shifts of the amide protons, as well as cathodic shifts in the ferrocene/ferrocenium couple in the presence of $H_2PO_4^-$, HSO_4^-, and Cl^-. Taken

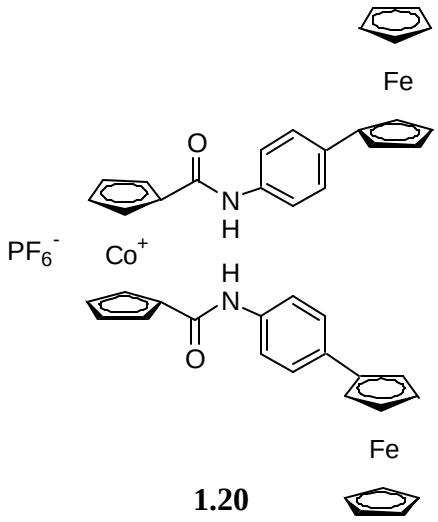

1.20

together, these findings support the initial assertion that these systems can function as redox-active electrochemical indicators for anions.

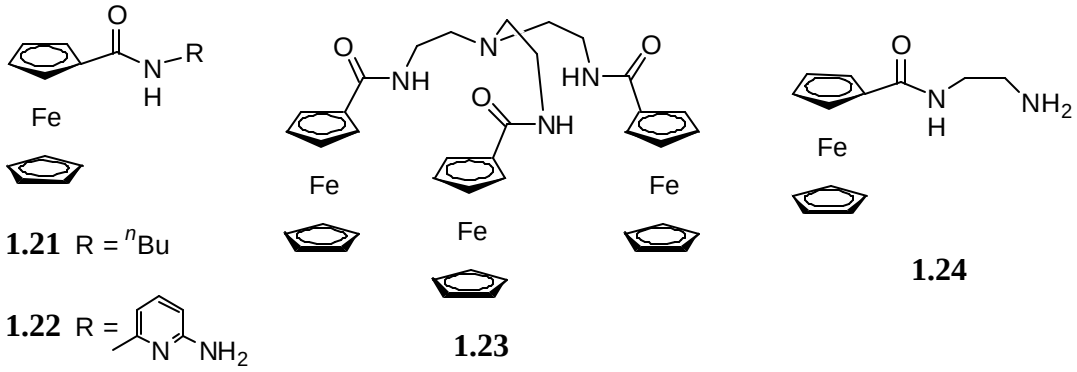

Interestingly, the tetrahedral cavity present in **1.23** resulted in the largest cathodic shift for $H_2PO_4^-$, a result that was initially rationalized in terms of anion-cavity shape complementarity. However, the other receptors in the series of **1.21-1.24** were also studied and found to be selective for $H_2PO_4^-$ in the presence of ten molar equivalents of HSO_4^- and Cl^- in a CD_3CN-$(CD_3)_2SO$ mixture (for **1.21-1.23**) and in CD_3CN (for **1.24**). Receptor **1.24** exhibited unique selectivity, binding HSO_4^- in preference to $H_2PO_4^-$ in acetonitrile, exactly the opposite selectivity seen in **1.21**. This novel selectivity is rationalized in terms of the terminal primary amine that becomes protonated in the presence of the relatively acidic HSO_4^- molecular anion. To the extent this protonation process occurs, it would add an electrostatic attraction to the anion recognition process. Consistent with this proposal, the binding constant for **1.24** is >10,000 M^{-1} in $CDCl_3$ compared to only 120 M^{-1} for the less acidic species $H_2PO_4^-$. As above, this set of

findings provided support for the notion that it is important to incorporate functionalities in the receptor that are complementary to the target anion.

As in the case of the cobaltocenium systems, receptor topology is known to play an important role in determining anion selectivity. For example, in the case of the ferrocene-amide porphyrin receptor **1.25**, different atropisomers are possible and these dictate the anion selectivity. The α,α,α,α and α,β,α,β isomers displayed selectivities in the order of $Br^- > NO_3^- > HSO_4^-$; the α,α,α,β isomer showed a preference for anions in the order $Cl^- > NO_3^- > HSO_4^-$, while the α,α,β,β isomer bound anions with relative K_a's in the order $Cl^- > Br^- > NO_3^-$.

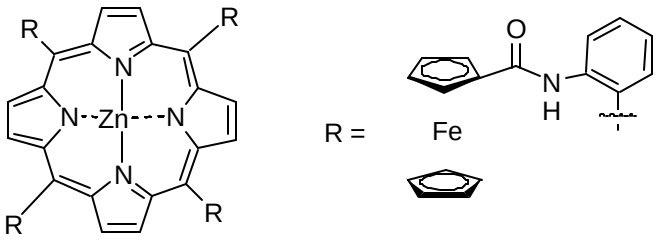

1.25

In addition to the systems already discussed, a wide variety of other ferrocene-based anion sensors have been developed. These include an extensive series of amide-substituted ferrocenes,[41-47] and ferrocene substituted porphyrins,[38,48] calixarenes,[49,50] and dendrimers.[51,52] A number of systems capable of sensing anions in aqueous solution have also been developed.[28,53-59] Ferroceneboronic acid derivatives have been found to be selective for fluoride anion, allowing this species to be recognized both electrochemically[60,61] and colorimetrically.[62] Other advances include the sensing of biologically relevant molecules, such as ferrocene-labeled nucleic acids[63] and a simple ferrocenylmethyltrimethylammonium cation[64] for the electrochemical detection of

DNA, as well as ferrocenyl derivatives immobilized on a gold electrode capable of sensing complementary DNA.[65-67]

1.1.3 Ferrocene-Substituted Calixpyrroles

In spite of this progress, there remains a need for ferrocene-based systems that display greater substrate selectivity, offer improved signal to noise ratios, and allow specific anions to be targeted more readily for binding. Obtaining systems that would be cheaper to produce on a commercial scale would also be beneficial. One way to address these challenges could come from using pyrroles to achieve anion binding.

Many systems incorporating multiple pyrrole units into their framework are known to act as anion receptors.[68-70] Depending on the design of the system, the binding can be tailored for strength or selectivity. The receptors can also be categorized on the basis of synthetic difficulty and cost. In this latter context, the so-called calixpyrroles are particularly attractive. They are very easy to make and display a high relative affinity for F^- in apolar media. Not surprisingly, therefore, initial attempts by the Sessler group at combining the anion binding affinity of pyrrole systems with the electrochemical detectability of ferrocenes relied on the use of calixpyrroles. These efforts resulted in ferrocene-calix[4]pyrrole conjugates **1.26** and **1.27** wherein the ferrocene moieties are tethered to the calix[4]pyrrole anion recognition unit through either a *meso*-like or β-pyrrolic site *via* amide linkages.[71] When performing cyclic voltammetry between 600 mV and –100 mV, a reversible ferrocene/ferrocenium wave was observed. Unfortunately,

both receptors revealed unpredictable and contradictory responses upon the addition of anions. For instance, in the case of both **1.26** and **1.27**, cathodic shifts were seen upon the addition of some anions (F^- and Cl^- for **1.26** and $H_2PO_4^-$ and F^- for **1.27**); however, anodic shifts were seen in the case of $H_2PO_4^-$ for **1.26** and Cl^- for **1.27**. While far from being understood, it is thought that these unexpected results, i.e., unanticipated shifts, are perhaps the result of fundamental differences in the conformational behavior manifest by these two ostensibly similar receptors (i.e., *meso* vs. β-pyrrole linked).

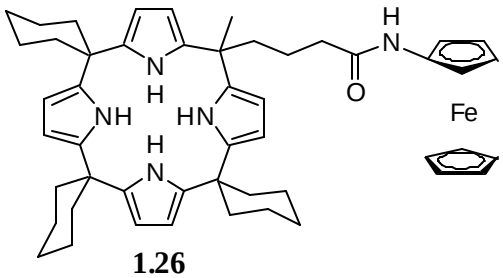

1.26

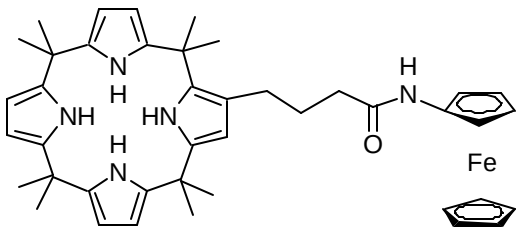

1.27

In an effort to improve on the above performance, the diferrocenyl substituted calix[4]pyrroles **1.28** and **1.29** were prepared by the author. These two products, a mixture of *cis* and *trans* isomers, were synthesized by condensing the *gem*-dimethyl substituted dipyrrolylmethane[72] with acetylferrocene. Their structures were elucidated by Dr. Vincent Lynch *via* a single crystal X-ray diffraction analysis (Figure 1.1). The *cis* isomer has the acetylferrocenes

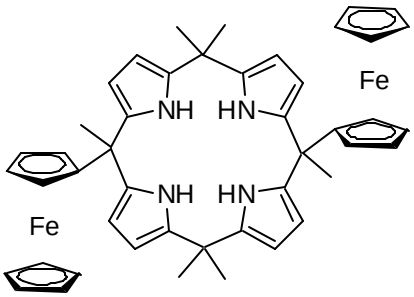

1.28 = cis
1.29 = trans

pointing outward and away from the calixpyrrole cavity (Figure 1.1a), with the pyrrole NHs hydrogen bonded to a molecule of methanol. By contrast, in the *trans* isomer, each ferrocene unit is folded over the top of the opposite face of the calixpyrrole (Figure 1.1b). This folded-over conformation is likely responsible for the unusual 1,2 orientation of the pyrrole units seen in the solid state structure of the *trans* isomer. Unfortunately, preliminary electrochemical results showed an ambivalence that was reminiscent of what was seen in the case of **1.26** and **1.27**. Currently, the reasons for this lack of useful response are unclear.

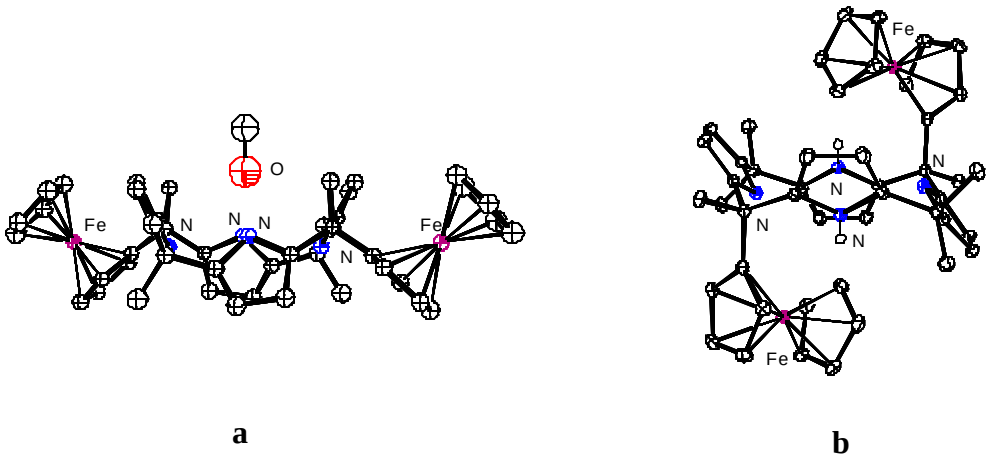

a **b**

Figure 1.1: Ortep views of the a) *cis* isomer **1.28** ; b) *trans* isomer **1.29**. Thermal ellipsoids are scaled to the 40% probability level.

Other work by Gale *et al.* showed that by linking the ferrocene to the calixpyrrole in a direct fashion through the condensation of acetylferrocene, cyclohexanone, and pyrrole to form **1.30**, the ability of the system to sense anions electrochemically dramatically improved.[73] Cathodic shifts occurred upon

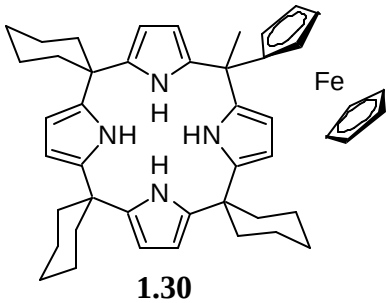

1.30

addition of halides as well as $H_2PO_4^-$ and HSO_4^-. Additionally, a C*H* ferrocene resonance was seen to shift downfield during ^{1}H NMR spectroscopic titrations with the anions, a finding that was interpreted in terms of direct coordination between the ferrocenyl C*H* atom and the anion. The results of this study indicate the importance of the orientation of the ferrocenyl group in relation to the anion binding site; in this instance, closer proximity to the anion binding site resulted in an improved electrochemical response. On the other hand, the ambivalent electrochemical results seen in the case of **1.28** and **1.29**, systems that also bear directly coordinated ferrocenyl groups, indicate that additional studies and derivatives are necessary to map out fully the rules for designing functioning redox-active calixpyrrole-based anion receptors.

1.2 *ANSA*-FERROCENE-PYRROLE CONJUGATES

In an effort to design other ferrocene-pyrrole conjugates, the *ansa*-ferrocene **1.31**, containing a ferrocene subunit covalently bound within a pyrrole-based macrocyclic framework, was synthesized by Dr. Marcus Scherer of the Sessler group. This receptor was found to display a high intrinsic affinity for Lewis basic anions while acting,

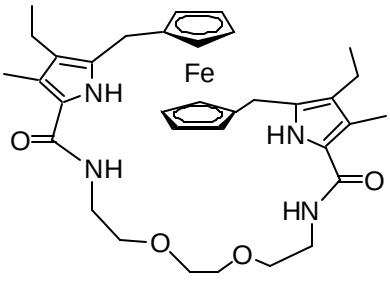

1.31

concurrently, as an effective electrochemical sensor for F^- and $H_2PO_4^-$.[74] In the initial *ansa*-ferrocene system **1.31** a single crystal X-ray diffraction study revealed the presence of a water molecule inside the cavity, as well as a second water molecule not constrained in the cavity but hydrogen bonded to the encapsulated water molecule (Figure 1.2). The water molecule bound in the cavity was stabilized by NH---O hydrogen bonds from an amide NH and a pyrrole NH, acting as hydrogen bond donors. It was linked as well *via* an OH---O hydrogen bond involving one of the bound ether oxygen atoms of the linker.

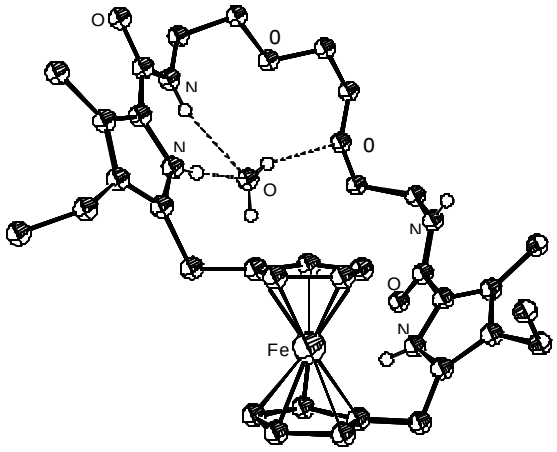

Figure 1.2: Solid state structure of **1.31**·$2H_2O$ (the second water molecule, not contained in the cavity, has been omitted for clarity). Dashed lines show a water molecule hydrogen bonded to an amide NH, a pyrrole NH, and an ether-type oxygen. Thermal ellipsoids are scaled to the 40% probability level.

It was the presence of this latter linker-derived hydrogen bonding interaction, along with evidence of strong dihydrogen phosphate binding in solution, that inspired the present study. Dihydrogen phosphate has two OH

hydrogen bond donor sites that could interact with an ether oxygen atom, acting as a hydrogen bond acceptor. To the extent dihydrogen phosphate is indeed binding to **1.31** through these kinds of interactions, a simple test of binding affinity versus number of oxygen atoms present in the linker (0, 1 or 2) should reveal differences. On this basis we decided to prepare receptors **1.51**, **1.52**, and **1.53** (the latter being analogous to **1.31**). Here, the goal was to investigate the effects of structural variations on the anion binding selectivity of *ansa*-ferrocene receptors for $H_2PO_4^-$, by varying the length and nature of the bridging arm. Both factors were expected to play a role in regulating the dihydrogen phosphate anion affinities as well as modulating the nature of the ferrocene/ferrocenium-based electrochemical response.

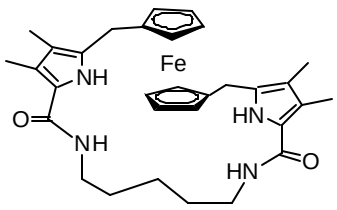

1.51

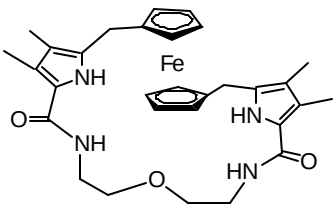

1.52

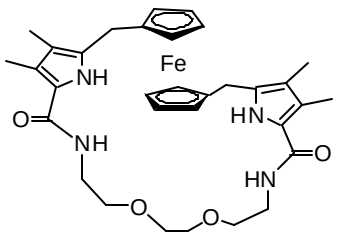

1.53

1.2.1 Synthesis of *ansa*-Ferrocenes 1.51-1.53

The synthesis of receptor **1.52** was initially attempted *via* the same multistep procedure that was used to make **1.31**.[74] Beginning with the pyrrole-cyclopentadiene conjugate, the ferrocene is formed, followed by an amide coupling of the linker. Specifically, the Knorr pyrrole synthesis proceeds by

starting with commercially available ethyl acetoacetate **1.32** (Scheme 1.1) and reacting it with sodium nitrite in acetic acid to form oxime **1.33**. This is condensed with 2,4-pentanedione under reductive conditions with zinc and sodium acetate to form pyrrole **1.34** in 70% yield. This ketone is then reduced using sodium borohydride in the presence of boron trifluoride to give **1.35** in 85% yield. The ethyl ester is then transesterified to give the easier-to-manipulate benzyl ester derivative **1.35** in 60% yield. This was done by heating in benzyl alcohol in the presence of sodium metal as a catalyst.

Scheme 1.1 Synthesis of pyrrolic precursor **1.36**

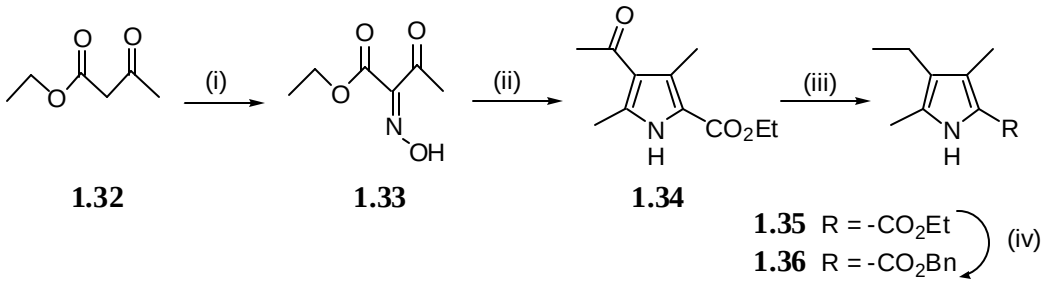

1.32 **1.33** **1.34** **1.35** **1.36**

Reagents: (i) $NaNO_2$, HOAc, 100%; (ii) Zn, NaOAc, 2,4-pentanedione, 70%; (iii) $BF_3 \cdot Et_2O$, $NaBH_4$, THF, 85%; (iv) BnOH, Na^o_{cat}, 60%.

Once in hand, pyrrole **1.36** is subject to oxidation using lead tetraacetate (Scheme 1.2). This gives the 5-acetoxy-substituted benzyl ester pyrrole **1.37** in 80% yield. Coupling to sodium cyclopentadienylide then gives the cyclopentadiene-pyrrole conjugate **1.38** in 20% yield. Thalium ethoxide is used

to effect deprotonation and stabilization of the cyclopentadienylide anion, which is reacted with iron(II) chloride to form ferrocene **1.39** in 50% yield. Unfortunately, hydrogenation of the benzyl esters with hydrogen and palladium on carbon followed by an amide coupling with 2,2'-oxybis(ethylamine) using benzotriazol-1-yloxy-tris(dimethylamino)phosphonium hexafluorophosphate (BOP) did not result in the desired macrocycle **1.40**. Initial attempts to effect this critical conversion by using various solvents and amide coupling reagents did not prove any more successful. As such, alternative synthetic routes were explored.

Scheme 1.2 Attempted synthesis of pyrrolic precursor **1.40**

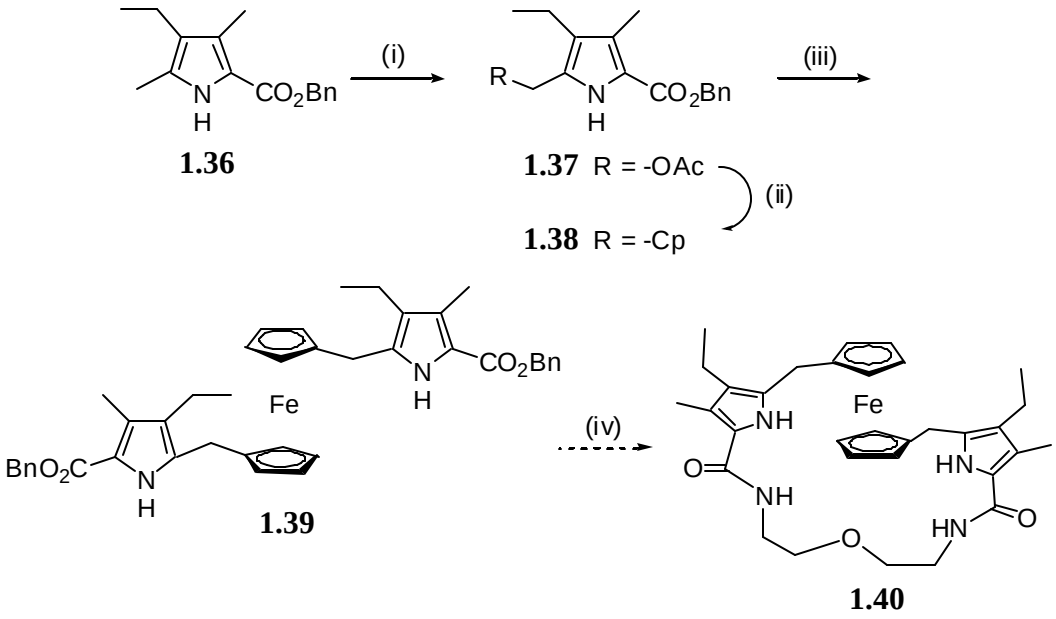

1.36 **1.37** R = -OAc **1.38** R = -Cp **1.39** **1.40**

Reagents: (i) $Pb(OAc)_4$, HOAc, 80%; (ii) NaCp, 20%; (iii) a)TlOEt, THF; b) $FeCl_2$, THF, 50%; (iv) a) H_2/Pd/C, Et_3N, THF; b) BOP, Et_3N, 2,2'-(ethylenedioxy)bis(ethylamine), DMF, 10%

The first alternative approach started with commercially available 1,1'-ferrocenedicarboxylic acid **1.41**. From it, 1,1'-ferrocenediacid chloride **1.42** was formed using oxalyl chloride in 95% yield (Scheme 1.3). This was coupled to α-benzyl ester pyrrole **1.43** using tin(IV) chloride to form **1.44** in 42% yield, a species whose synthesis had been previously reported in the literature.[75] A number of attempts were made to reduce **1.44** using a variety of reducing agents, including $LiAlH_4$ in the presence of catalysts such as P_2I_4, and $AlCl_3$. Ultimately, *tert*-butylamineborane and aluminum chloride was used to effect the reduction to **1.45** in 35% yield.[76]

Scheme 1.3 Alternative synthesis of ferrocenyl precursor **1.45**

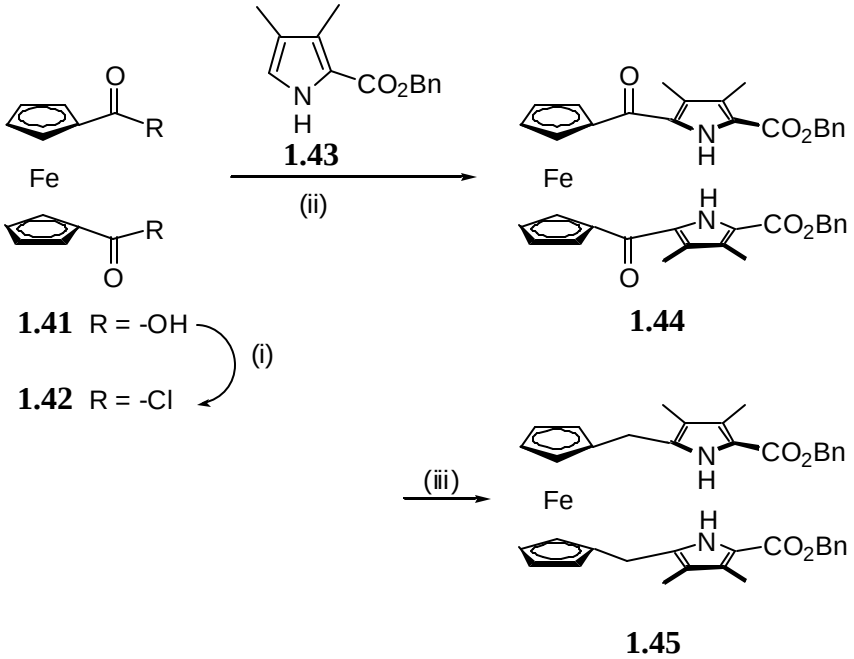

Reagents: (i) $COCl_2$, DCM, 95%; (ii) $SnCl_4$, DCM, 42%; (iii) $(CH_3)_3CNH_2 \cdot BH_3$, $AlCl_3$, DCM, 35%

This higher overall yield of **1.45** as compared to **1.40** allowed for additional coupling attempts with 2,2'-oxybis(ethylamine) dihydrochloride in the presence of amide coupling reagents such as BOP and 1,3-dicyclohexylcarbodiimide (DCC). However, unlike the original *ansa*-ferrocene **1.31**, these conditions resulted only in the recovery of starting material. At this point, it was hoped that a simple change in the order of reactivity would allow access to targets **1.51**-**1.53**. By placing the key amide coupling step earlier on in the synthetic sequence, we hoped to circumvent the relatively low yields seen in the case of the original synthesis as well as to elucidate the reasons for the difficulties encountered when trying to use 2,2'-oxybis(ethylamine) dihydrochloride to effect the amide couplings. In particular, it was hoped that by carrying out the coupling at an earlier stage with less hindered precursors, a presumed transition state would be involved that was less subject to steric strain, thereby allowing the reaction to proceed in decent yield.

In conjunction with Dr. Gregory Kirkovits, deesterification of α-benzyl ester pyrrole **1.43** under reductive conditions gave the corresponding acid **1.46**, which, when treated with the appropriate diamine under standard amide-forming conditions, gave the key precursors, **1.47**-**1.49** (Scheme 1.4). The macrocyclic receptors were subsequently prepared under pseudo high dilution conditions. 1,1'-Ferrocenedimethanol and the appropriate bispyrrole, each dissolved in an equal volume of CH_2Cl_2, were added simultaneously to a vigorously stirred solution of TFA in CH_2Cl_2 to generate the corresponding target molecules **1.51**-**1.53**.

Compounds **1.47** and **1.49** were obtained in 63% and 70% yield, respectively, by coupling pyrrole carboxylic acid **1.46** with the corresponding diamines, 1,5-diaminopentane and 2,2'-(ethylenedioxy)bis(ethylamine) using DCC with HOBT in DMF (Scheme 1.4). Compound **1.36** could not be obtained in this manner, however.

Scheme 1.4 Synthesis of dipyrrolic precursors **1.47**-**1.49**

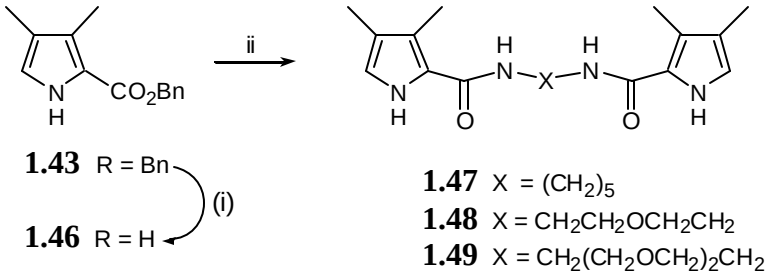

Reagents: (i) Pd/C-H_2, Et_3N, THF, 100%; (ii) $NH_2(CH_2)_5NH_2$, or $NH_2CH_2(CH_2OCH_2)_2CH_2NH_2$, DCC, HOBT, DMF for **1.51**, 63% and **1.53**, 70% or $NH_2CH_2CH_2OCH_2CH_2NH_2 \cdot 2HCl$, Et_3N, DCC, DCM for **1.52**, 18%.

The diamine precursor to **1.36**, 2,2'-oxybis(ethylamine), is commercially available only in the form of its dihydrochloride salt. Initial amide couplings in DMF, carried out in the presence of an excess of various bases such as triethylamine, TMEDA, and DBU, proved unsuccessful. The dihydrochloride salt was then subject to liquid-liquid extraction between a saturated potassium hydroxide solution and ether to obtain the neutral diamine.[77] The resulting free-base was then subjected to the same coupling conditions, but to no avail. Due to solubility problems this route was abandoned and efforts were again made to use

the dihydrochloride salt. Coupling this salt with **1.46** in dichloromethane with DCC in the presence of excess triethylamine was then found to afford **1.48** in 18% yield. With these precursors in hand, compounds **1.51**-**1.53** were obtained in 33%, 20% and 35% yields, respectively, by reacting **1.47**-**1.49** with 1,1'-ferrocenedimethanol in the presence of TFA in dichloromethane (Scheme 1.5).

Scheme 1.5 Synthesis of *ansa* ferrocenes **1.51**-**1.53**

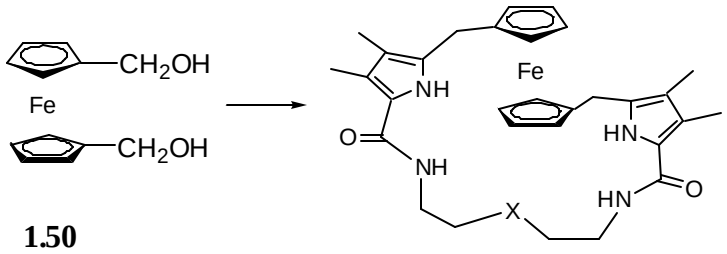

1.50

1.51 X = -CH_2-
1.52 X = O
1.53 X = -(OCH_2CH_2O)-

Reagents: **1.47**, **1.48** or **1.49** with TFA, DCM, 33% for **1.51**, 20% for **1.52**, 35% for **1.53**

1.2.2 Proton NMR Studies of *ansa*-Ferrocenes 1.51-1.53

The original *ansa*-ferrocene **1.31** was shown to have a binding affinity for dihydrogen phosphate anion (as its tetrabutylammonium salt) of 11,300 M^{-1} in CD_3CN. Unfortunately, solubility problems precluded similar studies of **1.51** and **1.52** in this solvent. Thus, dichloromethane-d_2 containing 2% dimethylsulfoxide-d_6 was used for all of the ^{1}H NMR titration studies, involving systems **1.51** and **1.52**. This specific solvent ratio was chosen so as to balance the need for

solubility (helped by DMSO) against the need to keep the affinity constant high enough to allow accurate detection (improved by the use of dichloromethane). The results of these studies are illustrated in Figures 1.3-1.6.

Receptor **1.51** showed a significant downfield shift in the amide N*H* proton from 6.9 ppm to 8.4 ppm. In this instance, the $H_2PO_4^-$ concentration was varied from 0-12 mM, and subsequent curve fitting[78] revealed a binding affinity, K_a, of 4,050 ± 300 M^{-1}. Unfortunately, a mole ratio plot[79] provided inconclusive evidence concerning the binding stoichiometry.

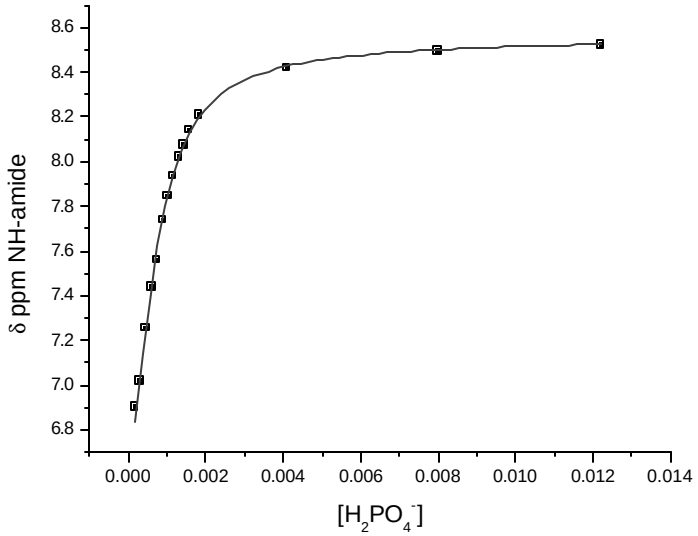

Figure 1.3: Proton NMR binding profile of **1.51** recorded in dichloromethane-d_2 containing 2% dimethylsulfoxide-d_6 at 1.12 x 10^{-4} M. Changes in the amide-N*H* chemical shift were recorded as the concentration of $Bu_4NH_2PO_4$ was varied between 0 – 12 mM. Nonlinear least squares analysis revealed an association constant, K_a = 4,050 ± 300 M^{-1}.

Receptor **1.52** was titrated with $H_2PO_4^-$, with the concentration varying from 0-73 mM, resulting in a downfield shift in the amide NH proton from 7.1 ppm to 8.6 ppm. Standard curve fitting then gave an association constant of 13,200 ± 1,500 (Figure 1.4). A mole ratio plot indicated a 1:1 binding stoichiometry of the receptor with $H_2PO_4^-$ (Figure 1.5).

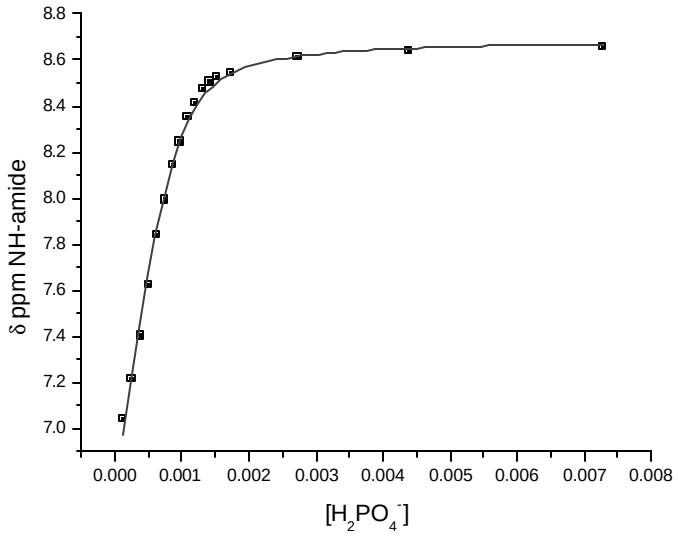

Figure 1.4: Proton NMR binding profile of **1.52** recorded in dichloromethane-d_2 containing 2% dimethylsulfoxide-d_6 at 8.99 x 10^{-4} M. Changes in the amide-N*H* chemical shift were recorded as the concentration of $Bu_4NH_2PO_4$ was varied between 0 – 73 mM. Nonlinear least squares analysis revealed an association constant, K_a = 13,200 ± 1,500 M^{-1}.

A titration with receptor **1.53** in the presence of concentrations of $H_2PO_4^-$ varying from 0-6 mM resulted in an association constant of 81,400 ± 9,700 M^{-1} (Figure 1.6a). Downfield shifts in the amide N*H* peaks occurred from 7.2 ppm to 8.9 ppm. A mole ratio plot confirmed the expected 1:1 binding stoichiometry (Figure 1.6b).

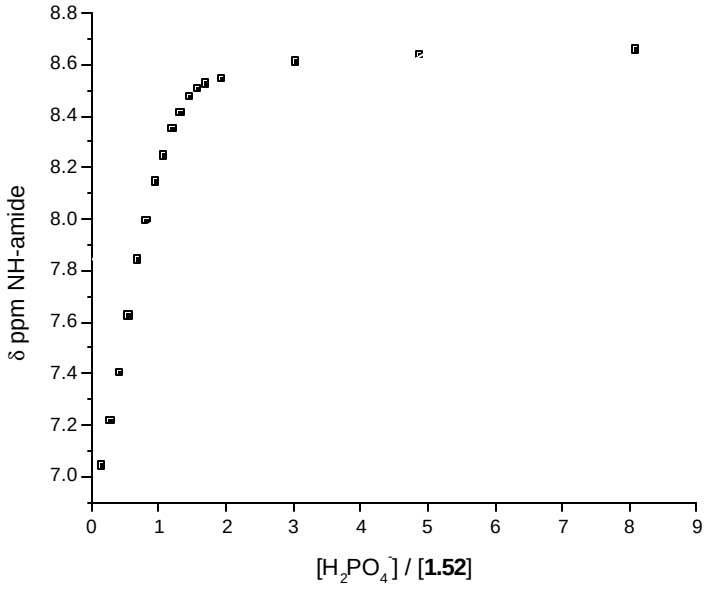

Figure 1.5: Mole ratio plot of a 8.99 x 10^{-4} M solution of **1.52** measured by ^1H NMR in dichloromethane-d_2 containing 2% dimethylsulfoxide-d_6 showing a 1:1 mole ratio of $[H_2PO_4^-]$/**1.52**.

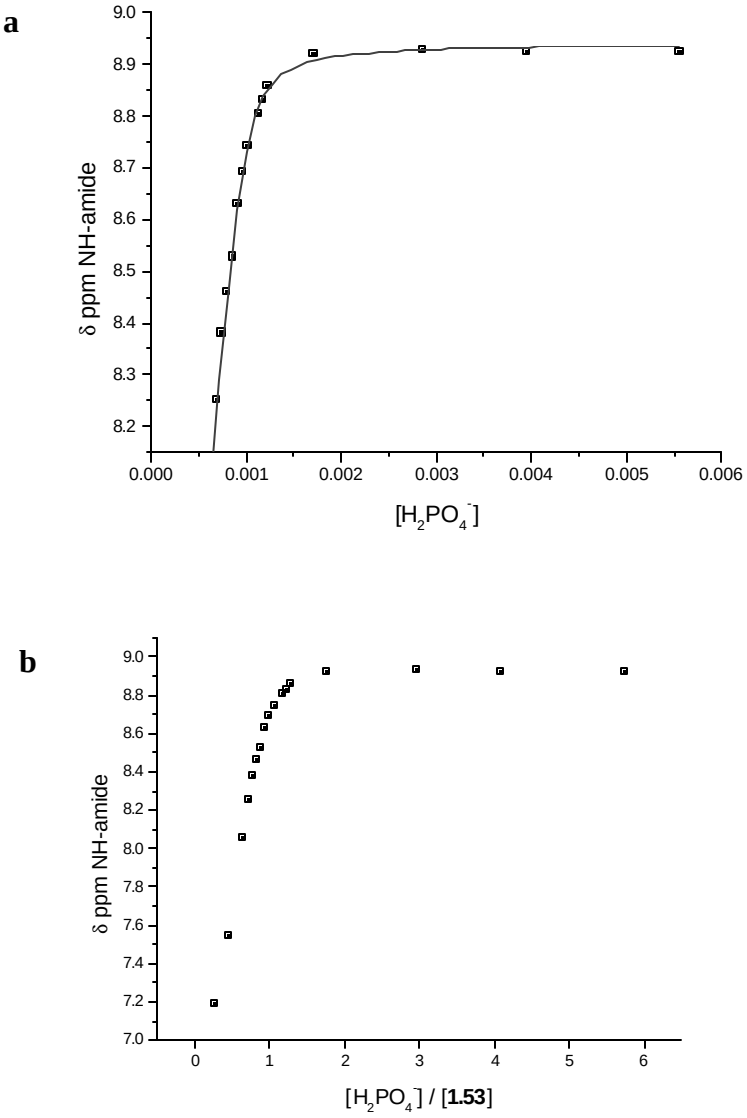

Figure 1.6 (a) Proton NMR binding profile of **1.53** at 9.66 x 10^{-4} M taken in dichloromethane-d_2 containing 2% dimethylsulfoxide-d_6 in the presence of an increasing concentration of $H_2PO_4^-$ from 0-6 mM. This resulted in a binding association of 81,400 ± 9,700 M^{-1}; (b) Mole ratio plot of this data indicating 1:1 binding stoichiometry of **1.53** with $H_2PO_4^-$.

1.2.3 Electrochemical Studies of *ansa*-Ferrocenes 1.51-1.53

The next set of experiments involved electrochemical studies of *ansa* ferrocenes **1.51**-**1.53**. These were carried out in spectroscopic grade dichloromethane, at approximately 1 mM. Tetrabutylammonium hexafluorophosphate, at a concentration of 100 mM, was used as the supporting electrolyte with Ag/AgCl as the reference electrode. Cyclic voltammograms were taken to test for reversibility of the ferrocene/ferrocenium redox couple. Unfortunately, reversibility was not maintained upon addition of the dihydrogen phosphate anion, although there was clearly a redox response. Square wave voltammetry was then performed on the free ligands and in the presence of 5 molar equivalents of $H_2PO_4^-$ to test for an anion-induced redox response.

Ansa-ferrocene **1.51** maintained reversibility in the cyclic voltammogram at all scan speeds recorded (Figure 1.7a), with $E_{1/2}$ = 432 ± 5 mV. The square wave voltammogram shows a cathodic shift of 128 mV upon the addition of 5 molar equivalents of $H_2PO_4^-$ (Figure 1.7b), which is consistent from 15 Hz to 100 Hz.

Likewise, receptor **1.52** exhibited reversibility of the ferrocene/ferrocenium redox couple, with $E_{1/2}$ = 428 ± 4 mV over a range of scan speeds from 40 mV/s – 1000 mV/s (Figure 1.8a). The square wave voltammogram showed a cathodic shift of 140 mV at 15, 50, and 100 Hz upon the addition of 5 molar equivalents of $H_2PO_4^-$ (Figure 1.8b).

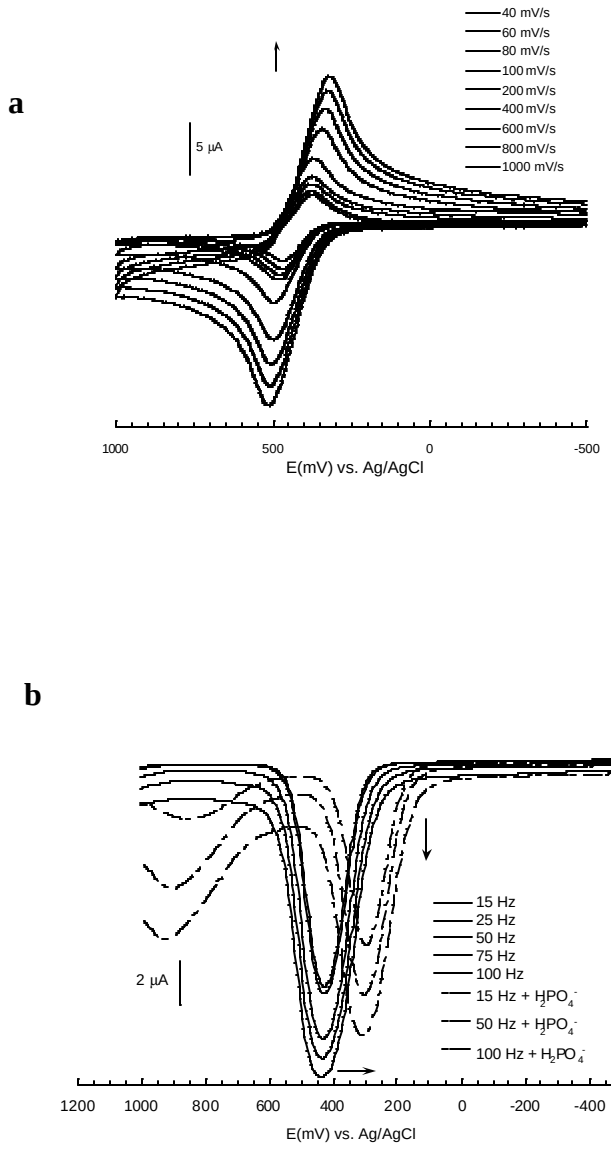

Figure 1.7 Results of electrochemical analyses carried out in dichloromethane at a 1 mM concentration using Bu_4NPF_6 as the supporting electrolyte and Ag/AgCl as the reference electrode (a) Cyclic voltammogram of **1.51** across scan speeds from 40 mV/s to 1000 mV/s; (b) Square wave voltammogram of **1.51** recorded in the absence and presence of 5 eqv. of $H_2PO_4^-$.

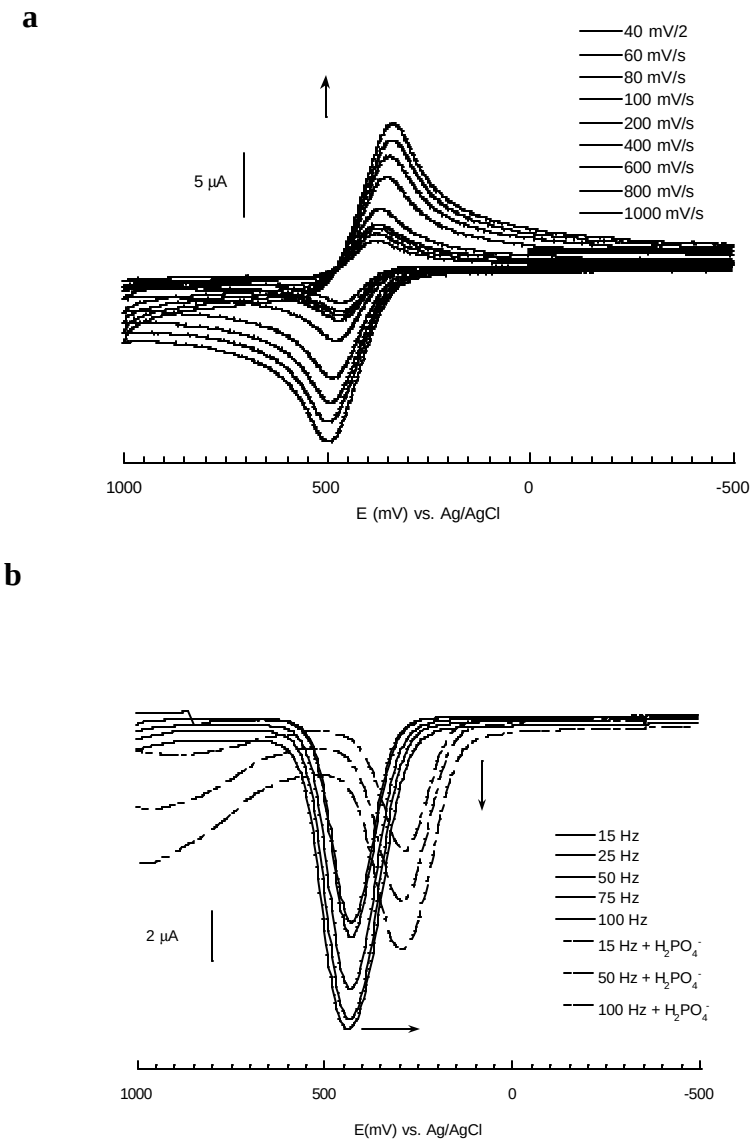

Figure 1.8 Results of electrochemical analyses in dichloromethane at a 1 mM concentration using Bu_4NPF_6 as the supporting electrolyte and Ag/AgCl as the reference electrode (a) Cyclic voltammogram of **1.52** recorded at speeds from 40 mV/s – 1000 mV/s; (b) Square wave voltammogram of **1.52** recorded in the absence and presence of 5 eqv. of $H_2PO_4^-$.

The reversibility of the ferrocene/ferrocenium redox couple present in receptor **1.53** remained intact across scan speeds from 20 mV/s – 1000 mV/s in the cyclic voltammogram (Figure 1.9a), with $E_{1/2}$ = 432 ± 4 mV. Additionally, square wave voltammtery showed a cathodic shift of 140 mV in the presence of 5 molar equivalents of $H_2PO_4^-$ (Figure 1.9b).

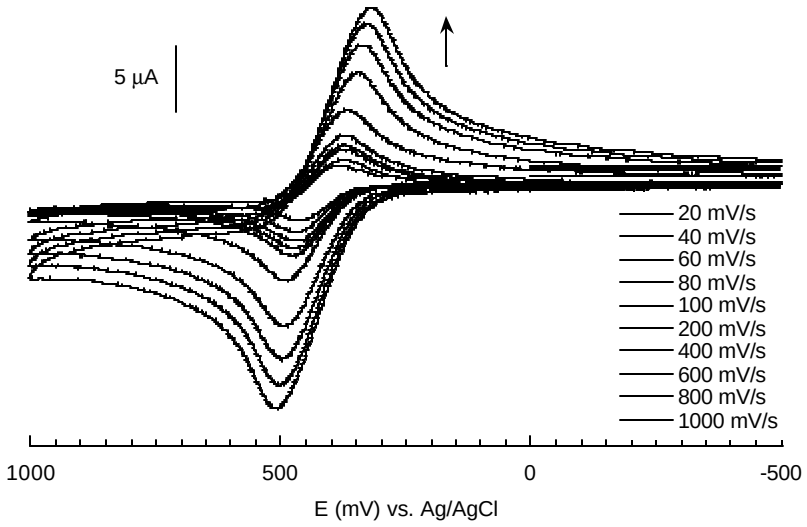

Figure 1.9 (a) Cyclic voltammogram recorded in dichloromethane at a 1 mM concentration of **1.53** using Bu_4NPF_6 as the supporting electrolyte and Ag/AgCl as the reference electrode showing reversibility across scan speeds from 20 mV/s – 1000 mV/s.

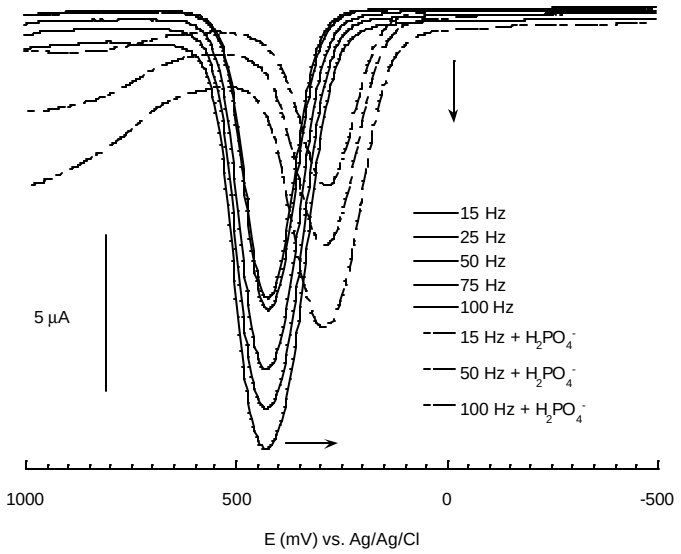

Figure 1.9 (b) Square wave voltammogram recorded in dichloromethane at a 1 mM concentration of **1.53** using Bu_4NPF_6 as the supporting electrolyte and Ag/AgCl as the reference electrode in the absence and presence of 5 equivalents of $H_2PO_4^-$.

The ^{1}H NMR and electrochemical results are summarized in Table 1.1. Unfortunately, reaction coupling efficiencies[39] could not be determined from the electrochemical data because it proved necessary to use different solvents for the ^{1}H NMR and electrochemical studies. In particular, unreliable electochemical results were seen when measurements were made in the 2% DMSO/dichloromethane mixture that was used for the ^{1}H NMR studies. This led us to use pure dichloromethane for the electochemical analyses. In spite of the fact that the electrochemical results could not accordingly be compared to those from the ^{1}H NMR studies, both the ^{1}H NMR and electrochemical results served to show that the affinity of the receptor for dihydrogen phosphate increases along the

series of **1.51** through **1.53**, a result that is interpreted in terms of the oxygen atoms in the linkers participating in the binding event. For instance, the stability constants were seen to increase incrementally from 4,050, to 13,200 to 81,400 M^{-1} as the number of oxygen atoms in the linkers increased from 0 to 1 to 2. The change in the cathodic shift of the electrochemical data increased from 128 mV for 0 oxygen atoms in the linker to 140 mV for both 1 and 2 oxygen atoms in the linker. Both of these trends indicate an increased affinity of the receptor for dihydrogen phosphate when there is at least one oxygen in the linker.

Table 1.1: Relevant stability constants and electrochemical data for $H_2PO_4^-$ complexes formed with receptors **1.51**-**1.53**

Receptor	Oxygens in linker	K_a / M^{-1}	$E_{1/2}$ / mV	ΔE_c / mV
1.51	0	4,050 ± 300	432 ± 5	128
1.52	1	13,200 ± 1,500	428 ± 4	140
1.53	2	81,400 ± 9,700	432 ± 4	140

E_c is the cathodically induced shift.

1.2.4 Conclusions

Based on the above observations, we conclude that the presence of oxygen atoms in the linker increases the electrochemical response of an *ansa*-ferrocene observed upon the addition of dihydrogen phosphate. The fact that we do not see

an increased response upon going from one to two oxygen atoms in the linker (i.e., upon going from **1.52** to **1.53**) means that the added electrostatic stabilization for the ferric state is equal in both molecules. This leads us to propose that the proximity of the bound dihydrogen phosphate anion to the ferrocene-bound iron center is similar in the case of both **1.52** and **1.53**. To the extent this is true, it would lead to identical through space interactions and similar electrochemical responses, as indeed is seen by experiment. The fact that the presumed electrostatic interaction relative to the iron center is identical in the case of both **1.52** and **1.53** highlights the fact that at least as far as an electrochemical "read-out" response is concerned, the nature of the linker (ether vs. all-alkyl) is more important than cavity size.

Compound **1.53** has a larger cavity than either **1.51** and **1.52**; if size were the dominating factor in terms of electrochemical response, a large anion-induced voltage change would be seen upon going from **1.52** and **1.53**, something that is not observed. Additionally, if size alone were the major determinant influencing the extent of the anion-induced cathodic shift, the same electrochemical response would be seen for both **1.51** and **1.52**, again something that is not observed. Still, it is important to appreciate that the factors regulating anion binding *per se* (i.e., as opposed to an electrochemical response) may be slightly different. In this case, the number of possible OH---O hydrogen bonding interactions appears important, as evidenced by the fact that in its neutral ferrocene form receptor **1.52** binds dihydrogen phosphate significantly less well than does receptor **1.53**, also in its neutral form.

Another, chemically similar explanation is that the association constants, measured in the Fe^{2+} state without the benefit of electrostatic interactions, show a steady increase correlated with the number of oxygens in the linker because the hydrogen bonding effects are dominant. Under the conditions of the electrochemical experiments, however, the importance of the electrostatic interaction of the anion with the Fe^{3+} center tends to outweigh the effects of hydrogen bonding. In other words, the effect of the presence of the second hydrogen bond acceptor site in the linker is overshadowed by inherent cation-anion ion pairing interactions. To the extent this hypothesis is correct, it would explain the similar electrochemical response behavior of **1.52** and **1.53**.

The above hypothesis could be tested by synthesizing the cobaltocenium analogs of **1.51**-**1.53**. In such a case, the initial "ground state" association constants would be measured with the cobalt center in a +3 oxidation state. Thus, if it is true that the electrostatics of a charged *ansa* metallocene system dominate over hydrogen bonding interactions, then it is likely that the difference in the association constants seen between the cobalt-containing versions of **1.52** and **1.53** would not be as large as that of the ferrocene analogs. Likewise, since electrochemical perturbations of the cobaltocenium analogs will result in the production of a Co^{2+} state, it is speculated that hydrogen bonding interactions will dominate. If this is the case, then it is likely that a difference will be seen in the magnitude of the cathodic shift for each analog.

These results highlight the importance of specific design in generating new pyrrole-based receptors while underscoring, in particular, the importance of

hydrogen bond acceptor sites in regulating both affinities and electrochemical response. As such, they offer a reference for the development of improved anion recognition and sensing systems.

1.3 TOWARD THE DEVELOPMENT OF A SCHIFF-BASE *ANSA*-FERROCENE

In an effort to continue to develop *ansa*-ferrocenes as electrochemical anion sensors, a Schiff base functionalized ferrocene receptor was conceived. Metal free Schiff base substituted polypyrrolic receptors have been successfully synthesized by the Sessler group in the past.[80-82] The relative ease of synthesis and versatility of the imine group make it an attractive linking functionality between an anion binding pocket and a redox active center. It was thought that incorporating this functionality into an *ansa*-ferrocenyl system would help to generalize this approach to anion sensor development while providing further insights into just what effects lead to redox reversibility in these kinds of systems.

1.3.1 Synthesis of the Schiff base *Ansa*-ferrocene

It was thought that a quick entry into the area of Schiff base *ansa*-ferrocene systems could be achieved by using a precursor, (2-pyrrolylmethene)-(2-pyrrolylmethyl)amine **1.57**, [83] that was available as the result of ongoing work on a different project being carried out by Dr. Bruno Andrioletti. Here, the starting material was commercially available pyrrole-2-carboxaldehyde **1.54**. This aldehyde was treated with hydroxylamine-*O*-sulfonic acid to give 2-cyanopyrrole **1.55** in 82% yield. After reducing **1.55** with lithium aluminum

hydride followed by quenching with Glauber's salt ($Na_2SO_4 \cdot 10H_2O$), self-condensation provided a mixture of (2-pyrrolylmethene)-(2-pyrrolylmethyl)imine **1.56** and (2-pyrrolylmethene)-(2-pyrrolylmethyl)amine **1.57**. Resubjecting the reaction mixture to lithium aluminum hydride reduction then effected complete conversion to **1.57** in 34% yield.

Scheme 1.6 Synthesis of dipyrrolyl precursor **1.57**.

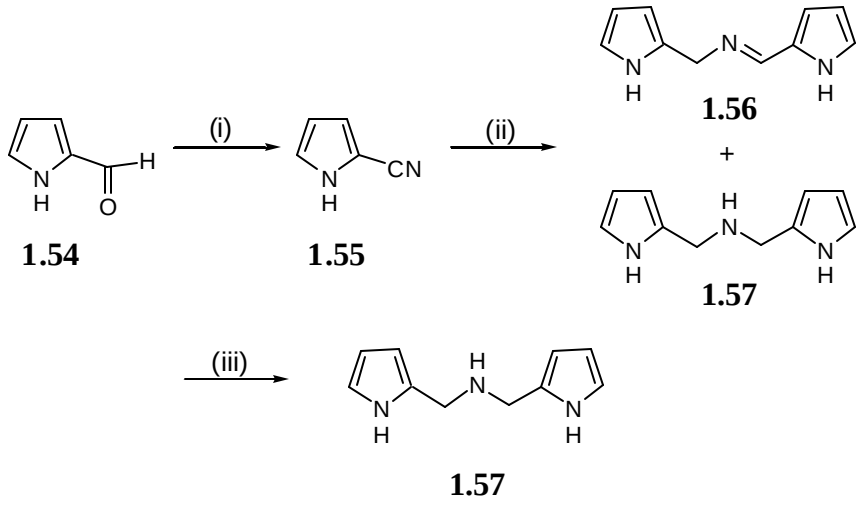

Reagents: (i) H_2NOSO_3H, H_2O, 0° C - 50° C, 82%; (ii) (a) $LiAlH_4$, THF, 0° C (b) $Na_2SO_4 \cdot 10\ H_2O$; (iii) $LiAlH_4$, THF, 0° C, 34%.

It was hoped that condensation of **1.57** with 1,1'-ferrocenediacid chloride would result in a unique and interesting anion binding system such as **1.58**. Unfortunately, all attempts to form the amide using standard condensations or various Lewis acid catalysts conditions failed to produce **1.58**. Lewis acid conditions degraded the dipyrrolyl starting material **1.57**, and under standard amide forming conditions an unusual and unexpected product was obtained. It

was this product, shown in Scheme 1.7 and discussed below, that provided the actual entry into Schiff base *ansa*-ferrocene systems.

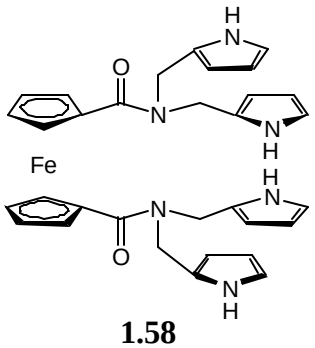

1.58

The synthesis of this unexpected product started with 1,1'-ferrocenediacid chloride **1.42**, whose synthesis was described previously (Scheme 1.3 p. 21). To this precursor, two equivalents of dipyrrolyl **1.57** were added, along with triethylamine in THF. This gave adduct **1.59** in 87% yield. Although not the desired product, it was recognized that this bis-pyrrole ferrocene could function as a useful starting material in its own right for the purpose of preparing novel *ansa*-ferrocene anion binding recpetors. In accord with such thinking, the pyrrole moieties were functionalized under Vilsmeier conditions using phosphorous oxychloride in DMF to give dialdehyde **1.60** in 26% yield. This latter species was then condensed with 4,5-dimethoxyphenalenediamine in methanol under conditions of nitric acid catalysis to form the novel Schiff base *ansa*-ferrocene **1.61**.

Scheme 1.7 Synthesis of Schiff base *ansa*-ferrocene **1.61**.

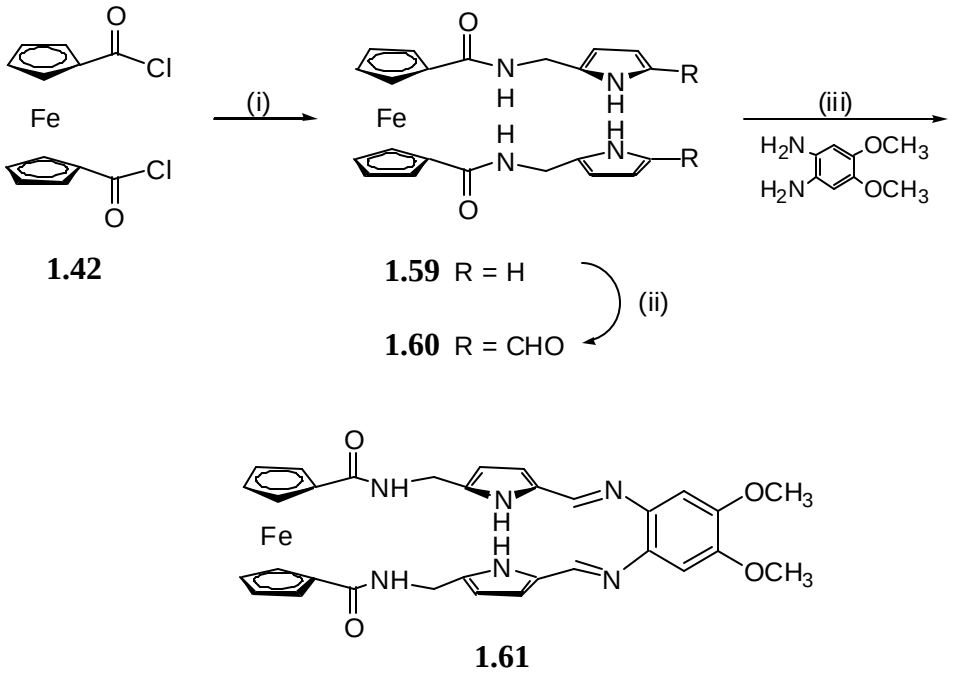

1.42 **1.59** R = H **1.60** R = CHO **1.61**

Reagents: (i) **1.57**, Et_3N, THF, 0º C - 25º C, 87%; (ii) $POCl_3$, DMF, DCE, 26%; (iii) HNO_3, CH_3OH, 52%.

1.3.2 Analytical Studies of the Schiff base *Ansa*-Ferrocene

Once prepared, the *ansa*-ferrocene **1.61** was tested for its anion binding ability using standard ^1H NMR spectroscopic titration methods and appropriately chosen tetrabutylammonium salts. Unfortunately, in dichloromethane-d_2 the amide and pyrrolic N*H* signals became too broad to follow during the course of the titrations carried out with F^- and $H_2PO_4^-$ or showed signs consistent with hydrolysis of the imine occurring. In the case of titrations with Br^- and Cl^-, the amide N*H* signal was followed and fitted to a nonlinear least squares equation.

The amide N*H* signals shifted downfield from 7.1 ppm to 8.4 ppm in the presence of increasing concentrations of Br^-, giving an association constant of 260 ± 12 M^{-1} (Figure 1.10a). In the presence of Cl^-, the amide NH shifted from 7.1 ppm to 8.8 ppm, resulting in an association constant of 960 ± 65 M^{-1} (Figure 1.10b).

Simultaneously, the electrochemical behavior of **1.61** in spectroscopic grade dichloromethane was investigated at a concentration of 1 mM using 100 mM of Bu_4NPF_6 as the supporting electrolyte. A cyclic voltammogram revealed irreversibility in the ferrocene/ferrocenium redox couple (Figure 1.11). Additionally, it appeared that redox activity was occuring elsewhere within the macrocycle, possibly at the imine functionalities, and that these ancillary processes were effecting the oxidation and subsequent reduction of the ferrocene center. Whether this interference is the true origin of the observed irreversibility or not remains to be elucidated. Nonetheless, it is clear that **1.61** is unable to function as an electrochemical sensor. This, in conjunction with the questionable stability of this *ansa*-ferrocene system (in terms of hydrolysis during the course of anion binding titrations), led to a hiatus in the development of analogs of **1.61**. Instead, a series of model ferrocene compounds was designed and studied in an effort to understand the potential reasons for irreversibility seen in the case of **1.61**.

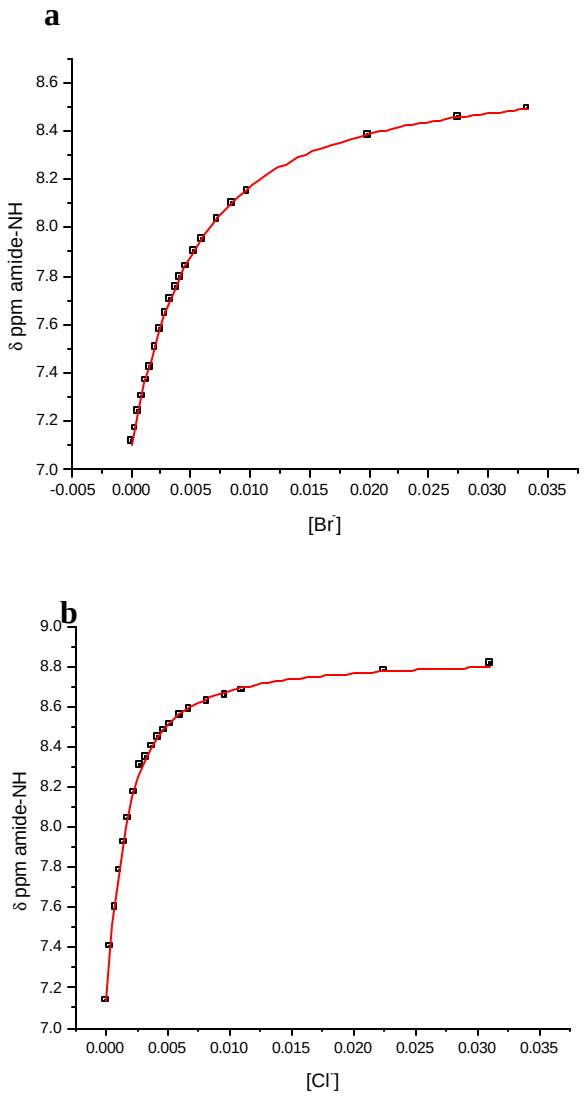

Figure 1.10: Proton NMR binding profile of **1.61** recorded in dichloromethane-d_2 at a concentration of (a) 1.97 x 10^{-4} M. Changes in the amide-N*H* chemical shift were recorded as the concentration of Bu_4NBr was varied between 0 – 33 mM. Nonlinear least squares analysis revealed an association constant, *K*a = 260 ± 12 M^{-1}; (b) 2.18 x zs3a210^{-3} M. Changes in the amide-N*H* chemical shift were recorded as the concentration of Bu_4NCl was varied between 0 – 42 mM. Nonlinear least squares analysis revealed an association constant, K_a = 960 ± 65 M^{-1}.

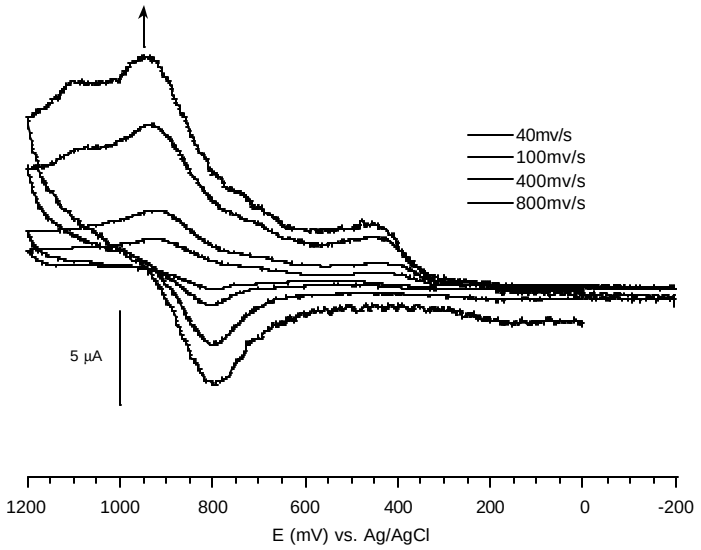

Figure 1.11 Cyclic voltammogram recorded in dichloromethane at a 1 mM concentration of **1.61**, scanned from 40 mV/s – 800 mV/s in the presence of Bu_4NPF_6 as the supporting electrolyte and Ag/AgCl as the reference electrode.

1.3.3 Synthesis and Studies of Acyclic Ferrocene-containing Analogs

The investigation was begun in the most logical and easily accessible manner, with ferrocenyl precursor **1.59** (Scheme 1.7, p. 40). The study of this compound, it was thought, would provide information concerning whether the electrochemical reversibility problem originates in the core of the binding pocket, or in the imine-phenylenediamine portion of the receptor. As a predicate to these studies, it was considered useful to obtain structural information. To do this, a single crystal X-ray diffraction analysis was carried out. It revealed two

intramolecular hydrogen bonding interactions between the pyrrole N*H* proton on one arm with the carbonyl oxygen on the adjacent arm (Figure 1.12). The result of these interactions is that the ferrocenyl arms both project outward from the same side of the ferrocene "core". A similar "cis" arrangement was seen by Beer *et al.* in his bis-arylamide cobaltocenium system **1.2**.[32] In spite of this precedent, this is an unusual conformation for disubstituted ferrocenes and is usually seen only in systems where there is intramolecular hydrogen bonding between the appended arms.[84-86] Absent such interactions, most disubstituted ferrocenes will have arms that point out in opposite directions from the ferrocene core for simple steric reasons.[87-89]

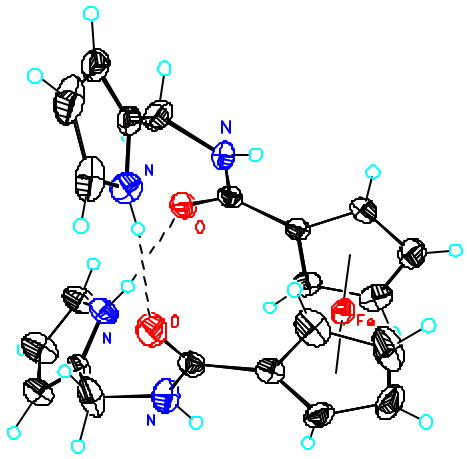

Figure 1.12: Solid state structure of **1.59** showing a partial atom labeling scheme. Dashed lines show two hydrogen bonding interactions between the pyrrole NH on one arm and the amide carbonyl on the second arm. Thermal ellipsoids are scaled to the 40% probability level.

It was unknown if the interactions revealed in the solid state structure of **1.59** would be present in solution, or whether they would have an adverse affect on anion binding. To address this latter question, cyclic voltammetry studies of **1.59** were performed in spectroscopic grade acetonitrile at a receptor concentration of 1 mM and in the presence of a 100 mM concentration of the supporting electrolyte, Bu_4NPF_6. The cyclic voltammogram displays a degree of reversibility, with $E_{1/2}$ = 900 mV vs. Ag/AgCl (Figure 1.13). This is a significantly higher potential than seen in the original *ansa*-ferrocenes **1.51**-**1.53**, an effect that is attributed to the electron withdrawing amide functionalities present in **1.59** that are in conjugation with the ferrocene unit. Further electrochemical investigations were undertaken to test the response, if any, that system **1.59** would display in the presence of various anions.

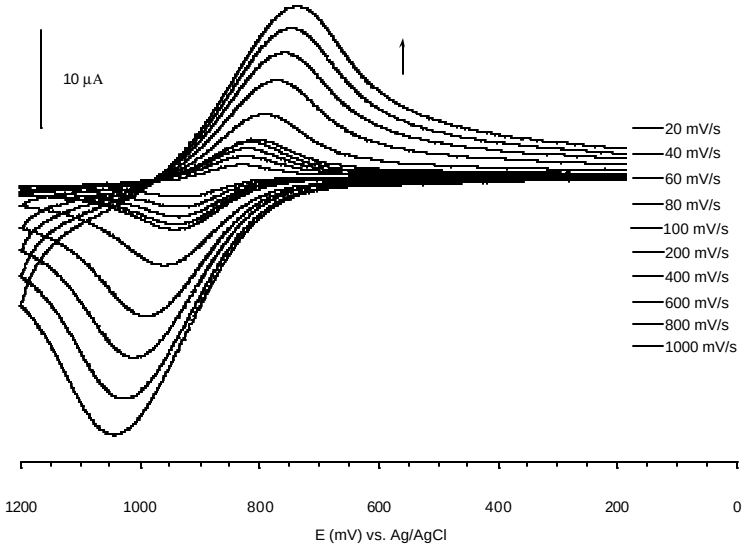

Figure 1.13: Cyclic voltammogram recorded in dichloromethane at a 1 mM concentration of **1.59**, scanned from 20 mV/s – 1000 mV/s in the presence of Bu_4NPF_6 as the supporting electrolyte and Ag/AgCl as the reference electrode.

In the presence of 5 molar equivalents of F^-, Cl^-, Br^-, $H_2PO_4^-$, and HSO_4^- cyclic voltammetric studies of **1.59** revealed electrochemical behavior that was not reversible (Figure 1.14). Initially, chloride and fluoride were tested, and both yielded voltammograms that were devoid of the typical ferrocene/ferrocenium redox wave (Figure 1.14a). In fact all vestiges of reversibility were absent. At this juncture, it was unknown whether this lack of a desired, reversible response was universal for all anions or specific to chloride and fluoride. Upon addition of 5 molar equivalents of tetrabutylammonium bromide, a different kind of voltammogram was seen. This made it apparent that the electrochemical response was indeed anion specific (Figure 1.14b). Once again, as in the case of chloride

and fluoride, no oxidation wave was apparent. However, across all scan speeds, the reduction wave indicated redox activity at 950, 1200, and 1400 mV. Clearly, all three reduction waves could not be attributed to the ferrocene center, and indicated that redox processes involving either the anion, the ligand, or both were occurring. Upon addition of dihydrogen phosphate anion (Figure 1.14c), there was once again an absence of ferrocene redox response upon oxidation; during reduction there was a broad wave at about 800 mV, presumably corresponding to the ferrocene center. The difference between what was seen with Br^- and $H_2PO_4^-$ led us to test the response of **1.59** toward hydrogen sulfate anion (Figure 1.14d). Here, reasonably clean cyclic voltammograms were seen. Although not reversible, there is a recognizable redox wave corresponding to the ferrocene/ferrocenium center that comes at $E_{1/2}$ ~ 800 mV vs. Ag/AgCl.

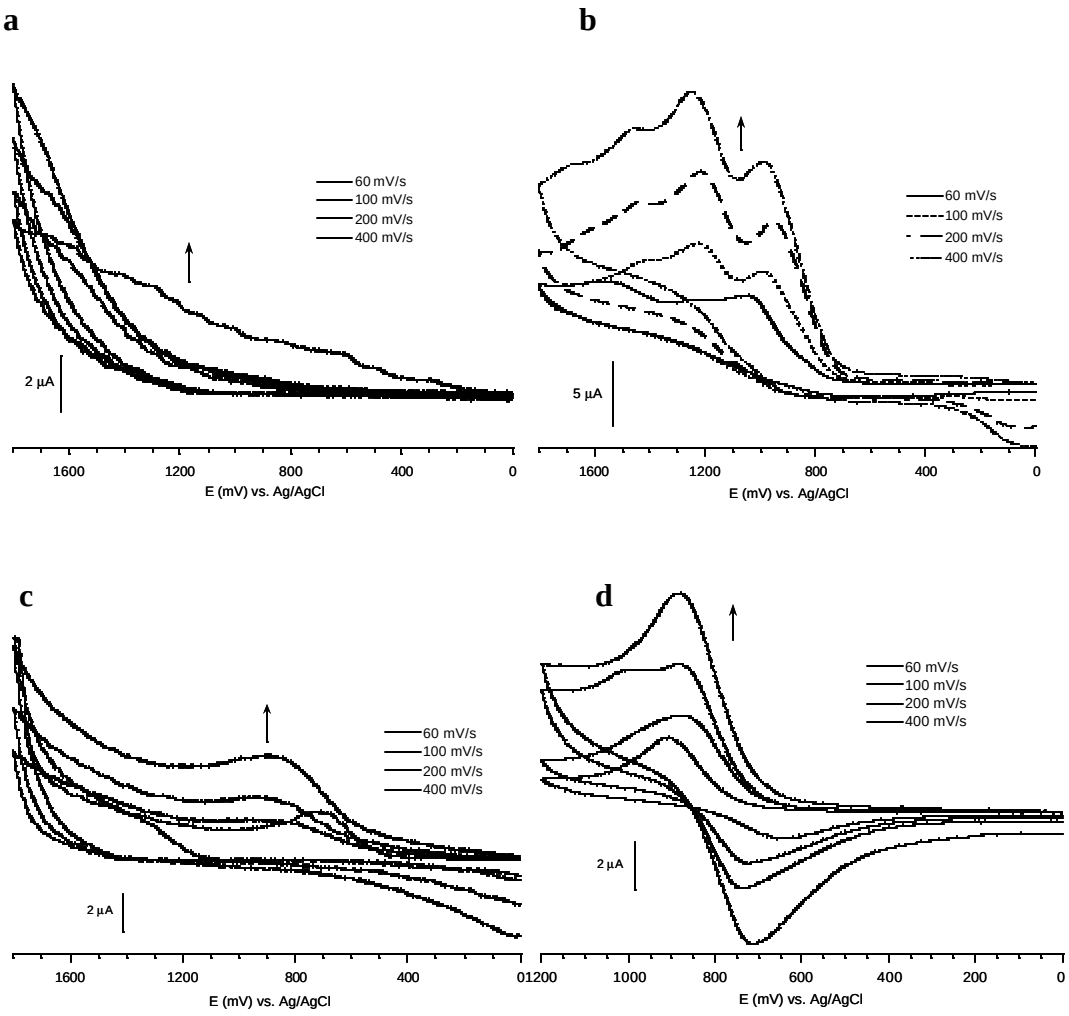

Figure 1.14: Cyclic voltammograms recorded in dichloromethane at 1 mM concentration of **1.59** in the presence of Bu_4NPF_6 as the supporting electrolyte and Ag/AgCl as the reference electrode. Scans taken from 60 mV/s – 400 mV/s. (a) In the presence of 5 eqv. of Bu_4NF. A similar voltammogram was observed in the presence of 5 eqv. of Bu_4NCl. (b) In the presence of 5 eqv. of Bu_4NBr. (c) In the presence of 5 eqv. of $Bu_4NH_2PO_4$. (d) In the presence of 5 eqv. of Bu_4NHSO_4.

To summarize, the differing patterns seen in these studies support the contention that there is some correlation between anion basicity and the degree of reversibility. The least basic anion, hydrogen sulfate, gave a relatively good electrochemical response, whereas the most basic anions, F^- and Cl^-, gave the worst response.

Despite the reduction in redox wave reversibility seen upon the addition of anions, it was possible to perform square wave voltammetry. This permitted an estimate of the cathodic perturbation induced by each anion. The results are summarized in Table 1.2. The interpretation of this preliminary data suggests that receptor **1.59** and any possible derivatives made from this core might prove effective as dihydrogen phosphate binders, as indicated by the 293 mV cathodic shift.

Table 1.2: Changes in the square wave voltammetric behavior of **1.59** observed upon the addition of various anions in dichloromethane. All anions were added in the form of their tetrabutylammonium salts.

Anion	E_p / mV	ΔE_c / mV
F^-	--	--
Cl^-	837	72
Br^-	878	31
$H_2PO_4^-$	616	293
HSO_4^-	834	75

E_p is the peak potential in the square wave voltammogram; E_c is the cathodically induced shift.

Based on the poor reversibility seen in the case of **1.59** upon addition of anions, it was established that the core binding pocket that comprises the Schiff base *ansa*-ferrocene **1.61** would likely not display a reversible response in the presence of anions. Accordingly, further studies of this receptor were abandoned. Before designing alternative *ansa*-ferrocenes, it was deemed prudent to devote yet further effort to probing the factors that can lead to irreversibility in receptors of this type. Therefore, three additional ferrocenyl compounds, namely **1.62**, **1.64**, and **1.66** were synthesized. Their preparation and electrochemical behavior is discussed below.

1.3.4 Synthesis and Analytical Studies of Additional Analogs

The first analog to be synthesized was **1.62**. By comparing this receptor, with its amine linker, to its parent **1.59**, containing diamide functionalities, it was hoped that insight into the role either functionality plays in adversely affecting the reversibility of ferrocenyl systems in the presence of anions might be obtained. Receptor **1.62** was made by reducing diamide **1.59** with lithium aluminum in THF to give diamine **1.62** in 17% yield (Scheme 1.8). Cyclic voltammetry in spectroscopic grade acetonitrile showed evidence of both an oxidation and a reduction wave; however, the redox couple does not exhibit reversibility (Figure 1.15). In light of the reversibility seen in the case of **1.59**, it was inferred that the presence of an amine functionality close to a ferrocene center, as in **1.62**, could interfere with redox reversibility. Such a conclusion is in accordance with literature precedence; when amines are proximal to the ferrocene center, the lone

electron pair can interact with the oxidized ferrocenium and destroy the reversibility.[90,91] At this point, there was sufficient evidence to suggest that the presence of a closely linked secondary amine in a ferrocenyl system would prevent its use as an electrochemical sensor in organic solvents. On this basis, it was concluded that reducing the Schiff base *ansa*-ferrocene **1.61** to the corresponding amine system would likely not solve the problem associated with its inherent lack of reversibility.

Scheme 1.8 Reduction of diamide *ansa*-ferrocene **1.59** to the diamine **1.62**

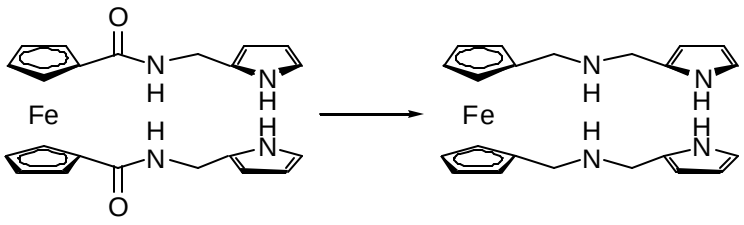

1.59 **1.62**

Reagents: $LiAlH_4$, THF, 0° C, 17%.

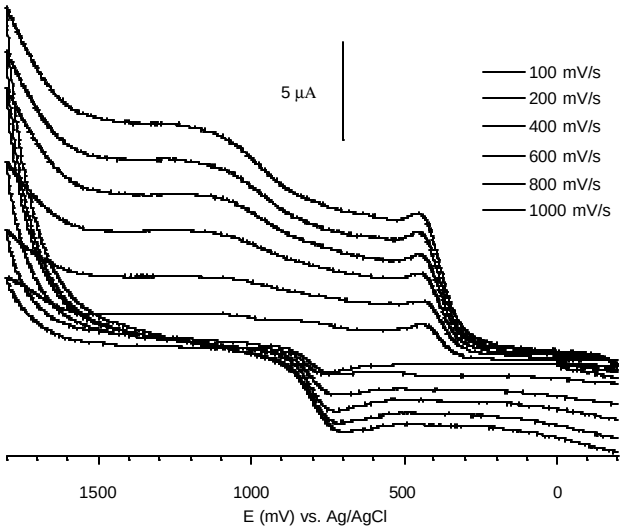

Figure 1.15 Cyclic voltammagram recorded in acetonitrile at a 1 mM of **1.62** in the presence of Bu_4NPF_6 as the supporting electrolyte and Ag/AgCl as the reference electrode. The voltammogram shows quasi-reversibility at scan speeds from 100 mV/s – 1000 mV/s.

Although the use of Schiff-base receptor **1.61** as an electrochemical sensor had been ruled out, it was considered worthwhile to study additional control systems to assist with the design of future generations of pyrrole-ferrocene conjugates. One such control was **1.45** (from Scheme 1.3, p. 21), a species that is a reduced, alkyl-linked analog of ferrocenyl precursor **1.44** that was originally used to try to prepare *ansa*-ferrocenes **1.51**-**1.53**. It was studied by cyclic voltammetry at a concentration of 1 mM in dichloromethane containing 100 mM Bu_4NPF_6, using Ag/AgCl as the reference electrode. Interestingly, this system maintained quasi-reversibility over scan speeds varying from 20 mV/s – 1000 mV/s (Figure 1.16). This finding, which appears to contradict what is seen with

1.62, leads to the question of why these two systems, which both contain pyrroles that are not conjugated to the ferrocene unit, give contradictory cyclic voltammetry results. The differences between the two receptors are that **1.62** contains secondary amides and **1.45** is substituted with electron withdrawing groups at the α position of the pyrroles.

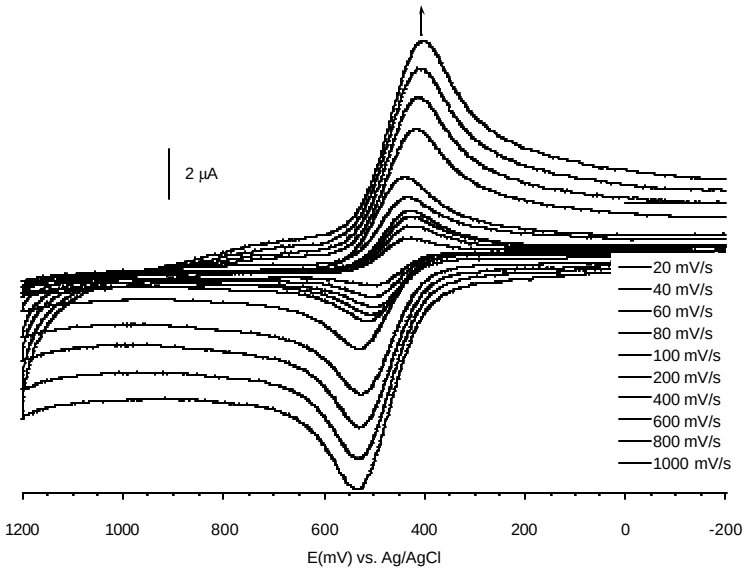

Figure 1.16 Cyclic voltammogram recorded in dichloromethane at a 1 mM of **1.45** in the presence of Bu_4NPF_6 as the supporting electrolyte and Ag/AgCl as the reference electrode. Variable scan speeds from 20 mV/s – 1000 mV/s show quasi-reversibility.

These results led us to look more closely at one of these variables, and to wonder if the α-free pyrroles in **1.62** were contributing to its electrochemical irreversibility; although receptor **1.59**, also with α-free pyrroles, did exhibit

electrochemical reversibility, literature precedence exists to suggest that α-free pyrroles can polymerize, causing the electrochemical signal to flatline.[92,93] To probe this discrepancy, an investigation was undertaken to look at the possible effect of substituents at the α position of the terminal pyrrole, if any. Attempts to synthesize the first set of chosen targets, **1.63** and **1.64**, were met with some difficulty. Surprisingly, the reaction of pyrrole and 2-methylpyrrole with 1,1'-ferrocenediacid chloride **1.42** in the presence of a number of Lewis acids and in a variety of solvents resulted in no reaction in the case of **1.63** and degradation of the starting material in the case of **1.64**.

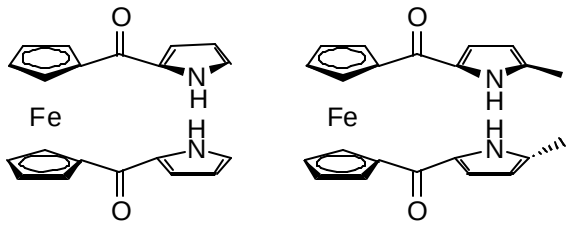

1.63 **1.64**

At this point it was thought that substituting the α and β positions of the pyrrole concurrently would serve the dual purpose of activating the pyrrole in order to enhance reactivity and blocking the extraneous unwanted reactive sites on the pyrrole unit. The first receptor designed along these lines, **1.66**, has a donating methyl group, and the second, **1.44**, whose synthesis was described previously in Scheme 1.3, p. 21, has an electron withdrawing benzyl ester group. The synthesis of **1.66** is similar to that of **1.44**. Specifically, 1,1'-ferrocenediacid chloride **1.42** was coupled to 3-ethyl-2,4-dimethylpyrrole **1.65** with tin(IV)

chloride in the presence of triethylamine. This gave the desired dipyrrole-substituted ferrocene **1.66** in 16% yield (Scheme 1.9).

Scheme 1.9 Synthesis of dipyrrole-substituted ferrocene **1.66**

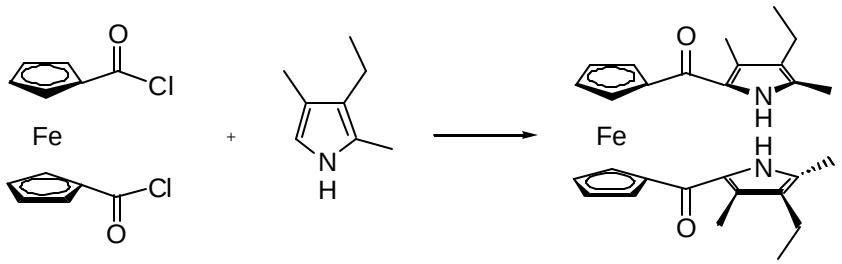

1.42 **1.65** **1.66**

Reagents: $SnCl_4$, Et_3N, THF, 16%

Electrochemical investigations of **1.66** show irreversibility in acetonitrile at scan speeds from 80 mV/s – 400 mV/s (Figure 1.17). The oxidation wave is distorted, with a corresponding reduction wave apparent at approximately 800 mV vs. Ag/AgCl. Additionally, reduction waves at 1400 mV and 1100 mV are seen that are considered indicative of ligand-centered redox activity. Once again, the reasons for the irreversiblity are not clear. It is questionable whether the conjugation present in **1.66** between the pyrrole and the ferrocene allows for the electron lone pair of the pyrrolic nitrogen, although "tied up" in an aromatic subunit, to communicate nonetheless with the ferrocenium center and disrupt the redox behavior. In an effort to address this question, efforts were made to reduce **1.66** with lithium aluminum hydride in both THF and dichloromethane.

Unfortunately, neither procedure effected full reduction to the dimethylene; either no reaction took place or mono-reduction was observed.

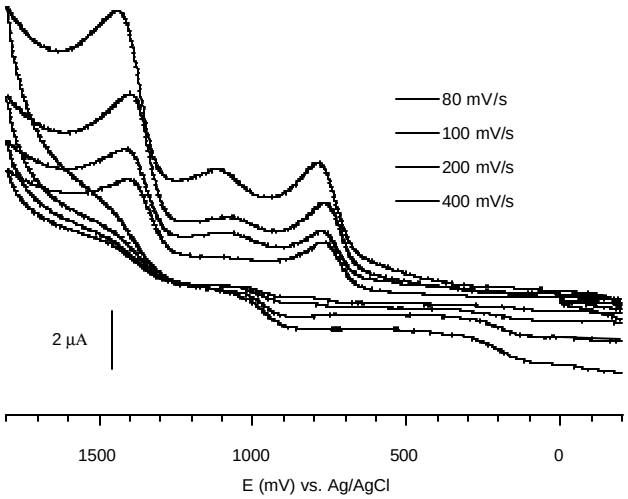

Figure 1.17 Cyclic voltammogram recorded in acetonitrile at a 1 mM concentration of **1.66** in the presence of Bu_4NPF_6 as the supporting electrolyte and Ag/AgCl as the reference electrode. Variable scan speeds taken from 80 mV/s – 400 mV/s. Although the system is irreversible, at scan speeds outside of this range the electrochemical signal flatlines.

The electrochemistry on the test compound with the benzyl ester electron withdrawing substituents, **1.44**, showed good reversibility at scans from 20 mV/s – 80 mV/s in acetonitrile (Figure 1.18). At 100 mV/s there is a sudden jump in amperage, and from this point upward to 1000 mV/s the oxidation wave becomes larger than the corresponding reduction wave, for unknown reasons.

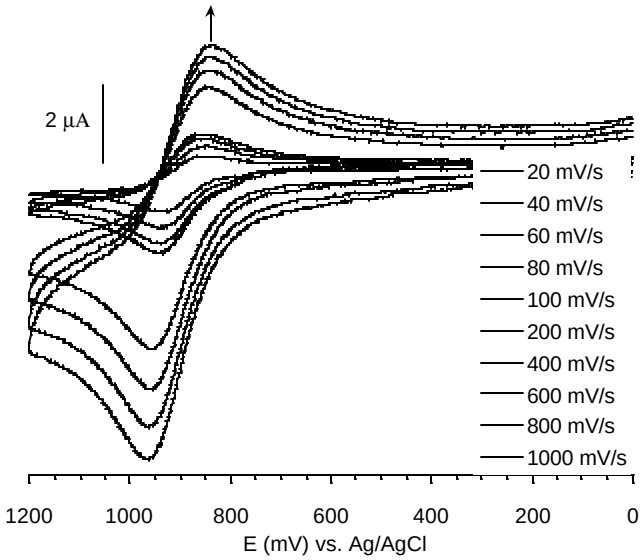

Figure 1.18 Cyclic voltammogram recorded in acetonitrile at a 1 mM concentration of **1.44** in the presence of Bu_4NPF_6 as the supporting electrolyte and Ag/AgCl as the reference electrode. Scans taken at variable scan speeds from 20 mV/s – 1000 mV/s. Reversibility occurs only from 20 mV/s – 80 mV/s.

At this point, the relative reversibility of this system led to a study of its electrochemical response to anions. Unfortunately, the addition of a range of anions led in all cases to the loss of the redox wave initially present in anion-free solutions of **1.44**. These results thus match what is seen upon the addition of anions to receptor **1.59**. Square wave voltammetric analyses were performed on **1.44** to gain preliminary insight into the types of changes that could be induced by the addition of anions. The results of this study are summarized in Table 1.3. Taken together, they highlight the fact that cathodically induced shifts are observed upon the addition of Cl^-, Br^-, HSO_4^-, and $H_2PO_4^-$.

Table 1.3: Square wave voltammetric behavior of **1.44** upon the addition of various anions in dichloromethane.

Anion	E_p / mV	ΔE_c / mV
F^-	--	--
Cl^-	847	59
Br^-	855	51
$H_2PO_4^-$	398, 917	508, +11
HSO_4^-	896	10

E_p is the peak potential in the square wave voltammogram; E_c is the cathodically induced shift.

From these studies, it appeared that the electron withdrawing benzyl ester substituents on the pyrroles may have helped to improve reversibility in these types of ferrocene systems. In all instances where electron withdrawing groups were in direct conjugation with the ferrocene core, as in receptor **1.59** and **1.44**, reversibility was maintained, even in the presence of most anions. On the other hand, the single example with an electron donating group, receptor **1.64**, was characterized by a disruption in reversibility. Examples in which conjugation between the ferrocene moiety and anion-binding pyrrole were disrupted, as in *ansa*-ferrocenes **1.51**-**1.53** and **1.45**, generally displayed electrochemical reversibility, although **1.62** appears to be an exception to this rule. Moreover, the irreversibility of **1.62** may be a consequence of the dialkyl-substituted amines perturbing the ferrocene/ferrocenium redox couple *via* the nitrogen atom lone

pairs. In light of this extra variable, it is not clear exactly what is causing the irreversibility of **1.62**.

At this point it appears that factors influencing reversibility of pyrrole-ferrocene receptors in the presence of a bound anion are not well understood. In general, future endeavors should focus on the design of receptors that do not contain secondary amines, and preferably that avoid the presence of electron donating substituents directly conjugated with the ferrocene unit.

1.4 CONCLUSION AND FUTURE DIRECTIONS

One of the problems in the design of anion receptors is the ability of the host to distinguish between chloride and dihydrogen phosphate anion. Since both anions are present in the same biological milieu, it is advantageous to be able to distinguish between them. Typically, most receptors that have a high affinity for one also have a high affinity for the other. Only a few metallocene receptors have shown a greatly enhanced affinity for the one anion over the other,[33,34,41] and of those that do, only a few have achieved this discrimination as the result of topological receptor design. The differences in affinity thus far have mainly been due to fortuitous size exclusion imposed by steric restrictions.

In the original *ansa*-ferrocene system **1.31**, the binding affinity was 9,030 M^{-1} for chloride and 11,300 M^{-1} for dihydrogen phosphate in acetonitrile-d_3. These values follow the typical trend for pyrrolic receptors, namely a comparable affinity for both anions. Instead of using size exclusion, it may be possible to design a receptor that possesses an inherent hydrogen bond architecture that

would allow for the preferential binding of one anion over the other. It became apparent that the scaffold of **1.31** may offer a base upon which to test this theory. For instance, if the *ansa*-ferrocenes **1.51-1.53** were to be tested for their chloride affinities, comparisons to the original system **1.31** could be used to help ascertain the relative affinity for dihydrogen phosphate and chloride. Depending on the resulting changes in K_a ratios, each *ansa*-ferrocene could be used to deduce insights into how minor ligand changes affect the anion binding process. Theoretically, by providing hydrogen bonding sites that are either topologically arranged (in a tetrahedral geometry) or arranged in a way that is chemically complementary to the dihydrogen phosphate anion (two hydrogen bond donors and two hydrogen bond acceptors), the affinity for dihydrogen phosphate anion could be enhanced relative to that of chloride anion.

This theory can be further tested by using different, commercially available linkers. For example, using 4,7,10-trioxa-1,13-tridecanediamine to synthesize the putative receptor **1.67** would lead to a receptor that contains an additional hydrogen bonding site. While the addition of this extra site is unnecessary in terms of establishing complementarity for dihydrogen phosphate binding (only two oxygen hydrogen bond acceptors are necessary), it will not likely have a detrimental effect on the ability of the receptor to bind anions; however, the additional electron density in the binding pocket may serve to decrease the affinity of the receptor for chloride.

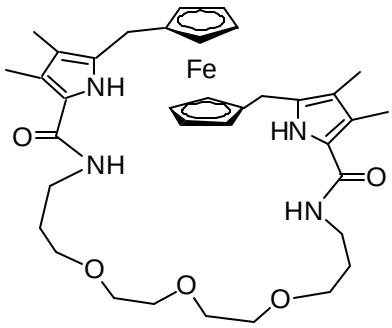

1.67

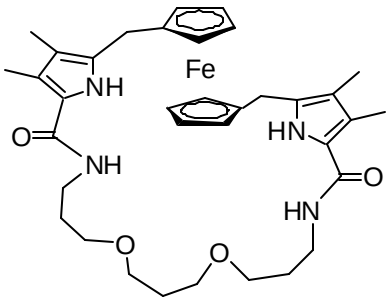

1.68

It is also possible that it is simply the size of the binding pocket that plays the dominant role in regulating selectivity. This latter hypothesis could be tested by increasing the length of the linker and hence the size of the binding pocket while maintaining the same number of oxygens as in **1.53**. Binding results from putative receptor **1.68** could then be directly compared to those from **1.53**. Another linker choice would be triethylenetetramine, a choice that gives target **1.69**. The lack of oxygens in this target and the absence of hydrogen bond acceptors in the linker will likely decrease the affinity for dihydrogen phosphate and increase it for chloride.

Another possible direction is to design an *ansa*-ferrocene such as **1.70** that could function as an electrochemical ditopic receptor. In this instance, the use of a 2-aminoethyl armed diaza-18-crown-6 as the linker would provide a metal binding site in close proximity to the pyrrolic anion binding site. This could potentially enhance the affinity of the receptor for both anions and cations.

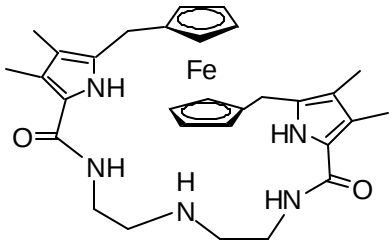

1.66

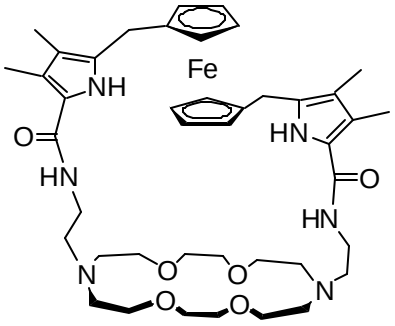

1.67

Future plans to expand the role of ferrocene-pyrrole conjugates include the incorporation of ferrocene into the backbone of a polypyrrolic system. Currently there are numerous examples of ferrocenes externally appended to various anion binding porphyrin or porphyrin analog receptors, including calixpyrroles as discussed in this chapter.[38,48,71,73] However, by incorporating ferrocene into the backbone of these systems in an *ansa*-type way, it is hoped that the closer proximity of the ferrocene unit to the actual binding event will result in a more sensitive electrochemical probe. For example, the calixpyrrole-inspired receptor **1.72** could be synthesized from 1,1'-ferrocenedimethanol **1.50** and tetrapyrrane **1.71** (Scheme 1.10, Path A) using reaction conditions analogous to those used to make *ansa*-ferrocenes **1.51**-**1.53**. In the event that the tetrapyrrane is too difficult to isolate or too reactive, **1.72** could also be synthesized from the appropriate *gem*-dimethyl substituted dipyrrolylmethane **1.73** through the open chain analog **1.74** (Scheme 1.10, Path B). The two dipyrrolylmethane arms on each cyclopentadiene ring could then be cyclized using standard calixpyrrole forming conditions with methanesulfonic acid and acetone.

Scheme 1.10 Possible synthetic routes showing how a ferrocene moiety could be incorporated into the backbone of a calixpyrrole-type *ansa* system.

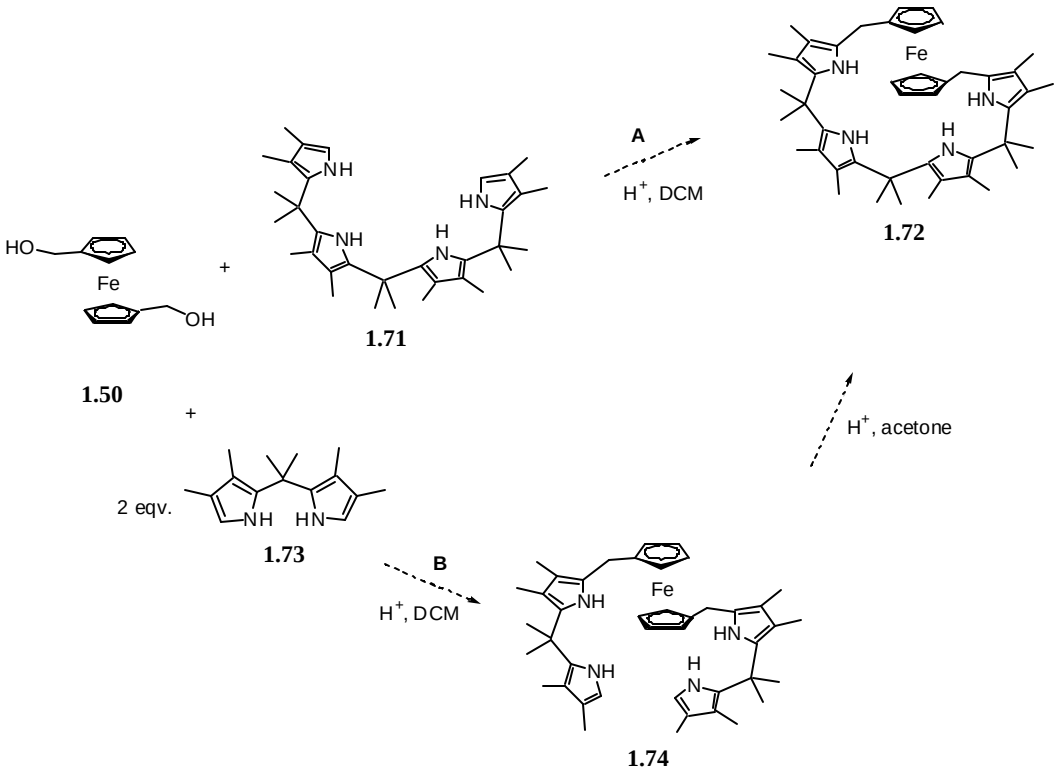

While difficulties remain to be overcome in the area of pyrrole ferrocene anion receptor development, it is an approach ripe with considerable promise. Electrochemical sensing is easy, requires relatively little sample, and has a low detection limit. The challenge is thus in the synthesis of viable targets that demonstrate electrochemical reversibility and thus would allow the inherent promise of this approach to be attained. On a more fundamental level, it is hoped that increasing the number of available ferrocene-pyrrole conjugates will provide further insights into why these systems often display irreversible electrochemical

behavior in the presence of anions, while simultaneously aiding in the design of yet-improved electochemically responsive ion-selective receptors.

This chapter is taken in part from a publication in which the author was a primary contributor, *J. Organomet. Chem*. **2001**, *637-639*, 343-348.

References

(1) Park, C. H.; Simmons, H. E. *J. Am. Chem. Soc.* **1968**, *90*, 2431-2432.

(2) Hosseini, M. W.; Lehn, J.-M. *J. Am. Chem. Soc.* **1982**, *104*, 3525-3527.

(3) Motekaitis, R. J.; Martell, A. E.; Lehn, J.-M. *Inorg. Chem.* **1982**, *21*, 4253-4257.

(4) Dietrich, B.; Fyles, D. L.; Fyles, T. M.; Lehn, J.-M. *Helv. Chim. Acta* **1979**, *62*, 2763-2787.

(5) Echavarren, A.; Galan, A.; de Mendoza, J.; Salmeron, A.; Lehn, J.-M. *Helv. Chim. Acta* **1988**, *71*, 685-693.

(6) Sanchez-Quesada, J.; Seel, C.; Prados, P.; de Mendoza, J.; Dalcol, I.; Giralk, E. *J. Am. Chem. Soc.* **1996**, *118*, 277-278.

(7) Sessler, J. L.; Cyr, M. J.; Lynch, V.; McGhee, E.; Ibers, J. A. *J. Am. Chem. Soc.* **1990**, *112*, 2810-2813.

(8) Fan, E.; Van Arman, S. A.; Kincaid, S.; Hamilton, A. D. *J. Am. Chem. Soc.* **1993**, *115*, 369-370.

(9) Neder, K. M.; Whitlock, J. H. W. *J. Am. Chem. Soc.* **1990**, *112*, 9412-9414.

(10) Sasaki, S.; Mizuno, M.; Naemura, K.; Tobe, Y. *J. Org. Chem.* **2000**, *65*, 275-283.

(11) Tobe, Y.; Sasaki, S.; Mizuno, M.; Naemura, K. *Chem. Lett.* **1998**, *8*, 835-836.

(12) Beer, P. D.; Smith, D. K. *Prog. Inorg. Chem.* **1997**, *46*, 1-96.

(13) Pham, H. V.; Pretsch, E.; Fluri, K.; Bezegh, A.; Simon, W. *Helv. Chim. Acta* **1990**, *73*, 1894-1903.

(14) Azuma, Y.; Newcomb, M. *Organometallics* **1984**, *3*, 9-14.

(15) Newcomb, M.; Blanda, M. T.; Azuma, Y.; Delord, T. J. *Chem. Commun.* **1984**, 1159-1160.

(16) Shriver, D. F.; Biallas, M. J. *J. Am. Chem. Soc.* **1967**, *89*, 1078-1081.

(17) Katz, H. E. *J. Am. Chem. Soc.* **1985**, *107*, 1420-1421.

(18) Reetz, M. T.; Niemeyer, C. M.; Harms, K. *Angew. Chem., Int. Ed. Engl.* **1991**, *30*, 1472-1476.

(19) Jung, M. E.; Xia, H. *Tetrahedron Lett.* **1988**, *29*, 297-300.

(20) Tamao, K.; Hayashi, T.; Ito, Y. *J. Organomet. Chem.* **1996**, *506*, 85-91.

(21) Ogawa, K.; Aoyagi, S.; Takeuchi, Y. *J. Chem. Soc., Perkin Trans. II* **1993**, *12,* 2389-2392.

(22) Aoyagi, S.; Ogawa, K.; Tanaka, K.; Takeuchi, Y. *J. Chem. Soc., Perkin Trans. II* **1995**, *2*, 355-358.

(23) Rothmaier, M.; Simon, W. *Anal. Chim. Acta* **1993**, *271*, 135-141.

(24) Zheng, Z.; Yang, X.; Knobler, C. B.; Hawthorne, M. F. *J. Am. Chem. Soc.* **1991**, *115*, 5320-5321.

(25) Goebel, M. W. *Angew. Chem., Int. Ed. Engl.* **1994**, 1141-1143.

(26) Beer, P. D.; Cadman, J. *Coord. Chem. Rev.* **2000**, *205*, 131-155.

(27) Beer, P. D.; Gale, P. A.; Chen, G. Z. *J. Chem. Soc. Dalton Trans.* **1999**, 1897-1909.

(28) Beer, P. D.; Gale, P. A.; Chen, Z. *Advances in Physical Organic Chemistry* **1998**, *31*, 1-90.

(29) Beer, P. D.; Keefe, A. D. *J. Organomet. Chem.* **1989**, *375*, C40-C42.

(30) Beer, P. D.; Hesek, D.; Hodacova, J.; Stokes, S. E. *Chem. Commun.* **1992**, 270-272.

(31) Beer, P. D.; Hazlewood, C.; Hesek, D.; Hodacova, J.; Stokes, S. E. *J. Chem. Soc. Dalton Trans.* **1993**, 1327-1332.

(32) Beer, P. D.; Drew, M. G. B.; Graydon, A.; Smith, D. K.; Stokes, S. E. *J. Chem. Soc. Dalton Trans.* **1995**, 403-408.

(33) Beer, P. D.; Hesek, D.; Kingston, J. E.; Smith, D. K.; Stokes, S. E.; Drew, M. G. B. *Organometallics* **1995**, *14*, 3288-3295.

(34) Beer, P. D.; Drew, M. G. B.; Hesek, D.; Shode, M.; Szemes, F. *Chem. Commun.* **1996**, 2161-2162.

(35) Beer, P. D.; Drew, M. G. B.; Hesek, D.; Nam, K. C. *Chem. Commun.* **1997**, 107-108.

(36) Beer, P. D.; Drew, M. G. B.; Hesek, D.; Jagessar, R. *Chem. Commun.* **1995**, 1187-1189.

(37) Beer, P. D.; Drew, M. G. B.; Hazlewood, C.; Hesek, D.; Hodacova, J.; Stokes, S. E. *Chem. Commun.* **1993**, 229-231.

(38) Beer, P. D. *Chem. Commun.* **1996**, 689-696.

(39) Beer, P. D.; Gale, P. A.; Chen, Z. *Coord. Chem. Rev.* **1999**, *185-186*, 3-36.

(40) Beer, P. D.; Chen, Z.; Goulden, A. J.; Graydon, A.; Stokes, S. E.; Wear, T. *Chem. Commun.* **1993**, 1834-1836.

(41) Beer, P. D.; Graydon, A.; Johnson, A. O. M.; Smith, D. K. *Inorg. Chem.* **1997**, *36*, 2112-2118.

(42) Kingston, J. E.; Ashford, L.; Beer, P. D.; Drew, M. G. B. *J. Chem. Soc. Dalton Trans.* **1999**, 251-257.

(43) Buda, M.; Ion, A.; Moutet, J.-C.; Saint-Aman, E.; Ziessel, R. *J. Electroanal. Chem.* **1999**, *469*, 132-138.

(44) Chen, Z.; Graydon, A.; Beer, P. D. *Journal of the Chemical Society, Faraday Transaction* **1996**, *92*, 97-102.

(45) Kavallieratos, K.; Hwang, S.; Crabtree, R. H. *Inorg. Chem.* **1999**, *38*, 5184-5186.

(46) Reynes, O.; Maillard, F.; Moutet, J.-C.; Royal, G.; Saint-Aman, E.; Stanciu, G.; Dutasta, J.-P.; Gosse, I.; Mulatier, J.-C. *J. Organomet. Chem.* **2001**, *637-639*, 356-363.

(47) Gallagher, J. F.; Kenny, P. T. M.; Sheehy, M. J. *Inorg. Chem. Commun.* **1999**, *2*, 327-330.

(48) Beer, P. D.; Drew, M. G. B.; Jagessar, R. *J. Chem. Soc. Dalton Trans.* **1997**, 881-886.

(49) Gale, P. A.; Chen, Z.; Drew, M. G. B.; Heath, J. A.; Beer, P. D. *Polyhedron* **1998**, *17*, 405-412.

(50) Tomapatanaget, B.; Tuntulani, T. *Tetrahedron Lett.* **2001**, *42*, 8105-8109.

(51) Valéro, C.; Fillaut, J.-L.; Ruiz, J.; Guittard, J.; Blais, J.-C.; Astruc, D. *J. Am. Chem. Soc.* **1997**, *119*, 2588-2589.

(52) Casado, C. M.; Cuadrado, I.; Alonso, B.; Morán, M.; Losada, J. *J. Electroanal. Chem.* **1999**, *463*, 87-92.

(53) Lloris, J. M.; Martínez-Máñez, R.; Padilla-Tosta, M. E.; Pardo, T.; Soto, J. *Helv. Chim. Acta* **1999**, *82*, 1445-1452.

(54) Beer, P. D.; Cadman, J.; Lloris, J. M.; Martínez-Máñez, R.; Soto, J.; Pardo, T.; Marcos, M. D. *J. Chem. Soc. Dalton Trans.* **2000**, 1805-1812.

(55) Beer, P. D.; Chen, Z.; Drew, M. G. B.; Johnson, A. O. M.; Smith, D. K.; Spencer, P. *Inorg. Chim. Acta* **1996**, *246*, 143-150.

(56) Lloris, J. M.; Martínez-Máñez, R.; Padilla-Tosta, M. E.; Pardo, T.; Soto, J.; Tendero, M. J. L. *J. Chem. Soc. Dalton Trans.* **1998**, 3657-3662.

(57) Beer, P. D.; Cadman, J.; Lloris, J. M.; Martínez-Máñez, R.; Padilla, M. E.; Pardo, T.; Smith, D. K.; Soto, J. *J. Chem. Soc. Dalton Trans.* **1999**, 127-133.

(58) Lloris, J. M.; Martínez-Máñez, R.; Padilla-Tosta, M. E.; Pardo, T.; Soto, J.; García-España, E.; Ramírez, J. A.; Burguete, M. I.; Luis, S. V.; Sinn, E. *J. Chem. Soc. Dalton Trans.* **1999**, 1779-1784.

(59) Lloris, J. M.; Martínez-Máñez, R.; Soto, J.; Pardo, T. *J. Organomet. Chem.* **2001**, *637-639*, 151-158.

(60) Dusemund, C.; Sandanayake, K. R. A. S.; Shinkai, S. *Chem. Commun.* **1995**, 333-334.

(61) Ori, A.; Shinkai, S. *Chem. Commun.* **1995**, 1771-1772.

(62) Yamamoto, H.; Ori, A.; Ueda, K.; Dusemund, C.; Shinkai, S. *Chem. Commun.* **1996**, 407-408.

(63) Ihara, T.; Nakayama, M.; Murata, M.; Nakano, K.; Maeda, M. *Chem. Commun.* **1997**, 1609-1610.

(64) Reynes, O.; Moutet, J.-C.; Pecaut, J.; Royal, G.; Saint-Aman, E. *New J. Chem.* **2002**, *26*, 9-12.

(65) Takenaka, S.; Yamashita, K.; Takagi, M.; Uto, Y.; Kondo, H. *Anal. Chem.* **2000**, *72*, 1334-1341.

(66) Yu, C. J.; Wan, Y.; Yowanto, H.; Li, J.; Tao, C.; James, M. D.; Tan, C. L.; Blackburn, G. F.; Meade, T. J. *J. Am. Chem. Soc.* **2001**, *123*, 11155-11161.

(67) Patolsky, F.; Weizmann, Y.; Willner, I. *J. Am. Chem. Soc.* **2002**, *124*, 770-772.

(68) Anzenbacher Jr., P.; Jursíková, K.; Sessler, J. L. *J. Am. Chem. Soc.* **2000**, *122*, 9350-9351.

(69) Anzenbacher Jr., P.; Try, A. C.; Miyaji, H.; Jursíková, K.; Lynch, V.; Marquez, M.; Sessler, J. L. *J. Am. Chem. Soc.* **2000**, *122*, 10268-10272.

(70) Sessler, J. L.; Weghorn, S. J. *Expanded, Contracted and Isomeric Porphyrins*; Elsevier: NY, 1997.

(71) Sessler, J. L.; Gebauer, A.; Gale, P. A. *Gazz. Chim. Ital.* **1997**, *127*, 723-726.

(72) Bucher, C.; Zimmerman, R. S.; Lynch, V.; Král, V.; Sessler, J. L. *J. Am. Chem. Soc.* **2001**, *123*, 2099-2100.

(73) Gale, P. A.; Hursthouse, M. B.; Light, M. E.; Sessler, J. L.; Warriner, C. N.; Zimmerman, R. S. *Tetrahedron Lett.* **2001**, *42*, 6759-6762.

(74) Scherer, M.; Sessler, J. L.; Gebauer, A.; Lynch, V. *Chem. Commun.* **1998**, 85-86.

(75) Zindel, J.; Lightner, D. A. *J. Heterocycl. Chem.* **1995**, *32*, 1219-1223.

(76) Lau, C. K.; Tardif, S.; Dufresne, C.; Scheigetz, J. *J. Org. Chem.* **1989**, *54*, 491-494.

(77) Martin Nelson, S. *J. Chem. Soc. Dalton Trans.* **1983**, 2525.

(78) Wilcox, C. W. *Frontiers in Supramolecular Organic Chemistry and Photochemistry*; VCH: Weinheim, 1991.

(79) Connors, A. K. *Binding Constants: the Measurement of Molecular Complex Stability*; Wiley: New York, 1987.

(80) Sessler, J. L.; Johnson, M. R.; Lynch, V.; Murai, T. *J. Coord. Chem.* **1988**, *18*, 99-104.

(81) Meyer, S.; Andrioletti, B.; Sessler, J. L.; Lynch, V. *J. Org. Chem.* **1998**, *63*, 6752-6756.

(82) Hannah, S.; Lynch, V.; Gerasimchuk, N.; Magda, D.; Sessler, J. L. *Org. Lett.* **2001**, *3*, 3911-3914.

(83) Brückner, C.; Xie, L. Y.; Dolphin, D. *Tetrahedron* **1998**, *54*, 2021-2030.

(84) Carr, J. D.; Coles, S. J.; Hassan, W. W.; Hursthouse, M. B.; Malik, K. M. A.; Tucker, J. H. R. *J. Chem. Soc. Dalton Trans.* **1999**, 57-62.

(85) Beer, P. D.; Sikanyika, H.; Slawin, A. M. Z.; Williams, D. J. *Polyhedron* **1989**, *8*, 879-886.

(86) Nomoto, A.; Moriuchi, T.; Yamazaki, S.; Ogawa, A.; Hirao, T. *Chem. Commun.* **1998**, 1963-1964.

(87) Scherer, M.; Sessler, J. L.; Moini, M.; Gebauer, A.; Lynch, V. *Chem. Eur. J.* **1998**, *4*, 152-158.

(88) Plenio, H.; Yang, J.; Diodone, R.; Heinze, J. *Inorg. Chem.* **1994**, *33*, 4098-4104.

(89) Beer, P. D.; Chen, Z.; Drew, M. G. B.; Pilgrim, A. J. *Inorg. Chim. Acta* **1994**, *225*, 137-144.

(90) Beer, P. D.; Chen, Z.; Drew, M. G. B.; Kingston, J.; Ogden, M.; Spencer, P. *Chem. Commun.* **1993**, 1046-1048.

(91) Beer, P. D.; Chen, Z.; Ogden, M. I. *Journal of the Chemical Society, Faraday Transaction* **1995**, *91*, 295-302.

(92) Bhat, N. V.; Gadre, A. P.; Bambole, V. A. *J. Appl. Polym. Sci.* **2001**, *80*, 2511-2517.

(93) Zhao, F.; Peng, Y.; Ding, X.; Zeng, B. *Electroanalysis* **2001**, *13*, 1367-1374.

Chapter 2: Design and Study of Expanded Calixphyrins and the First Cryptand-Like Calixpyrrole

2.1 INTRODUCTION TO CALIXPHYRINS

This chapter describes new developments in the area of calixphyrin chemistry. Calixphyrins encompass all porphyrin analogs that contain a mixture of sp^2 and sp^3 hybridized bridging meso carbon centers. In the case of hybrid systems containing four pyrroles, calix[4]phyrins, this definition encompasses systems with one, two, and three sp^2 hybridized bridging meso carbons. In contrast to calix[n>4]phyrins containing a greater number of pyrroles, such compounds have an established history and are known as porphomethenes **2.1** (one sp^2 hybridized meso carbon atom), porphodimethenes **2.2**, **2.3** (two sp^2 hybridized meso carbon atoms, arranged in either a "cis-" or "trans-like" (i.e., 5,10 or 5,15) fashion across the macrocycle), isoporphyrins **2.4** (three sp^2 hybridized meso carbon atoms, one NH hydrogen atom), and phlorins **2.5** (three sp^2 hybridized meso carbon atoms, three NH hydrogen atoms). This established history is underscored by the fact that several important calix[4]phyrin species are observed during classical porphyrin condensations involving pyrrole and an aldehyde. Here, initial condensation produces *inter alia* porphyrinogen, an octahydrocalixpyrrole.[1,2] This is then oxidized sequentially through a porphomethene and porphodimethene until a net 6 electron oxidation is achieved, leading to the formation of porphyrin.[3,4]

Historically, calix[4]phyrins have proved more difficult to isolate and study than porphyrins due to their relative conformational and electronic instability, something that abets oxidation to the corresponding porphyrin.[1] Initial proof of the formation of these species thus came from spectroscopic analyses carried out during studies of porphyrin formation or while subjecting well-characterized porphyrins to reduction.

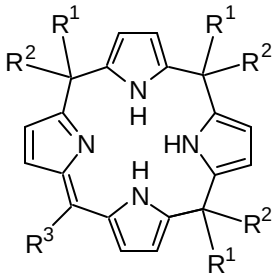

2.1

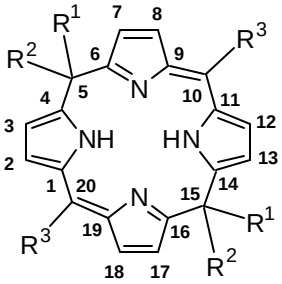

2.2

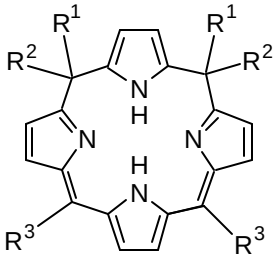

2.3

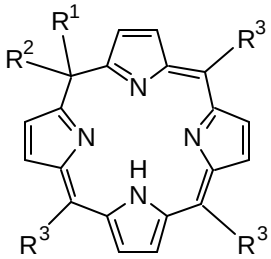

2.4

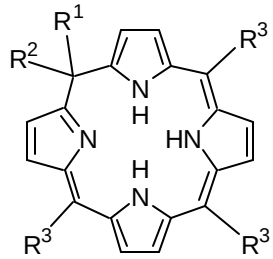

2.5

Many of the first calix[4]phyrin species were initially isolated as metal complexes.[5] The factors influencing stability were then studied in terms of electronic and steric effects, allowing the evolution of stable non-metalated species. Today, the field of free base calix[*n*]phyrin chemistry is growing rapidly and is opening up new opportunities in the porphyrin analog area. The

coordination and anion binding properties of calix[n>4]phyrins, in particular, promise to be unique and different, while the structural features of these hybrid systems, containing as they do both sp^2 and sp^3 hybridized bridging meso carbon atoms within their frameworks, are sure to be of interest. This introduction will outline the historical origins of calix[*n*]phyrin chemistry while placing an emphasis on current, rapidly emerging developments in the area, including new, modular syntheses that are permitting the preparation of higher order calix[*n*]phyrin species.

With the advent of higher order, or expanded calix[*n*]phyrins, a need arises for a systematic nomenclature. Following the pattern set in the expanded porphyrin and calix[*n*]pyrrole areas,[6] we propose a system based on distinguishing between the sp^2 and sp^3 meso carbon centers. For a calix[4]phyrin such as **2.2**, the systematic name, as proposed, would be calix[4]phyrin-(**1**.*1*.**1**.*1*). Starting with the highest order sp^2 center, the molecule is named in the direction in which the nearest sp^2 center lies. The bracketed number refers to the number of pyrroles in the macrocycle. Each individual bold and italicized number denotes the number of bridging meso centers between each pyrrole subunit. Bold numbers refer to sp^2 centers, and italicized numbers refer to sp^3 centers. This nomenclature, which will be elaborated on further in the section dealing with expanded calix[*n*]phyrins, will be used throughout this chapter. Common names for compounds with historical precedent will also be used.

2.1.1 Isoporphyrins

It is now known that isoporphyrins **2.4**, a class of calix[4]phyrin-(**1**.**1**.**1**.*1*), are byproducts of heme oxidation and intermediates in the biosynthesis of chlorophylls.[7] Initially, it was the discovery of phlorin **2.5** and the observation of its unexpected stability by Woodward[8] that led him to suggest that isoporphyrin could exist. The prescient nature of this prediction was subsequently demonstrated by Dolphin, who established that nucleophilic attack of methanol on the oxidized dication of Zn(II)TPP leads to the formation of its unstable isoporphyrin derivative.[9] Isoporphyrins are obtained from the chemical oxidation of metalloporphyrins, and are intermediates in electrophilic substitution reactions of porphyrins that involve attack at the meso positions.[10-20] Additionally, they are products of electrochemical and photooxidation of the parent metalloporphyrin (containing both transition and alkaline earth metal cations).[9,21-32] Isoporphyrins have also been obtained as the result of protonation of neutral meso-substituted metalloporophyrins.[33] Apparently, the presence of the metal center reduces the reactivity of the pyrrole nitrogens while simultaneously increasing the susceptibility of the meso carbons towards electrophilic attack. Unfortunately, the resulting metalated isoporphyrins exist in cationic form and tend to revert back to the parent porphyrin spontaneously.[7] On the other hand, they can undergo further nucleophilic attack to produce the corresponding porphodimethene.[34]

The first total synthesis of a stable isoporphyrin, at least with respect to unwanted conversion into a porphyrin, was obtained through a MacDonald condensation involving a dicarboxylic acid substituted dipyrrolylmethane and a

diformyl dipyrrolylmethane in the presence of zinc acetate and *p*-TSA. This resulted in a Zn(II) isoporphyrin with two methyl groups at the sp^3 meso position (**2.6**; R^1 = Me, R^2 = Me, R^3 = $-(CH_2)_2CO_2Me$, R^4 = H, X = ClO_4). This substitution prevented oxidative conversion into the corresponding porphyrin.[7,35]

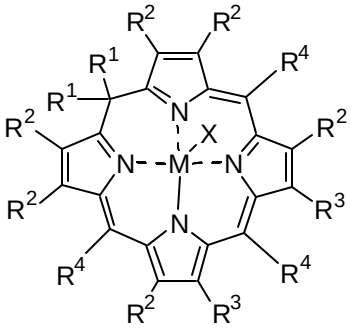

2.6

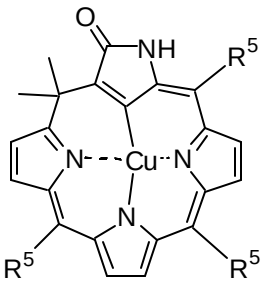

2.7

Recently, Furuta and Osuka reported the synthesis of an *N*-confused isoporphyrin system, **2.7**, obtained in 3% yield from the methanesulfonic acid-catalyzed cyclization of pyrrole, *p*-tolualdehyde, and acetone in a 4:3:1 molar ratio, followed by DDQ oxidation. The carbon atoms of the acetone component were found to be added in a *gem*-dimethyl fashion between the α- and the β'-position of two pyrrole subunits; no other confused isomers were found. Due to the lower reactivity of acetone as compared to tolualdehyde, at least when acting as an electrophile, it is thought that the *N*-confusion occurs in the final cyclization step. Crystal structures were obtained of the Ni(II) and Cu(II) complexes. These structures revealed the existence of dimers in the solid state, formed through hydrogen bonding interactions involving the outward-facing amide-like moiety present in the calixphyrin-type skeleton. Although the Ni(II) complex showed a typical ruffled structure, the Cu(II) complex was found to be relatively planar

despite the presence of an sp^3 bridging meso carbon. System **2.7** thus afforded the first example of a structurally characterized organocopper(II) complex and demonstrated that complete π-conjugation is not a necessary prerequisite for the formation of a metal-carbon bond in a polypyrrolic system.[36]

2.1.2 Phlorin

The study of phlorins **2.5**, a different, more reduced, class of calix[4]phyrins-(**1**.**1**.**1**.*1*), dates back to the days of Woodward, who discovered this class of compounds during the course of his studies directed towards the total synthesis of chlorophyll a,[8] and to Mauzerall and his work on the photoreduction of porphyrins.[37,38] Phlorins are formed during nucleophilic attack on a meso position of porphyrin; many can also be obtained by electrochemical- or photo-reduction.[39-41] As a general rule, metal-free phlorins proved to be unstable and easily oxidized[42-45] except when bearing sterically hindered substituents at the meso positions. It was also found that a ZnTPP-derived phlorin (TPP = tetraphenylporphyrinato dianion) could be synthesized in its anionic form. In the presence of excess methanol, this latter species was found to rearrange to the corresponding ZnTPP-type chlorin complex, the first phlorin to do so. Unfortunately, the low solubility and chemical lability of this latter species prevented proper characterization or further study.[40,41,46,47] The use of metalloporphyrins, and the increased electrophilic character they endowed, also permitted the use of nucleophiles in the addition-based formation of phlorins from porphyrins. In particular, Setsune *et al.* reported the formation of an air-sensitive

rhodium-phlorin complex obtained through the attack of organolithium reagents upon rhodium(III) OEP (OEP = 2,3,7,8,12,13,17,18-octaethylporphyrin).[48] Segawa and co-workers then described that the direct nucleophilic addition of hydroxide ion upon a nonoxidized porphyrin ring yielded hydroxyphlorin.[49] Similarly, Sugimoto synthesized a neutral phlorin with trivalent gold from Au(III)TPP using $NaBH_4$ in methanol; this provided a species that was stable for a relatively long period of time.[50]

Without the activation induced by a coordinated metal cation in a high oxidation state, nucleophilic additions to the meso positions of porphyrins (to form the corresponding phlorin) generally require strong nucleophiles such as alkyl lithium derivatives[51] In fact, H_2TPP reacts with *n*-BuLi in this fashion to yield the corresponding chlorin and phlorin congeners.[51,52] While stable in crystalline form, the phlorin produced in this manner readily decomposes in solution. The use of bulkier lithiating agents tended to lower the yield or give unwanted products.[53] Analogous alkylation reactions, involving the use of porphyrins not bearing substitutents in the meso positions, have also been reported.[54]

Historically, metal-free phlorins were difficult to isolate, and those that were stable showed strong *peri* interactions between peripheral meso and pyrrolic substituents.[8,42,55-57] Steric hindrance introduced by means of angular methyl groups,[58,59] *N*(21),*N*(22) bridges,[60-64] and the use of a tetra-*N*-substituted phlorin cation[65] resulted in stabilization. The use of *N*-methyl and *N*-phenyl substituted porphyrins as starting materials and treatment with reducing agents led to the

formation of the corresponding phlorin; however, attempts to carry out further chemistry involving the pyrrolic nitrogen centers led to aromatization (i.e., loss of phlorin character).[66] Smith showed that direct meso alkylation of *meso*-formylporphyrins results in substitution at the 15 position by way of a phlorin intermediate.[67]

Callot has proposed possible alternative pathways to the formation of phlorin derivatives. He found that electrochemical or $Na_2S_2O_4$–based reduction of *N*-arylporphyrins (**2.8**) gives stable phlorins (**2.9**) that are epimeric to the phlorins obtained by tosylhydrazine or $NaBH_4$ reduction of these same starting materials. While the former species was found to bear a *syn* arrangement of the meso sp^3 phenyl group with respect to the *N*-substituent, the products produced in the latter way possess an *anti* arrangement. Under cathodic conditions, it is thought that a radical anion is formed and that the meso carbon on the opposite face of the *N*-substituent is protonated, forcing the meso-phenyl substituent *syn* to the *N*-substituent. On the other hand, it is proposed that reducing agents effect reduction through hydride donation, a process that involves the irreversible donation of H^- to the porphyrin. In this case, steric factors that could hinder the approach of the reagent are expected to define the stereochemistry of the addition (i.e., *syn* or *anti*).[68]

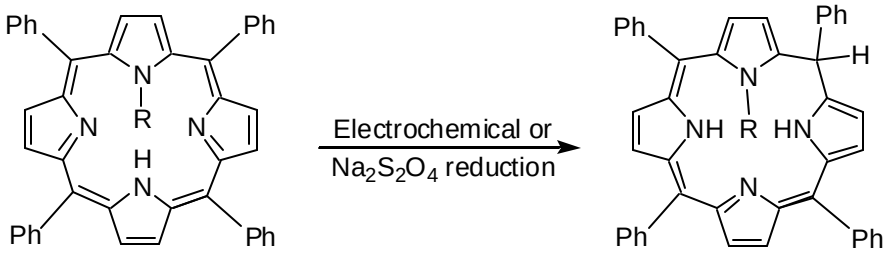

2.8 **2.9**

2.1.3 Porphodimethenes and Porphomethenes

Porphomethenes (calix[4]phyrin-(**1**.*1*.*1*.*1*), **2.1** as well as porphodimethenes (calix[4]phyrin-(**1**.*1*.**1**.*1*), **2.2** and calix[4]phyrin-(**1**.**1**.*1*.*1*), **2.3**) are known intermediates in the stepwise oxidation process leading to the production of porphyrin from porphyrinogen under many "normal" porphyrin-forming conditions.[69,70] The first air stable porphodimethenes that were isolated and characterized were di- or trivalent metalated species bearing alkyl substituents at the meso positions.[4,5,71-73] It is well known that relief of macrocyclic strain in overcrowded porphyrins can be achieved by converting to the corresponding porphodimethene; the larger the substituents, the more the strain is relieved by the conversion.[74,75] Although conjugation is lost, the relative energies of an overcrowded (and hence less than fully aromatic) porphyrin and the alternative porphodimethene are similar.[76]

Initially, the only method to prepare porphodimethenes was using Buchler's procedure, a process that involves subjecting a porphyrin to reductive alkylation at the meso position. Unfortunately, this approach proved limited to the synthesis of symmetric metalated porphodimethenes.[5,73,76,77] Further, this reductive alkylation strategy did not prove effective on all types of metalated porphyrins or compatible with all types of *beta*-pyrrolic substituents. These limitations, in turn, made it hard to obtain a range of porphodimethenes and restricted the extent to which this class of compounds could be subject to in-depth study.[78]

Today there are a number of alternative synthetic routes available that, taken in concert, have expanded greatly the range of metalated and non-metalated porphodimethenes available for study.[76] These include 2+2 MacDonald-like condensation-based approaches,[79] procedures based on acid catalyzed condensations of oligopyrroles with acetone,[80-82] and strategies based on the condensation of sterically hindererd aldehydes with pyrrole, an approach that precludes oxidation to the corresponding porphyrin.[3,83]

Porphodimethenes bearing alkyl groups at the meso sp^3 centers are stable since, in contrast to species with hydrogens on these bridging atoms, they are able to resist oxidative dehydrogenation to the corresponding porphyrin. Within the context of this general statement, it has been found that the exact extent of resistance towards oxidation is dependent on the relative configuration of the sp^3 hybridized meso carbon atoms.[77,84] For instance, in the case of 5,15-porphodimethene species (i.e., calix[4]phyrins(**1**.*1*.**1**.*1*) derived from unsymmetical ketones, the most stable products are those in which the more bulky substituents adopt a *syn* diaxial configuration. As a general rule, this is the species wherein the substituents at the tetravalent centers are at a maximum distance from the macrocycle and steric hindrance is at a minimum.

Porphodimethenes with unsymmetrically substituted carbon atoms at the meso sp^3 centers can exist in three isomeric forms: *syn* axial, *syn* equatorial, and *anti* (Figure 2.1). As noted above, in the case of the 5,15-disubstituted porphodimethenes, the solid state structure of **2.10**[85] as well as many metalated

species[5,86-89] adopt the common "roof-like" appearance, with a bend occurring along the 5,15 axis.

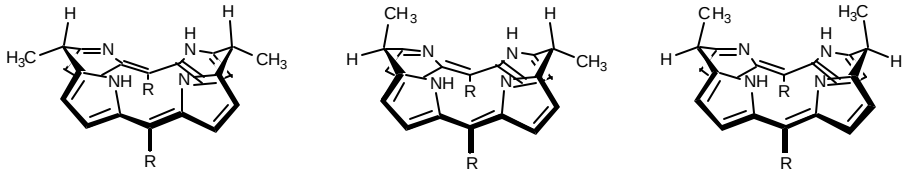

a **b** **c**

Figure 2.1 Porphodimethene conformations illustrating (a) *syn* equatorial (b) *anti* and (c) *syn* axial

Alternatively, a flat geometry has been observed in the case of a *syn* diaxial bis-lithiated system,[90] while an *anti*- configuration was seen in the case of a metal-free system containing bulky sp^3 meso groups and ethyl substituents in the eight β-pyrrolic positions. Interestingly, Ni(II) insertion of **2.11** resulted in complete conversion to a mixture of the *syn* diaxial and *anti* equatorial analogs. Moreover, heating **2.11** to reflux in glacial acetic acid for one hour resulted in complete isomerization to the *syn* diaxial conformation, lending credence to the idea that the conditions used for metal insertion result in ring opening and subsequent isomerization to the thermodynamically most stable *syn* diaxial isomer.

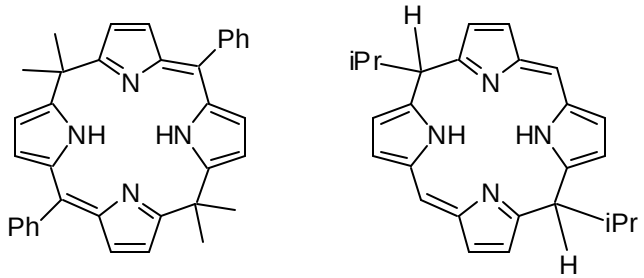

2.10 **2.11**

Lately, several advances have been made in the area of metalated porphodimethene chemistry.[76,91-94] Progress leading to a diversification in the number and type of substituents available at the meso carbons has also been made.[95] Recently, a 5,15-disubstituted porphodimethene (i.e., a calix[4]phyrin-(**1**.*1*.**1**.*1*)) was reported as the result of the first ever demonstrated reversible porphyrin- porphodimethene interconversion mediated by nucleophilic substituents proximal to the sp^3 meso carbon centers.

A different kind of porphodimethene is represented by the calix[4]phyrins-(**1**.**1**.*1*.*1*). Historically, references to these kinds of systems, bearing disubstituted sp^3 hybridized meso-like bridges in the 5 and 10 positions, have been infrequent; presumably, this reflects their lower stability arising from their inherently lower resonance stabilization energy compared to their 5,15 congeners.[96,97] The first fully characterized free-base 5,10-disubstituted porphodimethene was obtained by Callot *et al*. and was isolated while these workers were seeking to optimize their method of producing phlorins *via* the direct alkylation of porphyrins.[52] Specifically, the initial success in obtaining phlorins in this way using *n*-BuLi[51] led them to consider the use of more sterically demanding bases. This, it was thought, would improve the phlorin-to-chlorin ratio. When *s*-BuLi was used in this way, no isolable phlorin product was obtained. On the other hand, the use of *t*-BuLi yielded, surprisingly, not the phlorin, but rather a 1% yield of chlorin and 5% yield of a 5,10- disubstituted porphodimethene. In this latter calix[4]phyrin-(**1**.**1**.*1*.*1*), the bulky *t*-butyl groups are arranged in an *anti* diaxial fashion. The solid state structures of these

porphodimethenes reveal a characteristic nonplanar tripyrrolic helical twisting that is most manifest between the two planes defined by the isolated "calix'-type pyrrole, as exemplified in the solid state structure of **2.12** (Figure 2.2), an analog of Callot's calix[4]phyrin- (**1**.**1**.*1*.*1*) that was recently prepared by Sessler *et al*. [85]

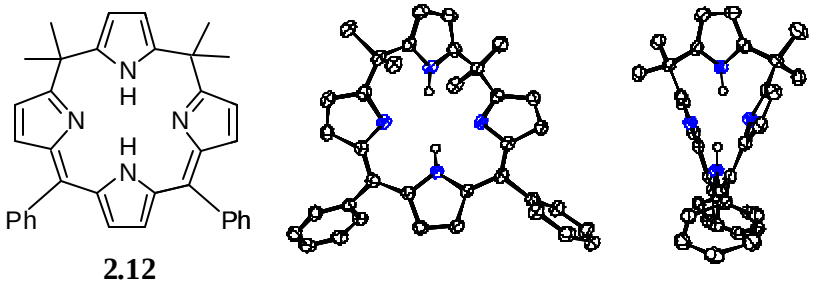

2.12

Figure 2.2 Drawing, top and side ORTEP views of **2.12**. Most hydrogen atoms have been omitted for clarity. Thermal ellipsoids are scaled to the 40 % probability level.[85]

Porphomethenes (calix[4]phyrins-(**1**.*1*.*1*.*1*); **2.1**) are less common than porphodimethenes due to their strained conformation, as illustrated in the solid state X-ray structures of **2.13** (Figure 2.3),[85] and the associated ease with which they may be "oxidized back" to the corresponding porphyrin species. Floriani *et al.* have developed a method that provides both metalated and metal free porphomethenes and 5,15-disubstituted porphodimethenes on a large scale. It is predicated on a tin-assisted dealkylation of *meso*-octaethylporphyrinogen, followed by transmetalation to a lithium derivative and subsequent hydrolysis. This procedure is noteworthy because at the time of its publication in 1999, it provided the first examples of oxidatively stable porphomethene and

porphodimethene derivatives bearing unsubstituted pyrroles and fully alkylated meso positions.[90]

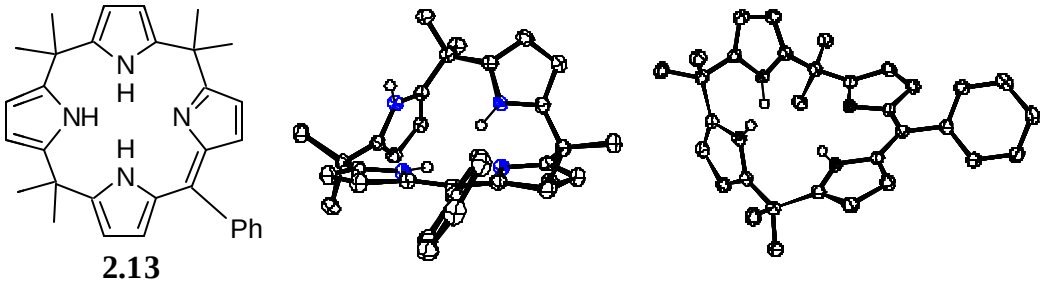

2.13

Figure 2.3 Drawing, top and side ORTEP views of **2.13**. Most hydrogen atoms have been omitted for clarity. Thermal ellipsoids are scaled to the 40% probability level.[85]

An important orthogonal development has been the discovery of reactions that allow for the preparation of multiple, mixed calixphyrin systems from single step reactions that involve only a few simple reactants. Senge developed a method using sterically hindered starting materials that yields stable free-base porphomethenes, as well as 5,10- and 5,15- disubstituted porphodimethenes. Specifically, by reacting pivalaldehyde with aryl-substituted aldehydes and pyrrole, oxidation-resistant hydroporphyrins were obtained.[98]

The Sessler group has been heavily involved in the development of modular methods for the synthesis of calix[4]phyrin derivatives. In particular, reacting a dipyrrolylmethane unit (one sp^3 hybridized bridging pro-meso carbon atom) with two molar equivalents of pyrrole in acetone, followed by DDQ oxidation, was found to yield a mixture of 5,15-disubstituted porphodimethene and porphomethene products (**2.10** and **2.13**). Starting with an appropriate

tripyrrane (two sp^3 hybridized pro-meso bridging atoms), the same conditions were found to yield a 5,10-porphodimethene which was shown to be highly distorted in the solid state (i.e., **2.12** a calix[4]phyrin-(**1**.**1**.*1*.*1*). Starting with the bilane (tetrapyrrane; three sp^3 hybridized pro-meso carbon atoms) under analogous reaction conditions did not yield the corresponding phlorin or isoporphyrin. Rather, a 5,15-disubstituted porphodimethene (calix[4]phyrin-(**1**.*1*.**1**.*1*)) with a meso-hydroxy substituent was obtained. Reaction of this latter species with $ZnCl_2$ under aerobic conditions induced dehydration of the molecule to form a metalated isoporphyrin-type species **2.6** (R^1 = Me, R^2 = R^3 = H, R^4 = Ph). This species, characterized by X-ray analysis,[85] is comparable to that initially observed by controlled potential oxidation of *meso*-TPP[9] or obtained by acid catalyzed condensation of dipyrrolylmethane precursors in the presence of zinc acetate.[7,35]

Sessler and Král and coworkers have also introduced an alternative synthetic methodology that involves switching the origin of the sp^3 and sp^2 centers. Specifically, by starting with a dialkyl substituted dipyrrolylmethane and condensing it with an aldehyde, the sp^3 hybridized centers get "built in" to the macrocyclic framework during the critical ring-forming step (Figure 2.4, pathway A). This "swap" allows for the incorporation of bulkier groups on the sp^3 bridging carbons than the original methodology would allow (Scheme 5, Pathway B). For instance, pentamethylene, phenyl, and 2,2'-biphenyldiyl entities may either be appended off these centers or incorporated into them. Presumably, this greater ability to incorporate large substituents into hydroporphyrins when they

are used as the electrophilic "partners" for oligopyrroles, reflects both the low reactivity of acetone and the steric encumbrance that would be inherent in using bulky oligopyrroles as reactants in such condensations.[82]

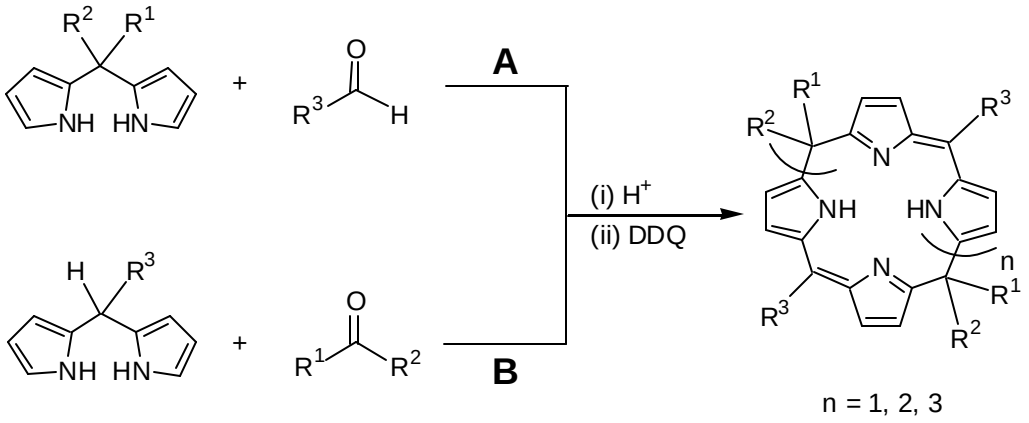

Figure 2.4 Synthesis of calix[n]phyrins using dipyrrolylmethane precursors.

2.1.4 Expanded Calixphyrins

The chemistry of higher order or "expanded" calix[*n*]phyrins (n > 4) is still in its infancy. While Smith has reported the synthesis of iso-oxopentaphyrin (obtained by oxidation of oxopentaphyrin),[99] only the Vogel group and the Sessler group have reported the preparation of purely pyrrole-derived expanded calixphyrins. Vogel's entry into this area came during attempts to synthesize a bimetallic nickel(II) complex of diketo-octaphyrin-(1.1.1.1.0.1.1.1.0). Instead of obtaining his desired product, Vogel and co-workers isolated the bis-nickel complex of the bicorrole **2.14**, a finding that raises the question of how the sp^3 bridging carbon atom (spiro center) influences the interactions between the two macrocyclic subunits.[100] Vogel has made further contributions to this area by

demonstrating that a range of cyclooctapyrroles (also known as octaphyrins) may be obtained from the MacDonald condensation of diformylbipyrrole with various dicarboxylic acid-substituted oligopyrroles under conditions that were expected to yield the tetrapyrrolic product, *trans*-corrphycene. While not extensively studied, larger materials, including a calix[12]phyrin-(**1**.0.**1**.*1*.**1**.0.**1**.*1*.**1**.0.**1**.*1*) analog, were also obtained. The octapyrrolic products obtained were all found to adopt chiral figure eight structure as illustrated by the line drawing of the calix[8]phyrin-(**1**.0.**1**.*1*.**1**.0.**1**.*1*) **2.15**.[100]

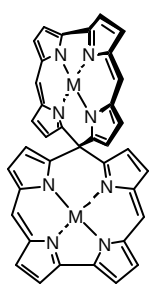

2.14

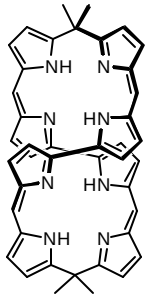

2.15

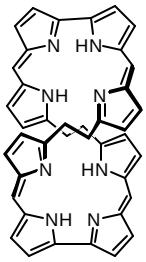

2.16

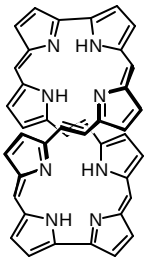

2.17

Vogel and coworkers also prepared a calix[8]phyrin-(**1**.0.**1**.*2*.**1**.0.**1**.*2*) species **2.16** that contains two bridging ethylene groups. (Here, the use of the digit 2 in italics is meant to denote the presence of the two atom sp^3 hybridized bridges.) They found that this calix[8]phyrin system could be oxidized to give the expanded porphyrin **2.17** with complete conjugation throughout the macrocycle. Interestingly, the conformations of the oxidized and non-oxidized forms of this octapyrrolic skeleton were found to be similar; apparently the conformation-defining influence of the apical bipyrrolic subunits dominates over that associated with a change in linking ethylene/ethene hybridization. Currently, these are the only free-base expanded calix[*n*]phyrin systems to incorporate direct α-linked oligopyrrolic subunits (e.g., bipyrrole) into

their frameworks. The octapyrrolic species were found to form binuclear metal complexes with Pd(II) and Cu(II).[101]

In work very different from that of the Vogel group, Sessler *et al*. have recently found that the condensation of mesityldipyrrolylmethane with acetone in the presence of a wide range of acid catalysts (*e.g*., TFA, MSA, etc.) at room temperature, followed by DDQ oxidation, produces not only the expected 5,15-disubstituted porphodimethene product but also the unprecedented higher order calix[6]phyrin-(**1**.*1*.**1**.*1*.**1**.**1**) and calix[8]phyrin-(**1**.*1*.**1**.*1*.**1**.*1*.**1**.*1*) species (Figure 2.4, Pathway B, R^1 = R^2 = Me, R^3 = mesityl, n= 2 and 3 respectively) along with trace quantities of acyclic oligopyrroles. The total and relative yields of each product were found to be strongly dependent on the amount and type of catalyst. The X-ray structure of the calix[8]phyrin **2.18** product formed in this way (Figure 2.5) reveals a distinct bowl-like conformation, with each pyrrole group oriented in a different direction than its neighbors.[80]

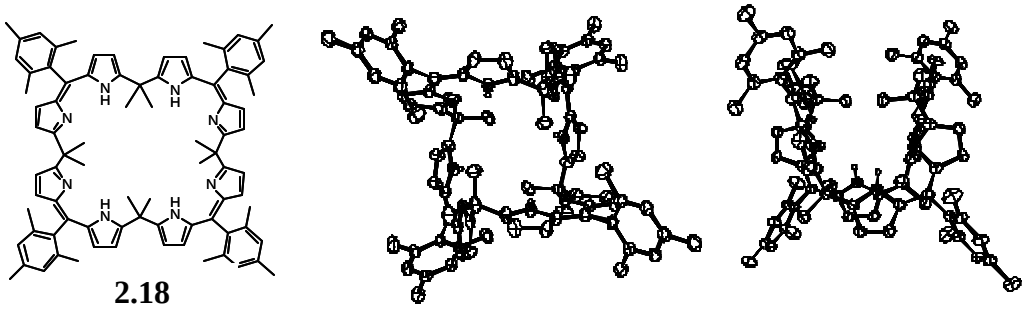

2.18

Figure 2.5 Drawing, top and side ORTEP views of **2.18**. Most hydrogen atoms have been omitted for clarity. Thermal ellipsoids are scaled to 40% probability level.[80]

This structure led Sessler and coworkers to infer that, as is true for typical 5,15-disubstituted porphodimethenes with their roof-like structures enforced by the sp^3 hybridized bridging meso carbon atoms, rather distorted structures will be the norm in higher order calix[*n*]phyrin chemistry. This is likely to be especially true in systems such as **2.18** and its smaller homologue, a calix[6]phyrin-(**1**.*1*.**1**.*1*.**1**.*1*) species, that contain meso-like carbons with alternating hybrization.[80] Preliminary anion binding studies of these "alternating" systems revealed a slight affinity for anions in the case of the calix[6]- and calix[8] products; however, the calix[4]phyrin-(**1**.*1*.**1**.*1*) was found to coordinate Cu(II) and Zn(II), and the calix[6]phyrin-(**1**.*1*.**1**.*1*.**1**.*1*) Co(III) and Ru(III), as judged from spectroscopic and mass spectrometric analysis.

2.1.5 Synthesis and Solid State Structure of 5,5-10,10-20,20-25,25-octamethylcalix[6]phyrin

As an extension of the initial foray of the Sessler group into expanded calixphyrin synthesis, Dr. Christophe Bucher discovered that by using appropriate acyclic polypyrrolic precursors it was possible to modify the ratio of higher order calix[*n*]phyrins as well as the distribution of these bridging centers within the macrocyclic skeleton. Condensation of a *gem*-dimethyl-substituted tripyrrane with pentafluorobenzaldehyde followed by DDQ oxidation gave the calix[6]phyrin-(**1**.*1*.*1*.**1**.*1*.*1*) **2.20** as well as trace quantities of the calix[9]-(**1**.*1*.*1*.**1**.*1*.*1*.**1**.*1*.*1*) analog **2.21** (see Figure 2.14, p. 111).[81]

Scheme 2.1 Synthesis of calixphyrin **2.20**

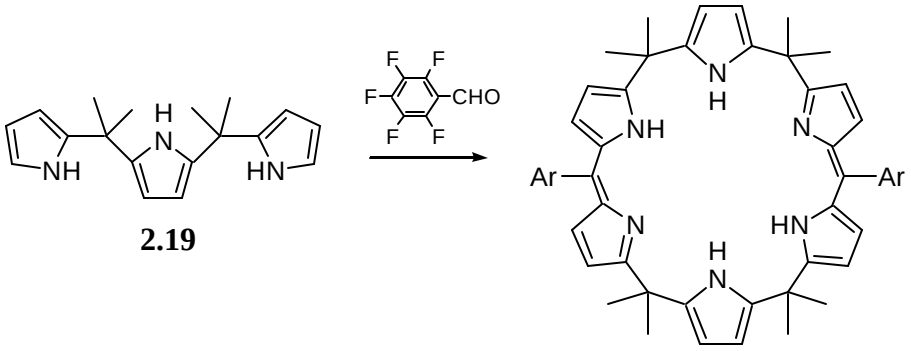

2.19 **2.20**

Reagents: (i) DCM, rt, Ar, 10h. (ii) DDQ

Single crystal X-ray diffraction analysis of **2.20**·H_2O revealed a semi-roof-like structure with apexes defined by the opposing sp^2 hybridized meso-like carbon centers (Figure 2.6). The phenyl groups were found to be oriented in a *syn* fashion with respect to one another. All the pyrrole subunits were oriented in towards the cleft-like cavity and were found to be bound to a water molecule. The alternating geometric arrangement of the sp^2 and sp^3 hybridized meso centers seen in the X-ray structure of **2.20**·H_2O was found to be reflected in the ^{1}H NMR spectroscopic properties of the system, particularly in the resonances ascribed to each pyrrole subunit. In the original calix[6]phyrin-(**1**.*1*.**1**.*1*.**1**.*1*) **2.18**, the macrocycle consists of four oxidized dipyrrolylmethane units separated by sp^3 hybridized bridging carbon atoms. This causes the pyrroles along the ring to contain alternatively imine N- and amine NH-type heteroatoms in a ratio of 3:3. Calix[6]phyrin-(**1**.*1*.*1*.**1**.*1*.*1*) **2.20**, on the other hand, is comprised of two oxidized dipyrryolylmethane units separated by a pyrrole that is, in turn, flanked by two

"insulating" sp^3 hybridized tetrasubstituted bridging carbon centers. This results in a NH to N ratio of 4:2, as well as two calixpyrrole-like pyrroles with NH heteroatoms oriented in a fashion that makes them potentially suitable for anion binding.[81] In both cases, the ratios are apparent from integrations of the relevant signals in the ^{1}H NMR spectra.

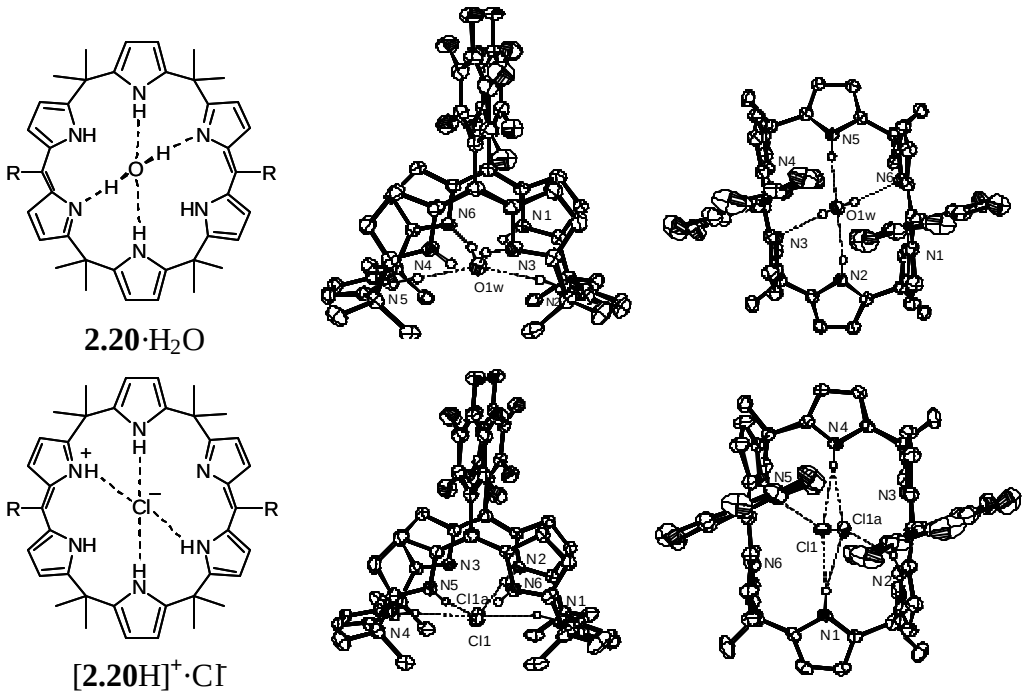

Figure 2.6 Drawing and ORTEP views of **2.20**·H_2O and [**2.20**H]$^+$Cl$^-$ (R = C_6F_5) showing the hetero atom labeling scheme. Hydrogen bonding interactions are indicated by dashed lines. Thermal ellipsoids are scaled to the 40 % probability level.[81]

2.1.6 Anion binding studies of 5,5-10,10-20,20-25,25-octamethylcalix[6]phyrin

One of the motivations for preparing larger calix[*n*]phyrins (n > 4) was to explore whether they, like the calix[*n*]pyrroles and expanded porphyrins to which they bear chimeric resemblence, would function as anion receptors. Surprisingly, standard UV-visible spectroscopy-based anion binding studies in acetone revealed that the unprotonated form of **2.20** displayed little affinity for various anions (e.g., Cl^-, Br^-, I^-, NO_3^-, HSO_4^-), possibly as a result of the strongly bound water molecule inside the cavity (Figure 2.7). As shown in Figure 2.6, the monoprotonated form of **2.20**, however, was shown to bind Cl^- in the solid state. This single X ray crystal was grown by slow evaporation of a dichloromethane solution that had been washed with a 1N HCl solution. In light of this, anion binding studies were initially attempted in dichloromethane. This same protonation could not be effected through the addition of dichloromethane soluble organic acids such as trifluoroacetic acid and methanesulfonic acid, however, and resulted in what appeared to be partial conversion from the free base directly to the diprotonated form as evidenced by the emergence of an absorption band at 540 nm (Figure 2.8).

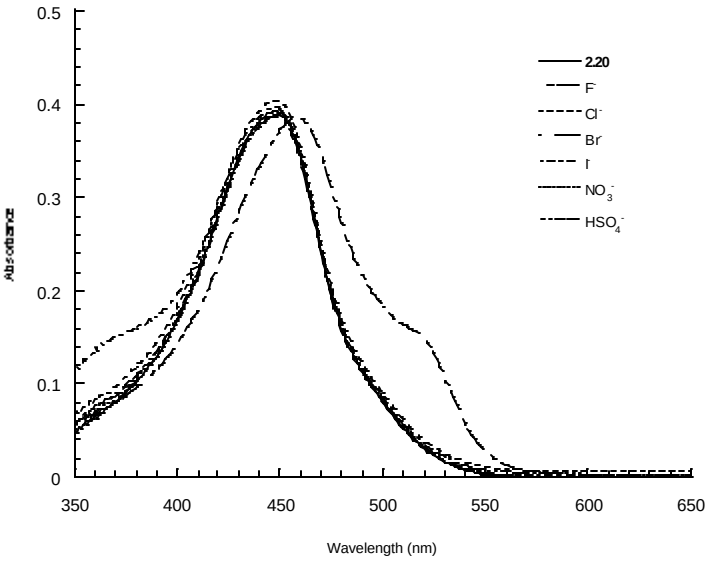

Figure 2.7 Qualitative UV-visible studies in acetone of **2.20** showing the effects, if any, caused by the addition of approximately 5 molar eqv. of F^-, Cl^-, Br^-, I-, NO_3^-, and HSO_4^- in the form of their tetrabutylammonium salts.

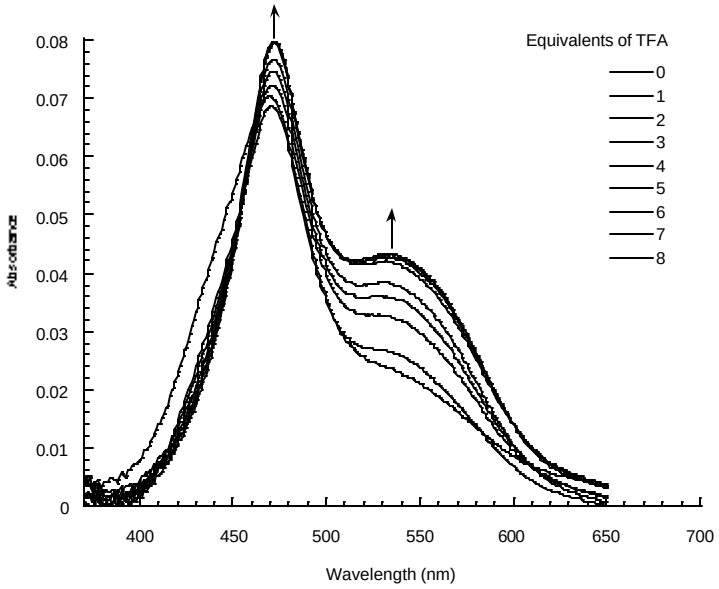

Figure 2.8 UV-visible spectroscopic titration of a 1.19 x 10^{-5} M solution of **2.20** titrated with trifluoroacetic acid from 0 – 8 eqv. in spectroscopic grade dichloromethane.

In light of this apparent complication, analogous titrations were undertaken in spectroscopic grade acetone. Unfortunately, the use of trifluoroacetic acid as well as methane sulfonic acid resulted in non-isosbestic behavior in the course of what was presumed to be the conversion of free base **2.20** into its corresponding diprotonated form [**2.20**·2H]$^{2+}$. Surprisingly, the use of H_2SO_4·30% SO_3 proved to be very effective, however. Addition of this acid to a solution of **2.20** in acetone resulted in the smooth conversion of the initial yellow solution of the free-base to a pink solution of the diprotonated form. This color change corresponded to a concomitant decrease in the absorption band at 449 nm and increase in the absorption band at 499 nm (Figure 2.9). Full

conversion to the protonated species occurred after the addition of 90 molar equivalents of $H_2SO_4 \cdot 30\%\ SO_3$.

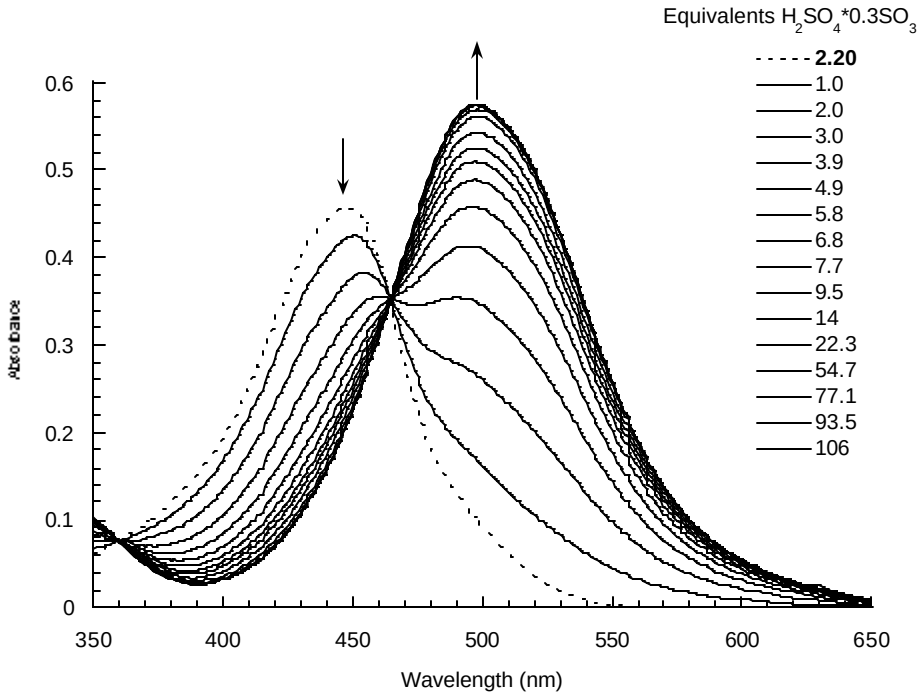

Figure 2.9 UV-visible spectroscopic titration of a 9.33 x 10^{-6} M solution of **2.20** with $H_2SO_4 \cdot 0.3SO_3$ from 0 – 106 eqv. in spectroscopic grade acetone. This effects conversion to $[\mathbf{2.20} \cdot 2H]^{2+}$.

Anion recognition studies were carried out using the fully (doubly) protonated species $[\mathbf{2.20} \cdot 2H]^{2+}$, and revealed an affinity of $[\mathbf{2.20} \cdot 2H]^{2+}$ for Br^-, Cl^-, and I^-. A control anion, HSO_4^-, was also tested for its binding affinity to assist in assessment of the binding mode of **2.20** prior to binding the halide. For instance, in the presence of 90 equivalents of $H_2SO_4 \cdot 0.3SO_3$ the host could bind the halides *via* direct "coordination" to $[\mathbf{2.20} \cdot 2H]^{2+}$, or *via* displacement of hydrogen sulfate counter anions in ion pairs such as $[\mathbf{2.20} \cdot 2H]^{2+} \cdot 2HSO_4^-$ or $[\mathbf{2.20} \cdot 2H]^{2+} \cdot HSO_4^-$.

Figure 2.10 shows the UV-visible titrations of [**2.20**·2H]$^{2+}$ with tetrabutyl ammonium salts of Cl$^-$ (Figure 2.10 a), Br$^-$ (Figure 2.10 b), I$^-$ (Figure 2.10 c) and HSO_4^- (Figure 2.10 d). Titrations with all four anions result in a decrease in the absorption band at 499 nm. In the case of both Cl$^-$ and Br$^-$, the emergence of peaks at 470 nm and 525 nm is seen with increasing concentration of the anion.

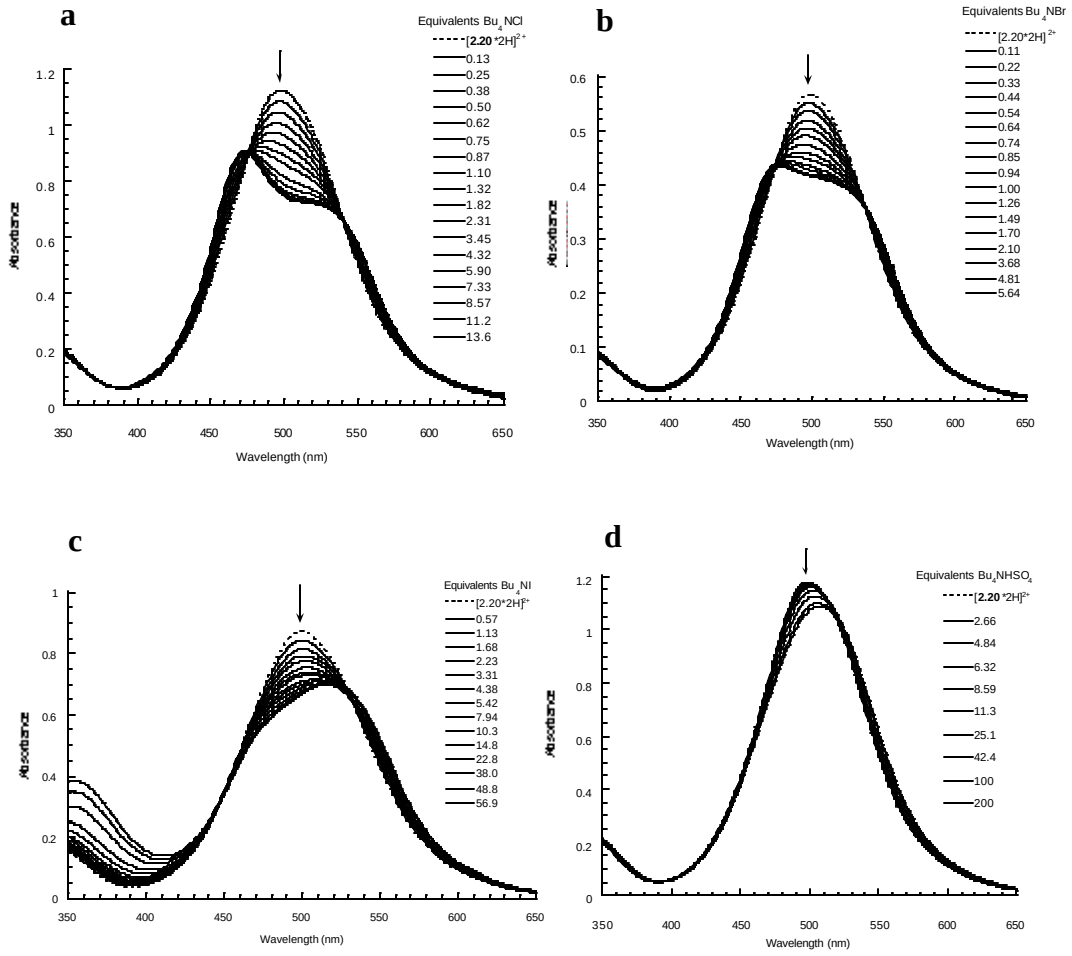

Figure 2.10 UV-visible titrations in acetone of (a) A 1.57 x 10^{-5} M solution of [**2.20**·2H]$^{2+}$ with Cl^- from 0– 14 eqv.; (b) A 9.80 x 10^{-6} M solution of [**2.20**·2H]$^{2+}$ with Br^- from 0 – 6 eqv.; (c) A 1.57 x 10^{-5} M solution of [**2.20**·2H]$^{2+}$ with I^- from 0 – 57 eqv.; (d) A 1.67 x 10^{-5} M solution of [**2.20**·2H]$^{2+}$ with HSO_4^- from 0 – 200 eqv.

A broad spectrum with a single decreasing peak at 525 nm was seen in the case of I^-, while the control experiment with HSO_4^- resulted only in a gradual decrease and red shift of the absorption intensity to 510 nm. Full saturation of the

binding events, as determined by a lack of subsequent spectral response, occurred after the addition of 13 equivalents of Cl^-, 6 equivalents of Br^-, 56 equivalents of I^-, and 200 equivalents of HSO_4^-. Figure 2.11 shows the non linear least squares curve fitting analysis of all four anions. In the case of Cl^- (Figure 2.11 a) and Br^- (Figure 2.11 b) a good fit to a 1:1 binding isotherm could not be made. Close examination of the curves showed a sharp leveling off and partial decrease in the change in absorbance values, which likely reflect more complex equilibria than simple anion binding or displacement processes (e.g., a mixture of anion binding and anion displacement or formation of 2:1 complexes). Both I^- (Figure 2.11 c) and HSO_4^- (Figure 2.11 d) curves could be fit nicely, however, and resulted in binding affinities of 25,500 ± 900 M^{-1} and 3,500 ± 390 M^{-1}, respectively.

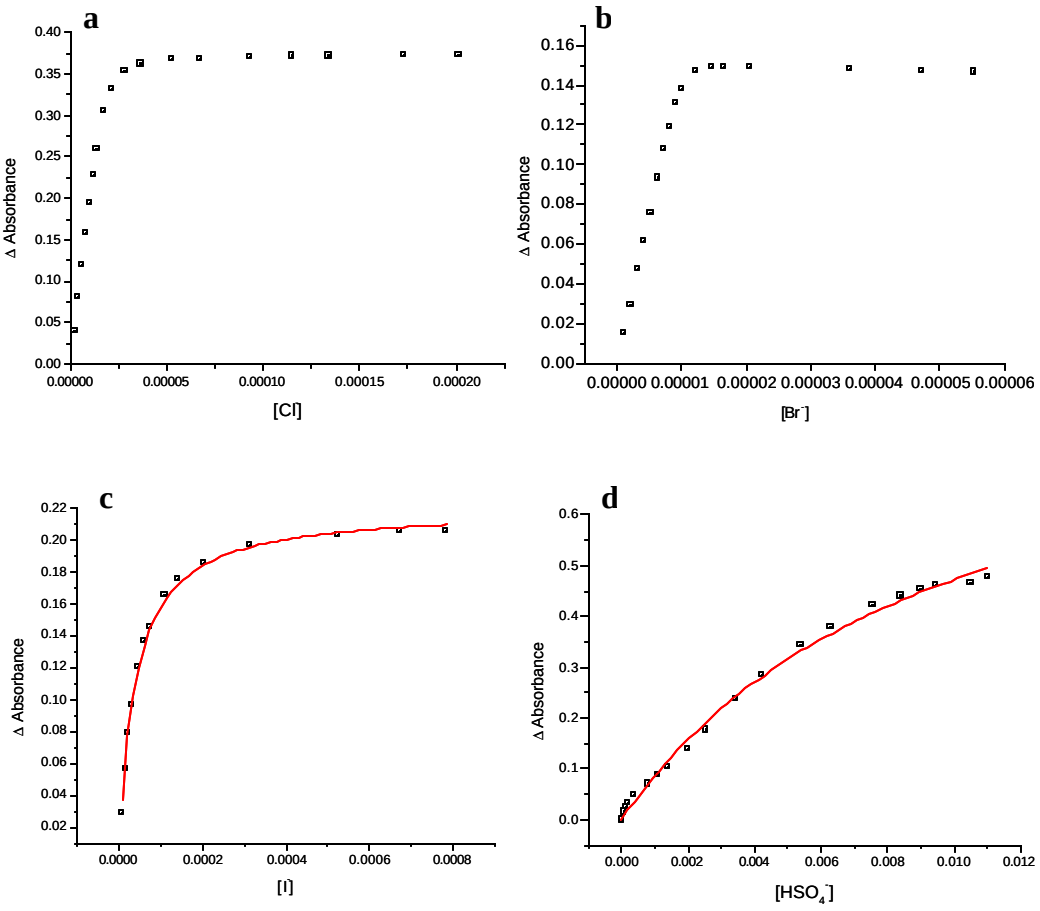

Figure 2.11 Nonlinear least squares analysis of titrations from Figure 2.10. (a) Unable to fit results from addition of Cl^-; (b) Unable to fit results from addition of Br^-; (c) Addition of I^- results in a binding affinity of 25,500 ± 900 M-1; (d) Addition of HSO_4^- results in a binding affinity of 3,500 ± 390 M-1.

The fitting of the binding isotherm for HSO_4^- was accomplished by taking into consideration the 90 molar equivalents of H_2SO_4. By assuming that **2.20** exists in its diprotonated form under these conditions, the co-existence of two

equivalents of HSO_4^- has to be assumed (Equation 2.1). This inference comes from an analysis of the potential competing equilibria that exist in solution.

Eq. 2.1

$$\mathbf{2.20} + 90\ H_2SO_4 \rightleftharpoons [\mathbf{2.20}\cdot H]^+ + 89\ H_2SO_4 + HSO_4^- \rightleftharpoons [\mathbf{2.20}\cdot 2H]^{2+} + 88\ H_2SO_4 + 2\ HSO_4^-$$

While the presence of these two molar equivalents of HSO_4^- cannot be ignored, it is also necessary to consider other potential sources of HSO_4^- other than from tetrabutyl ammonium sulfate since these would also compete for the receptor and thus modify the effective stoichiometry of the equilibrium. Additional sources of HSO_4^- include the sulfuric acid solution itself. The role of the sulfur trioxide is to remove water and maintain a fuming acidic medium; however, it is possible for an equilibrium to exist between the sulfur trioxide and the sulfuric acid, resulting in the production of hydrogen sulfate (Equation 2.2).

Eq. 2.2 $$H_2SO_4 + SO_3 \rightleftharpoons HSO_4^- + HSO_3^+$$

More important is the equilibria involving the acetone used as the solvent and the sulfuric acid solution (Equation 2.3). Based on the relative pK_a values of sulfuric acid (-3) and protonated acetone (-7.2) recorded in aqueous media, the equilibrium is expected to lie to the left, toward sulfuric acid. However, when the relative concentrations of sulfuric acid (approximately 2×10^{-4} M) and acetone employed as a solvent (ca. 14.6 M) are taken into consideration, the equilibrium is expected to lie to the right, toward hydrogen sulfate.

Eq. 2.3 $H_2SO_4 + (CH_3)_2CO \rightleftharpoons HSO_4^- + H(CH_3)_2CO^+$

These contradictory predictions correlated to a lack of certainty concerning the number of equivalents of hydrogen sulfate that would pre-exist in solution. Further complicating matters was the fact that the pK_a values used to make them are for aqueous solutions. Thus it was considered best to ascertain the effective number of HSO_4^- equivalents by experiment. A series of non linear least squares analyses was thus performed on the data obtained from the titration of $[\mathbf{2.20}\cdot 2H]^{2+}$ with HSO_4^- (Figure 2.10 d, p. 101). By varying the number of pre-existing hydrogen sulfate anions assumed to pre-exist in solution from 0 – 90 equivalents and looking for the best nonlinear least squares fit it was hoped that an accurate count could be made. The results of this analysis, which examined error, R value, and Chi^2, clearly indicate that the best fit for the data across all three of these variables is the assumption of two pre-existing equivalents of hydrogen sulfate (K_a = 3,550 M^{-1}) (Table 2.1). Because attempts to fit the binding profile using additional putative equivalents of HSO_4^- resulted in an increasingly poor fit, it was thus assumed that 1) either a minimal amount of HSO_4^- is produced from sulfuric acid self-ionization (Eq. 2) or solvent protonation (Eq. 3) or 2) that the species formed by solvent protonation, hydrogen sulfate anion and protonated acetone, exist in the form of a tightly bound ion pair.

Table 2.1 Nonlinear least squares curve fitting of the data from the titration of $[\mathbf{2.20}\cdot 2H]^{2+}$ with Bu_4NHSO_4 assuming differing quantities of pre-existing HSO_4^-.

Pre-existing HSO_4^- eqv.	K_a (M^{-1})	Error (%)	R	Chi^2
0	8,300	18	0.971	3.31×10^{-6}
1	5,500	11	0.991	1.01×10^{-6}
2	3,550	11	0.993	8.47×10^{-7}
3	2,280	17	0.988	1.33×10^{-6}
4	1,400	27	0.982	2.04×10^{-6}
5	800	47	0.975	2.83×10^{-6}
6	350	105	0.968	3.63×10^{-6}
7	10	3,500	0.961	4.41×10^{-6}
90	-750	--	--	--

Once the above predicative studies were complete, efforts were made to quantify the anion binding process. Both I^- and HSO_4^- yielded Job plots[102] with inconclusive maxima (an example of which is shown in Figure 2.12) and relatively linear analysis in the form of Benesi-Hildebrand plots[102] (Figure 2.13), revealing what appeared to be 1:1 binding stoichiometry in each case (Figure 2.13a for I^- and Figure 2.13c for HSO_4^-). However, upon analysis using x-reciprocal Scatchard plots,[102] curvature was seen for both I^- (Figure 2.13 b) and HSO_4^- (Figure 2.13d), which is indicative of complex solution state equilibria. In

light of this ambiguous data, absolute stoichiometry of the bound complexes cannot be stated with complete certainty.

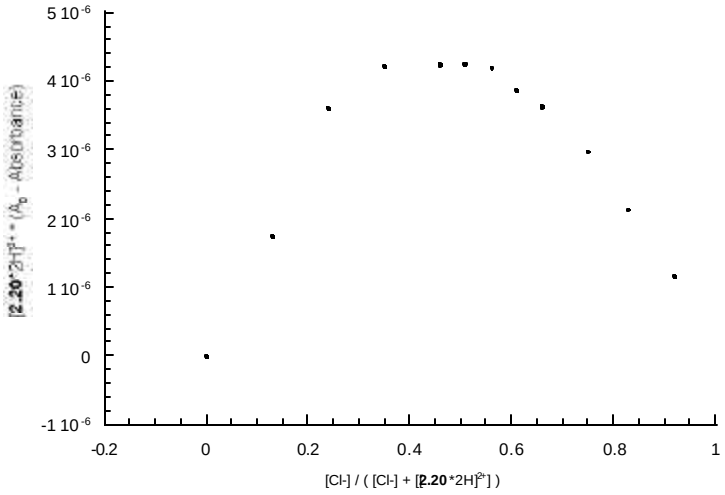

Figure 2.12 Inconclusive Job plot analysis of a concentration of 1.35 x 10^{-5} M **[2.20**·2H]$^{2+}$ with Bu_4NCl in acetone.

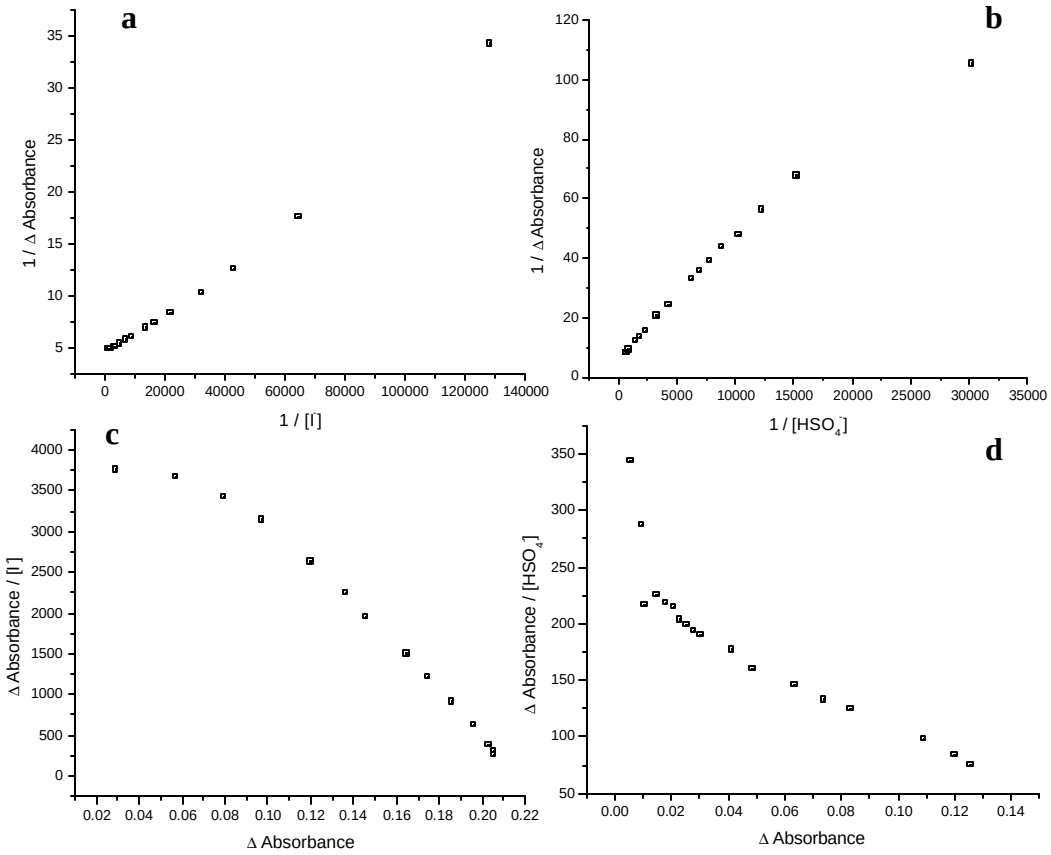

Figure 2.13 Data measured in acetone using a solution concentration of 1.57 x 10^{-5} M [**2.20**·2H]$^{2+}$ titrated with I⁻ from 0 – 56 eqv. to give (a) a Benesi-Hildebrand plot and (c) a Scatchard plot; a concentration of 1.67 x 10^{-5} M [**2.20**·2H]$^{2+}$ titrated with HSO_4^- from 0 – 200 eqv. to give (b) a Benesi-Hildebrand plot and (d) a Scatchard plot.

In order to obtain an estimate for the true binding affnity of [**2.20**·2H]$^{2+}$ for I⁻, it is necessary to consider the presence of the two pre-existing equivalents of HSO_4^- in solution before the addition of I⁻, and the presumed need to displace it from the binding pocket prior to I⁻ binding. Although it is possible that the true binding constant for I⁻ interacting with [**2.20**·2H]$^{2+}$ could be as high as 8 x 10^7 M^{-1}

(based on K_a (I^-) x K_a (HSO_4^-)), the fact that the binding stoichiometry of both anions was ambiguous throws an air of caution over this conclusion. Additionally, the fact that HSO_4^- binds [**2.20**·2H]$^{2+}$ with a lower affinity than I^- indicates that the true binding value of I^- is likely not a simple multiplication of the two binding affinities but rather only involves a portion of the binding affinity of [**2.20**·2H]$^{2+}$ with HSO_4^- since [**2.20**·2H]$^{2+}$ should prefer to bind with the more strongly bound I^- anion.

In any event, the magnitude of this binding is remarkable and provides an incentive to study additional calixphyrin receptors. It is possible that through the design of other systems, the problems of curve fitting and stoichiometry determination seen in this instance could be circumvented, thus leading to receptors with even higher affinities for the more strongly coordinating halide anions Cl^- and Br^-.

2.1.7 Future Directions

As noted in the introduction, the condensation used to produce **2.19** also produces the higher homologue, the [3+3] cyclization product **2.21** (calix[9]phyrin-(**1**.*1*.*1*.**1**.*1*.*1*.**1**.*1*.*1*).[81] Solid state X-ray diffraction analysis revealed a structure similar to that of the calix[6]phyrin **2.20** (Figure 2.6, p. 95).[81] As yet, however, no anion recognition studies have been carried out with this potentially interesting system. Recently Sessler *et al*. have succeeded in preparing the first-ever calix[5]phyrin-(**1**.*1*.*1*.*1*.*1*) **2.22**. This product was obtained by reacting a *gem*-dimethyl substituted pentapyrrane precursor with

pentafluorobenzaldehyde under similar conditions to those used to obtain **2.20**. X-ray diffraction analysis revealed that, as expected, this system is highly distorted, with the phenyl group and adjacent dipyrrolylmethane folded up over the tripyrrane (Figure 2.14). Future directions include probing the anion binding potential of these new systems.

In terms of the design of additional calixphyrins, it is possible to envision an extension of the previous work in terms of varying the combination of starting materials. For instance, condensation of terpyrrole with *gem*-dimethyl substituted diformyldipyrryolylmethane under Lewis acid catalyst conditions could result in a pentaphyrin analog such as **2.23**. Similarly, starting with bis-bipyrrole and using reaction conditions analogous to those used to prepare **2.20** could result in an isorubyrin analog, **2.24**. The resulting diversity in binding pocket size and conjugation pattern is expected to be reflected in interesting structural effects and anion binding properties.

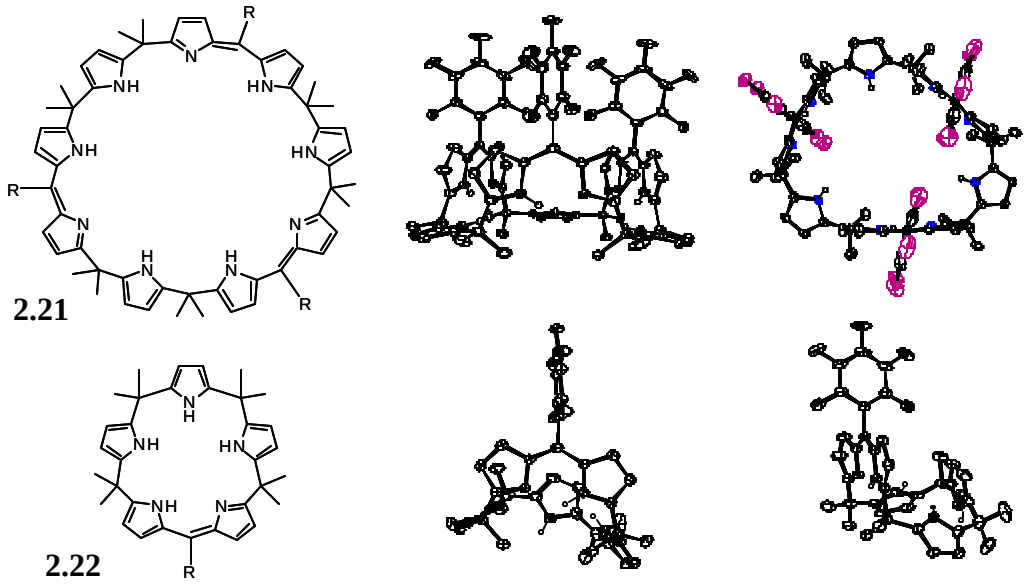

Figure 2.14 Drawing and ORTEP views of **2.21** and **2.22** (R = C_6F_5). Thermal ellipsoids are scaled to the 40 % probability level.[81]

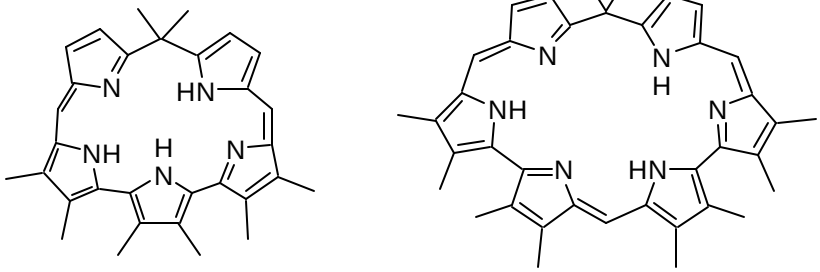

In summary, calix[*n*]phyrins represent an old-but-new set of porphyrin analogs that, because of their unique structures and potential utility in supramolecular cation and anion recognition applications, are beginning to receive increasing attention. The fact that new synthetic methodologies have been put forward in recent years that make efficient syntheses of the metal-free forms

possible will likely only serve to enhance the interest currently attendant to this class of compounds.

2.2 CRYPTAND-LIKE CALIXPYRROLES

A closely related field is the design of expanded or modified calix[*n*]pyrroles. Unlike calixphyrins, with their alternating sp^2 and sp^3 meso carbons, calix[*n*]pyrroles consist of an alternating succession of pyrrole subunits and sp^3-hybridized bridging carbon atoms. These systems are well known for their ability to bind fluoride and other anions both in solution and the solid state.[103,104] This anion-binding ability has been well established in the case of the easily made calix[4]pyrroles,[105-109] and has spawned recent efforts to design and synthesize new homologues. By varying the number of pyrrole moieties, the nature of the meso-like or β-pyrrolic substituents, the binding selectivity and strength of calix[*n*]pyrroles can be fine-tuned.[110] Still, recognizing what has proved to be true for cation recognition, namely that topographically nonplanar systems can display distinctive stabilities and selectivities,[111] increasingly interest has turned to the challenge of preparing three-dimensional polypyrrolic receptors. However, with the exception of a few limited strapped, capped, and catenated expanded porphyrins,[112-114] Schiff base cryptands,[115] and tripod-like open chain derivatives,[116] three-dimensional pyrrole-containing systems remain virtually unknown.[117] Therefore, in collaboration with Dr. Christophe Bucher the synthesis of a calixpyrrole-like cryptand was undertaken. As will be detailed below, this

new system displayed anion-binding behavior that differed substantially from that of simple calix[*n*]pyrroles.[118]

2.2.1 Synthesis and Solid State Structure of the bicyclic[3,3,3]nonapyrrole

The synthesis of the chosen target calixpyrrole-like cryptand **2.26** is summarized in Scheme 2.2. It starts with *gem*-dimethyl-substituted tripyrrane **2.19** (Scheme 2.1, p. 94). Subjecting this key precursor to Clezy formylation yields tripyrrane dialdehyde **2.25** in 20% yield. An acid-catalyzed condensation between this dialdehyde and two equivalents of tripyrrane **2.19** produces the three dimensional product **2.26** in up to 50% yield. While the yields proved highly variable and the synthesis of **2.19** always represented a challenge, it is important to appreciate that product **2.26** represents the first cryptand-like calixpyrrole to have been constructed solely from pyrrole subunits and bridging carbon atoms.

Scheme 2.2 Synthesis of bicyclic[3,3,3]nonapyrrole **2.26**

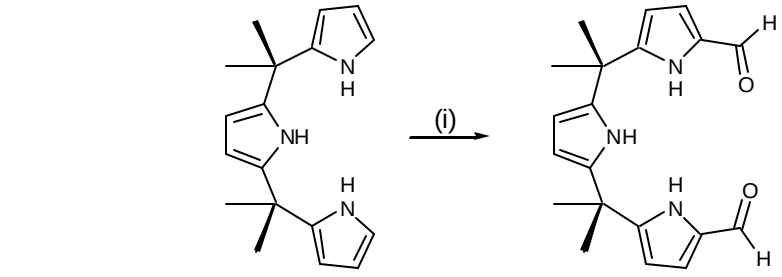

2.19 **2.25**

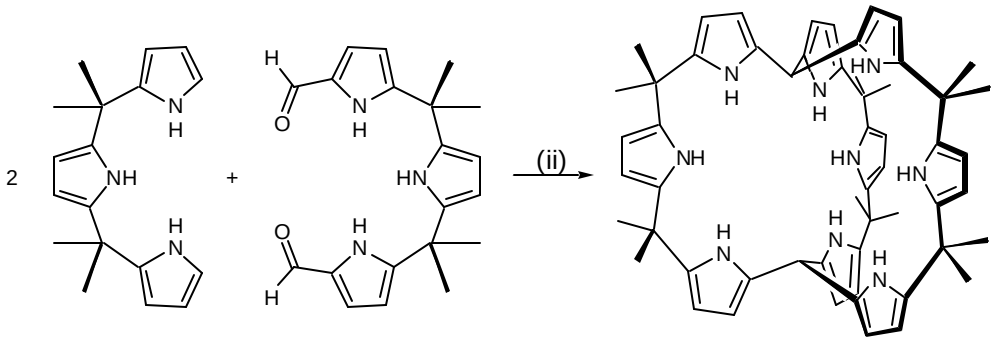

2.26

Reagents: (i) (a) TFA, $CH(OEt)_3$, -10° C; (b) NH_4OH, H_2O, 20%; (ii) TFA, CH_2Cl_2-CH_3CH_2OH, Ar, 0-50%.

Because of the bridge-head carbon atoms, **2.26** can exist, in principle, in the form of three configurational isomers. In the present instance, only one product was actually isolated, and its ^1H NMR spectral characteristics were consistent with a highly symmetrical species. In particular, both meso-like hydrogen atoms appear as a singlet at 4.69 ppm, while three signals attributed to the β-pyrrolic protons are observed between 5.3 and 6 ppm (CD_2Cl_2). Interestingly, the N*H* protons that resonate at 7.49 and 7.67 ppm as two broad signals in a 6:3 relative intensity ratio, shift downfield to 9 and 9.2 ppm,

respectively, when recorded in deuterated acetone. This observation is consistent with relatively strong solvent-pyrrole NH hydrogen-bonding interactions.

The structure of **2.26** was determined by X-ray diffraction analysis. As illustrated in Figure 2.15, the molecule adopts an *in-in* configuration with both meso-like bridging carbon atoms pointing in toward the center of the molecule. The distance between these atoms (C15-C30) is 4.3 Å. The fact that the two bridging CH hydrogen atoms point inward serves to close up the inner core. On the other hand, the resulting configurational, and it is assumed conformational ridigity, coupled with the overall three-dimensional structure, serves to define three identical cavities with three calixpyrrole-like NH motifs that could serve as potential binding sites. In the solid state, three different solvent species are observed in these cavities (Figure 2.16). Two water molecules, bound to each other, are located in one of these sites, whereas a molecule of dichloromethane interacts with the pyrrole moieties of a second cavity through three N–H···Cl hydrogen bonds and two C–H···π interactions. The third cavity, not shown in Figure 2.16, contains only one water molecule hydrogen bonded to two pyrrole NHs (N(3)H and N(1)H). On the basis of these initial solid state observations, anion binding studies were undertaken to determine possible solution state interactions.

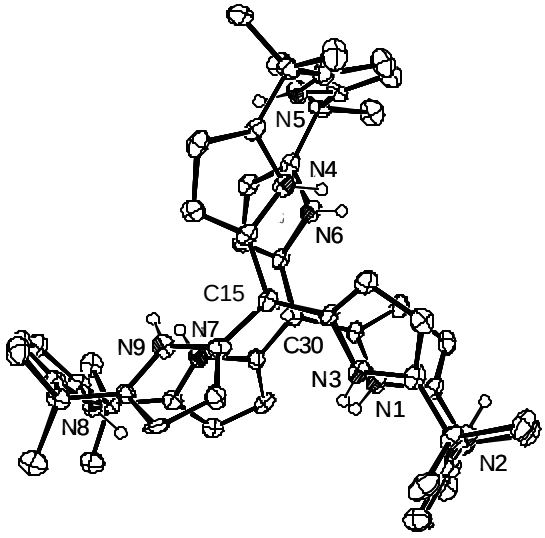

Figure 2.15 Ortep view of **2.26** showing heteroatom labeling scheme. Bound solvent molecules have been omitted for clarity. Thermal ellipsoids are scaled to the 30% probability level.

2.2.2 Proton NMR Anion binding studies of the bicyclic[3,3,3]nonapyrrole 2.26

Tetrabutylammonium salts of fluoride, chloride, bromide, nitrate, dihydrogen phosphate, and thiocyanate were used to determine the affinity of receptor **2.26** for anions. Titrations were performed using ^{1}H NMR spectroscopy in dichloromethane-d_2 in the absence of air. The existence of three identical binding cavities, as observed in the solid state, indicated that **2.26** might stabilize anion complexes of 1:1, 1:2, and 1:3 stoichiometry in solution.

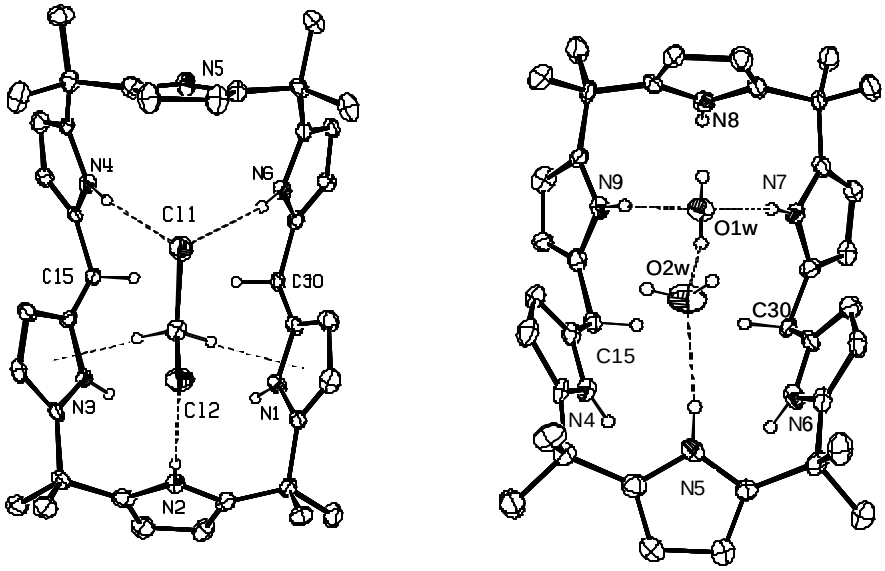

Figure 2.16 Partial Ortep views of two cavities present in **2.26**, showing bound neutral species. All protons are shown in calculated positions. Hydrogen bonding interactions are indicated by dashed lines. Thermal ellipsoids are scaled to the 30% probability level.

A detailed analysis of the ^{1}H NMR spectrum of receptor **2.26** (Figure 2.17) was undertaken prior to commencing the anion binding studies in order to establish a "baseline" against which putative anion induced changes could be judged. The N*H* signals were seen at 7.49 and 7.67 ppm, and correspond to three protons (signal a) and six protons (signal b). The β-C*H* resonances of the pyrroles, each corresponding to six protons (signals c, d and e) occured between 5.4 and 6.0 ppm. The apical C*H* (signal f) resonated at 4.72 ppm, and corresponds to two protons. These signals will be referred to throughout the anion binding discussion.

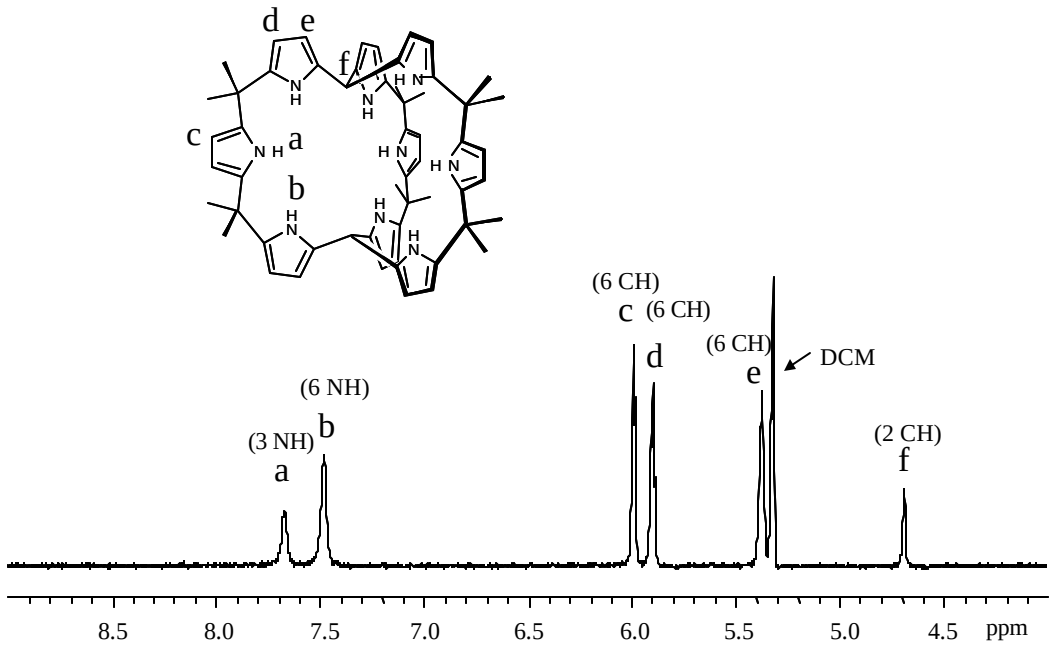

Figure 2.17 Proton spectrum of **2.26** as recorded in CD_2Cl_2.

During the course of the anion titrations, it became apparent that depending on the anion, receptor **2.26** was binding either through a fast or a slow equilibrium process. These processes were evaluated independently and subsequently compared and contrasted. The anions which exhibited a fast-exchange binding mechanism included nitrate, thiocyanate, and bromide. Nitrate induced the most reliable, and easiest to quantify spectral changes and its binding was the most thoroughly analyzed. Figure 2.18 shows a series of ^{1}H NMR spectra recorded during titration up to the point of saturation, something that occurs upon the addition of six molar equivalents of nitrate. At this point one of the N*H* resonances (signal a) have disappeared, while those of signal b have shifted from 7.49 to 8.52 ppm and broadened considerably.

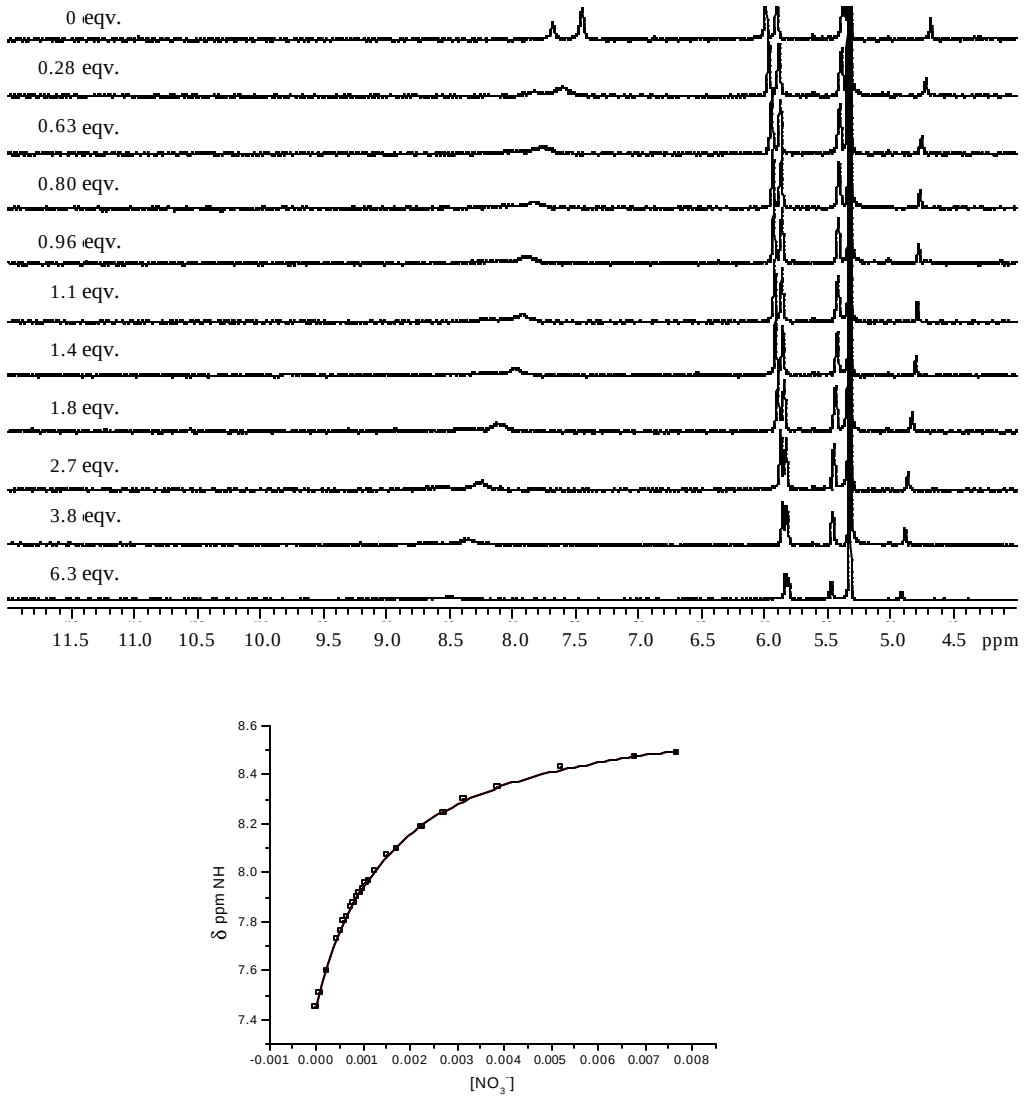

Figure 2.18 Proton spectroscopic titration of **2.26** in CD_2Cl_2 at 7.5 x 10^{-4} M with Bu_4NNO_3 from 0 – 6 eqv. A fit to the binding isotherm is consistent with a 2:1 binding stoichiometry (K_1 = 1,740 ± 75 M^{-1}, K_2 = 420 ± 20 M^{-1}) with two nitrate anions bound to one receptor.

Concurrently, there was a small shift seen in the apical C*H* (signal f) from 4.72 to 4.96 ppm. Nonlinear least squares analysis of the downfield shift of the N*H*s (signals a and b) was consistent with a 2:1 binding stoichiometry (i.e., two nitrate anions to one receptor) and affinity constants of $K_1 = 1{,}740 \pm 75\ M^{-1}$ and $K_2 = 420 \pm 20\ M^{-1}$. Unfortunately, no clear maximum was seen when a Job plot analysis was carried out.

Because the binding data fit only to a 2:1 stoichiometric profile,[102] and due to the fact that there was no loss of symmetry upon binding, a probable binding mode is that shown in Figure 2.19, where the three identical cavities seen in the solid state from Figure 2.15 are maintained, with two of the cavities containing a nitrate, leaving the third cavity empty. Looking down the axis of the apical C*H*s (C15-C30), the cryptand can be viewed as three identical "arms" pointing away from the center in a pinwheel fashion. Envisioning one possible binding mode, each cavity could share a nitrate anion between two adjacent arms of the cryptand, one of which has the N*H*s from the "terminal" pyrroles (signal a) oriented in one direction, and its neighbor with a N*H* from the "middle" pyrrole (signal b) pointed in the opposite direction, sandwiching the nitrate. Attempts to form a 3:1 stoichiometric complex by the addition of a large excess of tetrabutylammonium nitrate proved to be unsuccessful and resulted in the observation of complex spectroscopic features that will be discussed in detail later on in this chapter.

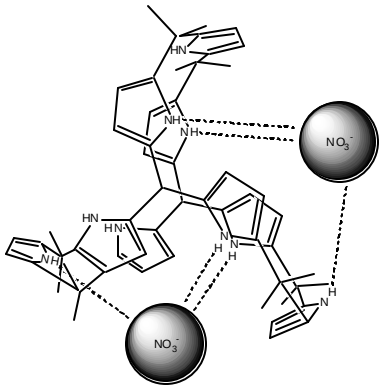

Figure 2.19 Proposed binding mode showing the 2:1 anion complex that is formed when **2.26** is treated with 6 eqv. of Bu_4NNO_3 in CD_2Cl_2.

Thiocyanate as its tetrabutylammonium salt also participated in a fast exchange equilibrium with **2.26** over a concentration range from 0 – 11 equivalents of anion (Figure 2.20). Unlike what is seen upon treatment with nitrate, increasing concentrations of thiocyanate anion produce a downfield shift in both N*H* signals. The N*H* signal corresponding to signal a shifted from 7.67 to 8.28 ppm, while that associated with signal b shifted from 7.49 to 7.93 ppm. The N*H* signals in this case did not broaden to the same extent as those associated with nitrate. Additionally, increasing concentrations of thiocyanate anion did not result in a shift in the apical C*H* peak (signal f); however, after the addition of approximately three equivalents of anion the signal started to broaden. Nonlinear least squares curve fitting of the N*H* (signal b) resulted in a fit to a 1:1 binding isotherm[119] (K_a = 290 ± 20 M^{-1}); attempts to fit a 2:1 binding isotherm[102] were unsuccessful. Unfortunately, as in the case of nitrate no well-defined maximum was seen in the Job plot. Thus, an independent confirmation of stoichiometry couldn't be made.

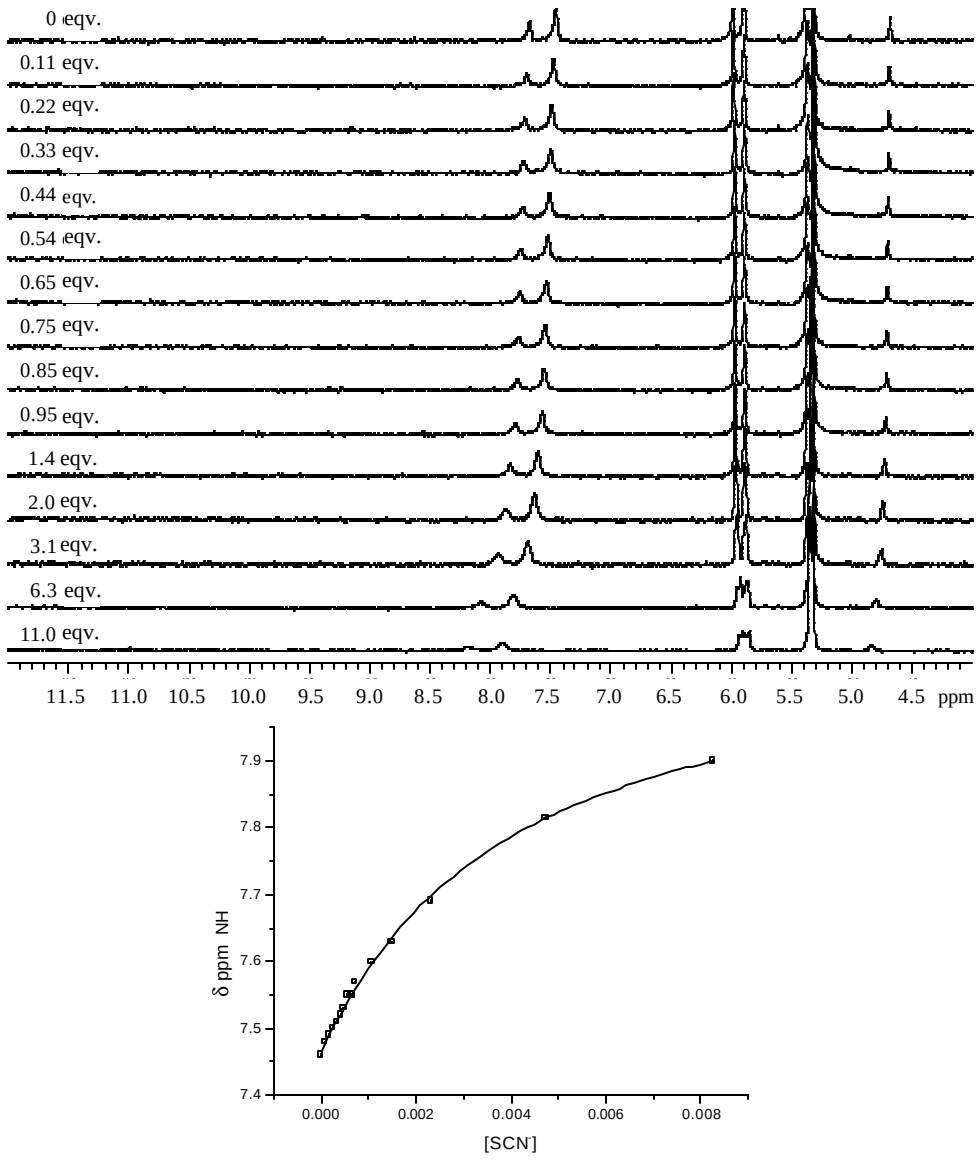

Figure 2.20 Proton spectroscopic titration of **2.26** at 8.3 x 10^{-4} M in CD_2Cl_2 with Bu_4NSCN from 0 – 11 eqv. A fit to the binding isotherm is consistent with a 1:1 binding stoichiometry (K_a = 290 ± 20 M^{-1}).

Evidence for a fast exchange equilibrium was also inferred from a titration of **2.26** with varying concentrations of tetrabutylammonium bromide ranging from 0 – 4.5 molar equivalents (Figure 2.21). As with nitrate, one N*H* (signal a) quickly disappeared and remained impossible to detect for the duration of the titration. Unfortunately, unlike the case with nitrate, the other N*H* peak (signal b) became too broad to locate a maximum after the addition of approximately 0.4 equivalents of bromide anion. Serendipitously, and unlike what was seen with nitrate and thicyanate, one of the β-C*H* protons (signal c) shifted upfield from 5.89 to 5.77 ppm. Due to the N*H* signal disappearing into the baseline, this β pyrrole C*H* signal was monitored in an effort to derive an association constant. Nonlinear least squares curve fitting showed that the binding isotherm could be fit to a 1:1 model[119] (K_a = 1,800 ± 190 M^{-1}) as well as to a binding 2:1 model[102] involving the interaction of two bromide anions to one receptor (K_1 = 1,440 ± 150 M^{-1}, K_2 = 580 ± 150 M-1); both binding modes gave values with acceptable errors (< 20%). Although the binding stoichiometry could not be determined due to an inconclusive Job plot, it is interesting to note that both binding models gave values for the first association process that were within close approximation to one another.

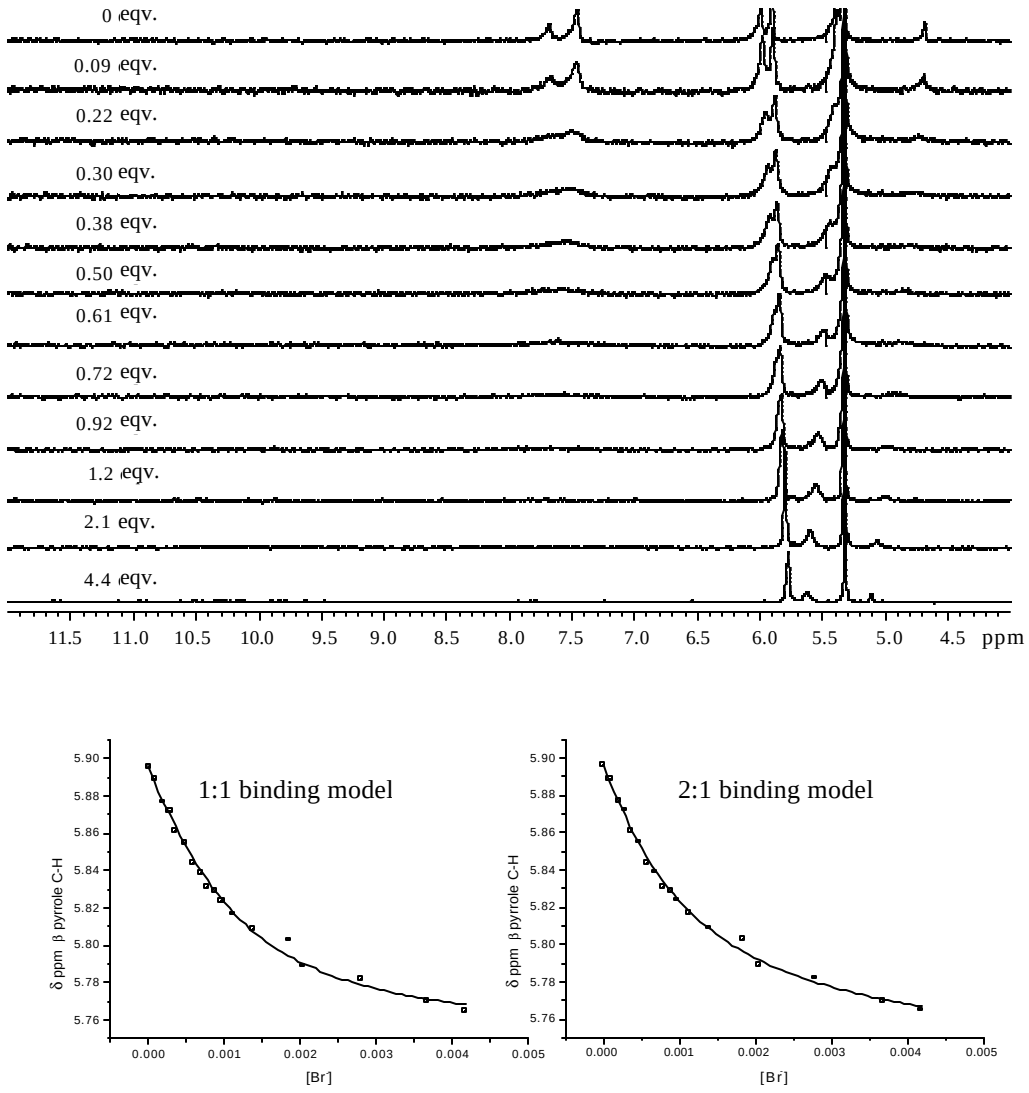

Figure 2.21 Proton spectroscopic titration of **2.26** at 9.5 x 10^{-4} M in CD_2Cl_2 with Bu_4NBr from 0 – 4 eqv. Nonlinear least squares analysis indicating possible 1:1 (K_a = 1,800 ± 190 M^{-1}) or 2:1 binding stoichiometry of two bromide anions to one receptor (K_1 = 1,440 ± 150 M^{-1}, K_2 = 580 ± 110 M^{-1}).

Evidence for a slow exchange binding mode was also seen when **2.26** was treated with dry tetrabutylammonium fluoride from 0 – 6.5 molar equivalents (Figure 2.22). In this instance, the N*H*s (signals a and b) disappeared after the addition of 0.3 equivalents of fluoride anion. After the addition of approximately two equivalents of fluoride, four N*H* signals reappeared at 6.78, 7.97, 10.56, and 11.99 ppm in a 1:2:2:4 relative intensity, respectively. Among these new N*H* signals, only those located at lower field were attributed to pyrrolic protons directly involved in the anion-binding process. The assumption that only six of these new N*H* protons interact with the fluoride anion was supported by low temperature (-10° C) ^{1}H NMR experiments, which revealed ^{19}F-^{1}H splitting (J = 32 and 11 Hz) only for these signals (Figure 2.23). No splitting was observed for the other N*H* signals. Unfortunately, even at this low temperature, no peaks from both **2.26** and [**2.26**·F^{-}] were observed concurrently. Attempts to fit a binding isotherm to the upfield shifts observed for the β-C*H* protons were unsuccessful. Additionally, due to the nature of the slow exchange equilibrium, no Job plot was performed. As a result, no reliable affinity constant or binding stoichiometry could be deduced for fluoride.

Despite the inability to determine stoichiometry conventionally, the fact that the binding event was not complete until the addition of three equivalents of fluoride is taken as an indication of 1:1 binding. Other supporting evidence includes the rise of four separate N*H* signals and their respective integration values. This deduction led to the proposed binding mode shown in Figure 2.24 as a probable conformation of [**2.26**·F^{-}].

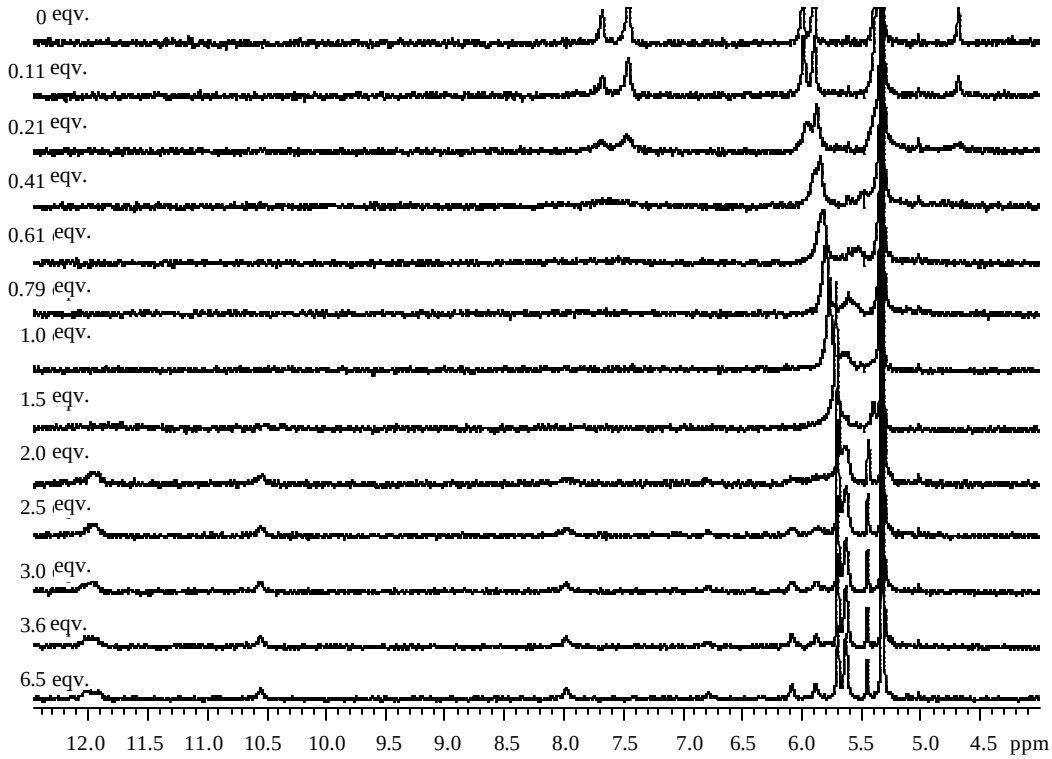

Figure 2.22 Proton spectroscopic titration of **2.26** at 7.3 x 10^{-4} M in CD_2Cl_2 with Bu_4NF from 0 – 6 eqv. No affinity constant could be determined.

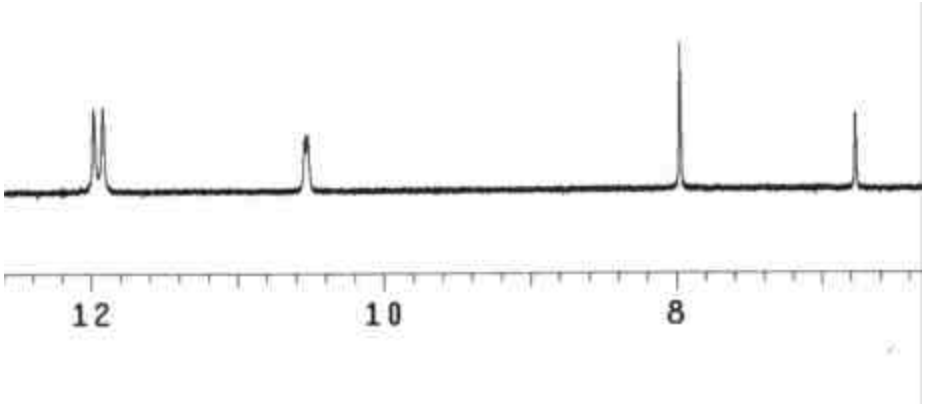

Figure 2.23 Low temperature (-10° C) ^{1}H NMR spectrum of [**2.26**·F^-] (3.5 eqv. of Bu_4NF in a 1.02 x 10^{-3} M solution of **2.26**) illustrating the ^{19}F-^{1}H splitting of the two downfield N*H* resonances (signals a and b) in CD_2Cl_2.

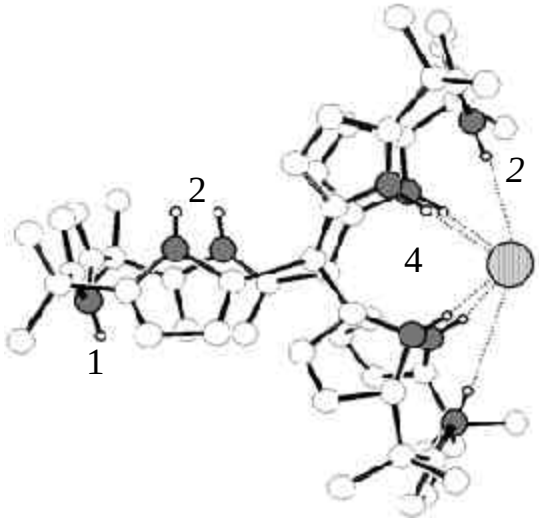

Final NH ppm	Relative Integration
6.78	1
7.97	2
10.56	*2*
11.99	4

Figure 2.24 Proposed binding mode for the fluoride complex formed when Bu_4NF is added to **2.26**.

Somewhat similar binding behavior was observed upon addition of tetrabutylammonium chloride to **2.26** (Figure 2.25). In this case, the two initial peaks located at 7.49 and 7.67 ppm attributed to the N*H* protons (signals a and b) decreased in intensity as chloride was added. Concurrently, four new NH peaks were seen to grow in at 6.86, 7.84, 10.51, and 10.94 ppm. The apex C*H* resonance (signal f) also decreased in intensity, while a new peak, ascribed to the same proton, appeared at 5.20 ppm. Although this spectal evolution compares roughly to what is observed in the course of the corresponding fluoride titration, the fact that saturation was observed upon the addition of only 0.7 molar equivalents in both dichloromethane-d_2 and tetrahydrofuran-d_8 leads to the suggestion that in these solvents two molecules of **2.26** bind to one chloride (in acetone-d_6, saturation did not occur until 1.1 equivalents of chloride were added). Based on this assumption, a proposed binding mode, shown in Figure 2.26, was generated.

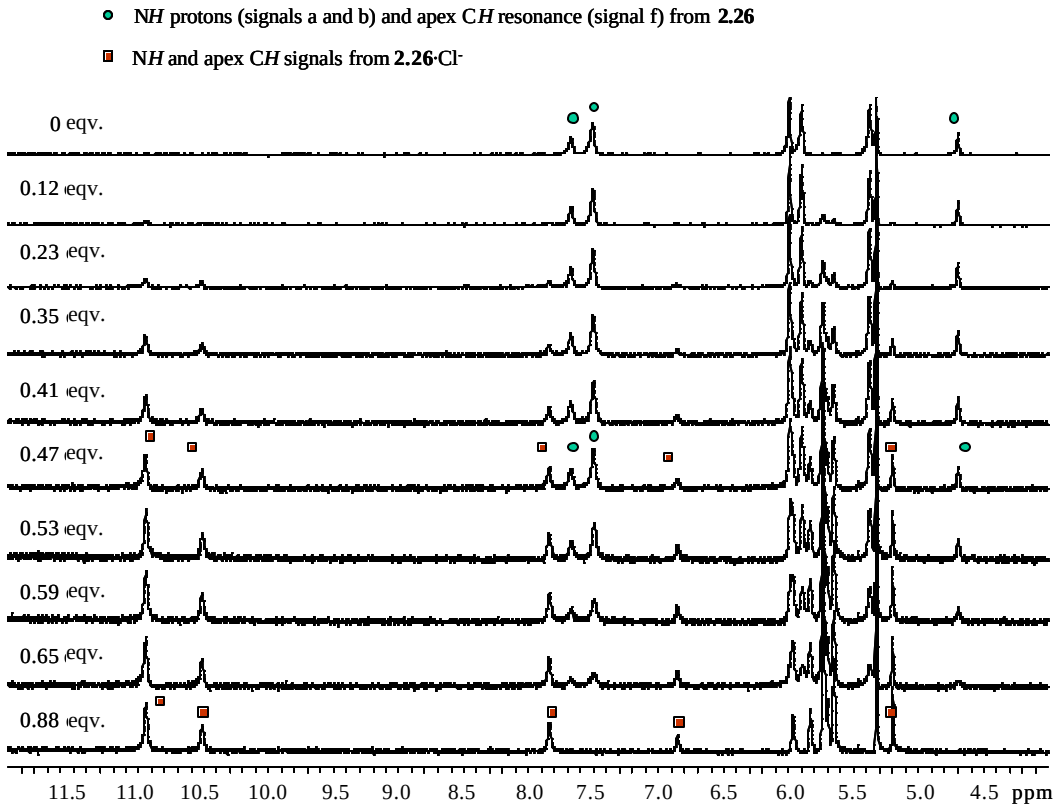

Figure 2.25 Proton spectroscopic tititation of **2.26** at 6.8 x 10^{-3} M in CD_2Cl_2 with Bu_4NCl from 0 – 0.8 eqv. Important peaks corresponding to **2.26** are indicated with a circle. Important peaks corresponding to **2.26**·Cl⁻ are indicated with a square.

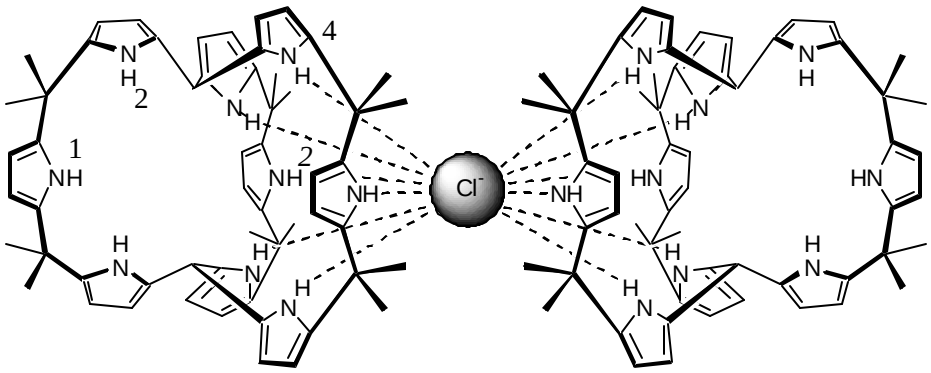

Final NH ppm	Relative Integration
6.86	1
7.84	2
10.51	*2*
10.94	4

Figure 2.26 Proposed binding mode of **2.26** with Bu_4NCl

The titration was redone in the presence of an internal standard, bicyclo[2.2.1]hepta-2,5-diene, in order to ensure a direct correlation between the integration and the concentration of **2.26**; only then could an accurate calculation of the binding affinity of **2.26**·Cl⁻ be assured. This standard was chosen for two reasons. First, it had easily distinguishible resonances at frequencies that did not interfere with signals from either the receptor or the receptor-anion species. Second, due to the somewhat unstable nature of receptor **2.26** to air, all sample preparation for this project was performed in an inert atmosphere box. Under these conditions, it was thought prudent to use an easily measured liquid standard to possibly correct for any error inherent in the weighing of the solid **2.26**.

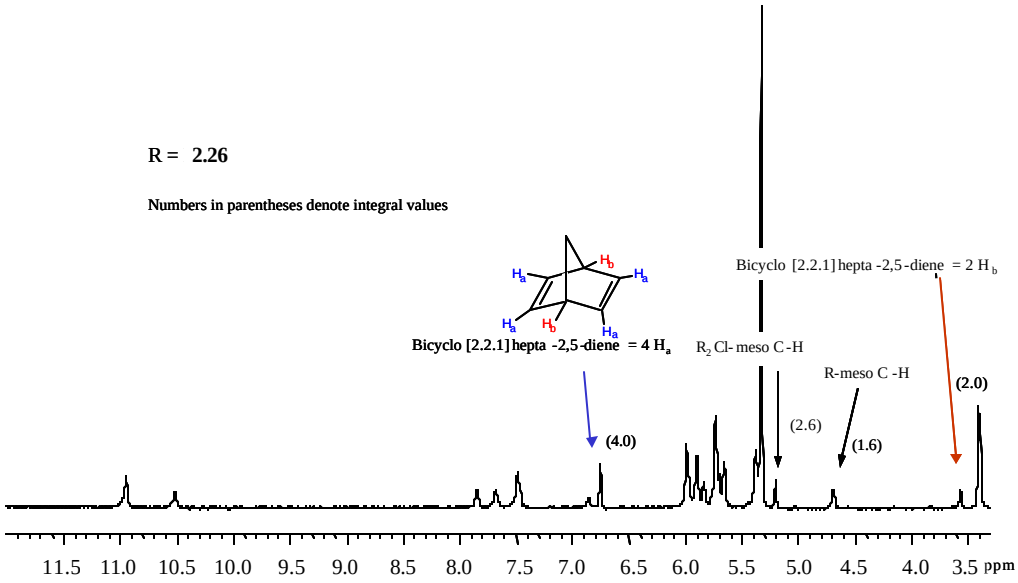

Figure 2.27 Proton spectroscopic titration of **2.26** (4.03 x 10^{-3} M), Bu_4NCl (1.63 x 10^{-3} M), and bicyclo[2.2.1]hepta-2,5-diene (9.76 x 10^{-4} M) in CD_2Cl_2.

To begin with, T_1 values were calculated for **2.26** and the internal standard to determine the relaxation delay necessary to achieve accurate integration of both species. A single datum point was then taken of the receptor and chloride source in the presence of a known amount of internal standard (Figure 2.27). The integration values of the internal standard were then compared to the integrals of both the receptor and the receptor-anion complex based on the apical C*H* protons (signal f). Since the concentration of the internal standard is known, the concentrations of both the receptor and the receptor-anion complex can then be calculated.

The theory behind this concept is explained by the fact that there is a finite amount of **2.26** in solution, the total of which exists divided between **2.26** and $(\mathbf{2.26})_2 \cdot Cl^-$ (Equation 2.4).

Eq. 2.4 $$[\mathbf{2.26}]_{true} = [\mathbf{2.26}]_{actual} + [(\mathbf{2.26})_2 \cdot Cl^-]_{actual}$$

In order to determine the "true" concentration, both $[\mathbf{2.26}]_{actual}$ and $[(\mathbf{2.26})_2 \cdot Cl^-]_{actual}$ were calculated from their integration values and ratioed to the concentration of the norbornyldiene (9.76×10^{-4} M). This resulted in a new $[\mathbf{2.26}]_{true}$ concentration of the receptor, which was adjusted from 4.03×10^{-3} M to 2.05×10^{-3} M. On this basis, solution equilibria equations were used to calculate the association constants based on a 2:1 binding model (Equation 2.5), resulting in an association constant of 3.08×10^6 M^{-2}. This promising result led us to perform similar experiments with dihydrogen phosphate anion.

Eq. 2.5 $$[\mathbf{2.26}]^2_{true} + [Cl^-]_{total} \underset{}{\overset{Ka}{\rightleftharpoons}} [(\mathbf{2.26})_2 \cdot Cl^-]$$

Titration of **2.26** with tetrabutylammonium dihydrogen phosphate from 0 – 1 equivalent resulted in spectral changes consistent with a slow exchange equilibrium similar to what was observed upon the addition of chloride anion (Figure 2.28). As the intensity of the N*H* resonances (signals a and b) at 7.49 and 7.67 ppm decreased, additional N*H* signals appeared at 10.01 and 7.61 ppm. Additionally, as the intensity of the apical C*H* (signal f) at 4.69 ppm decreased, a C*H* peak, corresponding to the bound species, appeared at 5.12 ppm.

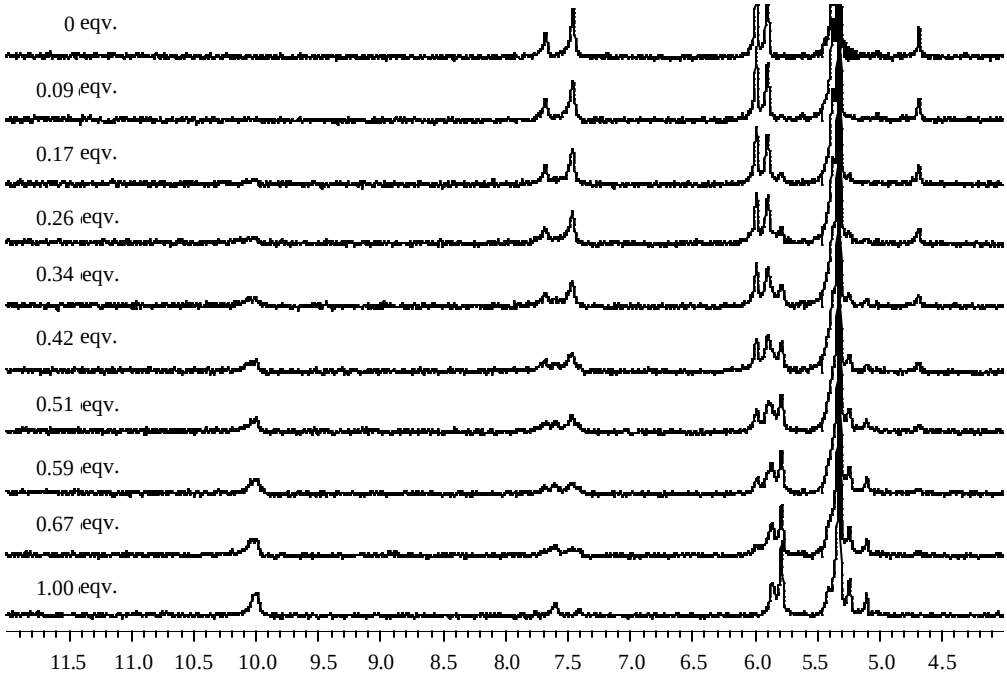

Figure 2.28 Proton spectroscopic titation of **2.26** at 8.1 x 10^{-4} M in CD_2Cl_2 with $Bu_4NH_2PO_4$ from 0 – 1 eqv.

In order to determine accurately the association constant of **2.26** with $Bu_4NH_2PO_4$, the same technique used in the case of chloride was employed. A ^1H NMR spectrum of a 5.17 x 10^{-3} M solution of **2.26** with $H_2PO_4^-$ and a 8.36 x 10^{-3} M solution of the standard bicyclo[2.2.1]hepta-2,5-diene was taken in CD_2Cl_2. As with chloride, the ratio of the integral values of the meso C-*H* signals of the receptor and receptor-anion complex to the signals of the internal standard was used to calculate an effective total concentration for all forms of **2.26**, bound and unbound, in solution. These values, in turn, were used to calculate the association constant from solution equilibria equations. Although complete conversion to the

bound species occurred before one equivalent of dihydrogen sulfate anion had been added, positive values for the association constant were obtained when the data was fit to a 1:1 as opposed to a 2:1 binding profile (Equation 2.6). From this it was concluded that 2:1 binding was not occurring. This contradiction between the number of equivalents necessary to reach saturation and the inability of the data to fit to a 2:1 binding mode of two receptors to one anion attests to the complexity of the system and precludes a fully reliable determination of the true association constant for $H_2PO_4^-$ binding.

Eq. 2.6 $$[\mathbf{2.26}]_{true} + [H_2PO_4^-]_{total} \underset{}{\overset{Ka}{\rightleftharpoons}} [\mathbf{2.26}\cdot H_2PO_4^-]$$

2.2.3 CONLUSION AND FUTURE DIRECTIONS

During the course of these studies, it was noted that at high concentrations of anion each species yielded similar NH shifts regardless of their rate of exchange in the binding equilibrium. Surprisingly, at these high concentrations of anions, even those species that were bound *via* presumed fast exchange anions caused the emergence of four N*H* peaks at resonances similar to those seen in the cases involving slow exchange anions. This point is reflected in the data summarized in Table 2.2. While perhaps fortuitous, the fact that the four NH resonances (labeled $NH_{a\text{-}d}$ in the table) have final values that are similar for all the anions could reflect the fact that under conditions of binding saturation, cryptand **2.26** adopts a similar conformation in its host-guest complexation regardless of the anion. Among the fast exchange anions, Br^-, NO_3^-, and SCN^-, it is interesting

to note that the number of equivalents required to reach these high-concentration NH resonances roughly correlates to the number of equivalents required to determine the association constant of the initial binding event; the weaker the interaction of the anion with the receptor, the greater the number of equivalents necessary to reach the "ultimate conformation". Currently there is no correlation between such factors as binding strength, anion basicity, size, or geometry with the adoption of either a fast or a slow exchange mechanism upon binding. The reasons for these unusual differences in the exchange rate between different anions are currently unknown.

Table 2.2 NH resonances of **2.26** with each anion at high anion concentrations

Bu_4N anion	Exchange	NH_a ppm	NH_b ppm	NH_c ppm	NH_d ppm	Eqv. to K_a	Eqv. to Final NH ppm
Cl^-	slow	6.86	7.84	10.51	10.94	0.8	--
$H_2PO_4^-$	slow	7.41	7.60	10.03	--	1.0	--
F^-	slow	6.78	7.97	10.56	11.99	6.0	--
Br^-	fast	6.85	7.88	10.52	10.97	4.5	100
NO_3^-	fast	--	7.76	10.02	10.92	6.0	457
SCN^-	fast	6.83	7.78	10.45	10.94	11.0	515

In light of these interesting findings regarding anion concentration and receptor configuration, a future direction in this area could involve the synthesis and study of the anion recognition chemistry of an analog of **2.26** bearing methyl

or ethyl substituents at the β-positions of all the pyrrole units. This would impose a conformational restriction on the system and allow for further investigation into the presumed conformational equivalence phenomena. Additionally, the increased solubility would allow for study in a wider range of solvents, which might help elucidate any correlations between the binding equilibria and anion basicity, as well as ruling out fortuitous solvent effects.

Additionally, current work by Dr. Christophe Bucher involves oxidation of the apex CH groups on **2.26**, something that results in the formation of new expanded cryptand-like calixphyrin **2.27**. Comparison of the anion binding studies of this new system with those of **2.26** would provide the first "link" between analogous expanded calixphyrin and calixpyrrole systems, and allow an opportunity to compare directly the effects of conformation and structure on anion binding in cryptand like polypyrrolic receptors.

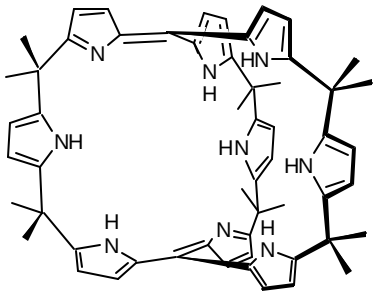

2.27

In summary, expanded calix[*n*]phyrins and calix[*n*]pyrroles represent a new frontier in expanded porphyrin analog chemistry. Their wide range of potential binding pocket size and their conformational flexibility make a determination of their anion binding properties interesting and challenging, but appears to allow for new anion binding motifs not previously seen with the smaller, more traditional polypyrrolic systems. This field thus promises to provide valuable information regarding topology, structure, flexibility and design

as it relates to anion binding, all of which represent important considerations as various “real world” applications start to be targeted.

This chapter was taken in part from three publications in which the author was either a primary or secondary contributor, *J. Am. Chem. Soc*. **2001**, *123*(9), 2099-2100, *J. Am. Chem*. *Soc*. **2001**, *123*(39), 9716-9717, and *Pure Appl. Chem*., **2001**, 73, 1041-1057.

References

(1) Kadish, K.; Smith, K. M.; Guilard, R., Eds.; Academic Press: San Diego, 1999; Vol. 1.

(2) Uno, H.; Inoue, T.; Fumoto, Y.; Shiro, M.; Ono, N. *J. Am. Chem. Soc.* **2000**, *122*, 6773-6774.

(3) Senge, M. O.; Runge, S.; Speck, M.; Ruhlandt-Senge, K. *Tetrahedron* **2000**, *56*, 8927-8932.

(4) Dolphin, D. *J. Heterocycl. Chem.* **1970**, *7*, 275-283.

(5) Dwyer, P. N.; Buchler, J. W.; Scheidt, W. R. *J. Am. Chem. Soc.* **1974**, *96*, 2789-2795.

(6) Gosmann, M.; Franck, B. *Angew. Chem., Int. Ed. Engl.* **1986**, *25*, 1107-1108.

(7) Barkigia, K. M.; Renner, M. W.; Xie, H.; Smith, K. M.; Fajer, J. *J. Am. Chem. Soc.* **1993**, *115*, 7894-7895.

(8) Woodward, R. B. *Ind. Chim. Belge* **1962**, *27*, 1293-1308.

(9) Dolphin, D.; Felton, R. H.; Borg, D. C.; Fajer, J. *J. Amer. Chem. Soc.* **1970**, *92*, 743-745.

(10) Barnett, G. H.; Hudson, M. F.; McCombie, S. W.; Smith, K. M. *J. Chem. Soc., Perkin Trans. I* **1973**, 691-696.

(11) Forman, A.; Borg, D. C.; Felton, R. H.; Fajer, J. *J. Am. Chem. Soc.* **1971**, *93*, 2790-2792.

(12) Cavaleiro, J. A. S.; Evans, B.; Smith, K. *Porphyrin Chemistry Advances*; Ann Arbor Science: Ann Arbor, 1979.

(13) Shine, H. J.; Padilla, A. G.; Wu, S.-M. *J. Org. Chem.* **1979**, *44*, 4069-4075.

(14) Gold, A.; Ivey, W.; Bowen, M. *Chem. Commun.* **1981**, *6*, 293-295.

(15) Gold, A.; Ivey, W.; Toney, G. E.; Sangaiah, R. *Inorg. Chem.* **1984**, *23*, 2932-2935.

(16) Lee, W. A.; Bruice, T. C. *Inorg. Chem.* **1986**, *25*, 131-135.

(17) Takeda, Y.; Takahara, S.; Kobayashi, Y.; Misawa, H.; Sakuragi, H.; Tokumaru, K. *Chem. Lett.* **1990**, 2103-2106.

(18) Haraldsson, G. G.; Baldwin, J. E.; Jones, J. G.; Debernardis, J. *Polyhedron* **1993**, *12*, 2453-2458.

(19) Murakami, T.; Watanabe, Y.; Morishima, I. *Chem. Lett.* **1998**, 27-28.

(20) Latos-Grazynski, L.; Rachlewicz, K.; Wojaczynski, J. *Coord. Chem. Rev.* **1999**, *190-192*, 109-125.

(21) Fuhrhop, J.-H.; Lumbantobing, T. *Tetrahedron Lett.* **1970**, *32*, 2815-2818.

(22) Wolberg, A.; Manassen, J. *J. Am. Chem. Soc.* **1970**, *92*, 2982-2991.

(23) Guzinski, J. A.; Felton, R. H. *Chem. Commun.* **1973**, 715-716.

(24) Felton, R. H.; Owen, G. S.; Dolphin, D.; Forman, A.; Borg, D. C. *Ann. N. Y. Acad. Sci.* **1973**, *206*, 504-515.

(25) Kadish, K. M.; Rhodes, R. K. *Inorg. Chem.* **1981**, *20*, 2961-2966.

(26) Harriman, A.; Porter, G.; Walters, P. *J. Chem. Soc., Faraday Trans. 1* **1983**, *79*, 1335-1350.

(27) Richoux, M. C.; Neta, P.; Christensen, P. A.; Harriman, A. *J. Chem. Soc., Faraday Trans. 2* **1986**, *82*, 235-249.

(28) Hinman, A. S.; Pavelich, B. J.; Kondo, A. E.; Pons, S. *J. Electroanal. Chem. Interfacial Electrochem.* **1987**, *234*, 145-162.

(29) Szulbinski, W.; Strojek, J. W. *J. Electroanal. Chem. Interfacial Electrochem.* **1988**, *252*, 323-334.

(30) Mosseri, S.; Mialocq, J. C.; Perly, B.; Hambright, P. *J. Phys. Chem.* **1991**, *95*, 2196-2203.

(31) Guilard, R.; Jagerovic, N.; Tabard, A.; Naillon, C.; Kadish, K. M. *J. Chem. Soc., Dalton Trans.* **1992**, 1957-1960.

(32) D'Souza, F.; Hsieh, Y.-Y.; Deviprasad, G. R. *Inorg. Chem.* **1996**, *35*, 5747-5749.

(33) Grigg, R.; Sweeney, A. *Chem. Commun.* **1970**, 1237-1238.

(34) Rachlewicz, K.; Latos-Grazynski, L. *Inorg. Chem.* **1995**, *34*, 718-727.

(35) Xie, H.; Smith, K. M. *Tetrahedron Lett.* **1992**, *33*, 1197-1200.

(36) Furuta, H.; Ishizuka, T.; Osuka, A.; Uwatoko, Y.; Ishikawa, Y. *Angew. Chem., Int. Ed. Engl.* **2001**, *40*, 2323-2325.

(37) Mauzerall, D.; Granick, S. *J. Biol. Chem.* **1958**, *232*, 1141-1162.

(38) Mauzerall, D. *J. Am. Chem. Soc.* **1960**, *82*, 1832-1833.

(39) Inhoffen, H. H.; Jäger, P.; Mälhop, C.-D. M. *Liebigs Ann. Chem.* **1967**, *704*, 188-207.

(40) Peychal-Heiling, G.; Wilson, G. S. *Anal. Chem.* **1971**, *43*, 550-556.

(41) Neri, B. P.; Wilson, G. S. *Anal. Chem.* **1972**, *44*, 1002-1008.

(42) Inhoffen, H. H.; Jäger, P.; Mählhop, R.; Mengler, C. D. *Justus Liebigs Ann. Chem.* **1967**, *704*, 188-207.

(43) Mauzerall, D. *J. Am. Chem. Soc.* **1962**, *84*, 2437-2445.

(44) Inhoffen, H. H.; Jäger, P.; Mälhop, C.-D. M. *Liebigs Ann. Chem.* **1971**, *749*, 109-116.

(45) Wilson, G. S.; Neri, B. P. *Ann. N. Y. Acad. Sci.* **1973**, *206*, 568-578.

(46) Closs, G. L.; Closs, L. E. *J. Am. Chem. Soc.* **1963**, *85*, 818-819.

(47) Lanese, J. G.; Wilson, G. S. *J. Electrochem. Soc.: Electrochemical Sciences and Technology* **1972**, *119*, 1039-1043.

(48) Setsune, J.; Yazawa, T.; Ogoshi, H.; Yoshida, Z. *J. Chem. Soc., Perkin Trans. 1* **1980**, 1641-1645.

(49) Segawa, H.; Azumi, R.; Shimidzu, T. *J. Am. Chem. Soc.* **1992**, *114*, 7564-7565.

(50) Sugimoto, H. *J. Chem. Soc., Dalton Trans.* **1982**, 1169-1171.

(51) Krattinger, B.; Callot, H. J. *Tetrahedron Lett.* **1996**, *37*, 7699-7702.

(52) Krattinger, B.; Callot, H. J. *Tetrahedron Lett.* **1998**, *39*, 1165-1168.

(53) Krattinger, B.; Callot, H. J. *Eur. J. Org. Chem.* **1999**, 1857-1867.

(54) Kalisch, W. W.; Senge, M. O. *Angew. Chem., Int. Ed. Engl.* **1998**, *37*, 1107-1109.

(55) Woodward, R. B. *Angew. Chem.* **1960**, *72*, 651-662.

(56) Holmes, R. T.; Lin, J. J.; Khoury, R. G.; Jones, K. M.; Smith, K. M. *Chem. Commun.* **1997**, 819-820.

(57) Lin, J. J.; Gerzevske, K. R.; Liddell, P. A.; Senge, M. O.; Olmstead, M. M.; Khoury, R. G.; Weeth, B. E.; Tsao, S. A.; Smith, K. M. *J. Org. Chem.* **1997**, *62*, 4266-4276.

(58) Liddell, P. A.; Olmstead, M. M.; Smith, K. M. *J. Am. Chem. Soc.* **1990**, *112*, 2038-2040.

(59) Swanson, K. L.; Snow, K. M.; Jeyakumar, D.; Smith, K. M. *Tetrahedron* **1991**, *47*, 685-696.

(60) Setsune, J.; Ikeda, M.; Iida, T.; Kitao, T. *J. Am. Chem. Soc.* **1988**, *110*, 6572-6574.

(61) Setsune, J.; Ishimaru, Y.; Kitao, T. *Chem. Lett*. **1990**, 1351-1354.

(62) Setsune, J.; Yamaji, H.; Kitao, T. *Tetrahedron Lett.* **1990**, *31*, 5057-5060.

(63) Setsune, J.; Wada, K.; Higashino, H. *Chem. Lett*. **1994**, 213-216.

(64) Setsune, J.-I.; Kashihara, K.; Wada, K.-I.; Shiozaki, H. *Chem. Lett*. **1999**, 847-848.

(65) Pohl, M.; Schmickler, H.; Lex, J.; Vogel, E. *Angew. Chem., Int. Ed. Engl.* **1991**, *30*, 1693-1697).

(66) Krattinger, B.; Callot, H. J. *Chem. Commun.* **1996**, 1341-1342.

(67) Jiang, X.; Nurco, D. J.; Smith, K. M. *Chem. Commun.* **1996**, 1759-1760.

(68) Ruppert, R.; Jeandon, C.; Sgambati, A.; Callot, H. J. *Chem. Commun.* **1999**, 2123-2124.

(69) Scheer, H.; Wolf, H. *Justus Liebigs Ann. Chem.* **1973**, *10*, 1741-1749.

(70) Fuhrhop, J. H.; Salek, A.; Subramanian, J.; Mengersen, C.; Besecke, S. *Justus Liebigs Ann. Chem.* **1975**, 1131-1147.

(71) Botulinski, A.; Buchler, J. W.; Lee, Y. J.; Scheidt, W. R.; Wicholas, M. *Inorg. Chem.* **1988**, *27*, 927-933.

(72) Inhoffen, H. H.; Buchler, J. W.; Jager, P. *Fortschr. Chem. Org. Natur.* **1968**, *26*, 284-355.

(73) Buchler, J. W.; Puppe, L. *Justus Liebigs Ann. Chem.* **1970**, *740*, 142-163.

(74) Ema, T.; Senge, M. O.; Nelson, N. Y.; Ogoshi, H.; Smith, K. M. *Angew. Chem., Int. Ed. Engl.* **1994**, *33*, 1879-1881.

(75) Senge, M. O.; Bischoff, I.; Nelson, H.; Smith, K. M. *J. Porphyrins Phthalocyanines* **1999**, *3*, 99-116.

(76) Bischoff, I.; Feng, X.; Senge, M. O. *Tetrahedron* **2001**, *57*, 5573-5583.

(77) Botulinski, A.; Buchler, J. W.; Lay, K. L.; Stoppa, H. *Liebigs Ann. Chem.* **1984**, 1259-1269.

(78) Botulinski, A.; Buchler, J. W.; Tonn, B.; Wicholas, M. *Inorg. Chem.* **1985**, *24*, 3239-3245.

(79) Harmjanz, M.; Scott, M. J. *Chem. Commun.* **2000**, 397-398.

(80) Král, V.; Sessler, J. L.; Zimmerman, R. S.; Seidel, D.; Lynch, V.; Andrioletti, B. *Angew. Chem., Int. Ed. Engl.* **2000**, *39*, 1055-1058.

(81) Bucher, C.; Zimmerman, R. S.; Lynch, V.; Král, V.; Sessler, J. L. *J. Am. Chem. Soc.* **2001**, *123*, 2099-2100.

(82) Kroulík, J.; Král, V.; Sessler, J. L.; Bucher, C.; Bour, P.; Lynch, V. *submitted*.

(83) Rhee, S. W.; Na, Y. H.; Do, Y.; Kim, J. *Inorg. Chim. Acta* **2000**, *309*, 49-56.

(84) Botulinski, A.; Buchler, J. W.; Abbes, N. E.; Scheidt, W. R. *Liebigs Ann. Chem.* **1987**, 305-309.

(85) Bucher, C.; Seidel, D.; Lynch, V.; Král, V. *Org. Lett.* **2000**, *2*, 3103-3106.

(86) Dwyer, P. N.; Puppe, L.; Buchler, J. W.; Scheidt, W. R. *Inorg. Chem.* **1975**, *14*, 1782-1785.

(87) Buchler, J. W.; Lay, K. L.; Smith, P. D.; Scheidt, W. R.; Rupprecht, G. A.; Kenny, J. E. *J. Organomet. Chem.* **1976**, *110*, 109-120.

(88) Buchler, J. W.; Lay, K. L.; Lee, Y. J.; Scheidt, W. R. *Angew. Chem., Int. Ed. Engl.* **1982**, *21*, 432-433.

(89) Buchler, J. W.; Dreher, C.; Lay, K. L.; Lee, Y. J.; Scheidt, W. R. *Inorg. Chem.* **1983**, *22*, 888-891.

(90) Benech, J.-M.; Bonomo, L.; Solari, E.; Scopelliti, R.; Floriani, C. *Angew. Chem., Int. Ed.* **1999**, *38*, 1957-1959.

(91) Bonomo, L.; Solari, E.; Scopelliti, R.; Floriani, C.; Latronico, M. *Chem. Commun.* **1999**, 2227-2228.

(92) Bonomo, L.; Solari, E.; Scopelliti, R.; Floriani, C.; Re, N. *J. Am. Chem. Soc.* **2000**, *122*, 5312-5326.

(93) Nelson, N. Y.; Khoury, R. G.; Nurco, D. J.; Smith, K. M. *Chem. Commun.* **1998**, 1687-1688.

(94) Bonomo, L.; Toraman, G.; Solari, E.; Scopelliti, R.; Floriani, C. *Organometallics* **1999**, *18*, 5198-5200.

(95) Senge, M. O.; Bischoff, I. *Eur. J. Org. Chem.* **2001**, 1735-1751.

(96) Balch, A. L.; Noll, B. C.; Phillips, S. L.; Reid, S. M.; Zovinka, E. P. *Inorg. Chem.* **1993**, *32*, 4730-4736.

(97) Balch, A. L.; Olmstead, M. M.; Phillips, S. L. *Inorg. Chem.* **1993**, *32*, 3931-3936.

(98) Senge, M. O.; Kalisch, W. W.; Bischoff, I. *Chem.--Eur. J.* **2000**, *6*, 2721-2738.

(99) Khoury, R. G.; Jaquinod, L.; Nguyen, L. T.; Smith, K. M. *Heterocycles* **1998**, *47*, 113-119.

(100) Wytko, J. A.; Michels, M.; Zander, L.; Lex, J.; Schmickler, H.; Vogel, E. *J. Org. Chem.* **2000**, *65*, 8709-8714.

(101) Werner, A.; Michels, M.; Zander, L.; Lex, J.; Vogel, E. *Angew. Chem., Int. Ed. Engl.* **1999**, *38*, 3650-3653.

(102) Connors, A. K. *Binding Constants: the Measurement of Molecular Complex Stability*; Wiley: New York, 1987.

(103) Allen, W. E.; Gale, P. A.; Brown, C. T.; Lynch, V. M.; Sessler, J. L. *J. Am. Chem. Soc.* **1996**, *118*, 12471-12472.

(104) Gale, P. A.; Sessler, J. L.; Král, V.; Lynch, V. *J. Am. Chem. Soc.* **1996**, *118*, 5140-5141.

(105) Sessler, J. L.; Gale, P. A.; Genge, J. W. *Chem. Eur. J.* **1998**, *4*, 1095-1099.

(106) Miyaji, H.; Anzenbacher, P. J.; Sessler, J. L.; Bleasdale, E. R.; Gale, P. A. *Chem. Commun.* **1999**, 1723-1724.

(107) Gale, P. A.; Twyman, L. J.; Handlin, C. I.; Sessler, J. L. *Chem. Commun.* **1999**, 1851-1852.

(108) Miyaji, H.; Sato, W.; Sessler, J. L. *Angew. Chem., Int. Ed. Engl.* **2000**, *39*, 1777-1780.

(109) Sessler, J. L.; Genge, J. W.; Gale, P. A.; Král, V. *ACS Symp. Ser.* **2000**, *757*, 238-254.

(110) Sessler, J. L.; Anzenbacher, P. J.; Miyaji, H.; Jursiková, K.; Bleasdale, E. R.; Gale, P. A. *Ind. Eng. Chem. Res.* **2000**, *39*, 3471-3478.

(111) Lehn, J.-M. *Supramolecular Chemistry, Concepts and Perspectives*; VCH: New York, 1995.

(112) Sessler, J. L.; Král, V.; Hoehner, M.; Chin, K. O.; Dávila, R. M. *Pure Appl. Chem.* **1996**, 1291-1295.

(113) Sessler, J. L.; Dávila, R. M.; Král, V. *Tetrahedron Lett.* **1996**, *37*, 6469-6472.

(114) Andrievsky, A.; Ahuis, F.; Sessler, J. L.; Vögtle, F.; Gudat, D.; Moini, M. *J. Am. Chem. Soc.* **1998**, *120*, 9712-9713.

(115) Lu, Q.; McKee, V.; Nelson, J. *Chem. Commun.* **1994**, 649-651.

(116) Sessler, J. L.; Hoehner, M.; Johnson, D. W.; Gebauer, A.; Lynch, V. *Chem. Commun.* **1996**, 2311-2312.

(117) Fox, O. D.; Rolls, T. D.; Drew, M. G. B.; Beer, P. D. *Chem. Commun.* **2001**, 1632-1633.

(118) Bucher, C.; Zimmerman, R. S.; Lynch, V.; Sessler, J. L. *J. Am. Chem. Soc.* **2001**, *123*, 9716-9717.

(119) Wilcox, C. W. *Frontiers in Supramolecular Organic Chemistry and Photochemistry*; VCH: Weinheim, 1991.

Chapter 3: Synthesis, Structural Characterization and Complexation Properties of the First 'Crowned'-Dipyrrolylquinoxalines

3.1 INTRODUCTION

For over thirty years now, supramolecular chemists have worked to develop abiotic receptors capable of binding positively or negatively charged species with ever-improving selectivities.[1,2] As a result, there is now abundant literature regarding the design, synthesis and study of such receptors. In spite of the progress this literature represents, significant challenges remain in this area. One of these involves the construction of so-called ditopic receptors, species that can complex cation and anion pairs concurrently within a single molecular system.[3-6] One of the goals of such a system is to effect through-membrane transport.[7-9]

Although most synthetic channels have been designed for cation transport, chloride transport is of particular interest due to its role in regulating cell volume and membrane potential.[10,11] To date there have been four major families of chloride channels identified,[12,13] and a number of synthetic peptides have been developed that act as Cl^- selective ion channels.[11] The ubiquity of Cl^- in all cells underscores its importance, with cystic fibrosis serving as a poignant example of what can happen when a particular chloride anion channel misfunctions. The net result is impaired Cl^- transport channels in epithelial cells and an increase in cell volume.[14] Thus far there is no treatment to compensate for this poor Cl^- transport. This renders cyctic fibrosis patients highly susceptible to infectious disease. Until

such time as an effective therapy is developed, the administration of suitable synthetic chloride anion channels or carriers could provide a way to control the disease by facilitating chloride anion transport.

One of the characteristics of such a treatment targeted carrier or channel is that they would need to be selective for a particular ion, while maintaining a high transport rate. Ideally they also should be able to regulate the ion flow.[15] These caveats must be taken into consideration when designing possible anion carriers. In recent years, the Sessler group has been involved in the design of dipyrrolylquinoxalines (DPQs) for the purpose of anion sensing.[16-18] These systems have typically displayed high affinities for fluoride anion; however, their lower chloride anion binding affinity initiated the idea that they could prove useful for the design of a ditopic receptor that might ultimately show utility as a physiologically compatible anion carrier. It is well established that relatively low binding affinities have been associated with rapid cross-membrane transport.[19] In addition, the high affinity of dipyrrolylquinoxaline for fluoride anion, which should correlate to more readily determined conditions for cooperativity, could provide an initial model system upon which to launch cooperative chloride binding studies. Further, the ability to control intimately counter cation binding could provide for a level of control that might not otherwise be possible. Thus, there was considerable incentive within the Sessler group to undertake preparation of DPQ-based ditopic receptors. Before describing the results of these efforts, a brief review of DPQ chemistry is in order.

3.1.1 Dipyrrolylquinoxalines

The initial impetus for the Sessler group to use dipyrrolylquinoxalines as anion sensors came from a desire to incorporate a fluorescent moiety (i.e., quinoxaline) into the body of an anion sensing unit (i.e., pyrrole). Effecting such a direct incorporation, rather than attaching a chromophore as an appendage, was considered promising in terms of achieving a high degree of anion recognition sensitivity. The first systems developed in accord with this strategy were based on the previously prepared 2,3-bis-(1*H*-pyrrol-2-yl)-quinoxaline scaffold **3.1a**. Although known in the literature since 1911,[20] its potential for anion binding was never recognized. Upon discovery of its anion binding properties, a series of receptors based on this scaffold were prepared (compounds **3.1a**, **3.1b**, **3.1c**[16] and **3.1d**[17]).

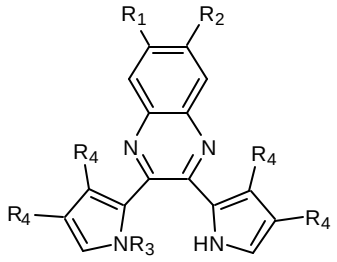

3.1a $R_1 = R_2 = R_3 = R_4 = H$
3.1b $R_1 = R_3 = R_4 = H$; $R_2 = NO_2$
3.1c $R_1 = R_2 = R_4 = H$; $R_3 = SEM$
3.1d $R_1 = R_2 = R_3 = H$; $R_4 = F$

Addition of fluoride to a dichloromethane or dimethylsulfoxide solution of **3.1a**, **3.1b**, and **3.1d** resulted in a colorimetric response that was reflected specifically in a dramatic color change from yellow to reddish-purple. Addition of chloride anion did not induce a similar color change, whereas dihydrogen phosphate anion induced a similar color change only in the case of receptor **3.1d**. Quantitative anion binding studies were undertaken to confirm that the observed colorimetric change did indeed reflect an anion binding process and to corroborate the intuitively appealing notion that a greater

color change upon addition of an anion was directly linked to a high anion binding affinity. Towards this end, binding affinities, K_a, for F^-, Cl^- and $H_2PO_4^-$ were calculated in dichloromethane based on results from fluorescence quenching experiments. The binding behavior of compounds **3.1a**, **3.1b** and **3.1d** proved similar in that they all displayed binding affinities at least three orders of magnitude higher for F^- than for either Cl^- or $H_2PO_4^-$ ($K_a \sim 10^4$ M^{-1} or 10^5 M^{-1} versus $K_a \sim 10$ M^{-1}). Control compound **3.1c**, with a SEM substituted pyrrole, displayed a binding affinity for fluoride of only 100 M^{-1}; this was taken as an indication that the full participation of both pyrrole NHs is necessary to achieve effective anion binding.

Studies of **3.1a**, **3.1b**, and **3.1d** also revealed that modifications of the particular peripheral substituents could be used to fine tune the anion binding affinities. In particular, the presence of electron withdrawing groups on both the quinoxaline as well as on the pyrrole was found to result in an enhanced binding affinity. For example, in the case of fluoride anion, the calculated K_a values were 1.18×10^5 M^{-1} for **3.1b** and 6.16×10^4 M^{-1} for **3.1d** compared to $K_a = 1.82 \times 10^4$ M^{-1} for **3.1**. Interestingly, receptor **3.1b** did not exhibit any significant enhancement in its binding affinity for Cl^- or for $H_2PO_4^-$. Receptor **3.1d**, with its four electron withdrawing fluorine substituents directly on the pyrrole units, as compared to the single electron withdrawing nitro substituent present in **3.1b**, did show a significant enhancement for $H_2PO_4^-$ ($K_a = 1.73 \times 10^4$ M^{-1} versus 60 M^{-1} for **3.1a**).

The success of these initial systems with regard to an ability to fine tune anion binding affinities led to the next generation of dipyrrolylquinoxaline sensors. Here, a new strategy was employed that relied on the presence of electron deficient metal centers to increase anion binding affinities. In accord with this thinking, Sessler *et al*. synthesized a fused dipyrrolylquinoxaline phenanthroline conjugate **3.2** and its Ru(II) and Co(III) complexes, **3.3** and **3.4**. It was hoped that the electron withdrawing properties of the metal placed in conjugation with the anion binding center would result in enhanced binding affinities.[18]

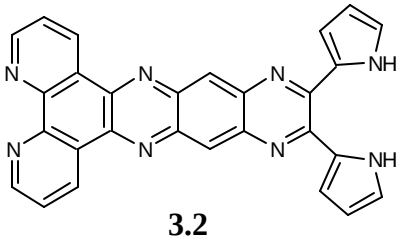

3.2

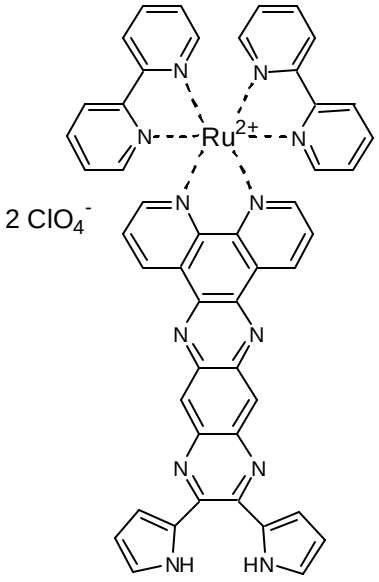

3.3

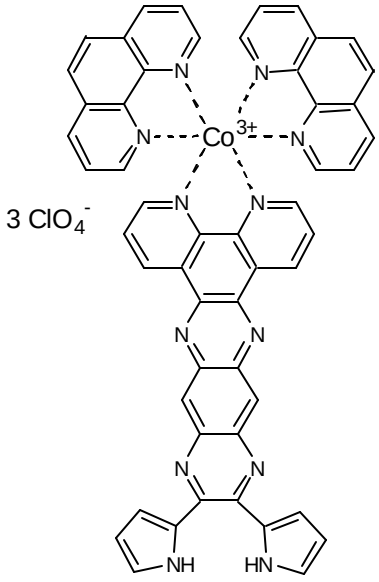

3.4

UV-visible titrations in spectroscopic grade dimethylsulfoxide were used to determine the F^-, Cl^-, and $H_2PO_4^-$ affinities. Compared to parent compounds **3.1a** and **3.2**, complexes **3.3** and **3.4** displayed fluoride anion (as 1 M Bu_4NF in THF) binding affinities of 1.20 x 10^4 M^{-1} and 5.40 x 10^4 M^{-1}, respectively, that were significantly enhanced relative to those of the non-metallated ligand **3.2** and the parent dipyrrolylquinoxaline **3.1a** (K_a = 440 M^{-1} and 100 M^{-1} for F^- binding in DMSO). Tetrafluorinated dipyrrolylquinoxaline **3.1d** was evaluated in dimethylsulfoxide as well, and was found to have a binding affinity of 5.90 x 10^4 M^{-1} for 1 M Bu_4NF in THF, which closely matches the values seen for **3.3** and **3.4**.

Similar findings of binding enhancement were made by Anzenbacher and coworkers who found that cyanide anion could be strongly bound using a $Ru(bpy)_2$ modified dipyrrolylquinoxaline **3.5**.[21] UV-visible and steady state emission spectroscopic titrations revealed significant binding affinities for tetrabutylammonium salts of fluoride and cyanide anions in 2% acetonitrile in dichloromethane (6.4 x 10^5 M^{-1} and 4.3 x 10^5 M^{-1}). This is a significant enhancement over the corresponding binding affinities for the control dipyrrolylquinoxaline **3.1a** (1.8 x 10^4 M^{-1} for F^- and 220 M^{-1} for CN^-).

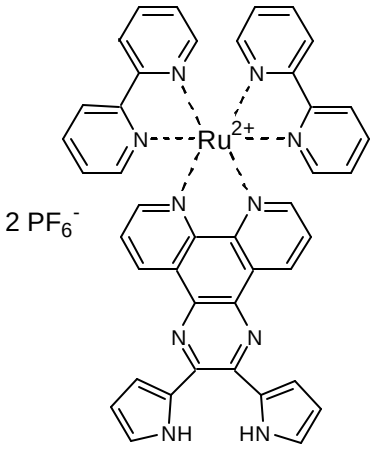

3.5

Recently, Sessler and coworkers reported an alternative approach to tuning the anion binding selectivity of dipyrrolylquinoxaline systems that involved

substitution at the α positions of the two pyrrolic substituents.[22] Specifically, they started with the original 2,3-bis-(1H-pyrrol-2-yl)-quinoxaline **3.1a** and converted it to the corresponding bis-formyl derivative. This was then reduced to produce the corresponding diol, an intermediate that immediately reacted with pyrrole to produce receptors **3.6** and **3.7**.

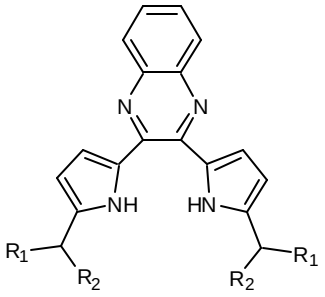

3.6 R_1 = H; R_2 = 

3.7 $R_1 = R_2$ = 

The results of anion binding studies, performed in dichloromethane using UV-visible spectroscopy, showed that these receptors possess dramatically enhanced anion binding affinities as compared to **3.1a**. For example, in the case of Bu_4NF, receptors **3.6** and **3.7** show binding affinities of 3.2×10^4 M^{-1} and $> 1.00 \times 10^6$ M^{-1} as compared to 1.82×10^4 M^{-1} for **3.1a**. As was the case with receptor **3.1d**, a significant enhancement was seen for $H_2PO_4^-$ (4.30×10^3 M^{-1} for **3.6**, 3.00×10^5 M^{-1} for **3.7**) over **3.1a** (60 M^{-1}). Most surprising was the previously unseen enhancement for Cl^-, to 550 M^{-1} and 5.80×10^3 M^{-1} for **3.6** and **3.7**, respectively, as compared to only 50 M^{-1} for **3.1a**. The increase in binding affinity for each anion as the number of pyrroles in the receptor increased was not surprising; however, presumably as a result of the number of pyrrole NHs increasing, the size of the binding pocket is augmented as the series **3.1a**, **3.6**, and **3.7** is traversed, and these latter systems showed a greater relative enhancement in the binding of $H_2PO_4^-$ and Cl^- than for F^-. These results were considered to be evidence that by

altering the hydrogen bond donating nature and size of the binding pocket, it is indeed possible to alter the selectivity ratio.

The fact that dipyrrolylquinoxalines proved both so easy to make and, based on initial studies, rather easy to modify, both in terms of structure and anion affinity, led us to choose them for the development of potential ditopic receptors, i.e., species capable of binding both an anion and a cation concurrently. Specifically, it was postulated that appending an appropriate cation recognition subunit to a dipyrrolylquinoxaline would not only lead to a possible enhancement of the anion binding, but also result in the generation of a successful ditopic receptor. In an effort to consider possible cation binding candidates, some background research was performed on the types of cation moieties that have been successfully incorporated into ditopic receptors to date.

3.1.2 Ditopic Receptors For Inorganic Ion Pairs

The preparation of ditopic receptors has received increasing attention in recent years due to their possible applications in the coordination of zwitterionic amino acids,[7,23,24] peptides,[25,26] and toxic materials,[27,28] as well as their potential to function as carriers that could enhance the through-membrane transport of various biologically important species, including drugs.[7-9] To date, most ditopic receptors have combined well-known anion binding functionalities such as Lewis acid centers, positively charged groups, pyrroles, amide, or (thio)urea groups with well-known cation binding functionalities.[6]

Reetz *et al*. synthesized crown ethers linked to a Lewis-acid boron center,[29,30] such as **3.8**, one of the earliest examples of a ditopic receptor. A solid state X ray diffraction analysis revealed a potassium ion bound within the crown ether and a fluoride ion interacting with the boron center. Solution state evidence for the formation of the ditopic complex was provided by ^{13}C and ^{11}B NMR spectroscopy.

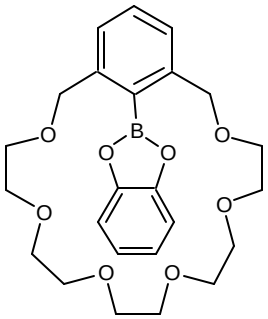

3.8

Later examples include receptors designed by Reinhoudt *et al*., such as **3.9** that consist of a Lewis-acid uranyl Schiff base complex appended to two amide-linked benzo[15]crown-5 subunits.[31,32] This particular receptor was shown by ^{1}H NMR spectroscopy and cyclic voltammetry to bind potassium and dihydrogen phosphate ions simultaneously. Other similar receptors designed by Reinhoudt have been shown to effect the transport of CsCl, KCl and $CsNO_3$ through a supported liquid membrane (SLM).[8,9,33]

Beer *et al*. have designed a number of ditopic receptors wherein a crown ether is attached *via* an amide linkage to ruthenium(II)- and rhenium(I)-bipyridyl groups.[34-37] Another class of ditopic receptors put forth by Beer contains two benzo[15]crown-5 groups covalently linked through amides to calixarenes. An example of this latter class of system is **3.10**.[38] Alone, **3.10** does not exhibit significant affinity for anions. The presence of potassium or ammonium ions, however, causes a sandwich complex to form between the two benzocrown units. This, the authors propose, forces the amide groups to move closer together and

leads dihydrogen phosphate to be bound with an affinity of > 10^4 M^{-1} in acetonitrile-d_3.

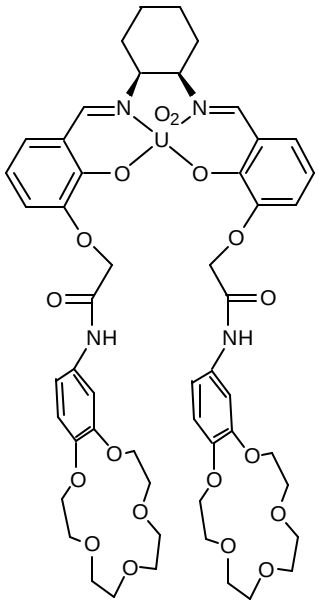

3.9

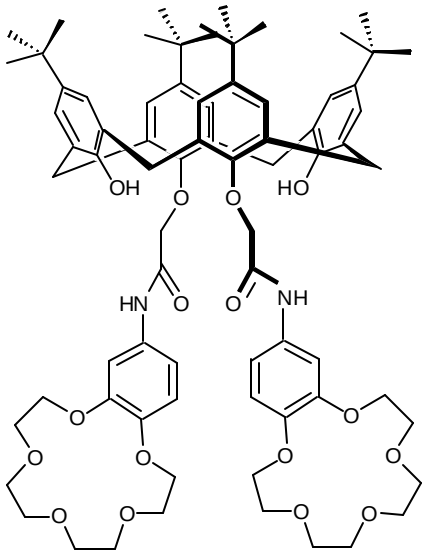

3.10

A different approach involving incorporation of the crown ether into the backbone of the macrocyclic framework was undertaken by Smith and co-workers. This resulted in preorganized macrobicyclic receptors such as **3.11** that combine dibenzo-18-crown-6 and 1,3-phenyldicarboxamide subunits and which demonstrate an ability to coordinate alkali metal and chloride ions concurrently.[39,40] The solid state structure of **3.11** obtained from a crystal of **3.11** grown after exposure to NaCl, shows the Na^+ cation and Cl^- anion co-coordinated as a solvent-separated ion pair. Solution state evidence for a similar interaction was inferred from ^1H NMR spectroscopic studies carried out in the presence of one equivalent of Na^+ or K^+. It was found that the presence of these cations

enhances the binding affinity of the receptor for Cl⁻ relative to what is seen in the absence of the cation (K_a for Cl⁻ = 410 M^{-1} with Na^+ and 470 M^{-1} with K^+ versus 50 M^{-1} for Bu_4NCl).

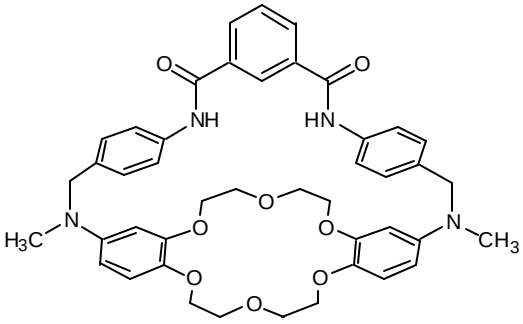

3.11

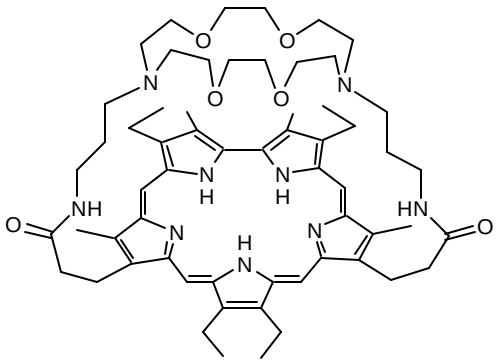

3.12

The Sessler group has also utilized crown ethers in conjunction with various oligopyrroles. For instance, Eric Bruker of the Sessler group prepared the HCl salt of the crowned sapphyrin **3.12**, a species that was shown to complex ammonium and fluoride ions simultaneously, as evidenced by ^{1}H NMR spectroscopic studies.[41] Additionally, the calix[4]pyrrole-crown ether **3.13** was recently prepared in conjunction with control **3.14**.[42,43] It was shown through ^{1}H NMR spectroscopic titrations in dichloromethane-d_2 that **3.13** bound the tetrabutylammonium salts of Cl⁻ and Br⁻ 15 times more strongly than the control **3.14**. This result was interpreted in terms of the crown ether acting to assist with the coordination of the tetrabutylammonium cation, thereby contributing an additional electrostatic component to halide binding. These examples of pyrrole units successfully incorporated into ditopic receptors provided one motivation for the present work, as well as an appreciation for how easily crown ethers could be

prepared and their well understood coordination chemistry.[44] These efforts had as their specific objective the development of dipyrrolylquinoxaline-crown ether conjugates. Other successful ditopic systems that contain calixarenes and Schiff base metal complexes, rather than crown ethers, as the cation coordinating site are discussed in a recent comprehensive review on this subject.[6]

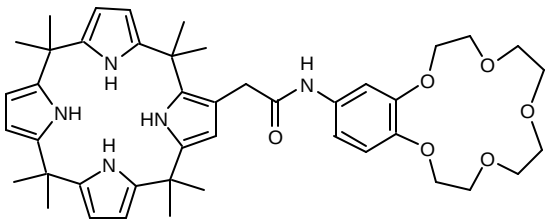

3.13

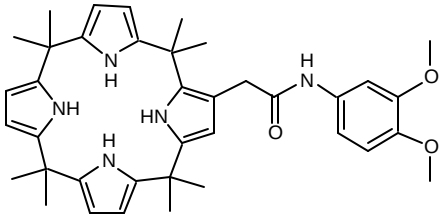

3.14

3.2 SYNTHESIS AND SOLID STATE STRUCTURES OF CROWN ETHER APPENDED DIPYRROLYLQUINOXALINES

In conjunction with Dr. Gregory Kirkovits, a series of dipyrrolylquinoxaline-crown ethers were synthesized that were substituted with a range of crown ethers including 15-crown-5, 18-crown-6, and their aza-substituted analogs; the purpose behind the variation in the crown ether analogs was to examine the versatility of their ditopic coordination chemistry. Key precursors to these systems include the appropriate benzo-crown and azo-benzo crown ethers, **3.18**-**3.21**. While **3.18** and **3.19** are commercially available, benzo-aza-crowns **3.20** and **3.21** had to be synthesized. They were obtained by

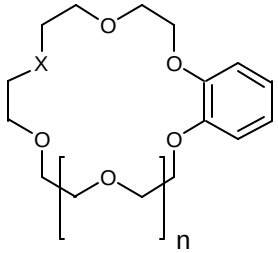

3.18 X = O, n = 1
3.19 X = O, n = 0
3.20 X = NH, n = 1
3.21 X = NH, n = 0

adapting the procedure of Okahara and co-workers that was developed to prepare mono-azacrown ethers (Scheme 3.1).[45] Specifically, 1,2-bis-(2-*para*-toulenesulfonylethoxy)benzene[46] **3.15** was reacted with aza-diol **3.16** or diethanolamine **3.17** in a *tert*-butyl alcohol / dioxane mixture in the presence of potassium *tert*-butoxide to give the products **3.20** and **3.21** in yields of 26 and 16%, respectively. To the best of our knowledge, this is the first time that the synthesis and full characterization of **3.20** has been described.

Scheme 3.1 Synthesis of aza-benzo-crown ether precursors

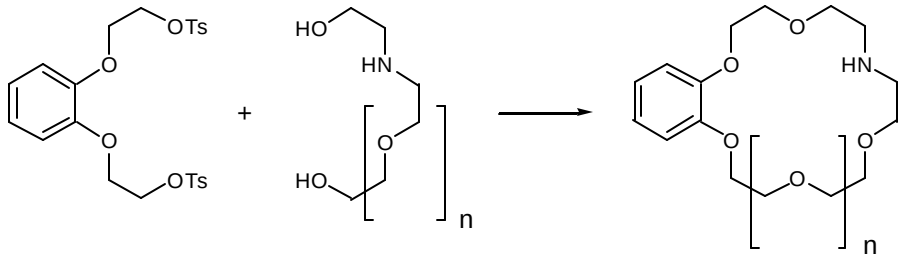

3.15 **3.16**, n = 1; **3.17**, n = 0 **3.20,** n = 1; **3.21**, n = 0

Reagents K^o, ^tBuOH, dioxane, 40° C, 2 h, 26% for **3.20**, 16% for **3.21**.

Nitration of benzo-crowns **3.18**-**3.21** was then carried out and produced the dinitro-intermediates **3.22**-**3.25** in moderate to high yields (44-88%) (Scheme 3.2). Reduction of the dinitro functionalities afforded the corresponding air-sensitive diamines **3.26**-**3.29**, which were used directly in the final quinoxaline-producing step. This step involved reaction of 1,2-bis-(1*H*-pyrrol-2-yl)-ethane-dione **3.30**[16] with the appropriate diamine (**3.26**-**3.29**) in an approximately 1:1

mixture of EtOH and acetic acid, under reflux conditions. This produced the 'crowned'-dipyrrolylquinoxalines **3.31**–**3.34** in moderate to quantitative yields (49–100%). Gratifyingly, the all-oxygen analogs **3.31** and **3.32** were isolated in analytically pure form without the need for column chromatography. Crystals suitable for X-ray diffraction analysis were then obtained by recrystallization from acetone. Compounds **3.33** and **3.34** were purified by column chromatography (neutral alumina; 1.5 % MeOH - CH_2Cl_2, eluent).

Scheme 3.2 Synthesis of Dipyrrolylquinoxaline Crown Ethers

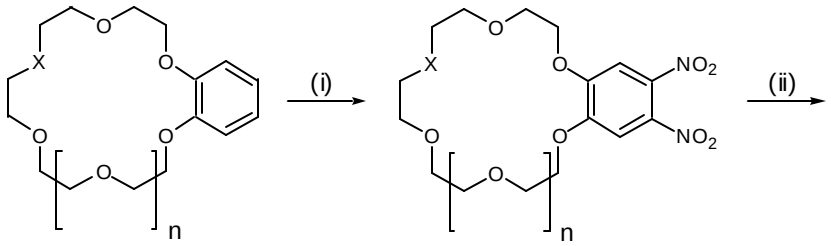

3.18 X = O, n = 1
3.19 X = O, n = 0
3.20 X = NH, n = 1
3.21 X = NH, n = 0

3.22 X = O, n = 1
3.23 X = O, n = 0
3.24 X = NH, n = 1
3.25 X = NH, n = 0

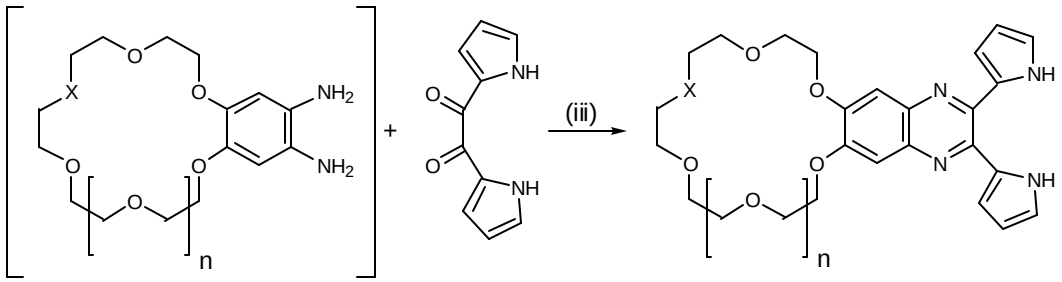

3.26 X = O, n = 1
3.27 X = O, n = 0
3.28 X = $NH_2^+AcO^-$, n = 1
3.29 X = $NH_2^+AcO^-$, n = 0

3.30

3.31 X = O, n = 1
3.32 X = O, n = 0
3.33 X = NH, n = 1
3.34 X = NH, n = 0

Reagents (i) 90% HNO_3, HOAc, 15° C, 88% for **3.22**, 84% for **3.23**, 78% for **3.24**, 44% for **3.25**; (ii) H_2, Pd/C, $AcOH_{cat}$, EtOH, 50 psi, 44 h; (iii) AcOH, EtOH, reflux, 100% for **3.31**, 100% for **3.32**, 62% for **3.33**, 44% for **3.34**.

In a manner similar to that outlined above, the control dimethoxy-dipyrrolylquinoxaline **3.35** was prepared by reaction of air-sensitive 1,2-dimethoxy-4,5-diamino-benzene[7] with 1,2-bis-(1*H*-pyrrol-2-yl)-ethane-dione **3.30**

(Scheme 3.3). The synthesis of 2,3-bis-(1*H*-pyrrol-2-yl)-quinoxaline **3.1a** is reported elsewhere.[16]

Scheme 3.3 Synthesis of control dipyrrolylquinoxaline **3.37**

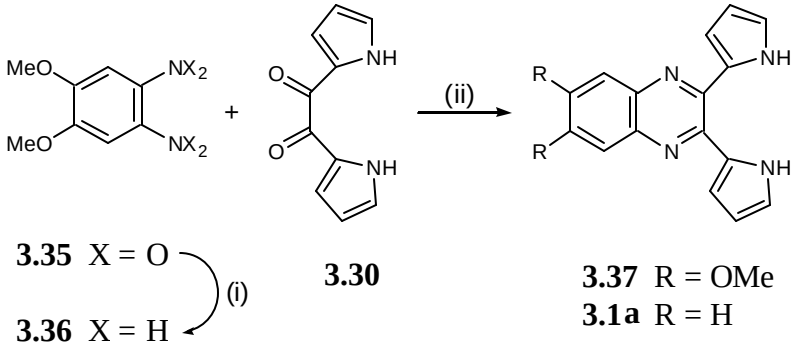

Reagents (i) H_2, Pd/C (ii) AcOH, EtOH, 89%.

Crystals of **3.31** suitable for X-ray structural analysis were grown by dissolving the receptor in boiling acetone, and allowing the solution to stand and cool overnight. A top face view of the basic unit of the solid state structure of 18-crown-6-dipyrrolylquinoxaline **3.31** shows a tetrameric arrangement held together by no fewer than ten hydrogen bonding interactions (Figure 3.1). In this ensemble, one pyrrole NH and one pyrazine nitrogen from each quinoxaline point inward into a water-filled pore. Additionally, the four crown ether moieties of each quinoxaline form the corners of a square.

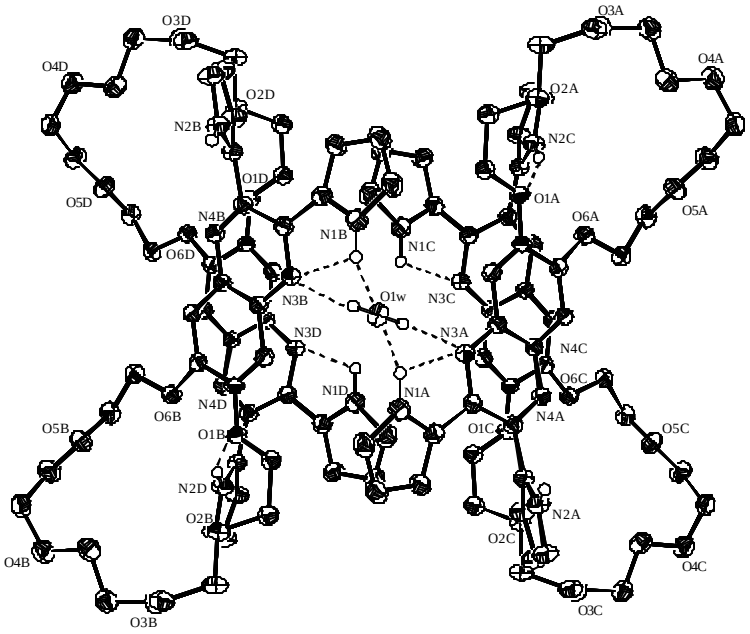

Figure 3.1 Ortep view of the supramolecular tetramer that exists as a repeating motif in crystals of **3.31**. Also shown is the heteroatom labeling scheme. Non-essential hydrogens have been omitted for clarity. Hydrogen bonding interactions are indicated by dashed lines. Thermal ellipsoids are scaled to the 50% probability level.

When looking at the crystal lattice from the top face (Figure 3.2a), the result of this conformation is the formation of five infinite sets of similarly oriented channels, four of which are formed by the "corner" crown ethers, and one in the center framed by a network of inward-pointing pyrrole and pyrazine nitrogens. The side view (Figure 3.2b) shows that the tetramer is comprised of two sets of two intermolecular interactions relative to the plane of each quinoxaline unit, one of which is perpendicularly directed, and the other of which is directed in a parallel fashion from this plane. More specifically, the set of

nearly perpendicular quinoxalines are oriented at a 103º angle to one another, with this arrangement being facilitated by hydrogen bonding interactions between the inward-facing pyrazine nitrogen atom of each quinoxaline and a bound water molecule. The set of nearly parallel interactions involves one of the molecules from the first set and a molecule directly above or below it at a distance ranging from 4.16 Å to 5.70 Å across the face of the two planes formed by the quinoxaline units.

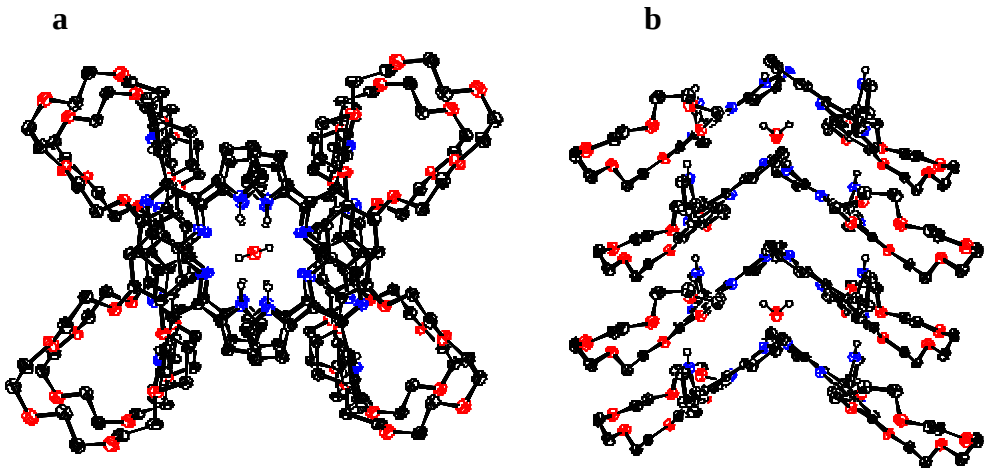

Figure 3.2 Ortep views of the top (a) and side (b) face of the crystal lattice of **3.31**. Encapsulated water molecules are repeated twice within each unit cell. Non-essential hydrogens have been omitted for clarity. Thermal ellipsoids are scaled to the 50% probability level.

The supramolecular motif highlighted in Figure 3.2 is reinforced by numerous hydrogen bonds, all of which occur in a regular pattern. Although difficult to see in two dimensions, within each unit cell of four molecules, two of the quinoxaline units opposite from each other lie above one of the quinoxaline

units on the molecule adjacent to it (Figure 3.2a). Only the inward facing pyrrole NH atoms (N1A and N1B) of the two overlaying molecules participate in hydrogen bonding to the encapsulated water molecule (NH···Ow of 2.13 Å). Likewise, it is also only the overlaying, inward facing pyrazine nitrogens (N3A and N3B) that participate in hydrogen bonding to this same molecule of water (N···H-Ow of 2.08 Å). Intramolecular hydrogen bonding interactions are present between the inward-pointing pyrazine nitrogen atoms of all four quinoxalines in the tetramer and the inward pointing pyrrole NH atoms, specifically N3A to N1A, N3B to N1B, N3C to N1C, and N3D to N1D; N···HN of 2.49 Å. Curiously, the only direct interactions between the two "layers" seen in this view are hydrogen bonds between one of the methoxy-like oxygens in the phenolic position of the overlaying quinoxaline and the NH of the outward-facing pyrrole of the corresponding underlying unit (O1A to N2C and O1B to N2D; NH···O of 2.20 Å). This extraordinary ensemble (the four molecules comprising the unit cell) is thus stabilized by ten hydrogen bonds: two NH···Ow, two N···H-Ow, four N···HN, and two NH···O interactions.

Crystallization of **3.32**, also from acetone, yielded the structure shown in Figure 3.3. This side view shows that **3.32** exists as a hydrogen-bound dimer in the solid-state, stabilized by two sets of identical intermolecular bifurcated hydrogen-bonds from N2···O4' (2.90 Å) and N2···O5' (3.36 Å). In this anti-parallel arrangement, the quinoxaline groups appear to be stacking, with atom-to-atom distances ranging from 4.15 to 4.28 Å. However, this distance is greater, by a considerable margin, than the approximately 3.3 to 3.6 Å separations typically

seen for stacked systems.[47] The fused aromatic rings are not completely planar, but are twisted slightly in opposite directions. This would appear to be the result of an intramolecular hydrogen bonding interaction involving the second out-of-plane pyrrole NH proton (N1) and the pyrazine nitrogen atom N3 (N1···N3 = 2.77 Å).

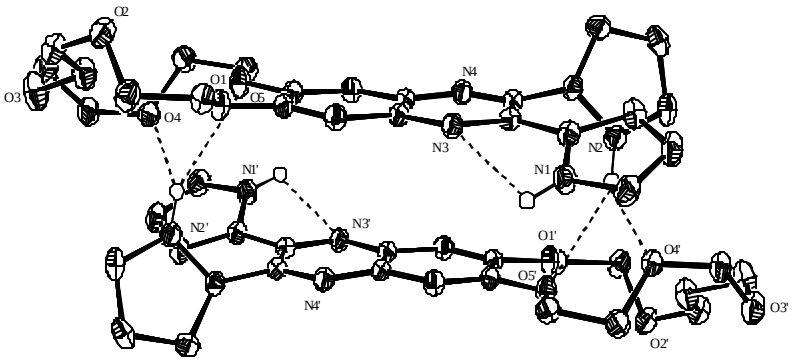

Figure 3.3 Ortep view of the hydrogen bonded dimer seen in crystals of **3.32**. Also shown is the heteroatom labeling scheme. Non-essential hydrogens have been omitted for clarity. Hydrogen bonding interactions are indicated as dashed lines. Thermal ellipsoids are scaled to the 50% probability level.

Crystals of the potassium complex of **3.32** suitable for X-ray structural analysis were grown by vapor diffusion of diethyl ether into an acetonitrile solution containing the ligand and potassium trifluoromethanesulfonate. The side view of the complex is shown in Figure 3.4. As anticipated, the receptor forms a 2:1, ligand:K^+ intermolecular complex with the benzo-15-crown-5 unit from each dipyrrolylquinoxaline acting to sandwich the potassium cation. The K···O distances range from 2.795(2) to 2.995(2) Å. The formation of such a sandwich complex is not uncommon, and the distances are well within the normal limits for

such contacts.[38,48-51] As a result of these interactions, the two sets of bifurcated hydrogen bonds between N2···O4' and N2···O5' seen in Figure 3.3 for the free receptor are no longer present. Presumably as a consequence, molecules of the 'crowned'-quinoxaline are offset from one another, giving what is presumably the lowest energy, least sterically hindered structure.

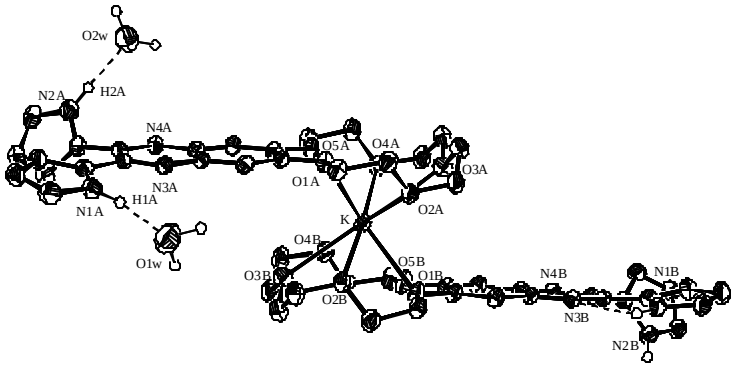

Figure 3.4 Ortep view of $(\mathbf{3.32})_2 \cdot K \cdot CF_3SO_3 \cdot 2H_2O \cdot CH_3CN$ showing the heteroatom labeling scheme. Non-essential hydrogens, the $CF_3SO_3^-$ counter anion, and a CH_3CN solvent molecule have been omitted for clarity. Hydrogen bonding interactions are indicated as dashed lines. Thermal ellipsoids are scaled to the 50% probability level.

In the above structure, examination of the pyrrole groups reveals that each such subunit is tilted out of the plane defined by the ten atom quinoxaline rings. Interestingly, two water molecules are present, but are hydrogen-bound to only one of the quinoxaline groups present in the K^+-bridged dimer *via* pyrrole NH···O interactions, with distances of 1.980 Å (H1A···O1w) and 1.984 Å (H2A···O2w). Also present is an intramolecular hydrogen bond of 2.70 Å length between N1B and N3B. This interaction is presumed to play an important role in defining the

dihedral angle between the quinoxaline core and this particular pyrrole. The counter trifluoromethanesulfonate anion and a molecule of acetonitrile are present in the crystal lattice but only as spectator species.

Crystallization of **3.37** from acetone yielded the structure shown in Figure 3.5. This side view shows that **3.37** exists, like the 15-crown-5 derivative, as an anti-parallel hydrogen-bound dimer, also stabilized by two sets of identical intermolecular hydrogen-bonds from N4···O1' (3.06 Å) and N4···O2' (3.29 Å). Interestingly, the two quinoxaline groups are offset from one another and hence "slipped" relative to what is seen for the 15-crown-5 analog **3.32** (Figure 3.3). The two fused benzene rings present in **3.37** appear to stack but the atom-to-atom distances of approximately 4 Å, although shorter than those observed for **3.32**, are greater than those expected for systems linked by strong π-π stacking interactions. In the unit cell, each dimer is further hydrogen-bound to an adjacent dimer, through a set of two pyrazine-N···pyrrole-NH interactions of 2.247 Å.

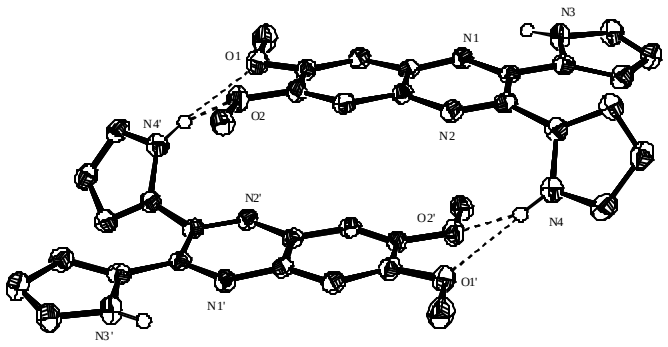

Figure 3.5 Ortep view of **3.37** showing the heteroatom labeling scheme. Non-essential hydrogens have been omitted for clarity. Hydrogen bonding interactions are indicated as dashed lines. Thermal ellipsoids are scaled to the 50% probability level.

3.3 PROTON NMR TITRATIONS

As mentioned in Section 3.1.1, previous studies of 2,3-bis-(1*H*-pyrrol-2-yl)-quinoxaline **3.1a** showed an enhanced affinity for fluoride anion over other halides; in addition to being confirmed by both fluorescence and ^{1}H NMR titrations, this selectivity was also recognizable as a colorimetric change from yellow to reddish-orange.[16] The addition of electron withdrawing groups to form, e.g., 6-nitro-2,3-bis-(1*H*-pyrrol-2-yl)-quinoxaline further enhanced the affinity for fluoride anion. During the design of the current crown-substituted bis-(1*H*-pyrrol-2-yl)-quinoxalines, it was thus speculated that the sigma-donating quality of the "methoxy-like" ethers would act to diminish the affinity of the pyrrole units for fluoride anion. To test this hypothesis, the control 6,7-dimethoxy-2,3-bis-(1*H*-pyrrol-2-yl)-quinoxaline **3.37** was studied using standard ^{1}H NMR spectroscopic titration techniques. The resulting nonlinear least squares analysis[52] gave K_a

values of 3,110 ± 565 M^{-1} for 6,7-dimethoxy-2,3-bis-(1*H*-pyrrol-2-yl)-quinoxaline **3.37** (Figure 3.6a) versus 7,480 ± 2200 M^{-1} for 2,3-bis-(1*H*-pyrrol-2-yl)-quinoxaline **3.1a** (Figure 3.6b), as determined in acetone-d_6. Despite this confirmation of compromised binding (by roughly a factor of two), it was hoped that the well-established ability of crown ethers to complex alkali metal cations would lead to systems in which good fluoride anion binding was observed. Specifically, it was considered possible that the electron withdrawing effects of cation complexation would overcome the electron donating effects of the ether-tethered crown substituents and thus giving rise to cooperative systems that would not show an appreciably reduced fluoride anion affinity.

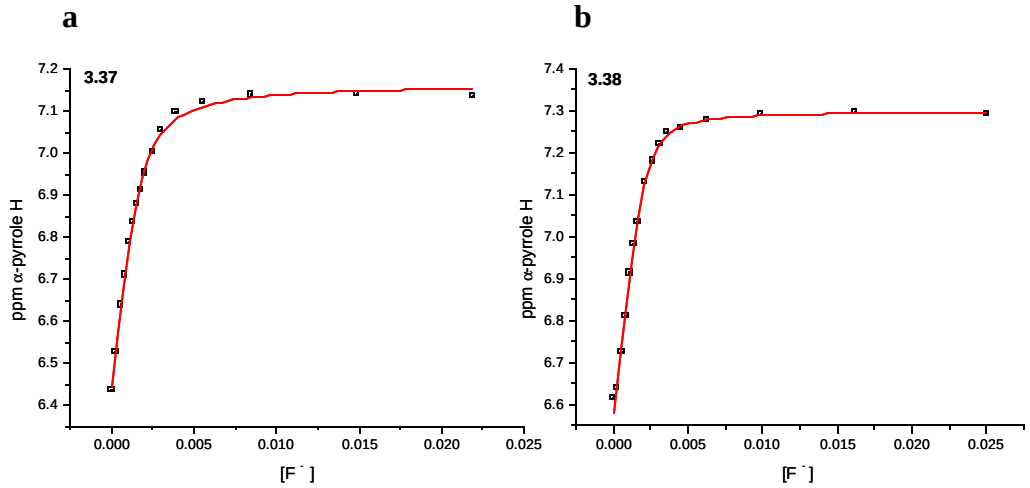

Figure 3.6 Nonlinear least squares analysis of data taken from ^{1}H NMR spectroscopic titrations in acetone-d_6 of Bu_4NF with (a) a solution containing a concentration of 8.06 x 10^{-4} M of **3.37** varying from 0 – 27 eqv. F^-; (b) a solution containing a concentration of 8.89 x 10^{-4} M of **3.38** varying from 0 – 28 eqv. F^-.

Against the backdrop of such considerations, solution state ^{1}H-NMR spectroscopic titrations of the four crown-substituted dipyrrolylquinoxalines **3.31**-**3.34** were undertaken. Acetone-d_6 was chosen as the solvent due to its ability to solubilize all of the species being studied, as well as to minimize potential ion pairing interactions. Initially, the binding of fluoride anion (as the tetrabutylammonium trihydrate salt) and the alkali metal cation (as the trifluoromethane sulfonate salt) to each receptor was performed separately in order to establish that each binding event was occurring independently, as well as to obtain a "baseline" of sorts against which evidence of cooperativity in mixed studies could be judged.

Data from ^{1}H NMR titrations showed that F^- bound to the all-oxygen receptors **3.31** and **3.32** (K_a = 6,950 ± 2,630 M^1 and 12,500 ± 5,480 M^1, respectively) more strongly than to the aza-substituted analogs **3.33** and **3.34** (K_a = 1,310 ± 565 M^{-1} and 1,220 ± 225 M^{-1}, respectively) (Figure 3.7); in each case, a color change was seen from yellow to reddish-orange upon the addition of fluoride anion. Rather surprisingly, the association constants for fluoride anion binding for the all-oxygen-analogs **3.31** and **3.32** were found to be of the same order of magnitude as the parent dipyrrolylquinoxaline **3.1** (K_a = 7,480 ± 2,20 M^{-1}). Hence, unlike the dimethoxy substituted system **3.37**, the "methoxy-like" ethers of **3.31** and **3.32** were not found to affect significantly the affinity of the pyrrole units for fluoride anion.

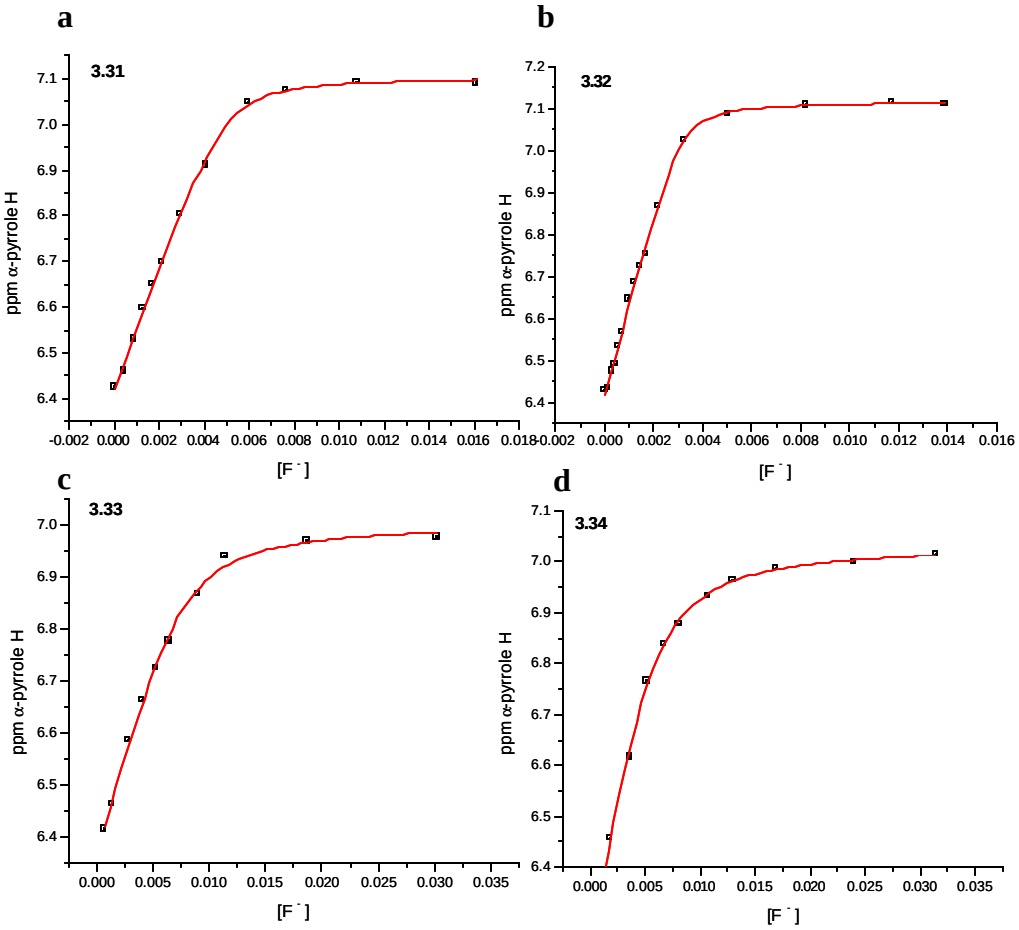

Figure 3.7 Nonlinear least squares analysis of data taken from ^{1}H NMR spectroscopic titrations in acetone-d_6 of Bu_4NF with (a) a solution containing a concentration of 1.31 x 10^{-3} M of **3.31** varying from 0 – 12 eqv. F^-; (b) a solution containing a concentration of 3.32 x 10^{-4} M of **3.32** varying from 0 – 16 eqv. F; (c) a solution containing a concentration of 3.33 x 10^{-3} M of **3.33** varying from 0 – 27 eqv. F^-; (d) a solution containing a concentration of 3.34 x 10^{-3} M of **3.34** varying from 0 – 24 eqv. F^-.

The cation binding behavior of receptors **3.31**-**3.34**, again studied in acetone-d_6, follows two distinct patterns for both Na^+ and K^+ in the form of their trifluoromethanesulfonate salts (Figure 3.8). First, the 18-crown-6 **3.31** (K_a =

57,500 ± 7,820 M^{-1}, Figure 3.8a) and the aza-18-crown-6 **3.33** (K_a = 11,400 ± 1,140 M^{-1}, Figure 3.8c) showed higher binding for Na^+ than their smaller 15-crown-5 counterparts **3.32** and **3.34** (K_a = 1,230 ± 22 M^{-1}, Figure 3.8b, and 195 ± 6 M^{-1}, Figure 3.8d, respectively), a finding that is consistent with the crown ether binding literature.[44] A similar comparison could not be made for K^+ since clean 1:1 binding was not observed in the case of **3.32** and **3.34**. This is fully consistent with our observation that **3.32** forms a 2:1 K^+ complex in the solid-state (Figure 3.4). Receptor 18-crown-6 **3.31** exhibited a binding affinity for K^+ of 86,900 ± 11,100 M^{-1} (Figure 3.9a) whereas the aza-18-crown-6 **3.33** bound K^+ with a K_a of 13,100 ± 2,070 M^{-1} (Figure 3.9b).

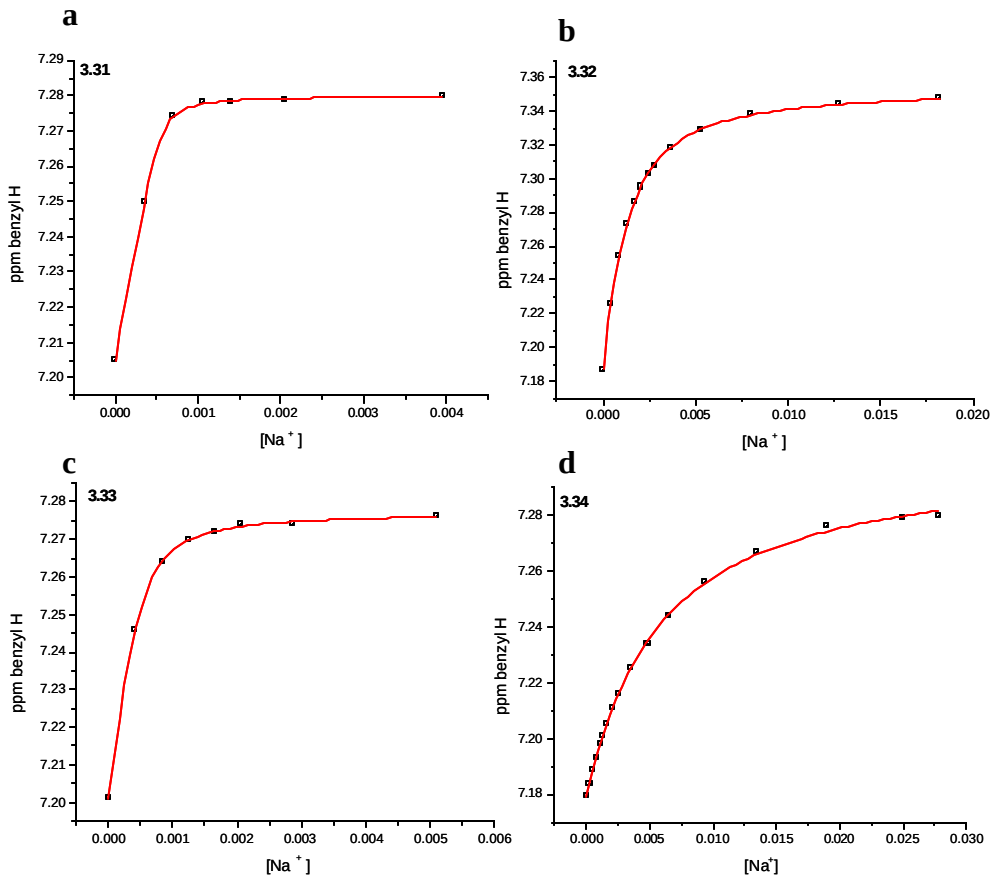

Figure 3.8 Nonlinear least squares analysis of data taken from ^{1}H NMR spectroscopic titrations in acetone-d_6 of $NaCF_3SO_3$ with (a) a solution containing a concentration of 8.63 x 10^{-4} M of **3.31** varying from 0 – 5 eqv. Na^+; (b) a solution containing a concentration of 8.58 x 10^{-4} M of **3.32** varying from 0 – 21 eqv. Na^+; (c) a solution containing a concentration of 9.25 x 10^{-4} M of **3.33** varying from 0 – 6 eqv. Na^+; (d) a solution containing a concentration of 1.04 x 10^{-3} M of **3.34** varying from 0 – 24 eqv. Na^+.

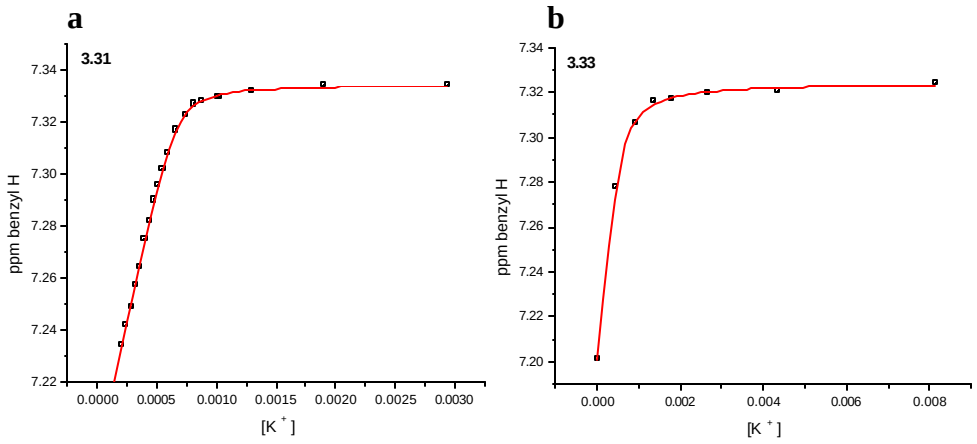

Figure 3.9 Nonlinear least squares analysis of data taken from ^{1}H NMR spectroscopic titrations in acetone-d_6 of KCF_3SO_3 with (a) a solution containing a concentration of 8.69 x 10^{-4} M of **3.31** varying from 0 – 3 eqv. K^+; (b) a solution containing a concentration of 9.52 x 10^{-4} M of **3.32** varying from 0 – 9 eqv. K^+.

Similar studies revealed that the all-oxygen receptors **3.31** and **3.32** exhibited stronger binding for Na^+ cation than the corresponding aza-analogs **3.33** and **3.34**, respectively. Likewise, **3.31** demonstrated enhanced binding for K^+ cation compared to its aza-analog **3.33**. This occurrence can be explained by classic crown ether coordination chemistry; the softer nitrogen donors in the aza analogs **3.33** and **3.34** do not bind alkali metals as strongly as their harder oxygen counterparts.[53] The results of these investigations are summarized in Table 3.1.

Table 3.1 Binding constants (K_a) measured in M^{-1} for **3.31**-**3.34**. Calculations taken from ^1H NMR spectroscopic titrations carried out in acetone-d_6.

Ion	**3.31**	**3.32**	**3.33**	**3.34**
F^-	6,950 ± 2,630	12,500 ± 5,480	1,310 ± 565	1,220 ± 225
Na^+	57,500 ± 7,820	1,230 ± 22	11,400 ± 1,140	195 ± 6
K^+	86,900 ± 11,100	[a]	13,110 ± 2,070	[a]

[a] Not determined due to the formation of a 2:1 complex.

Inspection of the anion and cation data generated in the above baseline studies engenders a fundamental question: why are there such large variations in the K_a values for fluoride anion seen in the four receptor systems? The portion of the receptor involved in the fluoride binding, namely the dipyrrolylquinoxaline moiety, is identical in each receptor. It was thus inferred that the crown ethers somehow influence the fluoride binding process, even though this binding presumably takes place far from the crown ether sites. Beyond the first set of methoxy-like, phenolic-type oxygens in the crown ethers (atoms that are identical for all four dipyrrolylquinoxaline units), it is unlikely that the specific nature of the crown ether will have a significant electronic effect on the system due to the lack of conjugation between the crown ether and the rest of the receptor. Therefore, various second order effects, including those associated with conformational changes, steric effects, or self-association must be considered.

Although there is no direct solution state evidence to implicate possible differences in complex equilibria between the receptors and their anionic and

cationic guests, it bears notice that in the solid state structures produced from crystals grown from acetone, the same solvent used for the solution state binding studies, there are distinct differences in terms of structure and self-association.

From the single crystal X-ray diffraction structure of the 15-crown-5-dipyrrolylquinoxaline **3.32** (Figure 3.3), for instance, it is clear that, in the solid state, there are hydrogen bonding interactions involving a pyrrole NH proton and two of the oxygen atoms in the crown ether (N2···O4' and N2···O5'), leading to a "back to front", face-to-face dimer comprised of four hydrogen bonds. The solid state interactions of the 18-crown-6 derivative **3.31** are more complicated. In addition to existing as a tetramer in the unit cell, the motif is stabilized by many hydrogen bonding interactions. The collective strength of these interactions, if present in solution, might be enough to have an effect on the K_a values. Certainly, to the extent they exist, such interactions would need to be disrupted by the addition of fluoride before the pyrrole NH protons would become available for anion binding. Indeed, according to the Jeffrey classification[54,55] of hydrogen bonds, four of the interactions are classified as "weak" (H···A > 2.2 Å, bond energy < 4 kcal mol^{-1}), and six are classified as "moderate" (H···A 1.5-2.2 Å, bond energy 4-15 kcal mol^{-1}). This results in a stabilization energy of at least 24 kcal mol^{-1}, a value that would represent a significant energy barrier if present in solution. Support for this rationalization comes from the observation that, in solution, higher fluoride anion binding is observed for **3.32** than for **3.31**. This is noteworthy because **3.32** forms a self-associated dimer in the solid-state, whereas **3.31** exists as an organized tetramer in the unit cell.

Unfortunately, attempts to grow X-ray quality crystals of both the aza-18-crown-6 and aza-15-crown-5 analogs **3.33** and **3.34** were unsuccessful. As a result, a definitive analysis of the structures and the possible hydrogen bonding interactions could not be made. However, interactions similar to those seen in **3.31** and **3.32** are considered likely. Further, additional hydrogen bonding interactions involving the NH in the azacrown ether are possible in these instances. To the extent they are present, they would be likely to have an adverse effect on the anion binding affinity for the reasons outlined above. The anion binding chemistry of these aza analogs is likely to be further complicated because the aza crown NH proton provides an additional hydrogen bond donating site with which a fluoride anion could interact. Indeed, a smaller K_a value for fluoride anion binding to the dipyrrolylquinoxaline core is seen for the aza-analogs **3.33** and **3.34** relative to the all-oxygen-analogs **3.31** and **3.32**, in solution. Not addressed by the present analyses, which probe only the pyrrole NH···anion interactions, is the K_a for the system as a whole (including possible azacrown-anion interactions). These could be higher for **3.33** and **3.34** than for **3.31** and **3.32**.

If the self-association effects seen in the solid state are retained in solution, it is reasonable to assume they should be reflected in the titration data. In fact, this appears to be the case. For instance, during the titration to determine the K_a of both aza analogs **3.33** and **3.34**, no changes in the chemical shift of the a-pyrrole protons was observed until 1.2 and 1.4 molar equivalents of tetrabutylammonium fluoride trihydrate had been added, respectively. This

contrasts with the results obtained when the 15-crown-5 **3.32** and 18-crown-6 **3.31** were subject to a similar analysis. In this latter case, displacements in the a-pyrrole proton resonances were seen after the addition of only 0.16 and 0.33 equivalents of tetrabutylammonium fluoride trihydrate, respectively. While not established unambiguously, we interpret this "delay" in response upon the addition of fluoride anion to the need to break up self-associated aggregates before the pyrrole NHs become available for binding. The stronger the self-association (assumed to increase from upon going from the all-oxygen to the aza-containing analogs), the greater the fluoride anion concentration needed to disrupt the interactions. As a control experiment, a ^{1}H NMR titration of **3.31** was carried out with H_2O alone. Little change in the ^{1}H NMR spectrum was seen upon the addition of 24 equivalents, leading to the conclusion that water by itself is not the decisive factor leading to deaggregation.

Solution state self-association is also supported by initial qualitative studies carried out using fluorescence methods. Here, an increase in the emission intensity was seen upon the addition of the first equivalents of tetrabutylammonium fluoride to **3.31**. However, after further additions, the fluorescence quenching typical of fluoride binding to dipyrrolylquinoxalines was observed.[16,17]

Yet additional support for the proposed solution state self-assembly came from ^{1}H NMR concentration dependence experiments involving **3.31**. Specifically, in acetone-d_6 solution, an upfield shift of 0.1 ppm in the benzylic proton was observed upon increasing the concentration of the receptor from 1 mM

to 50 mM. Such observations are consistent with the presence of concentration dependent π–π stacking interactions.[56]

Analyses made using Job plots[57] also support the proposed solution-phase self-association processes. Only the 15-crown-5-dipyrrolylquinoxaline **3.32**, which required the smallest quantity of fluoride anion to induce a chemical shift, yielded a plot that was clearly consistent with a 1:1 binding ratio between the receptor and fluoride (Figure 3.10). Strangely, a binding ratio could not be determined for the 18-crown-6-dipyrrolylquinoxaline **3.31**, even though there have been other hydrogen bonded systems in the literature with similar binding affinities that have exhibited clean Job plots.[58,59] Apparently, the need to add a small amount of fluoride anion to induce deaggregation and trigger the experimentally observed "delay" in the anion-induced chemical shift displacements was enough to prevent the first half of the Job plot from being determined accurately. Similar, but more severe, problems were seen when attempts were made to record Job plots for the interactions of F^- with the aza-crown-dipyrrolylquinoxalines **3.33** and **3.34**.

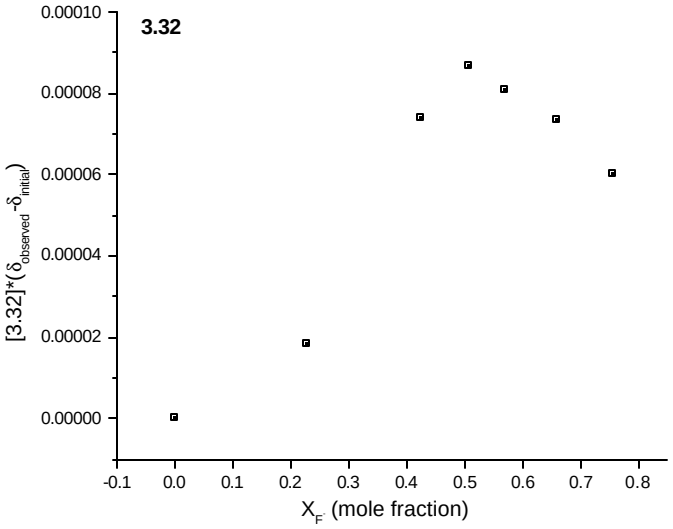

Figure 3.10 Job plot of **3.32** in acetone-d_6 with Bu_4NF showing 1:1 binding stoichiometry as determined by ^1H NMR spectroscopy at a concentration of 1.38 x 10^{-3} M.

Mole ratio plots were also used to confirm the classic (and expected) crown-ether type 1:1 binding stoichiometries for the 18-crown-6 **3.31** with both Na^+ and K^+, as well as for the aza-18-crown-6 **3.33** with Na^+ and K^+ (Figure 3.11). The binding of the 15-crown-5 **3.32** and the aza-15-crown-5 **3.34** with Na^+ was too weak to be determined by the mole ratio method; however, there is ample precedence to suggest a 1:1 binding mode.[44,53]

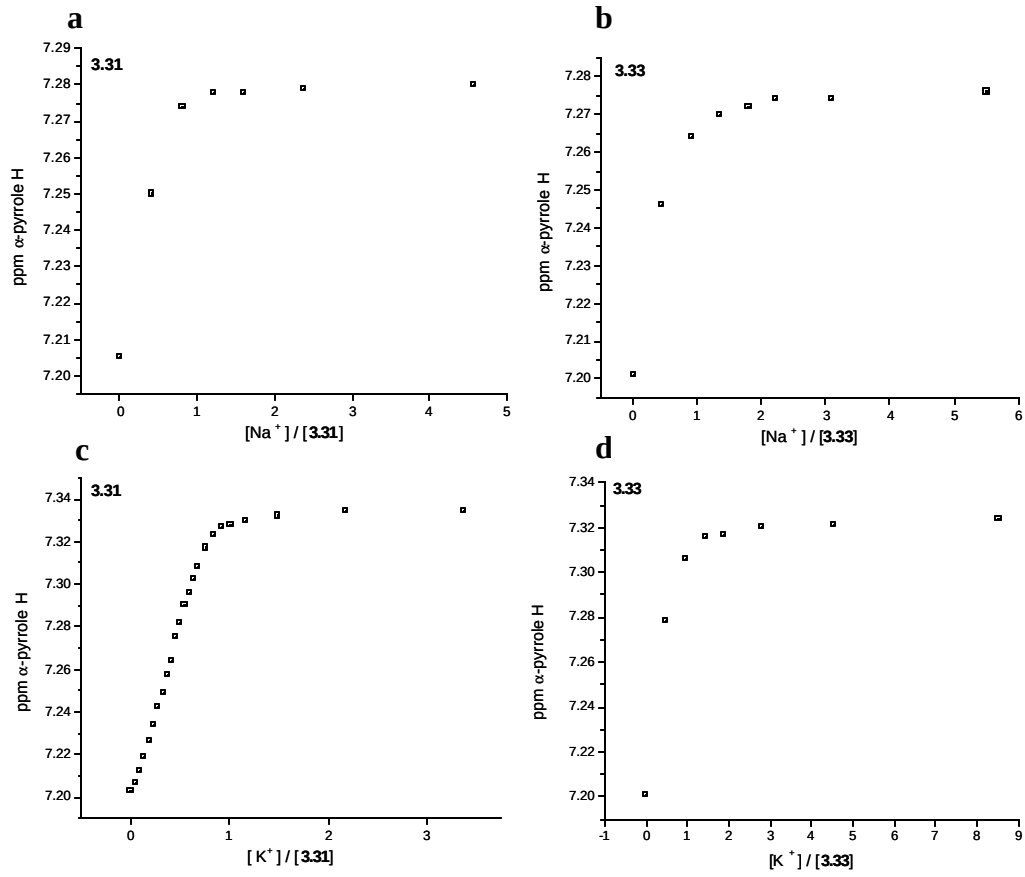

Figure 3.11 Mole ratio plot used to determine stoichiometry. These plots were derived from data of ^{1}H NMR spectroscopic titrations performed in acetone-d_6 of (a) $NaCF_3SO_3$ with a 8.63 x 10^{-4} M concentration of **3.31** from 0 – 5 eqv. Na^+; (b) $NaCF_3SO_3$ with a 9.25 x 10^{-4} M concentration of **3.33** from 0 – 6 eqv. Na^+; (c) KCF_3SO_3 with a 8.69 x 10^{-4} M concentration of **3.31** from 0 – 3 eqv. K^+; (d) KCF_3SO_3 with a 9.52 x 10^{-3} M concentration of **3.33** from 0 – 9 eqv. K^+.

As mentioned in the introduction to section 3.2, the hope and expectation was that systems **3.31**-**3.34** would act as ditopic receptors. Unfortunately, however, it was found that in the presence of one equivalent of Na^+ or K^+ cation, the fluoride anion binding affinities of dipyrrolylquinoxalines **3.31**-**3.34** were

significantly reduced, as determined by ^{1}H NMR spectroscopic titrations. For example, titration of **3.31** with tetrabutylammonium fluoride trihydrate gave a calculated K_a value of 6,950 ± 2630 M^{-1} (Figure 3.12a). However, repeating the titration in the presence of one molar equivalent of potassium trifluromethanesulfonate resulted in a K_a value of 685 ± 105 M^{-1} (Figure 3.12b).

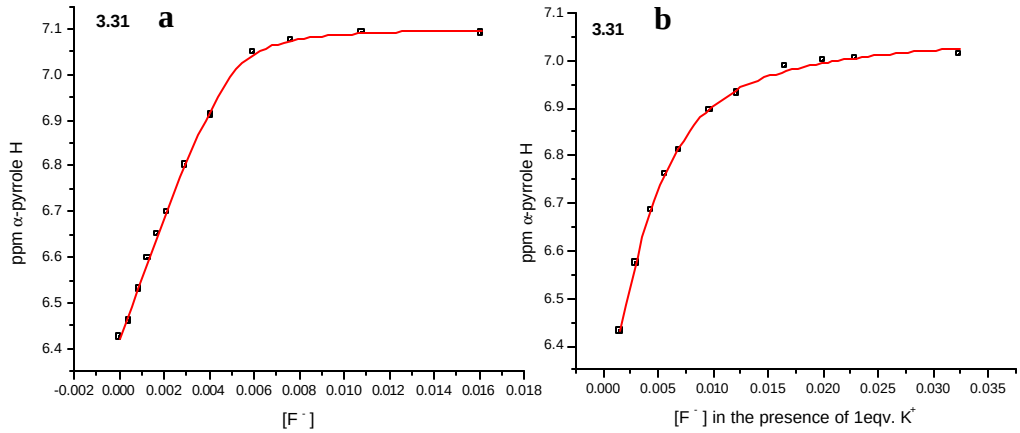

Figure 3.12 Nonlinear least squares analysis of data taken from ^{1}H NMR spectroscopic titrations in acetone-d_6 of Bu_4NF with (a) a solution containing a concentration of 1.31 x 10^{-3} M of **3.31** varying from 0 – 12 eqv. F^-; (b) a solution containing a concentration of 1.16 x 10^{-3} M of **3.31** varying from 0 – 28 eqv. F^- in the presence of 1 eqv. KCF_3SO_3.

The above findings are interpreted in terms of ion pairing effects. In particular, it is proposed that in studies involving NaF and KF, ion pairing between the cation and the fluoride anion occurs and it is this ion pair, rather than "free" fluoride or K^+ or Na^+ cations, that is bound. Because the affinity of the fluoride anion for the alkali metal cation within the contact ion pair, bound perhaps in part to the crown ether, is greater than that associated with the fluoride-

pyrrole hydrogen-bonding interaction, a reduced K_a is seen. Were the hydrogen bonding-based binding affinities of **3.31**-**3.34** greater for fluoride, then they might be able to compete with the K^+F^- or Na^+F^- ion pairing. Smith and co-workers also observed that the anion binding affinities of several neutral hosts were inhibited by the presence of alkali metal cations in polar organic solvents, and also attributed their findings to salt-type ion-pairing effects.[60]

3.4 UV-VISIBLE SPECTROSCOPIC TITRATIONS

Additional support for the above explanation was obtained from a series of UV-visible titrations carried out in spectroscopic grade acetone of dipyrrolylquinoxalines **3.31**-**3.34** using 1M Bu_4NF in THF in the presence of one equivalent of the trifluoromethane sulfonate salts of Li^+, K^+, Na^+ and Cs^+. If ion pairing is occurring, it should be reflected in the binding affinities across the series of cations. Specifically, as the ability of the cation to ion pair increases, the binding affinity between fluoride and the dipyrrolylquinoxaline should decrease. All titrations proceeded smoothly through two isosbestic points, with the original absorbance peak at 399 nm decreasing as the peak for the bound complex appeared at 475 nm, as exemplified by the titration of **3.31** with Bu_4NF in the presence of 1 eqv. Na^+ (Figure 3.13a). Unfortunately, in all instances nonlinear least squares analyses, although providing a value for the binding affinity, were characterized by poor fits with the R^2 value ranging from only 0.87 – 0.94 (Figure 3.13b). Benesi-Hildebrand analysis did not result in a linear fit in any instance,

indicating complex equilibria (Figure 3.13c). All additional binding affinity data for this series of titrations can be found in Appendix B.

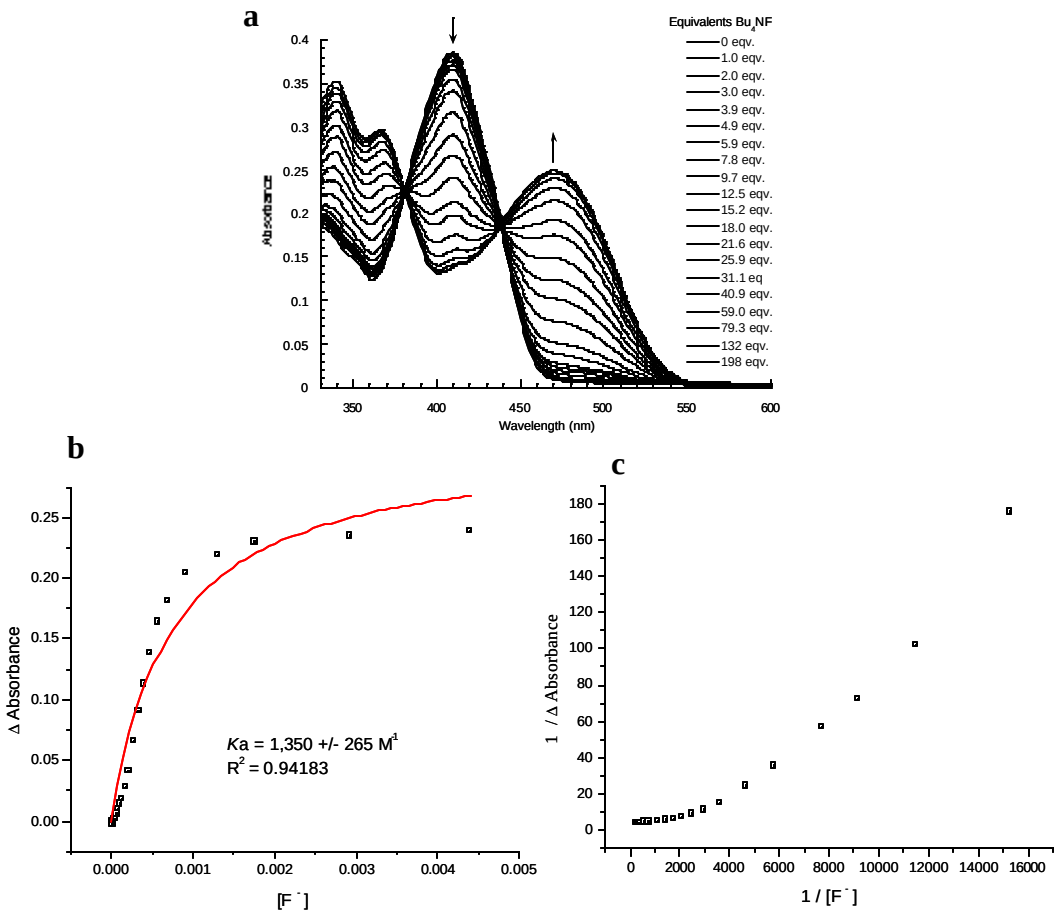

Figure 3.13 (a) UV-visible titration in spectroscopic grade acetone of a solution containing a concentration of **3.31** of 2.22 x 10^{-5} M varying Bu_4NF from 0 – 198 eqv. in the presence of 1 eqv. $NaSO_3CF_3$; (b) Nonlinear least squares analysis of the titration data; (c) Unsuccessful attempt to generate a linear Benesi-Hildebrand plot from the titration data.

In addition to fits that were less than optimal, the binding values obtained for fluoride with receptors **3.31**-**3.34** were as much as one order of magnitude

lower than what was observed from the ^{1}H NMR titrations. This disparity could reflect the greater sensitivity of UV-visible spectroscopy compared to ^{1}H NMR, although the lower initial concentrations of the dipyrrolylquinoxaline receptors employed would lead to the expectation that complications due to self assembly would be reduced. Certainly, it is difficult to rationalize why the UV-visible titrations of the receptors with F^- in the absence of a cation gave K_a values that were generally lower than the comparable results obtained from the ^{1}H NMR studies. Nonwithstanding these complications, the series of titrations revealed some insight into the behavior of the receptors with regard to ion pairing effects in acetone.

Table 3.2 shows the results from these titrations. Each receptor exhibited the highest binding affinity for F^- in the absence of a cation. Subsequently, the binding affinity of **3.31**-**3.34** for F^- decreased across the series of cations from Cs^+ - Li^+. Although these values cannot be considered to be truly quantitative, they are valuable in regards to their comparison with one another; since each exhibited the same pattern in their deviations from normal fitting behavior, it is likely that they undergo the same processes that cause this deviation, and can therefore be intercompared. To the extent such a supposition is valid, these results support the contention that the stronger the ability of the cation to participate in ion pairing ($Li^+ > Na^+ > K^+ > Cs^+$), the less likely the hydrogen bonding interactions of the dipyrrolylquinoxaline will be able to compete with the cation in question for the fluoride anion guest.

Table 3.2 Binding affinity of fluoride anion (as its tetrabutylammonium trihydrate salt) determined in the presence and absence of various cations as determined by UV-visible spectroscopy

		K_a for F^- binding determined in the presence of 1 eqv. of the specified cation (M^{-1})			
Receptor	K_a F^-	Cs^+	K^+	Na^+	Li^+
3.31	1960 ± 250	1900 ± 330	1820 ± 140	1350 ± 265	1010 ± 155
3.32	2350 ± 250	2120 ± 340	--	1640 ± 300	990 ± 200
3.33	2280 ± 340	2070 ± 140	1500 ± 260	--	790 ± 160
3.34	1840 ± 295	1470 ± 330	--	1350 ± 265	1120 ± 190

3.5 CONCLUSIONS AND FUTURE DIRECTIONS

Although these preliminary ^{1}H NMR and UV-visible data support the contention that ion pairing between the cation and the anionic fluoride guest is decreasing the affinity of the receptors for fluoride, there are a number of variables that need to be explored before this conclusion can be considered secure. One important consideration is the solvent medium, which has a direct effect on ion pairing; polar solvents inhibit ion pairing. Polar solvents also inhibit hydrogen bonding interactions by competing for the hydrogen bond donor or acceptor sites on the receptor. The balance between these competing factors is difficult to predict *a priori*. Given this concern and the fact that in the very early stages of this project fluoride anion binding was studied preliminarily *via* UV-visible and ^{1}H NMR spectroscopy using *dry* tetrabutylammonium fluoride, it was deemed prudent to revisit this issue. In these initial limited studies with dry

tetrabutylammonium fluoride, no significant binding occurred and a binding isotherm could not be obtained. It was this study that prompted the use of the commercially available trihydrate form of tetrabutylammonium fluoride. As noted earlier on in this chapter, using this hydrate gave rise to fluoride anion affinities that were substantial. It thus occurred to us that there likely might exist an optimal (relative) water concentration wherein the competing effects of decreased affinity and overly strong ion pairing might be weighed in favor of enhanced F^- recognition and, in the limit, good cation and anion cooperativity.

In an effort to explore the above possibility, precursory studies were undertaken with receptor **3.32** in acetone in the presence of 4%, 0.5% and 0.05% of water by volume in a solution of acetone. At 4% water, there was no visible color change upon addition of 1M Bu_4NF in THF. This was reflected in the UV-visible spectrum, which did not show any change even after the addition of 200 equivalents of fluoride, presumably due to competition from water for the receptor binding sites. The water content was then reduced to 0.5% water, resulting in a visible change upon addition of fluoride. However, no change was seen in the spectrum until after 122 equivalents of fluoride were added, which prevented the determination of a binding affinity. The water concentration was thus reduced to 0.05%, resulting in isosbestic behavior identical to that illustrated in Figure 3.13a. Interestingly, a change is seen in the UV-visible spectrum after the addition of only 0.5 eqv. of fluoride anion (Figure 3.14a); in the titration of **3.32** in plain acetone no change was seen until the addition of 2 eqv. of fluoride anion. This initial indication of stronger binding was confirmed by nonlinear

least squares analysis, which gave a binding affinity of 4,190 ± 550 M^{-1} (Figure 3.14b), a significant enhancement over the fluoride anion binding observed for **3.32** in plain acetone of 2,350 ± 250 M^{-1} with 1M Bu_4NF in THF. On the other hand, Benesi-Hildebrand analysis shows an S-shaped curve. This curve actually deviates from linearity to a greater extent than curves derived from plots generated from titrations of **3.31**-**3.34** with fluoride anion in the presence of a cation (as exemplified by Figure 3.13c). This supports the hypothesis that complex equilibria are being followed in solution, and that water is a significant contributor to the complexity of the equilibria.

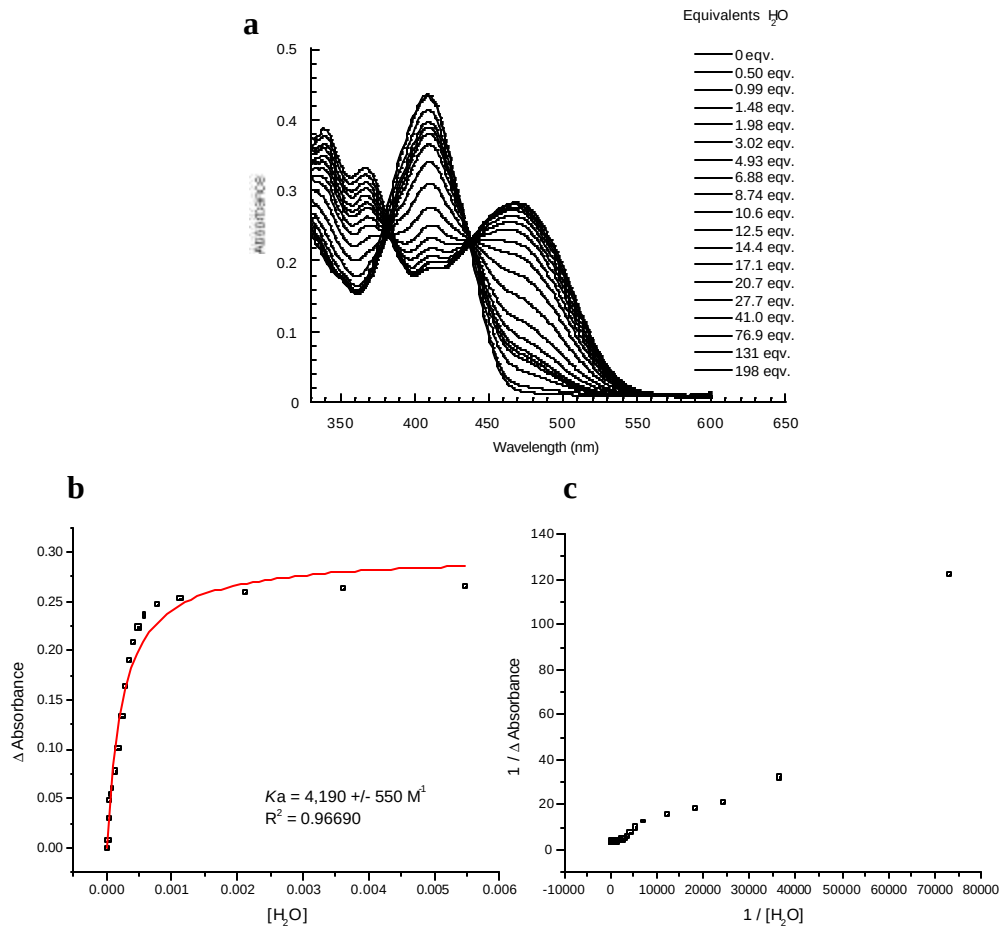

Figure 3.14: (a) UV-visible titration in a 0.05% water / acetone solution containing a concentration of **3.32** of 2.77 x 10^{-5} M varying Bu_4NF from 0 – 198 eqv.; (b) Nonlinear least squares analysis of the titration data; (c) Unsuccessful attempt to generate a linear Benesi-Hildebrand plot from the titration data.

To put the above conclusion on a more solid experimental footing, studies are ongoing to determine the water concentration that gives rise to the highest fluoride anion binding affinity. Additionally, the possibility of decomposition products in solutions made using Bu_4NF sources, which include FHF^-, are being

investigated to assist with quantification of the precise concentration of F^- in solution.[61]

Once this value is determined, attention will turn to studying the effect that Li^+, Na^+, K^+, and Cs^+ have on the fluoride anion binding process at this H_2O concentration. While not necessarily expected, it is hoped that under these optimized conditions, cation-anion binding will be seen in this series of quinoxaline receptors. To the extent that indications consistent with cooperativity are seen, detailed studies of the effect of varying cation concentration on the anion binding affinity will be carried out. Such studies should suffice to confirm the present indications of negative cooperativity.

Another effect which needs to be addressed is possible π stacking interactions. Although not seen in the solid state, there is considerable evidence that this may be occurring in solution. For example, it has already been noted that preliminary fluorescence quenching studies in dichloromethane and dimethylsulfoxide failed to give easily analyzable results due to the initial increase in emission seen upon anion addition, results that are indicative of π stacking behavior. The possibility of π stacking was also raised in the context of the ^1H NMR concentration study carried out in acetone. Here, an upfield shift of 0.1 ppm upon a 50-fold increase of the concentration of **3.31** was seen. Also, less-than-ideal Job plots resulted from the data. Likewise, in the UV-visible studies of receptors **3.31**-**3.34** (Table 3.2) the first addition of fluoride anion, usually approximately 0.5-1 eqv., was found not to give rise to the expected decrease in absorbance intensity. Rather, the addition of the first F^- equivalent either

maintains the initial absorbance level or increases it slightly (< 0.01 absorbance units). Such behavior is, again, consistent with possible π stacking interactions.

To the extent that a functioning ditopic recepor is sought, it is important to minimize these interactions. By performing studies at a lower concentration, it should be possible to mitigate these effects and possibly obtain more accurate data. Thus, after determining the optimal concentration of water for fluoride binding, it is proposed that studies be carried out at very low concentrations, perhaps as low as 1×10^{-7} M using fluorescence quenching methods to attain the needed sensitivity.

While it is hoped that the present systems can be made to function as ditopic receptors, it is likely that a different strategy will be needed if this ultimate goal is to be attained. In moving towards this objective the fact that ion pairing interactions appear to predominate over hydrogen bonding interactions, at least in this solvent (acetone) and with the receptors tested to date, leads to the supposition that reducing the large distance between the cation and anion binding sites might be useful. Such a strategy would allow the ions in question (e.g., Na^+ or K^+ and F^-) to pair with one another while simultaneously participating in a hydrogen bonding interaction with the corresponding portion of the crown appended dipyrrolylquinoxaline receptor. In a number of known ditopic receptors, the simultaneous binding of a cation and anion takes place over a shorter distance. The benefits of this approach are particularly well exemplified by the diazacrown-based receptor prepared by Smith and co-workers[40] that binds alkali halides within contact ion pairing distance. It is also of interest to note that

Nishizawa *et al.*[62] have successfully demonstrated the ditopic-binding properties of a thiourea-functionalized benzo-15-crown-5 that bears formal resemblance to our current generation of crowned dipyrrolylquinoxaline receptors, but which has an inherently shorter distance between the cation and anion binding sites. Given the geometric constraints and synthetic difficulties associated with working with crown ethers and dipyrrolylquinoxalines, it is likely that the preparation of a new generation of functional ditopic anion-cation receptors wherein such conditions are met will be challenging.

One particular approach to generating systems that fit the above design criteria and which stay within the present crown ether dipyrrolylquinoxaline paradigm, could involve attaching the crown ether moiety to the opposite end of the dipyrrolylquinoxaline unit. For instance, the known dialdehyde **3.38**, recently prepared by Hiromitsu Maeda in the Sessler group, could be condensed with the appropriate polyethylene glycol diamine **3.39**.[63] This would produce a receptor, **3.40**, that contains a cyclic ether-like linker bridged between the erstwhile open α positions on each pyrrole. By varying the length of the linker, the selectivity of the ditopic receptor for various cations could be fine tuned. In addition to providing a cation binding site in closer proximity to the anion binding site, this would lend preorganization to the entire binding pocket and potentially result in stronger fluoride binding even in the absence of a cation.

Scheme 3.4 Proposed synthesis of a new polyethylene glycol linked dipyrrolylquinoxaline.

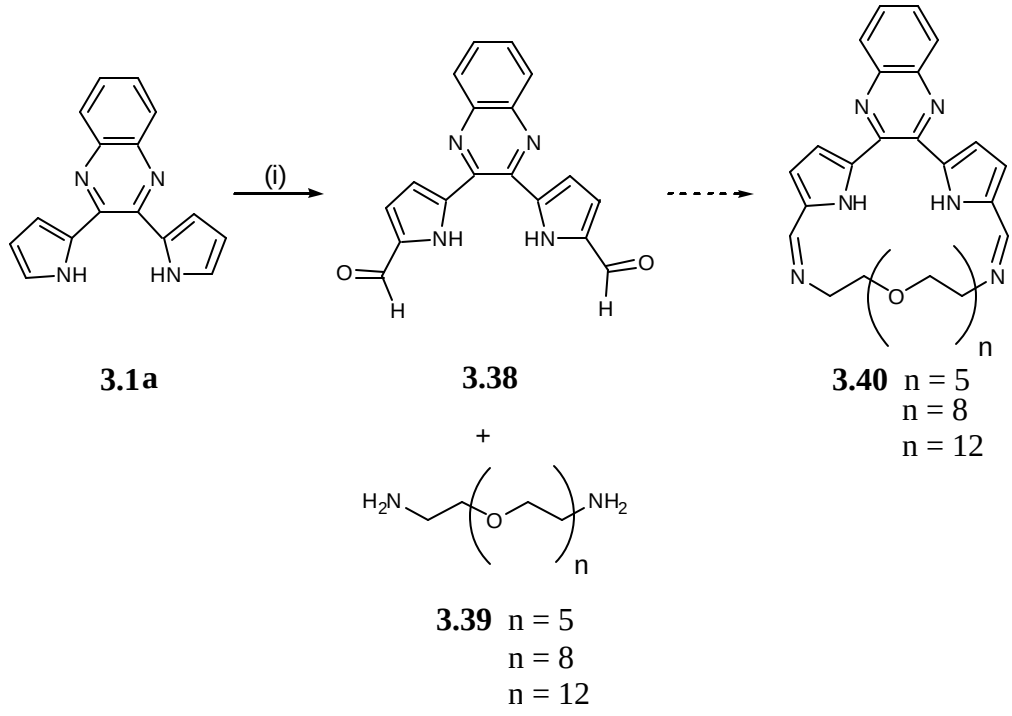

3.1a **3.38** **3.40** n = 5
n = 8
n = 12

3.39 n = 5
n = 8
n = 12

Reagents: (i) $POCl_3$, DMF[22]

Although significant effort must still be put forth to adapt the current crown appended dipyrrolylquinoxaline strategy to the production of an effective ditopic receptor, the solid state structure of **3.31** deserves comment. Unlike 15-crown-5-dipyrrolylquinoxaline **3.32** and dimethoxy-dipyrrolylquinoxaline **3.37**, which both form intermolecular dimers in the solid-state, the 'crowned' system **3.31** is found to form a tetramer in the solid-state that is chacterized by five infinite channels. The elegance of this structure coupled with the current interest in nanotube technology, particulary artificial ion channels, leads us to suggest that

supramolecular assemblies of this type could function as mimics of the biologically significant aquaporin water channels[64,65] or anion-conducting channels, of which there is currently only one example in the literature.[10] Thus, the present work, although not yet successful in terms of attaining its targeted goal of effecting cooperative cation-anion recognition, might yet serve an important role in terms of inspiring new transport studies and, as such, addressing a problem of even greater scientific significance.

References

(1) Lehn, J.-M. *Supramolecular Chemistry*; VCH: Weinheim, 1995.

(2) Steed, J. W.; Atwood, J. L. *Supramolecular Chemistry*; Wiley: Chichester, 2000.

(3) Reetz, M. T. In *Comprehensive Supramolecular Chemistry*; Atwood, J. L., Davies, J. E. D., MacNicol, D. D., Vögtle, F., Gokel, G. W., Eds.; Pergamon: Oxford, 1996; Vol. 2, pp 553-562.

(4) Antoinisse, M. M. G.; Reinhoudt, D. N. *Chem. Commun.* **1998**, 443-448.

(5) Beer, P. D.; Gale, P. A. *Angew. Chem., Int. Ed. Engl.* **2001**, *40*, 486-516.

(6) Kirkovits, G. J.; Shriver, J. A.; Gale, P. A.; Sessler, J. L. *J. Inclusion Phenom. Macrocyclic Chem.* **2001**, *41*, 69-75.

(7) Pike, J. D.; Rosa, D. T.; Coucouvanis, D. *Eur. J. Inorg. Chem.* **2001**, 761-777.

(8) Rudkevich, J. D.; Mercer-Chalmers, J. D.; Verboom, W.; Ungarro, R.; de Jong, F.; Reinhoudt, D. N. *J. Am. Chem. Soc.* **1995**, *117*, 6124-6125.

(9) Christoffels, L. A. J.; de Jong, F.; Reinhoudt, D. N.; Sivelli, S.; Gazzola, L.; Casanati, A.; Ungarro, R. *J. Am. Chem. Soc.* **1999**, *121*, 10142-10151.

(10) Schlesinger, P. H.; Ferdani, R.; Liu, J.; Pajewska, J.; Pajewski, R.; Saito, M.; Shabany, H.; Gokel, G. W. *J. Am. Chem. Soc.* **2002**, *124*, 1848-1849.

(11) Sidorov, V.; Kotch, F. W.; Abdrakhmanova, G.; Mizani, R.; Fettinger, J. C.; Davis, J. T. *J. Am. Chem. Soc.* **2002**, *124*, 2267-2278.

(12) Heiss, N. S.; Poustka, A. *Genomics* **1997**, *45*, 224-228.

(13) Jentsch, T.; Gunther, W. *Bioessays* **1997**, *19*, 117-126.

(14) Sessler, J. L.; Allen, W. E. *Chemtech* **1999**, *29*, 16-24.

(15) Jentsch, T. J. *Nature* **2002**, *415*, 276-277.

(16) Black, C. B.; Andrioletti, B.; Try, A. C.; Ruiperez, C.; Sessler, J. L. *J. Am. Chem. Soc.* **1999**, *121*, 10438-10439.

(17) Anzenbacher, J., P.; Try, A. C.; Miyaji, H.; Jursiková, K.; Lynch, V. M.; Marquez, M.; Sessler, J. L. *J. Am. Chem. Soc.* **2000**, *122*, 10268-10272.

(18) Mizuno, T.; Wei, W.-H.; Eller, L. R.; Sessler, J. L. *J. Am. Chem. Soc.* **2002**, *124*, 1134-1135.

(19) Gokel, G.; Royal Society of Chemistry: Cambridge, U. K., 1991, p 80.

(20) Oddo, B. *Gazz. Chim. Ital.* **1911**, *41*, 248.

(21) Anzenbacher, J., P.; Tyson, D. S.; Jursiková, K.; Castellano, F. N. *J. Am. Chem. Soc.* **2002**, in press.

(22) Sessler, J. L.; Maeda, H.; Mizuno, T.; Lynch, V. M.; Furuta, H. *Chem. Commun.* **2002**, 862-863.

(23) Sessler, J. L.; Andrievsky, A. *Chem. Commun.* **1996**, 1119-1120.

(24) Rosa, D. T.; Young, V. G.; Coucouvanis, D. *Inorg. Chem.* **1998**, *37*, 5042-5043.

(25) Hossain, M. A.; Schneider, H.-J. *J. Am. Chem. Soc.* **1998**, *120*, 11208-11209.

(26) Sirish, M.; Schneider, H.-J. *Chem. Commun.* **1999**, 907-908.

(27) Beer, P. D.; Hopkins, P. K.; McKinney, J. D. *Chem. Commun.* **1999**, 1253-1254.

(28) White, D. J.; Laing, N.; Miller, H.; Parsons, S.; Coles, S.; Tasker, P. A. *Chem. Commun.* **1999**, 2077-2078.

(29) Reetz, M. T.; Niemeyer, C. M.; Harms, K. *Angew. Chem., Int. Ed. Engl.* **1991**, *30*, 1472-1474.

(30) Reetz, M. T.; Johnson, B. M.; Harms, K. *Tetrahedron Lett.* **1994**, *35*, 2525-2528.

(31) Rudkevich, D. M.; Brzozka, Z.; Palys, M.; Visser, H. C.; Verboom, W.; Reinhoudt, D. N. *Angew. Chem., Int. Ed. Engl.* **1994**, *33*, 467-468.

(32) Rudkevich, D. M.; Verboom, W.; Reinhoudt, D. N. *J. Org. Chem.* **1994**, *59*, 3683-3686.

(33) Scheerder, J.; van Duynhoven, J. P. M.; Engbersen, J. F. J.; Reinhoudt, D. N. *Angew. Chem., Int. Ed. Engl.* **1996**, *35*, 1090-1093.

(34) Beer, P. D.; Dent, S. W. *Chem. Commun.* **1998**, 825-826.

(35) Beer, P. D.; Cooper, J. B. *Chem. Commun.* **1998**, 129-130.

(36) Cooper, J. B.; Drew, M. G. B.; Beer, P. D. *J. Chem. Soc., Dalton Trans.* **2000**, 2721-2728.

(37) Cooper, J. B.; Drew, M. G. B.; Beer, P. D. *J. Chem. Soc., Dalton Trans.* **2001**, 392-401.

(38) Beer, P. D.; Drew, M. G. B.; Knubley, R. J.; Ogden, M. I. *J. Chem. Soc., Dalton Trans.* **1995**, 3117-3123.

(39) Deetz, M. J.; Shang, M.; Smith, B. D. *J. Am. Chem. Soc.* **2000**, *122*, 6201-6207.

(40) Mahoney, J. M.; Beatty, A. M.; Smith, B. D. *J. Am. Chem. Soc.* **2001**, *123*, 5847-5848.

(41) Sessler, J. L.; Bruker, E. A. *Tetrahedron Lett.* **1995**, *36*, 1175-1176.

(42) Sessler, J. L.; Shriver, J. A.; Gebauer, A.; Gale, P. A. In *23rd ISMC*: Hawaii, 1998.

(43) Sessler, J. L.; Gale, P. A.; Genge, J. W. *Chem. Eur. J.* **1998**, *4*, 1095-1099.

(44) Izatt, R. M.; Pawlak, K.; Bradshaw, J. S.; Bruening, R. L. *Chem. Rev*. **1991**, *91*, 1721-1785.

(45) Maeda, H.; Furuyoshi, S.; Nakatsuji, Y.; Okahara, M. *Bull. Chem. Soc. Jpn.* **1983**, *56*, 212-218.

(46) Topal, G.; Demirel, N.; Togrul, M.; Turgat, Y.; Hosgören, H. *J. Heterocycl. Chem.* **2001**, *38*, 281-284.

(47) Dahl, T. *Acta Chem. Scand.* **1994**, *48*, 95-106.

(48) Mallinson, P. R.; Truter, M. R. *J. Chem. Soc., Perkin Trans. II* **1972**, 1818-1823.

(49) Shinkai, S.; Nakaji, T.; Ogawa, T.; Shigematsu, K.; Manabe, O. *J. Am. Chem. Soc.* **1981**, *103*, 111-115.

(50) Kikukawa, K.; He, G.-X.; Abe, A.; Goto, T.; Arata, R.; Ikeda, T.; Wada, F.; Matsuda, T. *J. Chem. Soc., Perkin Trans. II* **1987**, 135-141.

(51) Beer, P. D.; Tite, E. L.; Ibbotson, A. J. *J. Chem. Soc., Dalton Trans.* **1990**, 2691-2696.

(52) Wilcox, C. W. *Frontiers in Supramolecular Organic Chemistry and Photochemistry*; VCH: Weinheim, 1991.

(53) Weber, E.; Vögtle, F. *Top. Curr. Chem.* **1981**, *98*, 1-41.

(54) Steiner, T. *Angew. Chem., Int. Ed. Engl.* **2002**, *41*, 48-76.

(55) Jeffrey, G. A. *An Introduction to Hydrogen Bonding*; Oxford University Press: Oxford, 1997.

(56) Hamuro, Y.; Geib, S. J.; Hamilton, A. D. *J. Am. Chem. Soc.* **1997**, *119*, 10587-10593.

(57) Connors, A. K. *Binding Constants: the Measurement of Molecular Complex Stability*; Wiley: New York, 1987.

(58) Gale, P. A.; Camiolo, S.; Tizzard, G. J.; Chapman, C. P.; Light, M. E.; Coles, S. J.; Hursthouse, M. B. *J. Org. Chem.* **2001**, *66*, 7849-7853.

(59) Scheerder, J.; Fochi, M.; Engbersen, J. F. J.; Reinhoudt, D. N. *J. Org. Chem.* **1994**, *59*, 7815-7820.

(60) Shukla, R.; Kida, T.; Smith, B. D. *Org. Lett.* **2000**, *2*, 3099-3102.

(61) Sharma, R. K.; Fry, J. L. *J. Org. Chem.* **1983**, *48*, 2112-2114.

(62) Nishizawa, S.; Shigemori, K.; Teramae, N. *Chem. Lett.* **1999**, 1185-1186.

(63) Andrus, M. B.; Turner, T. M.; Updegraff, E. P.; Sauna, Z. E.; Ambudkar, S. V. *Tetrahedron Lett.* **2001**, *42*, 3819-3822.

(64) Verkman, A. S.; Mitra, A. K. *Am. J. Physiol. Renal Physiol.* **2000**, *278*, F13-F28.

(65) Sansom, M. S. P.; Law, R. J. *Curr. Biol.* **2001**, *11*, R71-R73.

Chapter 4: Experimental

Spectroscopic grade acetone, dichloromethane, and acetonitrile used for UV-visible sprectroscopic experiments were obtained from EM Science. All NMR solvents were purchased from Cambridge Isotope Laboratories, Inc. Anion tetrabutylammonium salts were purchased from Fluka. Trifluorosulfonate cation salts were purchased from Fluka or from Aldrich. All other reagents were purchased from Aldrich and used as received unless otherwise stated. TLC analyses carried out using Whatman K6F silica gel 60Å, 250 μm plates. Neutral aluminum oxide used was Aldrich Brockmann 1 type. ^{1}H NMR spectroscopic titrations were recorded on a Varian 300 MHz spectrometer. ^{1}H and ^{13}C NMR spectra used in the characterization of products were recorded on either a Varian Inova at 500 MHz (proton) and 125 MHz (carbon), a GE QE-300 or Bruker XX spectrometer at 300 MHz (proton) and 75 MHz (carbon). They were recorded in parts per million and referenced to the solvent. Low resolution FAB+ and CI+ mass spectra were obtained on a Finnigan MAT TSQ 70 mass spectrometer. High resolution FAB+ and CI+ mass spectra were recorded on a VG ZAB2-E mass spectometer. Elemental analyses were performed by Atlantic Microlabs. UV-Visible spectra were recorded on a Beckman DU-650 spectrophotometer. Cyclic and square wave voltammetric measurements were made on a BAS MF 9093 CV~50 W Version 2 instrument. The working electrode was a Pt disk with a Pt wire as the counter electrode, and Ag/AgCl as the reference electrode.

Diferrocene calixpyrrole (1.28 and 1.29). Gem dimethyl dipyrromethane (230 mg, 1.32 mmol) and acetylferrocene (150 mg, 0.66 mmol) were dissolved in dry methanol (50 mL). The orange solution was degassed for 15 minutes followed by addition of trifluoroacetic acid (83 mg, 0.73 mmol). The solution immediately turned dark green. Within one hour a yellow gelatinous precitate formed. It was stirred at room temperature for 20 hours, at which time the yellow precitate was filtered off. The crude product was purified by flash chromatography (silica gel, eluent benzene) to afford **1.28** (78 mg, 15%) and **1.29** (78 mg, 15%). ^{1}H NMR δ (300 MHz, $CDCl_3$): (**1.28**) 1.50 (s, 6H, C*H*$_3$), 1.54 (s, 6H, C*H*$_3$), 1.88 (s, 6H, C*H*$_3$), 3.87 (s, 4H, FcC*H*), 4.02 (s, 10H, FcC*H*), 4.08 (s, 4H, FcC*H*), 5.71 (s, 4H, pyr-*H*), 5.86 (s, 4H, pyr-*H*), 7.14 (s, 4H, N*H*); (**1.29**) 1.59 (s, 12H, C*H*$_3$) 1.78 (s, 6H, C*H*$_3$), 3.84 (s, 4H, FcC*H*), 3.94 (s, 10H, FcC*H*), 4.15 (s, 4H, FcC*H*), 5.81 (s, 4H, pyr-*H*), 5.95 (s, 4H, pyr-*H*), 8.09 (s, 4H, N*H*). CI MS (M + H) 769; CI HRMS (M + H) 769.2663 (calcd. for $C_{46}H_{48}FeN_4$, 769.2656).

1,1'-Bis-(2-carbonyl-3,4-dimethyl-1*H*-pyrrole-5-carboxylic acid benzyl ester) ferrocene (1.44). α-benzyl ester pyrrole **1.43** (591 mg, 2.58 mmol) was placed under an argon atmosphere and dissolved in a minimum of dry dichloromethane (4 mL). 1,1'-ferrocenediacid chloride **1.42** (400 mg, 1.29 mmol) was dissolved in a minimum of dry dichloromethane (5 mL) and added dropwise. It was placed in an ice water bath, and tin(IV) chloride (668 mg, 2.57 mmol) was added dropwise, slowly, which turned the solution from red to reddish green, and was stirred for 15 minutes. Ice water was added (2 mL), turning the solution back

to red. The dichloromethane layer was separated from the water layer. The dichloromethane was then washed with 1N HCl (2 x 10 mL), 10% NaOH (1 x 20 mL) and water (2 x 10 mL). The solution was concentrated *in vacuo* to a viscous solid. The crude product was purified by flash chromatography (silica gel, eluent increasing incrementally from dichloromethane to 2% methanol / dichloromethane) to afford **1.44** as a red solid (266 mg, 30%). ^{1}H NMR δ (300 MHz, $CDCl_3$): 2.18 (s, 6H, C*H*$_3$), 2.28 (s, 6H, C*H*$_3$), 4.55 (t, 4H, Fc-C*H*), 4.94 (t, 4H, Fc-C*H*), 5.30 (s, 4H, -C*H*$_2$Ph), 7.3-7.4 (m, 10H, Ph-*H*), 9.79 (bs, 2H, N*H*). CI MS (M + H) 696; CI HRMS (M + H) 696.1956 (calcd. for $C_{40}H_{36}FeN_2O_6$, 696.1913).

1,1'-Bis-(2-methylene-3,4-dimethyl-1*H*-pyrrole-5-carboxylic acid benzyl ester) ferrocene (1.45). Aluminum(III) chloride (64 mg, 0.480 mmol) was added to dry dichloromethane (10 mL) under an argon atmosphere. It was placed in an ice water bath for 5 minutes. *tert*-Butylamineborane was added (29 mg, 0.0939 mmol) and the solution stirred at 0º C for 10 minutes. Ferrocene **1.44** (50 mg, 0.0727 mmol) was dissolved in dry dichloromethane (10 mL) and added at once to the aluminum chloride solution, which immediately turned blue-green. It was stirred at 25º C for 12 h and quenched with 1N HCl (5 mL). The solution was washed with water (2 x 20 mL) and brine (2 x 20 mL) and dried over Na_2SO_4. It was concentrated in vacuo, and the crude product was purified by chromatography (silica gel, eluent dichloromethane) to afford **1.45** as a yellowish orange solid (17 mg, 35%). ^{1}H NMR δ (300 MHz, $CDCl_3$): 1.05 (s, 6H, C*H*$_3$),

2.29 (s, 6H, C*H*$_3$), 3.56 (s, 4H, Fc-C*H*$_2$-), 4.08 (s, 4H, Fc-C*H*), 4.09 (s, 4H, Fc-C*H*), 5.25 (s, 4H, -C*H*$_2$-Ph), 7.2-7.4 (m, 10H, Ph-H), 8.69 (bs, 2H, N*H*). ^{13}C NMR δ (75 MHz, $CDCl_3$): 10.6, 15.9, 17.6, 20.3, 22.5, 26.6, 65.5, 69.3, 69.6, 86.5, 117.0, 123.4, 127.7, 128.2, 128.7, 133.0, 137.4, 161.8. CI MS (M + H) 669; CI HRMS (M + H) 669.1956 (calcd. for $C_{40}H_{40}FeN_4O_4$, 669.1913).

3,4-Dimethyl-pyrrole-2-carboxylic acid (1.46). 3,4-Dimethyl-pyrrole-2-carboxylic acid benzyl ester (**1.43**) (500 mg, 2.18 mmol) and 10% palladium on carbon (250 mg) were suspended in THF (55 ml). Triethylamine (4 drops) was added to the reaction mixture, which was then placed under a hydrogen atmosphere and left to stir at 25° C for 24 h. The mixture was filtered through a pad of celite and the filtrate was concentrated *in vacuo* to give **3** as a pale pink solid (303 mg, 100%). The physical properties of this material agree with those previously reported.[1]

1,5-Bis-(3,4-dimethyl-pyrrole-2-carbonylamino)-pentane (1.47). 1,5-Diaminopentane (85 mg, 0.83 mmol), 3,4-dimethyl-pyrrole-2-carboxylic acid (**1.46**) (232 mg, 1.67 mmol) and 1-hydoxybenzotrizole hydrate (225 mg, 1.67 mmol) were dissolved in dry DMF (21 ml). The solution was stirred for 10 min, then *N*,*N*-dicyclohexylcarbodiimide (413 mg, 2.00 mmol) was added, and the reaction mixture was left to stir at 25° C for 24 h. The reaction mixture was filtered, the filtrate was concentrated *in vacuo* and the remaining residue was dissolved in $CHCl_3$ (30 ml). The organic phase was washed with 0.5 M HCl (3 ×

30 ml), saturated aqueous $NaHCO_3$ (3 × 30 ml), and a saturated NaCl solution (2 × 30 ml). The organic phase was then dried over $MgSO_4$ and the filtrate was concentrated *in vacuo* to give a light pink solid. Purification by column chromatography (silica, 3% MeOH/CH_2Cl_2) gave **1.47** as a white solid (179 mg, 63%). ^{1}H NMR (250 MHz, $CDCl_3$): δ 1.46 (quin., 2H, $NHCH_2CH_2C\mathit{H}_2CH_2CH_2NH$), 1.64 (quin., 4H, $NHCH_2C\mathit{H}_2CH_2C\mathit{H}_2CH_2NH$), 2.02 (s, 6H, pyr-C$\mathit{H}_3$), 2.24 (s, 6H, pyr-C$\mathit{H}_3$), 3.42 (br t, 4H, $CONHC\mathit{H}_2CH_2$), 5.95 (br s, 2H, $CON\mathit{H}CH_2$), 6.62 (d, 2H, pyr-*H*), 9.16 (br s, 2H, N*H*); ^{13}C NMR (62 MHz, $CDCl_3$): δ 10.1, 10.8, 24.0, 29.5, 39.1, 118.7, 119.6, 120.1, 122.7, 162.5; CI MS (M + H) 345; CI HRMS (M + H) 345.2294 (calcd. for $C_{19}H_{29}N_4O_2$, 345.2291).

1,5-Bis-(3,4-dimethyl-pyrrole-2-carbonylamino)-3-oxapentane (1.48). 3,4-dimethyl-pyrrole-2-carboxylic acid (**1.46**) (470 mg, 3.38 mmol), 2,2'-oxybis(ethylamine) (176 mg, 1.69 mmol) and *N*,*N*-dicyclohexylcarbodiimide (836 mg, 4.05 mmol) were suspended in dry CH_2Cl_2 (100 ml). Dry triethylamine (0.94 ml, 6.76 mmol) was added causing a momentary clearing of the solution before it became cloudy again. The reaction mixture was left to stir at 25° C for 24 h. The reaction mixture was filtered and the organic phase was washed with 0.5M HCl (3 × 50 ml), saturated aqueous $NaHCO_3$ (3 × 50 ml), and a saturated NaCl solution (2 × 50 ml). The organic phase was then dried over Na_2SO_4 and the filtrate was concentrated *in vacuo* to give a light pink solid. Purification by column chromatography (silica, 3.5% MeOH/CH_2Cl_2) gave **1.48** as a pale yellow solid

(103 mg, 18%). ^{1}H NMR (300 MHz, $CDCl_3$): δ 1.98 (s, 6H, pyr-C*H*$_3$), 2.17 (s, 6H, pyr-C*H*$_3$), 3.59-3.64 (m, 8H, CONHC*H*$_2$C*H*$_2$O), 6.20 (br s, 2H, CON*H*CH$_2$), 6.60 (d, 2H, pyr-*H*), 9.17 (br s, 2H, N*H*); ^{13}C NMR (75 MHz, $CDCl_3$): δ 10.0, 10.5, 39.1, 70.0, 118.6, 119.7, 120.0, 122.5, 162.3; CI MS (M + H) 347; CI HRMS (M + H) 347.2082 (calcd. for $C_{18}H_{27}N_4O_3$, 347.2083).

1,8-Bis-(3,4-dimethyl-pyrrole-2-carbonylamino)-3,6-dioxaoctane (1.49). This was made by the procedure used to prepare **1.47** but starting from 2,2'-(ethylenedioxy)bis(ethylamine) (162 mg, 1.09 mmol), 3,4-dimethyl-pyrrole-2-carboxylic acid (**1.46**) (303 mg, 2.18 mmol), 1-hydoxybenzotrizole hydrate (295 mg, 2.18 mmol) and *N*,*N*-dicyclohexylcarbodiimide (540 mg, 2.62 mmol) in DMF (26 ml). Purification by column chromatography (silica, 3.5% MeOH/CH_2Cl_2) gave **1.49** as a flaky white solid (295 mg, 70%). ^{1}H NMR (250 MHz, $CDCl_3$): δ 2.00 (s, 6H, pyrr-C*H*$_3$), 2.23 (s, 6H, pyr-C*H*$_3$), 3.56-3.69 (m, 12H, NHC*H*$_2$(C*H*$_2$OC*H*$_2$)$_2$C*H*$_2$NH), 6.40 (br s, 2H, CON*H*CH$_2$), 6.62 (d, 2H, pyr-*H*), 9.51 (br s, 2H, N*H*); ^{13}C NMR (62 MHz, $CDCl_3$): δ 10.1, 10.6, 39.1, 70.1, 70.4, 118.7, 119.9, 120.0, 122.6, 162.3; CI MS (M + H) 391; CI HRMS (M + H) 391.2350 (calcd. for $C_{20}H_{31}N_4O_4$, 391.2345).

1,1′-[1,5-Bis-(3,4-dimethyl-pyrrole-2-carbonylamino-5-diyldimethyl)-pentane]-ferrocene (1.51). 1,5-Bis-(3,4-dimethyl-pyrrole-2-carbonylamino)-pentane (**1.47**) (174 mg, 0.50 mmol) in CH_2Cl_2 (50 ml) and 1,1′-ferrocenedimethanol (124 mg, 0.50 mmol) in CH_2Cl_2 (50 ml) were

simultaneously added dropwise over 90 min to a stirred solution of trifluoroacetic acid (115 mg, 1.0 mmol) in CH_2Cl_2 (100 ml) held at 40° C. After the addition, the mixture was heated at reflux for a further 24 h. The mixture was allowed to cool and was then concentrated to *ca.* 50 ml. The solution was washed with 1M NaOH (3 × 50 ml), dried over $MgSO_4$ and concentrated *in vacuo* to yield a flaky yellow-brown solid. Purification by column chromatography (silica, 2% MeOH/CH_2Cl_2) gave **1.51** as a yellow solid (90 mg, 33%). ^{1}H NMR (250 MHz, $CDCl_3$): δ 1.57 (quin., 2H, $NHCH_2CH_2C\mathit{H}_2CH_2CH_2NH$), 1.76 (quin., 4H, $NHCH_2C\mathit{H}_2CH_2C\mathit{H}_2CH_2NH$), 1.91, (s, 6H, pyr-C$\mathit{H}_3$), 2.29 (s, 6H, pyr-C$\mathit{H}_3$), 3.41-3.59 (m, 8H, FcC$\mathit{H}_2$, $CONHC\mathit{H}_2CH_2$), 4.07 (br s, 4H, Fc-*H*), 4.14 (br s, 4H, Fc-*H*), 6.57 (br t, 2H, $CON\mathit{H}CH_2$), 9.89 (br s, 2H, N*H*); ^{13}C NMR (62 MHz, $CDCl_3$): δ 8.9, 11.0, 23.3, 25.4, 28.6, 38.5, 67.8, 68.9, 77.3, 116.5, 120.0, 122.9, 130.4, 163.1; CI MS (M + H) 555; CI HRMS (M + H) 555.2419 (calcd. for $C_{31}H_{39}N_4O_2Fe$, 555.2422); UV-vis (CH_2Cl_2) ?$_{max}$ [nm] (e) 426 (196).

1,1'-[1,5-Bis-(3,4-dimethyl-pyrrole-2-carbonylamino-5-diyldimethly)-3-oxapentane]-ferrocene (1.52). This was made by the procedure used to prepare **1.51** but starting from 1,5-bis-(3,4-dimethyl-pyrrole-2-carbonylamino)-3-oxaoctane (103 mg, 0.30 mmol), 1,1′-ferrocenedimethanol (73 mg, 0.30 mmol), and trifluoroacetic acid (74 mg, 0.60 mmol) in CH_2Cl_2 (60 ml). Purification by column chromatography (silica, 2% MeOH/CH_2Cl_2) gave **1.52** as an orange solid (33mg, 20%). ^{1}H NMR (300 MHz, DMSO-d_6): δ 1.78 (s, 6H, pyr-CH_3), 2.14 (s, 6H, pyr-CH_3), 3.20-3.78 (m, 12H, $NHC\mathit{H}_2C\mathit{H}_2OC\mathit{H}_2C\mathit{H}_2NH$, FcC*H*2,), 3.96 (br s,

8*H*, Fc-*H*), 7.68 (br s, 2H, CON*H*CH_2), 10.80 (br s, 2H, N*H*); ^{13}C NMR (125 MHz, DMSO-d_6) 8.8, 10.4, 25.4, 38.9, 67.1, 68.7, 69.8, 87.7, 114.5, 119.3, 122.8, 130.2, 161.7; CI MS (M + H) 557; CI HRMS (M + H) 557.2203 (calcd. for $C_{30}H_{36}N_4O_3Fe$, 557.2215); UV-vis (CH_2Cl_2) ?$_{max}$ [nm] (e) 404 (219).

1,1¢-[1,8-Bis-(3,4-dimethyl-pyrrole-2-carbonylamino-5-diyldimethyl)-3,6-dioxaoctane]-ferrocene (1.53). This was made by the procedure used to prepare **7** but starting from 1,8-bis-(3,4-dimethyl-pyrrole-2-carbonylamino)-3,6-dioxaoctane (**1.49**) (271 mg, 0.69 mmol), 1,1′-ferrocenedimethanol (171 mg, 0.69 mmol), and trifluoroacetic acid (158 mg, 1.39 mmol) in CH_2Cl_2 (180 ml). Purification by column chromatography (silica, 2.5% MeOH/CH_2Cl_2) gave **1.53** as an orange solid (145 mg, 35%). ^{1}H NMR (250 MHz, $CDCl_3$): δ 1.93 (s, 6H, pyr-C*H*$_3$), 2.26 (s, 6H, pyr-C*H*$_3$), 3.31 (br s, 4H, FcC*H*$_2$), 3.52-3.74 (m, 12H, NHC*H*$_2$(C*H*$_2$OC*H*$_2$)$_2$C*H*$_2$NH), 3.88-4.42 (br, 8H, Fc-*H*), 6.48 (br s, 2H, CON*H*CH_2), 9.54 (br s, 2H, N*H*); ^{13}C NMR (62 MHz, $CDCl_3$): δ 9.0, 11.1, 25.6, 39.8, 68.0, 69.4, 70.8, 71.3, 77.3, 116.5, 119.8, 122.5, 131.0, 161.9; CI MS (M + H) 601; CI HRMS (M + H) 601.2474 (calcd. for $C_{32}H_{40}N_4O_4Fe$, 601.2477); UV-vis (CH_2Cl_2) ?$_{max}$ [nm] (e) 413 (166).

1,1'-ferrocenedicarboxylic-*N*,*N*'-Bis-(1*H*-pyrrol-2-ylmethyl)-diamide (1.59). 1,1'-Ferrocenediacid chloride **1.42** (651 mg, 2.09 mmol) was dissolved in dry tetrahydrofuran (25 mL), resulting in a red solution. Triethylamine (465 mg, 4.59 mmol) was added dropwise and the reaction placed in an ice water bath. (2-

pyrrolylmethene)-(2-pyrrolylmethyl)amine **1.57** (733 mg, 4.19 mmol) was dissolved in a minimum of dry tetrahydrofuran (15 mL) and added dropwise, quickly. The solution immediately changed to a cloudy orange-brown suspension. It was stirred at room temperature for two hours, during which time an orange-brown precipitate formed. The solution was evaporated, dissolved in dichloromethane and washed sequentially with water (2 x 100 mL), $NaHCO_3$ (saturated, 2 x 100 mL), and brine (2 x 100 mL). It was then dried over Na_2SO_4 and concentrated *in vacuo*. The resulting crude product was purified by flash chromatography (silica gel, eluent 1% methanol / dichloromethane) to afford **1.59** as an orange solid (782 mg, 87%). ^{1}H NMR δ (250 MHz, $(CD_3)_2SO$): 1.85 (bs, 2H, N*H*), 4.38 (t, 4H, -CONHCH_2-), 4.51 (d, 4H, Fc-*H*), 4.54 (d, 4H, Fc-*H*), 6.01 (m, 2H, pyr-*H*) , 6.20 (m, 2H, pyr-*H*), 6.84 (m, 2H, pyr-*H*), 10.29 (bs, 2H, N*H*); ^{13}C NMR (60 MHz, $(CD_3)_2SO$): 36.0, 69.8, 71.6, 77.7, 105.9, 107.2, 117.2, 129.2, 168.6; CI MS (M + H) 430; CI HRMS (M + H) 430.1085 (calcd. for $C_{22}H_{23}N_4O_2Fe$, 430.1092).

1,1'-ferrocenedicarboxylic-*N*,*N*'-bis-(5-Formyl-1*H*-pyrrol-2-ylmethyl)-diamide (1.60). Dimethylformamide (0.5 mL) was added to a flask equipped with a condenser and a flow of argon. It was cooled in an ice water bath and freshly distilled phosphorous oxychloride (150 mg, 0.978 mmol) was added quickly, dropwise. It was stirred at room temperature for 10 minutes, during which time the solution turned pale yellow. It was placed in an ice water bath, and a suspension of **1.59** in dichloroethane (10 mL) was added dropwise. During

this time the solution turned to a reddish brown suspension. After the addition, the suspension was heated at reflux for 30 minutes. It was then cooled in an ice water bath and a half saturated sodium acetate solution (5 mL) was added slowly. The reaction was heated at reflux for 30 minutes, then stirred at room temperature for 12 h. It filtered to remove unwanted solids, after which the clear red filtrate was dried over Na_2SO_4 and concentrated *in vacuo*. The resulting crude product was purified by chromatography (silica gel, eluent increasing incrementally from 1% methanol / dichloromethane to 4% methanol / dichloromethane) to afford the orange solid **1.60** (116 mg, 26%). ^{1}H NMR δ (250 MHz, $(CD_3)_2SO$): 4.33 (t, 4H, Fc-*H*), 4.40 (d, 4H, -CONHC*H*$_2$-), 4.79 (t, 4H, Fc-*H*), 6.21 (d, 2H, pyr-*H*), 6.93 (d, 2H, pyr-H), 8.29 (bm, 2H, NH), 9.44 (s, 2H, C*H*O), 11.98 (bs, 2H, N*H*). CI MS (M + H) 486; CI HRMS (M + H) 486.1010 (calcd. for $C_{24}H_{23}N_4O_4Fe$, 486.1024).

Schiff base ferrocene (1.61). Diformyl ferrocene **1.60** (60 mg, 0.124 mmol) and 4,5-dimethoxyphenalenediamine (21 mg, 0.125 mmol) were dissolved in dry methanol (10 mL) under argon. The reaction was placed in the dark and one drop of concentrated nitric acid was added. It was stirred at room temperature for 1 h, then concentrated in vacuo. The dark solid was dissolved in dichloromethane (50 mL) and extracted with $NaHCO_3$ (saturated, 2 x 50 mL) and water (2 x 50 mL), then dried over Na_2SO_4. The crude product was purified by flash chromatography (silica gel, eluent ethyl acetate) to afford the orange product **1.61** (40 mg, 52%). ^{1}H NMR δ (300 MHz, $CDCl_3$): 3.82 (m, 4H), 3.93 (s, 6H),

4.30 (d, 4H), 4.36 (d, 4H), 4.55 (d, 2H), 6.24 (d, 2H), 6.55 (d, 2H), 6.76 (s, 2H), 7.2-7.3 (m, 2H), 8.25 (s, 2H). CI MS (M + H) 618; CI HRMS (M + H) 618.1683 (calcd. for $C_{32}H_{30}N_6O_4Fe$, 618.1678).

***N*,*N*'-Bis-(1*H*-pyrrol-2-ylmethyl)-1,1'-dimethylamino ferrocene (1.62)**. Ferrocene **1.59** (257 mg, 0.600 mmol) was placed under an argon atmosphere and dissolved in dry tetrahydrofuran (100 mL). Lithium aluminum hydride (90 mg, 2.37 mmol) was added, resulting in vigorous bubbling. The orange-yellow solution was heated at reflux for 12 h. The solution was cooled to room temperature and ice water was added dropwise to quench the excess lithium aluminum hydride. The mixture was filtered, and the filtrate was concentrated in vacuo. The crude product was purified by chromatography (silica gel, eluent increasing incrementally from 1% methanol / dichloromethane to 5% methanol / dichloromethane) resulting in the light orange solid **1.59** (41 mg, 17%). ^{1}H NMR δ (300 MHz, $CDCl_3$): 3.51 (s, 2H), 3.73 (bs, 4H), 4.03 (s, 4H), 4.16 (s, 4H), 6.08 (bd, 2H), 6.23 (s, 2H), 8.52 (bs, 2H), 9.19 (bs, 2H). CI MS (M + H) 402; CI HRMS (M + H) 402.1563 (calcd. for $C_{22}H_{26}N_4Fe$, 402.1577).

1,1'-Bis-(2-carbonyl-3-ethyl-2,5-dimethyl-1*H*-pyrrole)ferrocene (1.66). 1,1'-Ferrocenediacid chloride **1.42** (807 mg, 2.60 mmol) was dissolved in dry tetrahydrofuran (50 mL) under an argon atmosphere. It was chilled in an ice water bath and α-benzyl ester pyrrole **1.43** (639 mg, 5.19 mmol) was added dropwise, followed by triethylamine (653 mg, 6.46 mmol). Tin(IV) chloride

(1.36 g, 5.21 mmol) was added dropwise, slowly. It was stirred for 1 h in the ice bath, then quenched with water (10 mL). The layers were separated and the dichloromethane layer was washed with 1N HCl (2 x 50 mL), 10% NaOH(aq) (2 x 50 mL), and water (1 x 50 mL). It was dried over Na_2SO_4 and evacuated in vacuo. The crude product was purified by chromatography (silica gel, eluent 1% methanol / dichloromethane) to afford **1.66** as a red solid (203 mg, 16%). ^{1}H NMR δ (300 MHz, $CDCl_3$): 1.15 (t, 6H, -CH_2CH_3), 2.24 (s, 6H, CH_3), 2.38 (s, 6H, CH_3), 2.89 (m, 4H, -CH_2CH_3), 4.52 (d, 4H, Fc-*H*), 4.73 (d, 4H, Fc-*H*), 10.23 (bs, 2H, N*H*). CI MS (M + H) 484; CI HRMS (M + H) 484.1869 (calcd. for $C_{28}H_{32}N_4O_2Fe$, 484.1862).

The remaining work was carried out by Dr. Gregory Kirkovits and is included here for completeness of this yet unpublished work.

3-Aza-5-oxaoctane-1,8-diol (3.16): was prepared in accord with the procedure used to synthesize 6-aza-3,9-dioxaundecane-1,11-diol.[2] 2-Chloroethanol (38.29 g, 0.48 mol) in toluene (120 mL) was added to a mixture of 2-(2-aminoethoxy)ethanol (200.0 g, 1.90 mol) and Na_2CO_3 (55.44 g, 0.52 mol) heated at reflux in toluene (1.2 L). The resulting mixture was stirred at reflux for a further 2 days using a condenser equipped with a Dean-Stark adaptor. The reaction mixture was allowed to cool, filtered and concentrated *in vacuo*. The remaining residue was purified by fractional distillation to give **3.16** as a pale

yellow oil (28.68 g, 40%). The physical properties of this material agree with those previously reported.[3]

Benzo-aza-18-crown-6 (3.20). 3-Aza-5-oxaoctane-1,8-diol (**3.16**) (18.41 g, 0.123 mol) and potassium metal (5.79 g, 0.118 mol) were dissolved in *tert*-butyl alcohol (160 mL), with stirring at 40 ºC. 2,2'-[1,2-Phenylenebis(oxy)]bis(4-methylbenzenesulfonate) **3.15** (25.00 g, 0.049 mol) dissolved in dioxane (140 mL) was added dropwise over 90 min. After the addition was complete, heating and stirring was continued for a further 2 h. The reaction mixture was then allowed to cool, upon which point it was passed through a sintered funnel. The resulting precipitate was washed with CH_2Cl_2 and the combined filtrates were concentrated *in vacuo*. The residue obtained in this way was redissolved in water (30 mL), washed with hexanes (40 mL), and then extracted with CH_2Cl_2 (3 × 50 mL). The combined CH_2Cl_2 extracts were concentrated to *ca.* 50 mL, and extracted with 1 M HCl (50 mL). The aqueous layer was adjusted to pH 10 – 11 using Na_2CO_3, and extracted with CH_2Cl_2 (2 × 100 mL) and the combined organic extracts were concentrated *in vacuo*. Purification by column chromatography (neutral alumina, 2.5% MeOH - CH_2Cl_2 eluent) gave a pale orange oil which solidified on standing. Recrystallization from hexanes afforded **3.20** as a white crystalline solid (3.96 g, 26%). ^{1}H NMR (250 MHz, $CDCl_3$) d = 2.21 (br-s, 1H, NH), 2.77-2.83 (m, 4H, CH_2N), 3.60-3.74 (m, 8H, CH_2O), 3.80-3.84 (m, 2H, CH_2O), 3.88-3.92 (m, 2H, CH_2O), 4.12-4.19 (m, 4H, $PhOCH_2$), 6.88 (*pseudo*-s, 4H, Ph-H). ^{13}C NMR (62 MHz, $CDCl_3$) d = 49.3, 68.6, 68.8, 69.4,

69.8, 70.3, 70.7, 113.9, 114.6, 121.3, 121.4, 149.0, 149.06. HRMS (CI^+): calcd for $C_{16}H_{26}N_1O_5$ $[M + H]^+$ 312.1811; found *m/z*: 312.1812. Anal. calcd for $C_{16}H_{25}N_1O_5$: C, 61.72; H, 8.09; N, 4.50; found C, 61.73; H, 8.13; N, 4.44.

Benzo-aza-15-crown-5 (3.21). This compound was prepared in accord with the procedure used for **3.20** but starting from diethanolamine **3.17** (10.38 g, 0.10 mol) and potassium metal (4.63 g, 0.12 mol) in *tert*-butyl alcohol (160 mL), and **3.15** (25.00 g, 0.05 mol) in dioxane (140 mL). Purification by column chromatography (neutral alumina, 1.5% MeOH - CH_2Cl_2 eluent) gave the product as a white solid. Recrystallization from n-heptane afforded **3.21** as a white crystalline solid (2.12 g, 16%). ^1H NMR (250 MHz, $CDCl_3$) d = 2.60 (br-s, 1H, NH), 2.80-2.84 (m, 4H, CH_2N), 3.71-3.75 (m, 4H, CH_2O), 3.85-3.88 (m, 4H, CH_2O), 4.09-4.12 (m, 4H, CH_2O), 6.80-6.89 (m, 4H, Ph-H). ^{13}C NMR (62 MHz, $CDCl_3$) d = 49.1, 67.6, 68.9, 70.2, 112.4, 120.8, 148.7. HRMS (CI^+): calcd for $C_{14}H_{21}NO_4$ $[M + H]^+$ 268.1549; found *m/z*: 268.1558. Anal. calcd for $C_{14}H_{21}N_1O_4$: C, 62.90; H, 7.92; N, 5.24; found C, 63.12; H, 7.89; N, 5.03.

General Procedure – Synthesis of dinitro-3*n*-benzo-*n*-crowns 3.22 – 3.24: To a stirred solution of the appropriate benzo-3*n*-crown-*n* (**3.19 – 3.21**) (4.6 – 20.8 mmol) in glacial acetic acid (7 – 30 mL) cooled to less than 15 ºC, was added conc. nitric acid (70%, 5 – 20 mL) dropwise over 15 min. After the addition the solution was stirred at ambient temperature for 15 min. The solution was again cooled to less than 15 ºC and fuming nitric acid (90%, 11 – 50 mL) was

added dropwise over a period of 30 min. The orange solution was poured into water (100 mL) and extracted with CH_2Cl_2 (3 × 100 mL). The combined organic extracts were dried ($MgSO_4$) and concentrated *in vacuo*.

Dinitro-benzo-18-crown-6 (3.22) was synthesized from benzo-18-crown-6 **3.18** (6.5 g, 20.8 mmol). Product **3.22** was obtained as a yellow solid after recrystallization from acetone (7.34 g, 88%). ^{1}H NMR (250 MHz, $CDCl_3$): d = 3.64 (*pseudo*-s, 4 H, CH_2O), 3.66-3.70 (m, 4H, CH_2O), 3.73-3.76 (m, 4H, CH_2O), 3.93-3.96 (m, 4H, CH_2O), 4.26-4.30 (m, 4H, $PhOCH_2$), 7.34 (*pseudo*-s, 2H, Ph-H). ^{13}C NMR (62 MHz, $CDCl_3$): d = 68.8, 69.8, 70.4, 70.7, 71.0, 108.3, 133.3, 151.6. HRMS (CI^+): calcd for $C_{16}H_{23}N_2O_{10}$ $[M + H]^+$: 403.1353; found *m/z*: 403.1345. Anal. calcd for $C_{16}H_{22}N_2O_{10}$: C, 47.76; H, 5.51; N, 6.96; found C, 47.80; H, 5.53; N, 6.98.

Dinitro-benzo-15-crown-5 (3.23) was synthesized from benzo-15-crown-5 **3.19** (2.50 g, 9.3 mmol). Product **3.23** was obtained as a yellow solid after recrystallization from acetone (2.78 g, 84%). ^{1}H NMR (250 MHz, $CDCl_3$): d = 3.70-3.77 (m, 8H, CH_2O), 3.91-3.95 (m, 4H, CH_2O), 4.23-4.26 (m, 4H, $PhOCH_2$), 7.31 (s, 2H, Ph-H). ^{13}C NMR (62 MHz, $CDCl_3$) d = 68.7, 69.7, 70.1, 71.1, 108.5, 136.8, 151.9. HRMS (CI^+): calcd for $C_{14}H_{19}N_2O_9$ $[M + H]^+$ 359.1091; found *m/z*: 359.1082. Anal. calcd for $C_{14}H_{18}N_2O_9$: C, 46.93; H, 5.06; N, 7.82; found C, 47.02; H, 5.04; N, 7.88.

Dinitro-benzo-aza-18-crown-6 (3.24) was synthesized from benzoaza-18-crown-6 **3.20** (3.6 g, 11.6 mmol). However, the work-up was modified in the following manner: The orange solution was poured into water (150 mL), and washed with CH_2Cl_2 (3 × 150 mL). The aqueous layer was adjusted to pH 10 – 11 using Na_2CO_3 and extracted with CH_2Cl_2 (3 × 150 mL). The combined organic extracts were dried ($MgSO_4$) and concentrated *in vacuo* to afford **3.24** as a yellow solid (3.61 g, 78%). ^{1}H NMR (250 MHz, $CDCl_3$) d = 2.33 (br-s, 1H, NH), 2.76-2.82 (m, 4H, CH_2N), 3.59-3.72 (m, 8H, CH_2O), 3.84-3.92 (m, 4H, CH_2O), 4.24-4.29 (m, 4H, $PhOCH_2$), 7.30 (s, 1H, Ph-H), 7.31 (s, 1H, Ph-H). ^{13}C NMR (62 MHz, $CDCl_3$) d = 49.4, 68.3, 68.7, 69.3, 69.6, 70.1, 70.6, 70.7, 107.8, 108.1, 136.5, 151.5, 151.6. HRMS (CI^+): calcd for $C_{16}H_{24}N_3O_9$ $[M + H]^+$ 402.1513; found *m/z*: 402.1510. Anal. calcd for $C_{16}H_{23}N_3O_9$: C, 47.88; H, 5.78; N, 10.47; found C, 47.94; H, 5.87; N, 10.37.

Dinitro-benzo-aza-15-crown-5 (3.25) was synthesized from benzoaza-15-crown-5 **3.21** (1.24 g, 4.6 mmol). Work-up in the manner described for **3.24**, afforded **3.25** as a yellow solid (1.15 g, 44%). ^{1}H NMR (250 MHz, $CDCl_3$) d = 2.50 (br-s, 1H, NH), 2.79-2.83 (m, 4H, CH_2N), 3.73-3.76 (m, 4H, CH_2O), 3.88-3.92 (m, 4H, CH_2O), 4.20-4.23 (m, 4H, $PhOCH_2$), 7.27 (s, 2H, Ph-H). ^{13}C NMR (62 MHz, $CDCl_3$) d = 49.2, 68.1, 68.8, 70.5, 107.5, 136.7, 151.6. HRMS (CI^+): calcd for $C_{14}H_{19}N_3O_8$ $[M + H]^+$ 358.1250; found *m/z*: 358.1252. Anal. calcd for $C_{14}H_{19}N_3O_8$: C, 47.06; H, 5.36; N, 11.76; found C, 47.02; H, 5.35; N, 11.73.

General Procedure – Synthesis of 3*n*-crown-*n*-dipyrrolylquinoxalines (3.31 – 3.34) and 6,7-dimethoxy-2,3-bis-(1*H*-pyrrol-2-yl)-quinoxaline (3.37). The appropriate dinitro-3*n*-benzo-*n*-crown **3.22 – 3.25** (2.35 - 7.0 mmol) or 1,2-dimethoxy-4,5-dinitro-benzene (3.58 g, 15.70 mmol), and 10% Pd/C (170 - 500 mg) were suspended in ethanol (33 - 135 mL) and glacial acetic acid (2 - 7 mL) and shaken in a Parr hydrogenation apparatus at 50 psi H_2 pressure and ambient temperature for 44 h. The resultant diamine was assumed to form in quantitative yield and was used immediately in the subsequent reaction. The reaction mixture was filtered through a pad of Celite into the next reaction vessel and washed with ethanol (50 mL). 1,2-Bis-(1*H*-pyrrol-2-yl)ethane-dione (**3.30**) (1.1 – 7.24 mmol) dissolved in glacial acetic acid (80 - 180 mL) was added to the solution and the resultant mixture was heated at reflux for 24 h. The reaction mixture was allowed to cool, and then concentrated *in vacuo*. The remaining residue was redissolved in a mixture of CH_2Cl_2 (75 mL) and water (75 mL). The aqueous layer was further extracted with CH_2Cl_2 (3 × 75 mL). The combined organic extracts were washed sequentially with saturated $NaHCO_3$ solution (100 mL), water (100 mL), and brine (100 mL), before being dried ($MgSO_4$) and concentrated *in vacuo*.

18-Crown-6-dipyrrolylquinoxaline (3.31). The intermediate diamine **3.26** was synthesized from **3.22** (2.82 g, 7.0 mmol) using the general procedure given above. It was then reacted with **3.30** (0.60 g, 3.2 mmol). Product **3.31** was obtained in pure form as a fine brown powder (1.58 g, 100%). ^{1}H NMR (250 MHz, $CDCl_3$) d = 3.68-3.84 (m, 16H, CH_2O), 4.10-4.13 (m, 4H, $PhOCH_2$), 6.26

(m, 2H, pyr-H), 6.55 (m, 2H, pyr-H), 6.96 (s, 2H, Ph-H), 6.99 (m, 2H, pyr-H), 9.64 (br-s, 2H, pyr-NH). ^{13}C NMR (62 MHz, $CDCl_3$) d 68.8, 69.0, 70.4, 70.9, 71.1, 106.9, 109.8, 111.2, 120.2, 120.2, 129.3, 136.7, 141.9, 151.5. HRMS (CI^+): calcd for $C_{26}H_{31}N_4O_6$ $[M + H]^+$ 495.2244; found *m/z*: 495.2235. Anal. calcd for $C_{26}H_{30}N_4O_6.H_2O$: C, 60.93; H, 6.29; N, 10.93; found C, 60.97; H, 6.16; N, 10.51. UV-vis: λ_{max} (nm) (ε, M^{-1} cm^{-1}) (CH_3CN): 271 (28,947), 407 (23,331).

Crystallization of 3.31. Receptor **3.31** was dissolved in boiling acetone and then allowed to cool to RT. Yellow-green crystals of **3.31**, suitable for X-ray diffraction analysis, were obtained by letting stand overnight.

15-Crown-5-dipyrrolylquinoxaline (**3.32).** The intermediate diamine **3.27** was synthesized from **3.23** (2.50 g, 6.98 mmol) using the general procedure given above. This was then reacted with **3.30** (0.60 g, 3.2 mmol). Product **3.32** was obtained, pure, as a fine brown powder (1.44 g, 100%). ^{1}H NMR (250 MHz, $CDCl_3$) d = 3.78-3.85 (m, 12H, CH_2O), 4.06-4.09 (m, 4H, $PhOCH_2$), 6.26 (m, 2H, pyr-H), 6.54 (m, 2H, pyr-H), 6.93 (s, 2H, Ph-H), 6.98 (m, 2H, pyr-H), 9.62 (br-s, 2H, pyr-NH). ^{13}C NMR (62 MHz, $CDCl_3$) d = 68.2, 69.1, 70.3, 71.3, 106.9, 109.8, 111.2, 120.9, 129.3, 136.8, 141.9, 151.5. HRMS (CI^+): calcd for $C_{24}H_{27}N_4O_5$ $[M + H]^+$: 451.1981; found *m/z*: 451.1964. Anal. calcd for $C_{24}H_{26}N_4O_5$: C, 63.99; H, 5.82; N, 12.44; found C, 63.73; H, 5.72; N, 12.22. UV-vis: λ_{max} (nm) (ε, M^{-1} cm^{-1}) (CH_3CN): 269 (27,796), 402 (17,747).

Crystallization of 3.32 and its KCF_3SO_3 complex: Receptor **3.32** was dissolved in boiling acetone and then allowed to cool to RT. Pale yellow crystals

of **3.32**, suitable for X-ray diffraction analysis, were obtained by letting stand overnight. The complex was obtained by dissolving **3.32** and excess KCF_3SO_3 in MeCN at ambient temperature, and allowing vapor diffusion of Et_2O in a screw-capped vial. In this manner, amber crystals, suitable for X-ray diffraction analysis, were obtained after several days.

Aza-18-crown-6-dipyrrolylquinoxaline (3.33). The protonated form of the intermediate diamine **3.28** was synthesized from **3.24** (2.01 g, 5.0 mmol) using the general procedure given above. It was then reacted with **3.30** (0.43 g, 2.3 mmol) to yield the crude product as the acetate salt. Therefore, the work-up was modified in the following manner: The reaction mixture was redissolved in a mixture of CH_2Cl_2 (100 mL) and a 20% w/v aqueous Na_2CO_3 solution (100 mL). The aqueous solution was further extracted with CH_2Cl_2 (2 × 100 mL). The combined organic extracts were washed sequentially with saturated $NaHCO_3$ solution (100 mL), water (100 mL), and brine (100 mL), before being dried ($MgSO_4$) and concentrated *in vacuo*. Purification by column chromatography (neutral alumina, 1.5 % MeOH - CH_2Cl_2 eluent) afforded **3.33** as a fine brown powder (0.697 g, 62%). ^{1}H NMR (250 MHz, $CDCl_3$) d = 2.84-2.87 (m, 4H, CH_2N), 3.64-3.81 (m, 12H, CH_2O), 4.10-4.14 (m, 4H, $PhOCH_2$), 6.25 (m, 2H, pyr-H), 6.55 (m, 2H, pyr-H), 6.94 (s, 1H, Ph-H), 6.97 (s, 1H, Ph-H), 6.99 (2H, pyr-H), 9.64 (br-s, 2H, pyr-NH). ^{13}C NMR (62 MHz, $CDCl_3$) d = 49.2, 49.3, 68.3, 68.4, 68.6, 69.0, 70.0, 70.1, 71.2, 70.7, 106.7, 106.8, 109.8, 111.2, 120.1, 129.3, 136.7, 142.0, 151.3. HRMS (CI^+) calcd for $C_{26}H_{32}N_5O_5$ $[M + H]^+$: 494.2403;

found *m/z*: 494.2408. UV-vis: λ_{max} (nm) (ε, M^{-1} cm^{-1}) (CH_3CN): 270 (25,688), 405 (20,945).

Aza-15-crown-5-dipyrrolylquinoxaline (3.34). The protonated form of the intermediate diamine **3.29** was synthesized from **3.25** (0.84 g, 2.35 mmol) using the general procedure given above. It was then reacted with **3.30** (0.20 g, 1.1 mmol) to yield the acetate salt of **3.34** in impure form. Work-up was effected in the manner described for **3.33**. Purification by column chromatography (neutral alumina, 1.5 % MeOH - CH_2Cl_2, eluent) then afforded **3.34** as a fine red-brown powder (0.234 g, 49%). ^{1}H NMR (250 MHz, $CDCl_3$) d = 2.98-3.01 (m, 4H, CH_2N), 3.84-3.88 (m, 4H, CH_2O), 3.97-4.01 (m, 4H, CH_2O), 4.22-4.26 (m, 4H, $PhOCH_2$), 6.27 (m, 2H, pyr-H), 6.72 (m, 2H, pyr-H), 6.97 (m, 2H, pyr-H), 7.13 (s, 2H, Ph-H), 9.49 (br-s, 2H, pyr-NH). ^{13}C NMR (62 MHz, $CDCl_3$) d = 49.0, 67.5, 68.7, 69.3, 106.6, 109.8, 111.3, 120.1, 129.3, 136.8, 141.8, 151.5. HRMS (CI^+) calcd for $C_{24}H_{28}N_5O_4$ $[M + H]^+$ 450.2141; found *m/z*: 450.2142. UV-vis: λ_{max} (nm) (ε, M^{-1} cm^{-1}) (CH_3CN): 270 (24,765), 404 (13,262).

6,7-Dimethoxy-2,3-bis-(1*H*-pyrrol-2-yl)-quinoxaline (3.37). The requisite intermediate, 1,2-diamino-4,5-dimethoxy-benzene was synthesized from 1,2-dimethoxy-4,5-dinitro-benzene (3.58 g, 15.70 mmol). It was then reacted with **3.30** (1.36 g, 7.24 mmol) in accord with the standard procedures described above. This gave product **3.37** as a yellow powder (2.05 g, 89%) after purification by column chromatography (silica, 2% MeOH - CH_2Cl_2, eluent). ^{1}H

NMR (250 MHz, $CDCl_3$) d = 4.04 (s, 6H, OCH_3), 6.28 (m, 2H, pyr-H), 6.77 (m, 2H, pyr-H), 6.97 (m, 2H, pyr-H), 7.24 (s, 2H, Ph-H), 9.48 (br-s, 2H, pyr-NH). ^{13}C NMR (62 MHz, $CDCl_3$) d = 56.2, 106.1, 109.9, 111.5, 120.2, 129.3, 136.8, 141.7, 152.2. HRMS (CI^+) calcd for $C_{18}H_{17}N_4O_2$ $[M + H]^+$ 321.1352; found *m/z*: 321.1352. Anal. calcd for $C_{18}H_{16}N_4O_2.¼H_2O$: C, 66.55; H, 5.12; N, 17.25; found C, 66.55; H, 5.08; N, 17.11.

Crystallization of 3.37. Receptor **3.37** was dissolved in boiling acetone and then allowed to cool to RT. Yellow crystals of **3.37**, suitable for X-ray diffraction analysis, were obtained by letting stand overnight.

References

(1) Byun, Y.-S.; Lightner, D. A. *J. Org. Chem*. **1991**, *56*, 6027-6033.

(2) Bordunov, A. V.; Hellier, P. C.; Bradshaw, J. S.; Dalley, N. K.; Kou, X.; Zhang, X. X.; Izatt, R. M. *J. Org. Chem*. **1995**, *60*, 6097-6102.

(3) Maeda, H.; Furuyoshi, S.; Nakatsuji, Y.; Okahara, M. *Bull. Chem. Soc. Japan* **1983**, *56*, 212-218.

Appendix A: X-ray Crystallographic Data

X-ray crystallographic analysis described in this appendix were grown by the author (**1.28** and **1.29**), and Dr. Bruno Andrioletti (**1.59**). All structures were solved by Dr. Vincent Lynch. Structures described in this work but not included in this appendix are deposited with the Cambridge Crystallographic Data Base and can be obtained from there. A general experimental method (as per Dr. V. Lynch) used in obtaining these structures, as well as relevant data tables for each structure follows.

General Experimental

The data were collected on a Nonius Kappa CCD diffractometer using a graphite monochromator with MoKα radiation (λ = 0.71073Å). The data were collected at –120 °C using a Oxford Cryostream low temperature device. Data reduction were performed using DENZO-SMN.[1] The structure was solved by direct methods using SIR92[2] and refined by full-matrix least-squares on F^2 with anisotropic displacement parameters for the non-H atoms using SHELXL-97.[3] The hydrogen atoms on carbon were calculated in ideal positions with isotropic displacement parameters set to 1.2xUeq of the attached atom (1.5xUeq for methyl hydrogen atoms). Definitions used for calculating R(F),$R_w(F^2)$ and the goodness of fit, S, are given below.[4] The data were corrected for secondary extinction effects. The correction takes the form: $F_{corr} = kF_c/[1 + (1.8(3)x10^{-6})* F_c^2 \lambda^3/(\sin 2\theta)]^{0.25}$ where k is the overall scale factor. Neutral atom scattering factors

and values used to calculate the linear absorption coefficient are from the International Tables for X-ray Crystallography (1992).[5] All figures were generated using SHELXTL/PC.[6]

X-ray Experimental for $C_{46}H_{48}N_2Fe_2$ (**1.29**): Crystals grew as very nicely formed yellow-orange prisms by diffusion of a solution of **1.29** in dichloromethane into methanol. The data crystal was a small prism of approximate dimensions; 0.27 x 0.25 x 0.22 mm. A total of 305 frames of data were collected using ω-scans with a scan range of 1° and a counting time of 44 seconds per frame. The hydrogen atom positions on the pyrrole nitrogen atoms were located in a ΔF map and refined with isotropic displacement parameters. The function, $\Sigma w(|F_o|^2 - |F_c|^2)^2$, was minimized, where $w = 1/[(\sigma(F_o))^2 + (0.0385*P)^2 + (1.8937*P)]$ and $P = (|F_o|^2 + 2|F_c|^2)/3$. $R_w(F^2)$ refined to 0.0814, with R(F) equal to 0.0305 and a goodness of fit, S, = 1.04.

Table 1. Crystal data and structure refinement for **1.29**.

Empirical formula	C46 H48 Fe2 N4	
Formula weight	768.58	
Temperature	153(2) K	
Wavelength	0.71073 Å	
Crystal system	Orthorhombic	
Space group	Pbca	
Unit cell dimensions	a = 11.6370(1) Å	α= 90°.
	b = 16.5300(2) Å	β= 90°.
	c = 18.5091(2) Å	γ = 90°.
Volume	3560.40(7) $Å^3$	Z=4
Density (calculated)	1.434 Mg/m^3	
Absorption coefficient	0.856 mm^{-1}	
F(000)	1616	
Crystal size	0.27 x 0.25 x 0.22 mm	
Theta range for data collection	3.1 to 27.5°.	
Index ranges	-15<=h<=15, -21<=k<=21, -23<=l<=24	
Reflections collected	7606	
Independent reflections	4078 [R(int) = 0.0163]	
Completeness to theta = 27.48°	99.8 %	
Max. and min. transmission	0.8341 and 0.8018	
Refinement method	Full-matrix least-squares on F^2	

Data / restraints / parameters	4078 / 0 / 244
Goodness-of-fit on F^2	1.040
Final R indices [I>2sigma(I)]	R1 = 0.0305, wR2 = 0.0759
R indices (all data)	R1 = 0.0426, wR2 = 0.0814
Extinction coefficient	$1.8(3)x10^{-6}$
Largest diff. peak and hole	0.33 and -0.38 e.$Å^{-3}$

Table 2. Atomic coordinates (x 10^4) and equivalent isotropic displacement parameters ($Å^2$ x 10^3) for **1.29**. U(eq) is defined as one third of the trace of the orthogonalized U^{ij} tensor.

Atom	x	y	z	U
Fe	5006(1)	1004(1)	3119(1)	16(1)
N1	5809(1)	813(1)	5908(1)	17(1)
N2	6852(1)	166(1)	4450(1)	17(1)
C1	4902(1)	1237(1)	6197(1)	16(1)
C2	5156(1)	2043(1)	6121(1)	21(1)
C3	6252(1)	2104(1)	5781(1)	22(1)
C4	6645(1)	1335(1)	5660(1)	17(1)
C5	7805(1)	1029(1)	5402(1)	17(1)
C6	7678(1)	251(1)	4979(1)	16(1)
C7	8329(1)	-438(1)	4963(1)	23(1)
C8	7891(1)	-948(1)	4408(1)	24(1)
C9	6974(1)	-559(1)	4096(1)	16(1)
C10	6160(1)	-819(1)	3499(1)	17(1)
C11	8383(1)	1672(1)	4923(1)	23(1)
C12	8580(1)	876(1)	6061(1)	24(1)
C13	6808(1)	-1432(1)	3020(1)	21(1)
C14	5818(1)	-117(1)	3009(1)	17(1)
C15	4799(1)	-79(1)	2578(1)	20(1)
C16	4904(1)	575(1)	2084(1)	23(1)

C17	5980(1)	955(1)	2208(1)	23(1)
C18	6546(1)	531(1)	2775(1)	20(1)
C19	5303(2)	1887(1)	3885(1)	25(1)
C20	4834(1)	2224(1)	3243(1)	25(1)
C21	3741(1)	1858(1)	3124(1)	22(1)
C22	3540(1)	1294(1)	3692(1)	22(1)
C23	4503(1)	1316(1)	4164(1)	23(1)

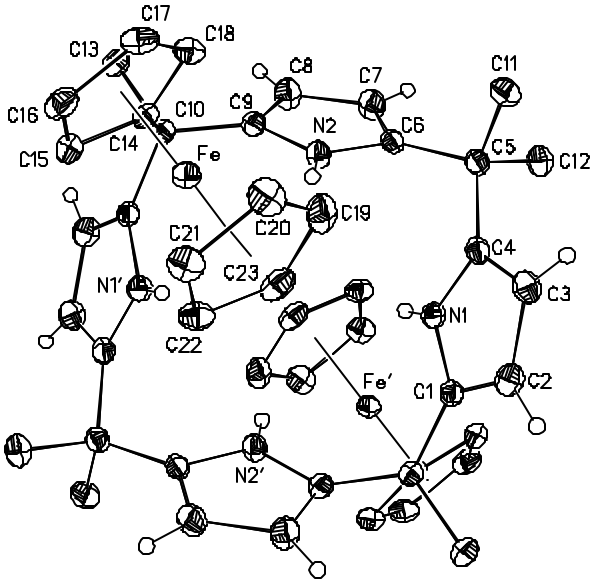

Figure 1. Single crystal X-ray structure of **1.29** showing the atom labeling scheme.

X-ray Experimental for $C_{46}H_{48}N_4Fe - CH_3OH$: Crystals grew as yellow-orange plates by diffusion of a solution of **1.28** in dichloromethane into methanol. A total of 168 frames of data were collected using ω-scans with a scan range of 1.8° and a counting time of 36 seconds per frame. The hydrogen atoms on the pyrrole nitrogen atoms were observed in a ΔF map and initially refined with isotropic displacement parameters. However, while the geometry of these hydrogen atoms were reasonable the isotropic displacement parameters were quite low. The isotropic displacement parameter for H2n refined to a negative value. The isotropic displacement parameters for the two N-H hydrogen atoms were finally refined with values set to 1.2xUeq of the attached nitrogen atom.

The complex lies around a crystallographic two-fold rotation axis at 0, y, ¼ . A solvent molecule was found to be disordered and centered around this two-fold axis. The molecule appeared to be methanol and was initially refined as such. A third peak, lying on the two-fold axis, of about 1.5 $e^-/Å^3$ persisted near the carbon atom of the methanol molecule and perhaps was due to a mixture of methanol and acetonitrile lying along the two-fold axis. Because of the uncertainty of the identity of the solvent and the difficulty in modeling it, the utility SQUEEZE[4] was employed to remove the contribution of the solvent from the data. The function, $\Sigma w(|F_o|^2 - |F_c|^2)^2$, was minimized, where $w = 1/[(\sigma(F_o))^2 + (0.0322*P)^2]$ and $P = (|F_o|^2 + 2|F_c|^2)/3$. $R_w(F^2)$ refined to 0.110, with R(F) equal to 0.0555 and a goodness of fit, S, = 0.921.

Table 3. Crystal data and structure refinement for **1.28**.

Empirical formula	C47 H52 Fe2 N4 O	
Formula weight	800.63	
Temperature	153(2) K	
Wavelength	0.71073 Å	
Crystal system	Monoclinic	
Space group	C2/c	
Unit cell dimensions	a = 30.4448(9) Å	α= 90°.
	b = 7.1250(3) Å	β= 121.960(2)°.
	c = 21.1495(8) Å	γ = 90°.
Volume	3892.3(2) $Å^3$	
Z	4	
Density (calculated)	1.366 Mg/m^3	
Absorption coefficient	0.788 mm^{-1}	
F(000)	1688	
Crystal size	0.20 x 0.16 x 0.08 mm	
Theta range for data collection	2.97 to 27.40°.	
Index ranges	-35<=h<=39, -7<=k<=9, -27<=l<=27	
Reflections collected	6960	
Independent reflections	4341 [R(int) = 0.0799]	
Completeness to theta = 27.40°	98.0 %	

Absorption correction	None
Refinement method	Full-matrix least-squares on F^2
Data / restraints / parameters	4341 / 0 / 241
Goodness-of-fit on F^2	0.921
Final R indices [I>2sigma(I)]	R1 = 0.0555, wR2 = 0.0922
R indices (all data)	R1 = 0.168, wR2 = 0.110
Largest diff. peak and hole	0.51 and -0.37 e.$Å^{-3}$

Table 4. Atomic coordinates (x 10^4) and equivalent isotropic displacement parameters ($Å^2$ x 10^3) for **1.28**. U(eq) is defined as one third of the trace of the orthogonalized U^{ij} tensor.

Atom	x	y	z	U
Fe	2071(1)	3556(1)	5957(1)	27(1)
N1	844(1)	3324(5)	2768(2)	29(1)
N2	320(1)	3718(5)	3817(2)	27(1)
C1	818(1)	4603(6)	2260(2)	27(1)
C2	1084(1)	6171(6)	2656(2)	35(1)
C3	1272(1)	5813(6)	3417(2)	34(1)
C4	1117(1)	4048(5)	3480(2)	25(1)
C5	1225(1)	2907(5)	4151(2)	23(1)
C6	734(1)	2486(5)	4129(2)	26(1)
C7	586(1)	993(5)	4383(2)	33(1)
C8	75(1)	1328(6)	4213(2)	31(1)
C9	-87(1)	3018(6)	3856(2)	28(1)
C10	-586(1)	4075(6)	3553(2)	31(1)
C11	1480(1)	1046(5)	4157(2)	28(1)
C12	1591(1)	4100(5)	4835(2)	21(1)
C13	1445(1)	5227(5)	5255(2)	25(1)
C14	1884(1)	6322(5)	5765(2)	30(1)
C15	2296(1)	5926(5)	5653(2)	30(1)
C16	2113(1)	4569(5)	5080(2)	26(1)

C17	2023(2)	2653(6)	6826(2)	48(1)
C18	2532(2)	3141(6)	7077(2)	44(1)
C19	2700(2)	2006(6)	6714(2)	37(1)
C20	2309(2)	850(6)	6235(2)	39(1)
C21	1876(2)	1206(7)	6289(2)	48(1)
C22	-493(2)	5903(6)	4001(2)	43(1)
C23	-981(1)	2833(6)	3609(2)	43(1)

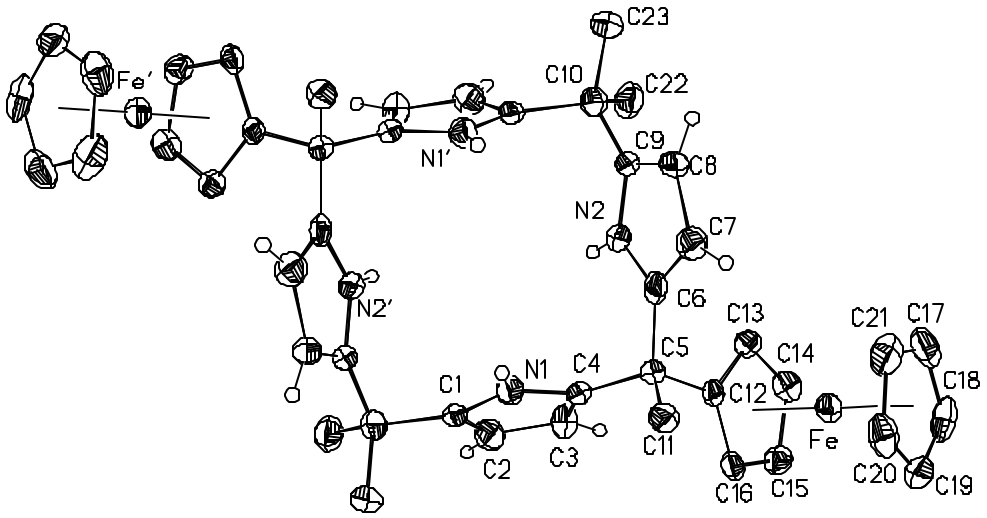

Figure 2. Single crystal X-ray structure of **1.29** showing the atom labeling scheme.

X-ray Experimental for $(C_{11}H_{11}N_2O)_2Fe$: Crystals grew as beautiful orange prisms by slow evaporation from a solution of **1.59** dissolved in methylene chloride. The data crystal had approximate dimensions; 0.42 x 0.46 x 0.62 mm. The data were collected using the ω-scan technique at 8 - 12°/min., with a scan range of 1.2° in ω at -85 °C on a. Four reflections (-1,-4,0; 2,-4,-7; 2,-4,7; -1,2,5) were remeasured every 96 reflections to monitor instrument and crystal stability. A smoothed curve of the intensities of these check reflections was used to scale the data. The scaling factor ranged from 0.983 - 1.00. The data were corrected for Lp effects but not for absorption. The structure was solved by direct methods and refined by full-matrix least-squares on F^2 with anisotropic displacement parameters for the non-H atoms. The hydrogen atoms were observed in a ΔF map and refined with isotropic displacement parameters. The function, ? $w(|F_o|^2 - |F_c|^2)^2$, was minimized, where $w = 1/[(\sigma(F_o))^2 + (0.0221*P)^2 + (3.6045*P)]$ and $P = (|F_o|^2 + 2|F_c|^2)/3$. The data were corrected for secondary extinction effects. The correction takes the form: $F_{corr} = kF_c/[1 + (1.6(2)x10^{-6})* F_c^2 \lambda^3/(\sin 2\theta)]^{0.25}$ where k is the overall scale factor. The direction of the c-axis was determined by refining the Flack parameter.[2]

Table 5. Crystal data and structure refinement for **1.59**.

Empirical formula	C22 H22 Fe N4 O2
Formula weight	430.29
Temperature	188(2) K
Wavelength	0.71073 A
Crystal system	Orthorhombic
Space group	Pna21
Unit cell dimensions	a = 9.7812(7) A alpha = 90°
	b = 13.2533(9) A beta = 90°
	c = 15.1360(10) A gamma = 90°
Volume, Z	1962.1(2) A^3, 4
Density (calculated)	1.457 Mg/m^3
Absorption coefficient	0.795 mm^-1
F(000)	896
Crystal size	0.42 x 0.46 x 0.62 mm
Theta range for data collection	2.04 to 27.50 deg.
Limiting indices	-1<=h<=12, -1<=k<=17, -1<=l<=19
Reflections collected	3036
Independent reflections	2518 [R(int) = 0.0153]
Refinement method	Full-matrix least-squares on F^2
Data / restraints / parameters	2517 / 1 / 352
Goodness-of-fit on F^2	1.007
Final R indices [I>2sigma(I)]	R1 = 0.0303, wR2 = 0.0649

R indices (all data)	R1 = 0.0443, wR2 = 0.0719
Absolute structure parameter	-0.05(4)
Extinction coefficient	0.0103(7)
Largest diff. peak and hole	0.219 and -0.242 e.A^-3

Table 6. Atomic coordinates (x 10^4) and equivalent isotropic displacement parameters ($Å^2$ x 10^3) for **1.59**. U(eq) is defined as one third of the trace of the orthogonalized U^{ij} tensor.

Atom	x	y	z	U
Fe	1037(1)	1048(1)	7424(1)	22(1)
C1	-176(3)	2008(3)	8119(3)	22(1)
C2	-953(3)	1477(2)	7468(3)	27(1)
C3	-396(4)	1717(3)	6628(3)	32(1)
C4	721(5)	2377(3)	6759(3)	35(1)
C5	867(4)	2552(3)	7677(2)	27(1)
C6	-466(4)	1991(2)	9078(2)	24(1)
O7	-1615(3)	1735(2)	9352(2)	33(1)
N8	537(3)	2282(2)	9625(2)	27(1)
C9	362(5)	2357(3)	10581(3)	35(1)
C10	1482(4)	1867(3)	11090(2)	29(1)
N11	2018(4)	944(2)	10875(2)	33(1)
C12	2967(4)	662(4)	11483(3)	42(1)
C13	3057(5)	1411(4)	12096(3)	48(1)
C14	2133(4)	2165(3)	11852(3)	39(1)
C1'	1381(4)	-250(3)	8103(3)	24(1)
C2'	1152(4)	-463(3)	7190(2)	30(1)
C3'	2183(6)	45(4)	6707(3)	47(1)

C4'	3025(4)	568(3)	7295(4)	46(1)
C5'	2546(4)	400(3)	8162(3)	36(1)
C6'	582(4)	-587(2)	8873(2)	24(1)
O7'	1019(3)	-467(2)	9634(2)	40(1)
N8'	-615(3)	-1045(3)	8713(2)	32(1)
C9'	-1461(4)	-1474(3)	9421(3)	40(1)
C10'	-2884(3)	-1079(3)	9443(2)	27(1)
N11'	-3178(3)	-78(2)	9403(2)	30(1)
C12'	-4554(4)	53(3)	9502(3)	40(1)
C13'	-5137(4)	-875(3)	9613(4)	45(1)
C14'	-4069(4)	-1587(3)	9569(3)	35(1)

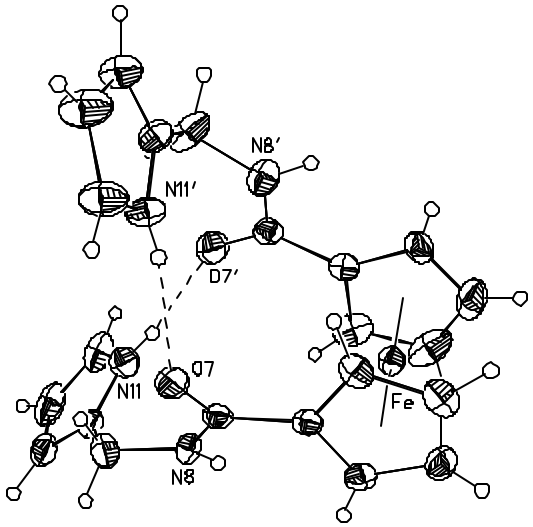

Figure 3. Single crystal X-ray structure of **1.59** showing the atom labeling scheme.

Appendix B: UV-Visible Titration Data Taken in Acetone of Receptors 3.31-3.34 with F^- in the Presence and Absence of Various Cations.

The fluoride anion was studied in the form of its tetrabutylammonium trihydrate salt. See individual captions for experimental details.

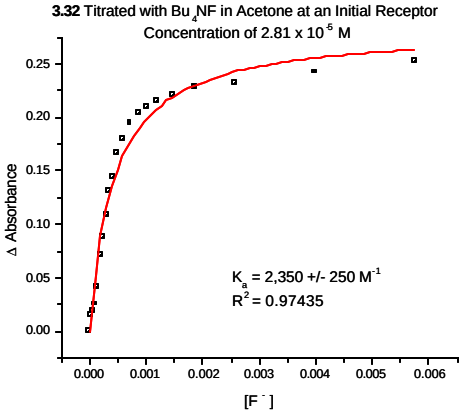

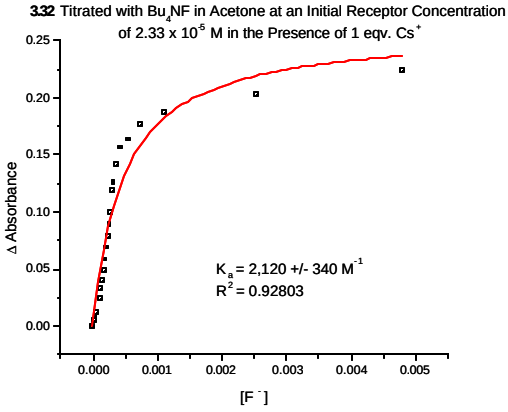

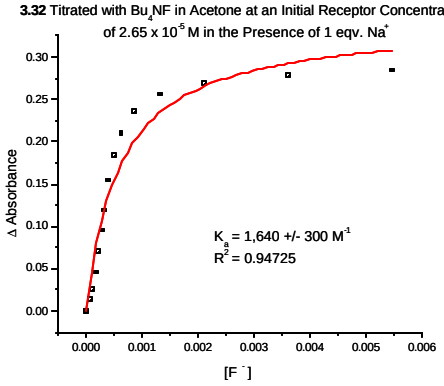

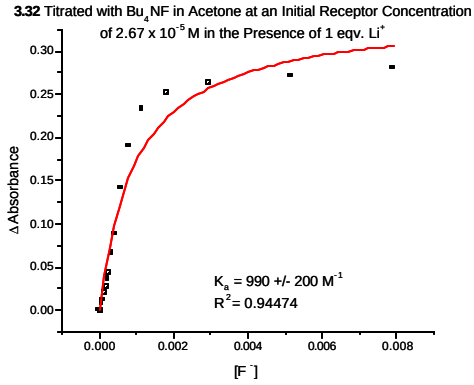

3.31 Titrated with Bu_4NF in Acetone at an Initial Receptor Concentration of 3.09×10^{-5} M

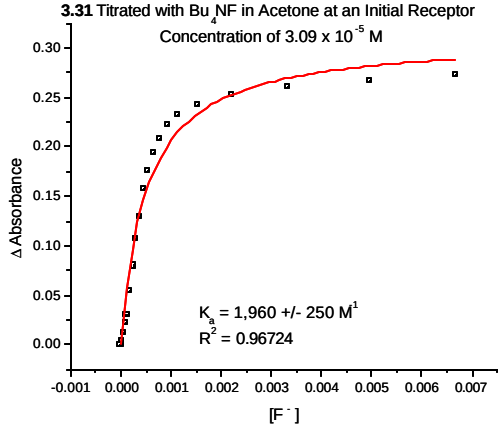

3.31 Titrated with Bu_4NF in Acetone at an Initial Receptor Concentration of 2.51×10^{-5} M in the Presence of 1 eqv. Cs^+

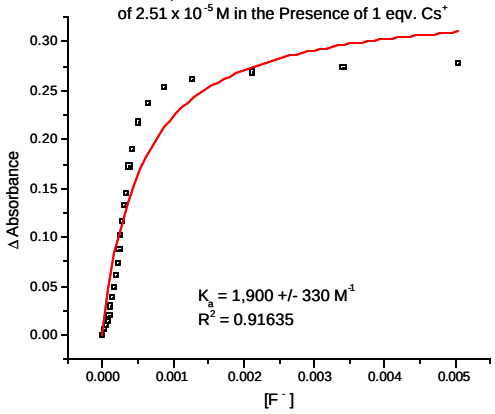

3.31 Titrated with Bu_4NF in Acetone at an Initial Receptor Concentration of 2.50×10^{-5} M in the Presence of 1 eqv. K^+

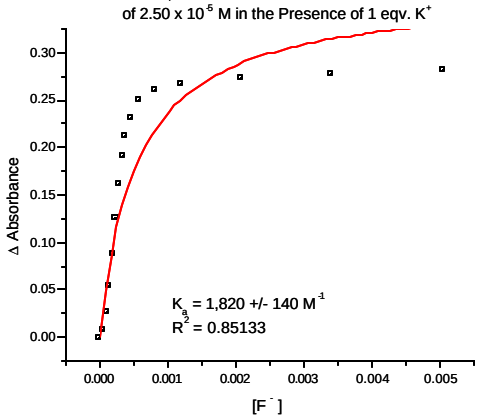

3.31 Titrated with Bu_4NF in Acetone at an Initial Receptor Concentration of 2.65×10^{-5} M in the Presence of 1 eqv. Na^+

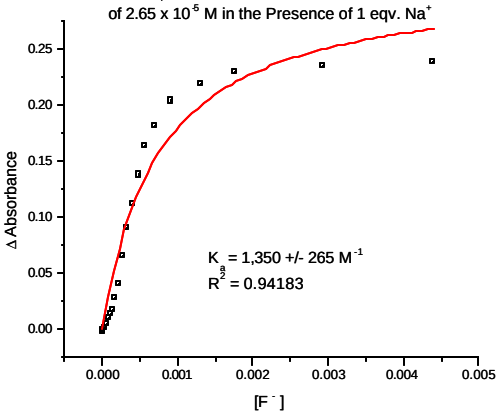

3.31 Titrated with Bu_4NF in Acetone at an Initial Receptor Concentration of 2.47×10^{-5} M in the Presence of 1 eqv. Li^+

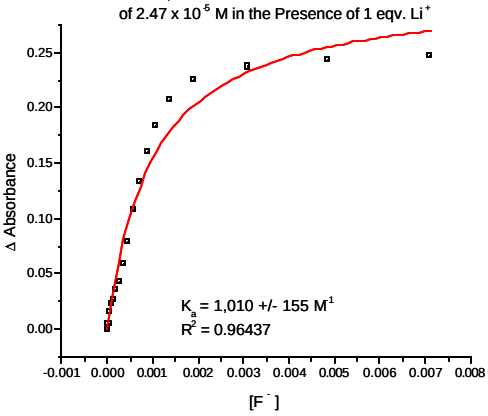

3.34 Titrated with Bu_4NF in Acetone at an Initial Receptor Concentration of 2.76 x 10^{-5} M

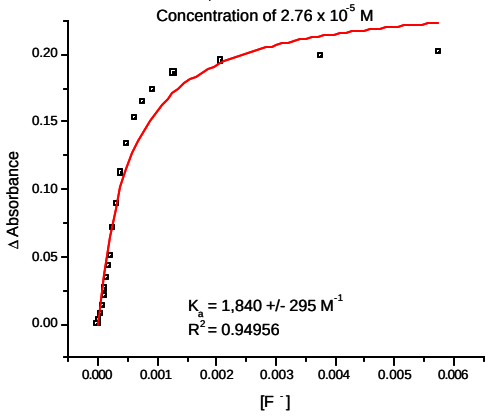

3.34 Titrated with Bu_4NF in Acetone at an Initial Receptor Concentration of 3.48 x 10^{-5}M in the Presence of 1 eqv. Cs^+

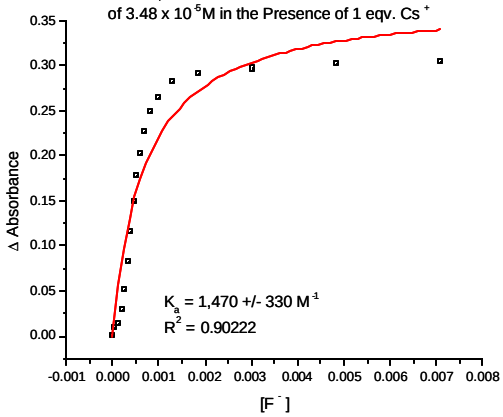

3.34 Titrated with Bu_4NF in Acetone at an Initial Receptor Concentration of 2.76 x 10^{-5} M in the Presence of 1 eqv. Na^+

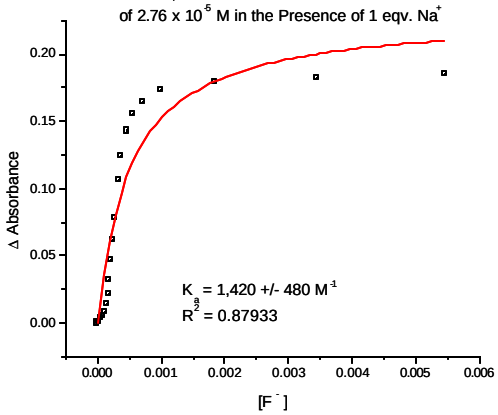

3.34 Titrated with Bu_4NF in Acetone at an Initial Receptor Concentration of 2.36 x 10^{-5} M in the Presence of 1 eqv. Li^+

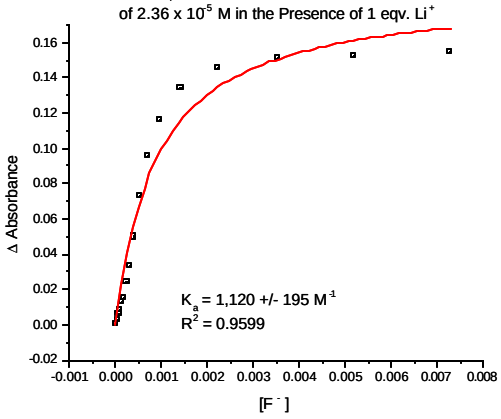

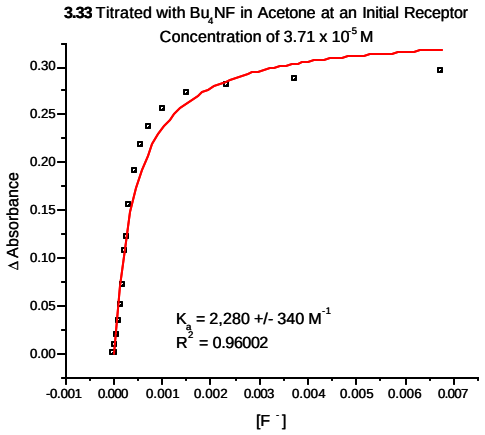
3.33 Titrated with Bu4NF in Acetone at an Initial Receptor Concentration of 3.71 x 10-5 M
Δ Absorbance
[F -]
Ka = 2,280 +/- 340 M-1
R2 = 0.96002

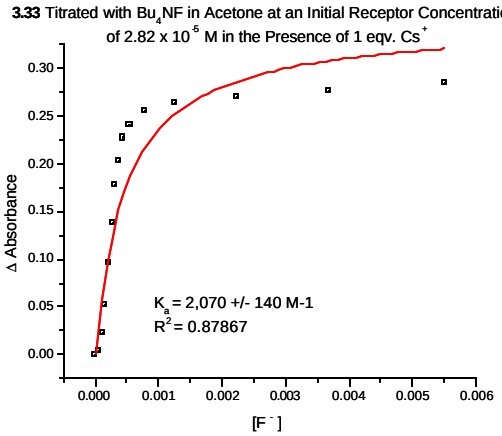
3.33 Titrated with Bu4NF in Acetone at an Initial Receptor Concentration of 2.82 x 10-5 M in the Presence of 1 eqv. Cs+
Δ Absorbance
[F -]
Ka = 2,070 +/- 140 M-1
R2 = 0.87867

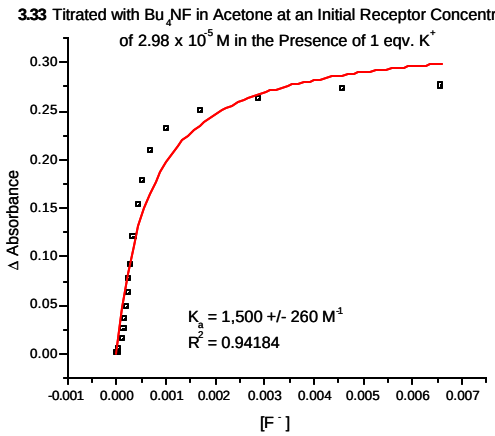
3.33 Titrated with Bu4NF in Acetone at an Initial Receptor Concentration of 2.98 x 10-5 M in the Presence of 1 eqv. K+
Δ Absorbance
[F -]
Ka = 1,500 +/- 260 M-1
R2 = 0.94184

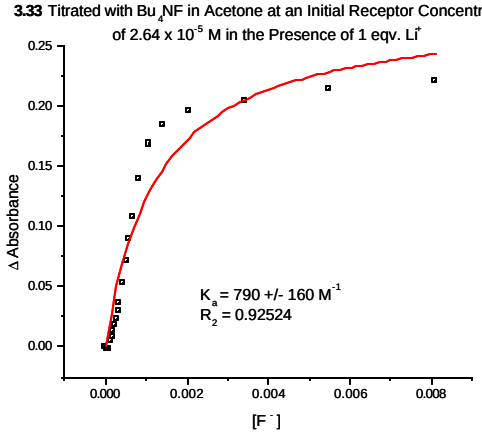
3.33 Titrated with Bu4NF in Acetone at an Initial Receptor Concentration of 2.64 x 10-5 M in the Presence of 1 eqv. Li+
Δ Absorbance
[F -]
Ka = 790 +/- 160 M-1
R2 = 0.92524

Vita

Rebecca Suzanne Zimmerman was born in Detroit, Michigan on September 26, 1972, the first child of Dennis and Suzanne Zimmerman. In 1990 she enrolled at Shippensburg University of Pennsylvania, where she earned a B.A. in Geoenvironmental Studies and a B.S. in Chemistry in 1995. She then worked as an environmental consultant at Dyncorp and at her favorite place in the world, Home Depot, before coming to The University of Texas at Austin in the fall of 1996 to pursue her doctorate. She was awarded the Henze Teaching Excellence Award and Texas Excellence in Teaching Award in 2000. She finished three Austin Motorola marathons, saved five stray cats and successfully hand raised two birds during her time here.

Permanent address: 3271 Blue Heron Dr., Falls Church, VA 22042

This dissertation was typed by the author.